QUARTERLY JOURNAL
OF THE
ROYAL METEOROLOGICAL SOCIETY

Editor: J. S. SAWYER

Vol. 86 OCTOBER 1960 No. 370

CONTENTS

PAGE

R. FJØRTOFT—Symons Memorial Lecture for 1960—On the control of kinetic energy of the atmosphere by external heat sources and surface friction 437

F. SINGLETON and D. J. SMITH—Some observations of drop-size distributions in low layer clouds 454

D. ATLAS, W. G. HARPER, F. H. LUDLAM and W. C. MACKLIN—Radar scatter by large hail 468

F. K. BALL—Control of inversion height by surface heating 483

H. A. PANOFSKY and R. A. MCCORMICK—The spectrum of vertical velocity near the surface 495

E. KNIGHTING and M. K. HINDS—A report on some experiments in numerical prediction using a stream function 504

C. L. MATEER and W. L. GODSON—The vertical distribution of atmospheric ozone over Canadian stations from *umkehr* observations 512

C. D. WALSHAW—The accuracy of determination of the vertical distribution of atmospheric ozone from emission spectrophotometry in the 1,043 cm^{-1} band at high resolution 519

M. W. RAMSAY and J. A. CHALMERS—Measurements on the electricity of precipitation 530

Shorter Contributions—

R. A. EBDON—Notes on the wind flow at 50 mb in tropical and sub-tropical regions in January 1957 and January 1958 540

C. S. DURST—The statistical variation of wind with distance 543

B. C. V. ODDIE—The variation in composition of sea-salt nuclei with mode of formation 549

B. J. MASON—Ice-nucleating properties of clay minerals and stony meteorites .. 552

R. G. BARRY—A note on the synoptic climatology of Labrador-Ungava 557

Correspondence—

R. W. LONGLEY; C. I. JACKSON—Snowfall measurements in northern Canada .. 566

F. BAUR—Physical-statistical rules as bases for forecasts of weather and weather-character 567

Discussions—

E. B. KRAUS—Synoptic and dynamic aspects of climatic change (*Q.J.*, **86**, p. 1) .. 569

D. W. MARTIN and A. W. BREWER—A synoptic study of day-to-day changes of ozone over the British Isles (*Q.J.*, **85**, p. 393) 575

F. K. HARE—The summer circulation of the arctic stratosphere below 30 km (*Q.J.*, **86**, p. 127) 576

J. I. P. JONES and F. PASQUILL—An experimental system for directly recording statistics of the intensity of atmospheric turbulence (*Q.J.*, **85**, p. 225) 578

J. L. MONTEITH—The reflection of short-wave radiation by vegetation (*Q.J.*, **85**, p. 386) 579

Announcement—

L. F. RICHARDSON PRIZE 579

Proceedings at meetings of the Society 580

Reviews—

Dynamics of climate, R. L. Pfeffer (G.A.C.); *Weathercraft*, L. P. Smith (R.W.G.); *Turbulent flows and heat transfer*, (Ed.) C. C. Lin (R.S.S.); *Alfred Wegener*, E. Wegener (H.H.L); *Sonnenstrahlung und Lufttrübung*, L. Foitzik and H. Hinzpeter (D.B.L.) 583

Index 586

PUBLISHED AND SOLD BY THE
ROYAL METEOROLOGICAL SOCIETY
49 CROMWELL ROAD, LONDON, S.W.7
PRICE THIRTY SHILLINGS ($4.50)
ANNUAL SUBSCRIPTION £5 - 4 - 0 ($16), POST FREE

ROYAL METEOROLOGICAL SOCIETY

Founded on 3 April 1850, for the advancement of meteorological science. The Society was incorporated by Royal Charter in 1866.

MEMBERSHIP

Membership is open to all persons genuinely interested in meteorology. The annual subscription is as follows :

Fellows ..	..	£4-4-0 (Entrance fee, 1 guinea)
Foreign Members ..		£4-4-0 „ „
Students ..	..	£1-10-0
Corporate Members ..		£21-0-0

All Members receive free the regular publications of the Society, including the monthly publication *Weather* (annual subscription to non-members 24s. plus 2s. 6d. postage).

The Descriptive Account of the Society and an application form will be sent on request to the Assistant Secretary.

Quarterly Journal

EDITING COMMITTEE

J. S. Sawyer — *Editor and Chairman*

G. A. Corby A. G. Forsdyke R. F. Jones B. J. Mason
F. Pasquill R. C. Rainey R. S. Scorer

The primary purpose of the *Quarterly Journal* is to publish results of original research and reports of the Society's scientific meetings. Papers intended for the *Journal* **should be submitted in accordance with standards laid down by the Council in the Society's memorandum** ' Preparation of Papers for the *Quarterly Journal* ' which is available on request. Failure to conform with these standards involves the Society's officers and staff in much needless work and the Society in unnecessary expense. **Manuscripts will therefore not be considered for publication unless they conform reasonably closely with the procedure laid down.** The attention of authors is drawn particularly to the requirements in regard to mathematics and diagrams and the Assistant Secretary will be pleased to advise authors on their special problems of illustration before papers are formally submitted. Diagrams should, if possible, be submitted flat, not rolled, and a duplicate rough set for refereeing purposes should be included. Where rulings on a diagram are desirable the closest acceptable spacing is approximately 1 cm and this may be done on **blue-lined** graph paper by thickening the centimeter rulings. Manuscripts may be submitted in duplicate to expedite refereeing, but authors must retain complete copies in their possession.

Price to non-members is £5-4-0 (post free) per annum and £1-10-0 for single issues (postage extra).

PUBLICATIONS

Copies of the publications *Centenary Proceedings of the Royal Meteorological Society*, 1950 (£1. 1s.) and *Proceedings Toronto Meteorological Conference* 1953 (£1. 10s.) are still available.

Reprints of papers recently published in the *Quarterly Journal* are generally available, the prices being as follows (postage extra): 8 pp., 1s. 2d.; 16 pp., 1s. 10d.; 20 pp., 2s. 2d.

Weather Lore. Fourth edition of the late Richard Inwards's unique compilation, revised, augmented and edited for the Society by E. L. Hawke. Published in 1950. Price 15s. Price to Members, 10s. 6d., postage 9d.

Rainfall Atlas of the British Isles. Published in 1926. Price to Members, 15s. post free.

Collected Scientific Papers of William Henry Dines, F.R.S. This memorial volume contains reproductions of nearly sixty papers and other original communications by W. H. Dines. Price 15s., postage 1s.

Cloud study : a pictorial guide. By F. H. Ludlam and R. S. Scorer. 75 photographs. Published in 1957 under the auspices of the Society by John Murray. 12s. 6d. (11s. to Members), postage 1s.

THE SOCIETY'S OFFICES

Assistant Secretary — R. H. Levinson, M.A., F.C.A.

49 Cromwell Road, London, S.W.7.

(*Telephone :* KENsington 0730)

The offices and library of the Society are open daily (Monday to Friday) from 10 a.m. to 5 p.m. All enquires and correspondence concerning the Society and its publications should be addressed to the Assistant Secretary.

treatment presented in most works on the subject. The methods and practices included have been tested in day-to-day forecasting and have withstood the critical appraisal of working forecasters, have produced consistently superior results, and, above all, have proved practical in use. The text contains detailed, instructive illustrations throughout.

In addition to meteorologists directly concerned with weather forecasting for aeronautical purposes, other scientists interested in forecasting will find this book useful as a thorough survey of current methods and accuracy in weather prediction.

P. W. FUNKE

R. J. SHAFER

A. H. STAKELY

H. B. VISSCHER

R. M. WHITING

Members of the Weather Department, Eastern Air Lines

Table of contents and sample pages ▶

ACADEMIC PRESS, *New York and London*

111 FIFTH AVENUE, NEW YORK 3, NEW YORK

17 OLD QUEEN STREET, LONDON, S.W.1

GERMAN AGENCY: Minerva, G.m.b.H., Holbeinstrasse 25-27, Frankfurt am Main

INDIAN AGENCY: Asia Publishing House, Nicol Road, Ballard Estate, Bombay 1

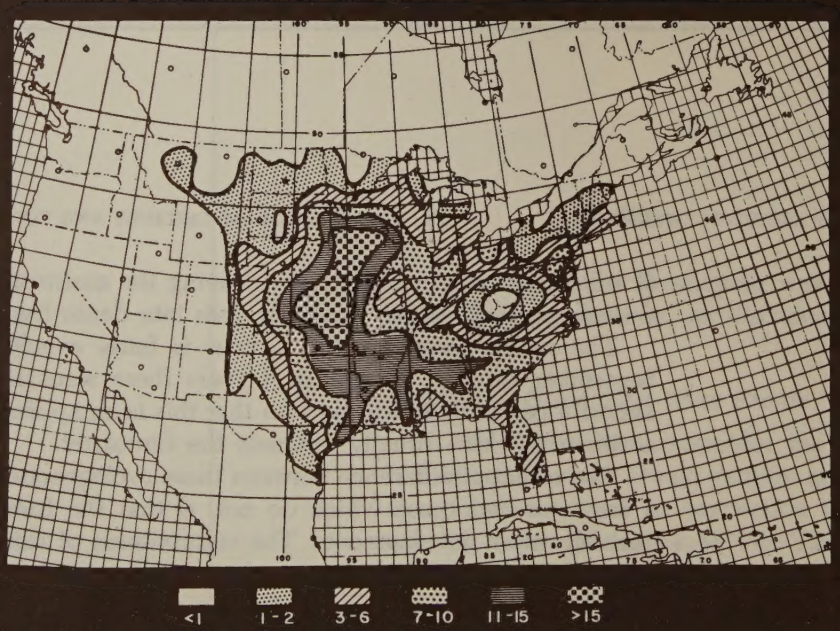

Weather Forecasting for Aeronautics

By JOSEPH J. GEORGE

Eastern Air Lines
Atlanta, Georgia

Fig. 14.36. **Total number of tornadoes per 50-mile square reported in the period 1920-1949**

June 1960, 673 pp., 650 illustrations, $15.00
£5.7.6

WEATHER LORE

Compiled and arranged by the late

RICHARD INWARDS, F.R.A.S.

FORMER PRESIDENT OF THE
ROYAL METEOROLOGICAL SOCIETY

Edited, revised and amplified by

E. L. HAWKE, M.A., F.R.A.S.

FORMER VICE-PRESIDENT OF THE
ROYAL METEOROLOGICAL SOCIETY

A collection of several thousand sayings and rules relating to the weather, taken from the world's literature and the age-old wisdom of farmers, mariners, bird watchers . . . . . concerning flowers, plants, trees, birds, animals, fish, tides, clouds, rainbows, stars, mock moons, haloes . . . . .

This bedside book for the would-be weather-wise is available from the *Assistant Secretary, Royal Meteorological Society, 49 Cromwell Road, London, S.W.7.* Price 4s. 6d. (postage 1s. extra).

CLOUD PHOTOGRAPHS

The Society is publishing in postcard form a new series from its unique CLARKE AND CAVE COLLECTION.

The set contains three groups of eight photographs of high, medium and low-level clouds.

These are available as complete sets of 24 cards (price 7s. 6d. or 8s. post free) from the *Assistant Secretary, Royal Meteorological Society, 49 Cromwell Road, London, S.W.7.*

BACK NUMBERS OF THE *QUARTERLY JOURNAL* OF THE ROYAL METEOROLOGICAL SOCIETY

With the growing number of scientific institutions and libraries throughout the world frequent requests are received by the Society for back issues of the *Quarterly Journal.*

Stocks have, however, now fallen very low and it is becoming difficult to meet the demands. The Society is dealing with this problem, so far as Journals for the years since 1945 are concerned, by reprinting those which are approaching exhaustion, and about a dozen numbers have been so reprinted in the last year. But for 1944 and earlier years the demand is insufficient to justify reprinting. On the other hand, requests are received from time to time, and the Society, as a scientific institution, evidently has a duty to meet them if possible.

Council will be most grateful to Members who will help in this matter by handing in their pre-1945 *Quarterly Journals.* Such Members are invited to write to the Assistant Secretary, saying what Journals they have available. The Society will pay 7s. 6d. for each usable number, and will refund postage.

LIBRARY. Members of the Royal Meteorological Society are reminded that Lists of Accessions to the library are issued at irregular intervals. Copies can be obtained on application to the *Assistant Librarian.*

Lists containing details of lantern slides, films and film strips are also available, on application, and may be obtained on loan by Members.

TRADE HEZZANITH MARK

Meteorological and Scientific Instruments

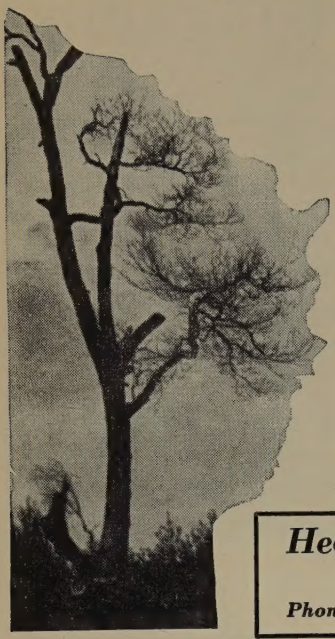

There is a century of rich experience behind the manufacture of every **"HEZZANITH"** *Instrument*

CATALOGUES ARE AVAILABLE UPON REQUEST (RMS.A1)

Heath, Hicks & Perken (THERMOMETERS) Ltd.
New Eltham, London, S.E.9
Phone : ELTHAM 3836. Grams : "OPTIMUS," Southphone, London

HORSTMANN

CHART CLOCK

The robustly constructed movements and high quality jewelled lever escapements of Horstmann Chart Clocks ensure the extremely accurate timekeeping necessary in meteorological equipment. The clocks, which are used extensively by the Air Ministry Meteorological Office, are available in two types – one to drive chart drums revolving once every 24 hours and the other for 7 day rotation.

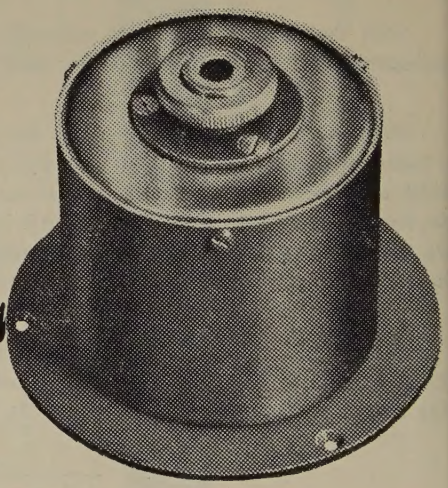

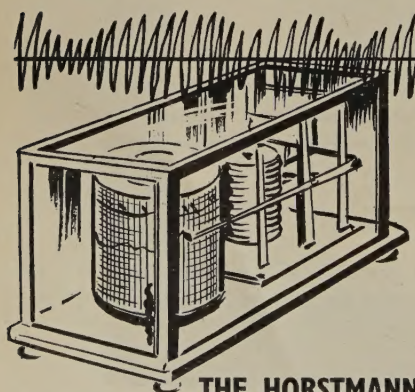

Chart Clocks with speeds other than those mentioned above can also be supplied to special order.

THE HORSTMANN GEAR CO. LTD.
NEWBRIDGE WORKS · BATH · Tel. : Bath 7241

NEWBRIDGE WORKS BATH
REGISTERED TRADE MARK

THE FINEST SOUNDING AND PILOT BALLOONS AVAILABLE

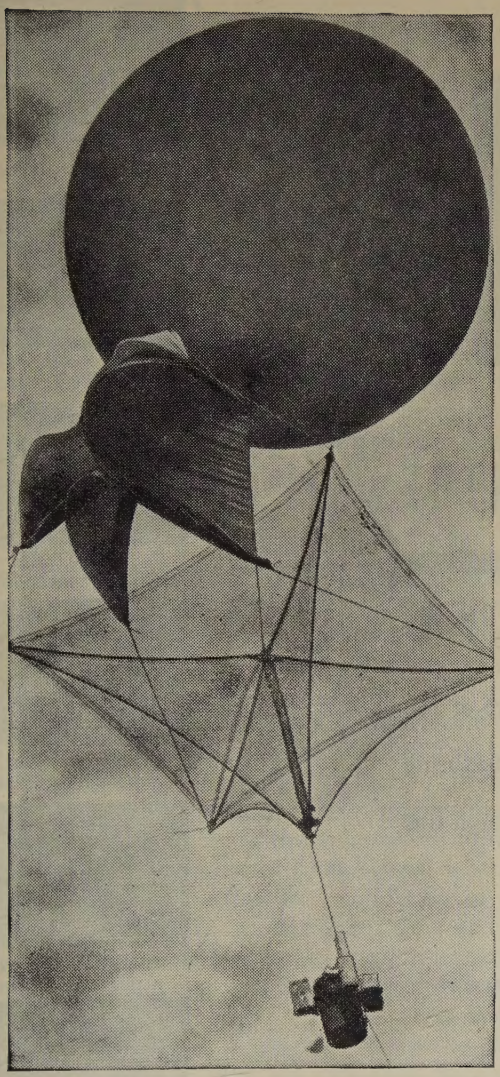

Manufactured by the Guide Bridge Rubber Company of Vulcan Mill, Bury, these balloons are in use throughout the world.

OVERSEAS SALES

Phillips Patents Limited
250 Western Avenue, Acton, London, W.3

HOME SALES

Guide Bridge Rubber Co. Ltd, Vulcan Mill, Butcher Lane, Bury, Lancs

Beritex SEAMLESS REGD.

ask SIMA

INSTRUMENT CENTRE

20 QUEEN ANNE STREET, LONDON, W.1.

The specialised knowledge and advice of 160 British Manufacturers of Scientific Measuring Instruments are available to you through this one source.

Telephones:

Technical Enquiries — IMPerial 6000
Secretarial Enquiries — LANgham 4251

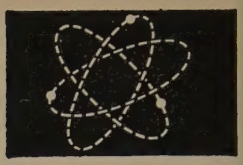

NUCLEAR INSTRUMENTS

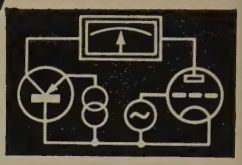

ELECTRONIC INSTRUMENTS

NAVIGATIONAL AND SURVEY EQUIPMENT

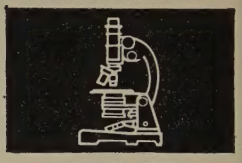

OPTICAL AND OPHTHALMIC INSTRUMENTS

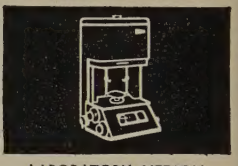

LABORATORY MEDICAL AND X-RAY APPARATUS

KINEMATOGRAPH AND ALLIED INSTRUMENTS

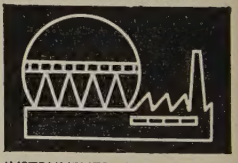

INSTRUMENTS FOR PROCESS CONTROL AND AUTOMATION

Space donated by :

C. F. CASELLA & CO. LTD.

Regent House, Fitzroy Square, London, W.1

Manufacturers of a complete range of meteorological instruments for measurement of wind, pressure, temperature, humidity, rainfall and sunshine.

SIMA

SCIENTIFIC INSTRUMENT MANUFACTURERS' ASSOCIATION OF GREAT BRITAIN

QUARTERLY JOURNAL
OF THE
ROYAL METEOROLOGICAL SOCIETY

Vol. 86 OCTOBER 1960 No. 370

551.511.3 : 551.513.1

On the control of kinetic energy of the atmosphere by external heat sources and surface friction

By R. FJØRTOFT
Det Norske Meteorologiske Institutt, Oslo

(Symons Memorial Lecture, delivered 4 May 1960)

When your President asked me to deliver the Symons Lecture, I had recently been studying some aspects of the energetics of the general circulation of the atmosphere; several of my results have recently appeared in an article (Fjørtoft 1959) in the *Rossby Memorial Volume*, and as I believe they add to our fundamental understanding of the general circulation, I have decided, with your President's concurrence, to review the energy transformations of the atmosphere along similar lines, tonight.

1. Introduction

With regard to the long-term behaviour of the atmosphere, this, undoubtedly, is controlled externally by the sun and the earth's surface. Although it seems as if the atmosphere, with seemingly constant external conditions, can have a number of different dynamical regimes which can persist for some time, it is very likely that, for periods which are sufficiently long, these regimes will average out to one which is uniquely defined by the external conditions.

The radiation from the sun, together with the spherical shape of the earth, the inclination of the axis of the earth's rotation, and the inhomogeneities of the earth's surface, as well as the way in which the thermodynamical properties of the earth's surface differ from those of the atmosphere, are fundamentally the reasons for the maintenance of the temperature differences in the atmosphere. Firstly, by the motion of the air the temperature distribution is constantly rearranged whereby all those solenoid fields are maintained which are responsible for the production of kinetic energy against the dissipative loss by friction. Secondly, the frictional drag at the surface forces the atmosphere to rotate basically with the earth, whereby the atmosphere is given an important dynamical property. Thirdly, the character of the roughness of the earth's surface influences the dissipation of kinetic energy.

In this lecture it is intended to discuss the problem of how, in certain respects, the external conditions define the long-term state of the atmosphere. The complexity of this problem, when taken in all detail, is, of course, so great that it is necessary to simplify the problem greatly. Essentially this will be accomplished by restricting the dynamical degrees of freedom to what seems a permissible minimum, and by using very simple laws for frictional dissipation and heating. In spite of this it is hoped that some qualitatively correct results have been derived.

2. The mechanical energy equation and the vertical distribution of temperature

In the following, $\int$ symbolizes an average with respect to mass over the whole atmosphere and over a period sufficiently extended to have a long-term steady state. Approximately, the hydrodynamic equations may be written as :

Equation of motion :

$$\frac{d\mathbf{V}}{dt} = \Theta \nabla\phi - f\mathbf{k} \times \mathbf{V} + \mathbf{F} + \text{a laminar vector} \quad . \quad . \quad (1)$$

$$\left(\Theta = \frac{\theta - \int \theta}{\int \theta}; \quad \theta = \text{potential temperature}\right)$$

Thermodynamic energy equation in terms of Θ :

$$\frac{d\Theta}{dt} = H \quad . \quad . \quad . \quad . \quad . \quad (2)$$

Continuity equation :

$$\nabla \cdot Q\mathbf{V} = 0 \; . \quad . \quad . \quad . \quad . \quad (3)$$

(Q = standard density)

Boundary conditions :

$$Qw = 0 \quad \text{for} \quad z = 0, \quad z = \infty \quad . \quad . \quad . \quad (4)$$

Hence the mechanical energy equation :

$$\frac{d}{dt}\int \tfrac{1}{2}\mathbf{V}^2 Q \, d\tau = \int g\Theta \, wQ \, d\tau - \int \delta Q \, d\tau \quad . \quad . \quad (5)$$

(δ = dissipation)

Integration in (5) is over the whole atmosphere. Correspondingly we get for the long-term steady state :

$$0 = \frac{d}{dt}\int \tfrac{1}{2}\mathbf{V}^2 = \int g\Theta \, w - \int \delta \quad . \quad . \quad . \quad . \quad (6)$$

For an atmosphere in motion, $\delta > 0$. Accordingly there is, on an average, an upwards flux of Θ. Because of the boundary conditions this must tend to warm the upper parts of the atmosphere and cool the lower ones. In the steady state there must therefore be compensating cooling and warming due to the ' heating ' function H. Explicitly this is stated by :

$$\frac{1}{Q}\frac{d}{dz}(\Theta w \, Q)_0 = H_0 \quad . \quad . \quad . \quad . \quad (7)$$

Here the subscript zero denotes a horizontal average and it is further understood that $(\Theta w)_0$ and H_0 are long-term averages.

It will now be assumed that Eqs. (1) to (4) are smoothed equations valid only for the large-scale components of motion, say for scales larger than those of the smallest-scale frontal wave perturbations. The corresponding dissipation is roughly proportional to kinetic energy of surface geostrophic velocity :

$$\int \delta = \nu \int \mathbf{V}^{\circ 2}; \quad \nu \approx 2 \times 10^{-6} \, \text{sec}^{-1} \quad . \quad . \quad . \quad (8)$$

($\mathbf{V}^\circ$ = surface geostrophic velocity)

We are then dealing only with a fraction of total dissipation. This is consistent, however, with the fact that ' heating ' now includes turbulent heating due to the smaller-scale components of motion excluded from Eqs. (1) to (4).

To see, by order of magnitude, what the warming amounts to which is due to convergence of vertical flux of Θ, we first note that we have the identity :

$$\int \Theta \, w = -\int \frac{z}{Q}\frac{d(\Theta w \, Q)_0}{dz} \quad . \quad . \quad . \quad . \quad (9)$$

We next fit a linear dependence upon height to $\frac{1}{Q}\frac{d}{dz}(\Theta w\, Q)_0$:

$$\frac{1}{Q}\frac{d}{dz}(\Theta w\, Q)_0 = \gamma(z - \hat{z}) \quad . \quad . \quad . \quad (10a)$$

$$\left(\hat{z} \equiv \int_0^\infty zQ\, dz \Big/ \int_0^\infty Q\, dz \equiv d \approx 7{\cdot}10^3 \text{ m}\right)$$

By substitution into Eq. (9) we get:

$$\gamma = \frac{1}{d^2}\int \Theta w \quad . \quad . \quad . \quad . \quad (10b)$$

The numerical value of Eq. (10a) averaged vertically with respect to mass gives us next:

$$\overbrace{\left|\frac{1}{Q}\frac{d}{dz}(\Theta w\, Q)_0\right|} = \frac{\int \Theta w}{d^2}\,\overbrace{|z - \hat{z}|}. \quad . \quad . \quad . \quad (11)$$

Inserting here $\int \delta = 2{\cdot}10^{-6}\int \mathbf{V}^{\circ 2}$

and the typical winter value $\int \mathbf{V}^{\circ 2} = 100 \text{ m}^2 \text{ sec}^{-2}$

for the Northern Hemisphere, it is found that the large-scale motions in winter contribute to a vertical differential warming whose numerical value averaged with respect to mass is about 2°C. This is of fairly the same magnitude as the radiative cooling in the troposphere, showing that the large-scale motions cannot be neglected when the actual vertical temperature distributions are to be explained.

To see next to what extent the warming influences the vertical temperature distributions we must first adopt a heating law. Formally we may then write:

$$H = H(E_1, E_2, \ldots;\ (EI)_1, (EI)_2, \ldots),$$

where E_1 and E_2 denote parameters which exclusively are subject to an external control, and where $(EI)_1$ and $(EI)_2$ denote parameters which are, in part, controlled internally. An important parameter of the latter kind is ' temperature ' Θ. This is true for the warming by radiation, but also for the eddy warming and warming by release of latent heat.

We now firstly consider Θ as the only parameter of this kind and secondly H will furthermore be assumed to depend linearly upon Θ. Accordingly H_0 shall be written

$$H_0 = k(\Theta_e - \Theta_0);\quad k = \text{const.} > 0. \quad . \quad . \quad . \quad (12)$$

Here k and Θ_e are parameters controlled externally. Using Eqs. (7) and (10) we get, in the steady state:

$$k(\Theta_e - \Theta_0) = \frac{\int \Theta w}{d^2}(z - \hat{z})$$

or

$$\left.\begin{aligned} \frac{d\Theta_0}{dz} &= \frac{d\Theta_e}{dz} + \kappa \int \Theta w \\ \kappa &= 1/kd^2 \end{aligned}\right\} \quad . \quad . \quad . \quad (13)$$

This equation may be said to state the following result : In a number of hypothetical long-term steady states with constant values of the external parameters $d\Theta_e/dz$ and κ, vertical stability $d\Theta_0/dz$ will increase proportionally to $\int \Theta w$. In the actual transition process from the one such stationary state to another, caused by a gradual change of the proper external conditions, it must be the corresponding new values of Θw that set up the new vertical temperature gradients until equilibrium is reached with the warmings due to $k(\Theta_e - \Theta_0)$. The question of how much in the real atmosphere the vertical stability $d\Theta_0/dz$ is influenced by $\int \Theta w$ depends upon the proportionality factor κ which in turn is inversely proportional to the heating coefficient k. The latter, like Θ_e, is, however, difficult to determine with sufficient accuracy from the actual heating laws, as these are not properly known. For the same reason it is also difficult to determine by what amount the overall vertical stability would increase from summer to winter as a result of the higher winter-dissipation. It is interesting to note that in the Northern Hemisphere the overall vertical stability is observed to be significantly greater in winter than in summer. In Table 1 the conditions are shown for January-February 1949 and July-August 1949. Here the summer and winter values of the vertical mass average of the vertical temperature lapse-rate, averaged zonally, is given in different latitude zones north of approximately 20° together with the values averaged over all latitude zones.

TABLE 1. VERTICALLY AVERAGED TEMPERATURE LAPSE-RATES IN DIFFERENT LATITUDE ZONES

10 sin Φ (Φ = latitude)	2-3	3-4	4-5	5-6	6-7	7-8	8-9	9-10	2-10
$-10^3 \widehat{\frac{\partial T}{\partial z}}$ °/m									
July-August	4·0	4·1	4·2	4·3	4·6	4·9	5·2	5·7	4·6
January-February	5·0	5·2	5·4	5·7	6·0	6·6	6·8	7·2	6·0

The fact that the winter stability is significantly greater in *all* latitude zones considered, together with the fact that we have given zonal averages, reduces the possibility of explaining the difference as mainly being due to different values of the external parameters κ and $d\Theta_e/dz$. In fact it would probably not be easy to show that this could be explained by the different thermodynamic properties of the earth's surface in winter and summer. We shall now by hypothesis assume that the summer-winter difference in overall vertical stability is due mainly to the corresponding difference in overall dissipation.

Assuming that Eq. (13), which is strictly valid only for a closed system and for a long-term steady state, can also be applied with sufficient accuracy to the atmosphere north of approximately 20° and for a period of two months, we obtain by solving for $d\Theta_e/dz$ and κ and after taking vertical mass averages :

$$\left.\begin{aligned} \widehat{\frac{d\Theta_e}{dz}} &= \frac{\widehat{\frac{d\Theta_0}{dz}}_{\text{summer}} \cdot \int \Theta w_{\text{winter}} - \widehat{\frac{d\Theta_0}{dz}}_{\text{winter}} \cdot \int \Theta w_{\text{summer}}}{\int \Theta w_{\text{winter}} - \int \Theta w_{\text{summer}}} \\ \kappa &= \frac{\widehat{\frac{d\Theta_0}{dz}}_{\text{winter}} - \widehat{\frac{d\Theta_0}{dz}}_{\text{summer}}}{\int \Theta w_{\text{winter}} - \int \Theta w_{\text{summer}}} \end{aligned}\right\} \quad . \quad . \quad (14)$$

In 1949, $\int \mathbf{V}^{\circ 2}$, taken as an average north of 20°, was approximately 110 $m^2\,sec^{-2}$ in January-February, and 40 $m^2\,sec^{-2}$ in July-August. Using Eq. (6) and (8), and substituting in Eq. (14) for $\widehat{\frac{d\Theta_0}{dz}}_{\text{summer}}$ and $\widehat{\frac{d\Theta_0}{dz}}_{\text{winter}}$ the values corresponding to those of $\widehat{\frac{\partial T}{\partial z}}$ given at the end of Table 1, it is found:

$$\left.\begin{aligned} \widehat{\frac{d\Theta_e}{dz}} &\approx 1{\cdot}9 \times 10^{-6}\ m^{-1} \\ \kappa &\approx 4 \times 10^{-1}\ sec\ m^{-2} \\ k &\approx 5 \times 10^{-8}\ sec^{-1} \end{aligned}\right\} \quad . \quad . \quad . \quad (15)$$

We may here note that the corresponding value of $-10^3 \widehat{\frac{dT_e}{dz}}$ is 3·8 °/m, which is only slightly less than the summer values of $-10^3 \widehat{\frac{\partial T}{\partial z}}$ at lower latitudes. Averaged over the four southern zones, this amounts to 4·15 °/m. This conforms with the fact that dissipation is small at these latitudes in summer. If it is permissible to apply Eq. (13) to a region of this limited extension it follows directly that here $\widehat{\frac{d\Theta_0}{dz}} \gtrsim \widehat{\frac{d\theta_e}{dz}}$.

3. Mechanical energy equation, vertical stability, and the horizontal temperature field

From the thermodynamic-energy equation and the long-term constancy of the variance of Θ follows:

$$0 = \frac{d}{dt} \int \tfrac{1}{2} \Theta^2 = \int H\,\Theta \quad . \quad . \quad . \quad . \quad (16)$$

Writing

$$\Theta = \Theta_0 + \vartheta; \quad H = H_0 + h$$

we obtain $\int \Theta^2$ written as the sum of two partial variances:

$$\int \Theta^2 = \int {\Theta_0}^2 + \int \vartheta^2$$

Correspondingly:

$$\int H\,\Theta = \int H_0\,\Theta_0 + \int h\vartheta$$

From the long-term constancy of the partial variances $\int {\Theta_0}^2$ and $\int \vartheta^2$ we get further:

$$0 = \frac{d}{dt} \int \tfrac{1}{2} {\Theta_0}^2 = \int H_0\,\Theta_0 + \left[\int \vartheta^2 \rightarrow \int {\Theta_0}^2\right] \quad . \quad . \quad (17a)$$

$$0 = \frac{d}{dt} \int \tfrac{1}{2} \vartheta^2 = \int h\vartheta - \left[\int \vartheta^2 \rightarrow \int {\Theta_0}^2\right] \quad . \quad . \quad . \quad (17b)$$

Here

$$\left[\int \vartheta \rightarrow \int {\Theta_0}^2\right] = \int \frac{d\Theta_0}{dz}\,\vartheta w \quad . \quad . \quad . \quad (17c)$$

This additional term, which does not appear in Eq. (16), expresses simply the fact that as long as partial variances are considered, the one kind of variance may, owing to the motion of air, be a source or sink for the other. Defining an overall vertical stability S by means of :

$$\int \frac{d\Theta_0}{dz}\,\vartheta w = S \int \vartheta w \quad . \quad . \quad . \quad . \quad (18)$$

Eq. (17) can now be written :

$$\int H_0\,\Theta_0 = -\,S \int \vartheta w \quad . \quad . \quad . \quad . \quad (19a)$$

$$\int h\vartheta = S \int \vartheta w \quad . \quad . \quad . \quad . \quad . \quad (19b)$$

Adopting for h a law analogous to that for H_0 in Eq. (12), we have, in addition, the heating laws :

$$H_0 = k\,(\Theta_e - \Theta_0); \quad k = \text{const.} > 0 \text{ (as in Eq. (12))}$$

and

$$h = r\,(\vartheta_e - \vartheta); \quad r = \text{const.} > 0 \quad . \quad . \quad . \quad . \quad (20)$$

Correspondingly :

$$\int H_0\,\Theta_0 = k \int (\Theta_e\,\Theta_0 - \Theta_0^2) \quad . \quad . \quad . \quad (21a)$$

$$\int h\vartheta = r \int (\vartheta_e\,\vartheta - \vartheta^2) \quad . \quad . \quad . \quad . \quad (21b)$$

Two distinctly different cases can now be studied :

(I) $S > 0$.

In this case we obtain :

(a) The vertical variance of 'temperature,' $\int \Theta_0^2$ increases kinematically at the expense of the horizontal variance $\int \vartheta^2$.

(b) The loss of horizontal variance is compensated by an externally conditioned build-up due to differential heating in the horizontal $\int h\vartheta > 0$, which is possible only if $\int \vartheta_e\,\vartheta > \int \vartheta^2$.

(c) The increase in vertical variance of temperature is compensated owing to differential heating in the vertical $\left(\int H_0\,\Theta_0 < 0\right)$.

(II) $S < 0$.

In this case the same conclusions will apply by using the words horizontal for vertical and vice versa.

In the following we shall confine ourselves to the vertically stable case. By performing the averaging involved in Eq. (18) on Eq. (13), we obtain :

$$S = S_e + \kappa \int \Theta w \quad . \quad . \quad . \quad . \quad (13)'$$

We shall now derive some results which have some bearing on more complete results to be obtained later when the influence of the earth's rotation is taken into account.

By substitution from Eq. (13)′ into (19b) we obtain first :

$$\kappa\left(\int \Theta w\right)^2 + S_e \int \Theta w - \int h\vartheta = 0$$

Since $\int \Theta w = \frac{1}{g}\int \delta > 0$, this equation shows :

$$\int \Theta w \sim \int h\vartheta \quad \text{for small values of } \int h\vartheta \qquad . \qquad . \qquad (23a)$$

$$\int \Theta w \sim \sqrt{\int h\vartheta} \quad \text{for large values of } \int h\vartheta \qquad . \qquad . \qquad (23b)$$

Secondly, since we can write $\int h\vartheta = r\,\sigma_{\vartheta_e,\vartheta}\left(\int \vartheta_e^2 \cdot \int \vartheta^2\right)^{\frac{1}{2}} - r\int \vartheta^2$, where $\sigma_{\vartheta_e,\vartheta}$ is the correlation coefficient between ϑ_e and ϑ, we get :

$$\int h\vartheta = \max = \tfrac{1}{4}\int \vartheta_e^2 \text{ when } \int \vartheta^2 = \frac{\sigma^2_{\vartheta_e,\vartheta}}{4}\int \vartheta_e^2 \text{ and } \sigma_{\vartheta_e,\vartheta} = 1 \qquad . \qquad (24)$$

Since $\int \Theta w_{\max}$ is obtained when $\int h\vartheta = \max$, we obtain :

$$\int \Theta w_{\max} \sim \int \vartheta_e^2 \quad \text{for small values of } \int \vartheta_e^2 \qquad . \qquad . \qquad (25a)$$

$$\int \Theta w_{\max} \sim \sqrt{\int \vartheta_e^2} \quad \text{for large values of } \int \vartheta_e^2 \qquad . \qquad . \qquad (25b)$$

Finally, it may also be mentioned that in order to have $\int h\vartheta > 0$, we must have :

$$\int \vartheta^2 < \int \vartheta_e^2 \qquad . \qquad . \qquad . \qquad . \qquad . \qquad (26)$$

4. The influence of rotation on the condition for creation of kinetic energy

In the atmosphere the horizontal wind velocity $\mathbf{V}_h$ satisfies approximately the thermal wind equation :

$$\frac{\partial \mathbf{V}_h}{\partial z} = -\frac{g}{f}\nabla_h \vartheta \times \mathbf{k} \qquad . \qquad . \qquad . \qquad . \qquad (27)$$

This equation expresses *firstly* the fact that in a rotating atmosphere, horizontal temperature differences can exist in a state of equilibrium between Coriolis and gravity forces. *Secondly*, the fact that the actual horizontal velocities satisfy approximately the thermal wind equation, is a result of a dynamical stability. The criterion for this stability is expressed by the Richardson number :

$$g\frac{d\Theta}{dz}\Big/\left(\frac{d\mathbf{V}_h}{dz}\right)^2 > 1 \qquad . \qquad . \qquad . \qquad . \qquad (28)$$

Because of this stability it is impossible to obtain a free production of kinetic energy by the most simple vertical overturning of the isentropic surfaces. Instead, a simultaneous distortion of the temperature field by horizontal motions becomes essentially important. It is now well known that for motions satisfying approximately the thermal wind equation and the condition for dynamic stability mentioned above, vertical velocity is not an independent variable, but is instead determined when the non-divergent part of horizontal velocity (approximately the geostrophic velocity) is given together with heating and friction.

We now assume a two-parametric representation of $\mathbf{V}_h$ in the vertical :

$$\mathbf{V}_h = \widehat{\mathbf{V}}_h - \frac{g\,\nabla_h \vartheta \times \mathbf{k}}{f} \cdot (F(z) - \widehat{F(z)}); \quad \vartheta = \widehat{\vartheta}. \qquad (29a)$$

Friction is neglected above the friction layer. (29b)

If we carry out the mentioned elimination of vertical velocity in the energy equation (6) we obtain :

$$-\frac{g^2 D^2}{f_c^2} \int \widehat{\psi}\, J(\vartheta, \nabla_h^2 \vartheta) + \frac{gl\nu}{f_c} \int \vartheta\, \nabla_h \times \mathbf{V}^\circ \cdot \mathbf{k} = \nu \int \mathbf{V}^{\circ 2}. \qquad (30)$$

Here $D^2 = \overline{(F(z) - \widehat{F(z)})^2}$.

$l = \widehat{F(z)} - F(z = 0)$

f_c = an average value of the Coriolis parameter.

$-\nabla_h \widehat{\psi} \times \mathbf{k} = \mathbf{V}_h$

J = horizontal Jacobian.

We note that

$$-\int \widehat{\psi}\, J(\vartheta, \nabla_h^2 \vartheta) = -\int \nabla_h^2 \vartheta\, J(\widehat{\psi}, \vartheta)$$

Here $-J(\widehat{\psi}, \vartheta) = -\widehat{\mathbf{V}} \cdot \nabla_h \vartheta$

and thus equals the change in ϑ caused if advection is acting alone. Symbolizing this change by $\left(\frac{\partial \vartheta}{\partial t}\right)_{\text{adv}}$, we may write :

$$-\int \nabla_h^2 \vartheta\, J(\widehat{\psi}, \vartheta) = \int (\nabla_h^2 \vartheta) \left(\frac{\partial \vartheta}{\partial t}\right)_{\text{adv}} = \frac{d}{dt}_{\text{adv}} \int \tfrac{1}{2} (\nabla_h \vartheta)^2.$$

Eq. (30) may then also be written

$$\frac{g^2 D^2}{f_c^2} \frac{d}{dt}_{\text{adv}} \int \tfrac{1}{2} (\nabla_h \vartheta)^2 + \frac{gl\nu}{f_c} \int \vartheta\, \nabla_h \times \mathbf{V}^\circ \cdot \mathbf{k} = \nu \int \mathbf{V}^{\circ 2} \qquad (30),$$

The second term in the above equation depends upon a correlation between temperature and the vertical velocities caused by the frictional inflow and outflow in areas with surface cylonic and anticyclonic velocity, respectively. As will be shown later we have reason to believe that this term is of minor importance as compared to the first term. The latter depends upon the change in the integrated square of the horizontal temperature gradients. Noting that :

$$\frac{d}{dt}_{\text{adv}} \int \tfrac{1}{2} \vartheta^2 = -\int \vartheta\, J(\widehat{\psi}, \vartheta) = 0, \qquad (31)$$

it is understood that $\int (\nabla_h \vartheta)^2$ cannot increase by advection unless horizontal temperature variance is moved (advectively), on an average, from large horizontal scales to smaller ones. In the preceding section we were naturally led to consider total ' temperature ' variance $\int \Theta^2$ as consisting of a horizontal and vertical part. In a vertically stable atmosphere it was found, as a general feature, that vertical motions, excluding other effects, would lead to an increase in vertical variance $\int \Theta_0^2$ if the dissipative loss of kinetic energy is balanced by a corresponding production. In the present case, when we are considering the more restrictive types of motion which satisfy the thermal wind equation (27), we observe correspondingly the appearance of additional and more specific conditions for

production of kinetic energy. These lead us to consider horizontal variance $\int \vartheta^2$ as consisting of more parts characterized by different horizontal scales. For a spectral representation of ϑ we suppose now that ϑ is developed in a series of functions ϑ_q satisfying

$$\nabla_h^2 \vartheta_q = -A_q \vartheta_q; \quad A_q = \frac{q(q+1)}{R^2}; \quad q = 1, 2, \ldots \quad . \quad . \quad (32)$$

(R = radius of the earth).

Eq. (31) can now be written :

$$\sum_q \frac{d}{dt}_{\text{adv}} \int \vartheta_q^2 = 0, \quad . \quad . \quad . \quad . \quad (33)$$

while

$$\frac{d}{dt}_{\text{adv}} \int (\nabla_h \vartheta)^2 = \sum_q A_q \frac{d}{dt}_{\text{adv}} \int \vartheta_q^2 \quad . \quad . \quad . \quad (34)$$

Suppose further that r denotes an arbitrary one of the q's for which $\frac{d}{dt}_{\text{adv}} \int \vartheta_r^2 < 0$, whilst r' denotes the remainder. We can then write the above equations as :

$$\sum_r \frac{d}{dt}_{\text{adv}} \int \vartheta_r^2 + \sum_{r'} \frac{d}{dt}_{\text{adv}} \int \vartheta_{r'}^2 = 0$$

$$\frac{d}{dt}_{\text{adv}} \int (\nabla_h \vartheta)^2 = \sum_r A_r \frac{d}{dt}_{\text{adv}} \int \vartheta_r^2 + \sum_{r'} A_{r'} \frac{d}{dt}_{\text{adv}} \int \vartheta_{r'}^2.$$

We can now define two average scales characterized by the scale parameters a and a' given by :

$$\left.\begin{aligned} a \sum_r \frac{d}{dt}_{\text{adv}} \int \vartheta_r^2 &= \sum_r A_r \frac{d}{dt}_{\text{adv}} \int \vartheta_r^2 \\ a' \sum_{r'} \frac{d}{dt}_{\text{adv}} \int \vartheta_{r'}^2 &= \sum_{r'} A_{r'} \frac{d}{dt}_{\text{adv}} \int \vartheta_{r'}^2 \end{aligned}\right\} \quad . \quad . \quad (35)$$

Accordingly we get :

$$\frac{d}{dt}_{\text{adv}} \int (\nabla_h \vartheta)^2 = (a - a') \sum_r \frac{d}{dt}_{\text{adv}} \int \vartheta_r^2 \gtrless 0 \quad . \quad . \quad (36)$$

when $a' \gtrless 0$.

We anticipate now that the large-scale advective loss of horizontal variance cannot, to any substantial degree, be replaced by a corresponding loss of vertical variance, caused by large-scale vertical motions. Considering further that the horizontal differential heating which maintains the large-scale horizontal temperature variance, is basically zonal, it is natural to assume that we have approximately :

$$\sum_r \vartheta_r = \overline{\vartheta}$$

($\overline{\vartheta}$ = zonal average)

Then

$$\sum_{r'} \vartheta_{r'} = \vartheta' \text{ where } \vartheta' = \vartheta - \overline{\vartheta} \text{ is the corresponding eddy field.}$$

We now obtain :

$$\sum_r \frac{d}{dt}_{\text{adv}} \int \tfrac{1}{2} \vartheta_r^2 = \frac{d}{dt}_{\text{adv}} \int \tfrac{1}{2} \overline{\vartheta}^2 = -\int \overline{\vartheta} \frac{\partial \widehat{v'} \vartheta}{\partial y} = \int \frac{d\overline{\vartheta}}{dy} v'^\circ \vartheta'$$

(The replacement of $\widehat{v'}$ by v'° may be done because of Eq. (29a).

By substitution into Eq. (30)′ this can now be written :

$$\frac{g^2 D^2}{f_c^2}(a' - a) \int \frac{d\overline{\vartheta}}{dy} v'^\circ \vartheta' + \frac{gl\nu}{f_c} \int \vartheta \nabla_h \times \mathbf{V}^\circ \mathbf{k} = \nu \int \mathbf{V}^{\circ 2} \quad . \quad . \quad (30)''$$

5. Derivations of the lacking equations

In the *five* equations (6), (13), (19b), (21b) and (30)'', we have the *seven* variables w, Θ_0, $\bar{\vartheta}$, ϑ', h, v'° and $\mathbf{V}^{\circ 2}$. The sufficient number of equations are obtained if Eqs. (6), (19b), (21b) and (30) are replaced by the corresponding two sets of equations valid separately for the zonal mean, and the eddy motion. First Eq. (6), which is $\int g\vartheta\, w = \nu \int \mathbf{V}^{\circ 2}$ splits into two equations as follows :

$$\int g\bar{\vartheta}\, \bar{w} + [\mathbf{V}'^2 \to \bar{\mathbf{V}}^2] = \nu \int \bar{\mathbf{V}}^{\circ 2} \quad . \quad . \quad . \quad (37)$$

$$\int g\vartheta' w' - [\mathbf{V}'^2 \to \bar{\mathbf{V}}^2] = \nu \int \mathbf{V}'^{\circ 2} \quad . \quad . \quad . \quad (38)$$

$[\mathbf{V}'^2 \to \mathbf{V}^2]$ symbolizes the Reynolds term and expresses what the zonal mean motion gains of kinetic energy from the corresponding eddy motion.

Next, Eq. (19b) which is $\int h\vartheta = S \int \Theta w$ splits into two equations as follows :

$$\int \left(\bar{h} - \frac{\partial \vartheta' v'^\circ}{\partial y}\right) \bar{\vartheta} = S \int \bar{\vartheta}\, \bar{w} \quad . \quad . \quad . \quad (39)$$

$$\int \left(h' + \frac{\partial \vartheta' v'^\circ}{\partial y}\right) \vartheta' = S \int \vartheta' w' \quad . \quad . \quad . \quad (40)$$

In these $-\frac{\partial \vartheta' v'^\circ}{\partial y}$ is the warming due to convergence of geostrophic meridional eddy flux of ϑ.

Then Eq. (21b), which is $\int h\vartheta = r \int (\vartheta_e \vartheta - \vartheta^2)$ splits into :

$$\int \bar{h}\, \bar{\vartheta} = r \int (\vartheta_e \bar{\vartheta} - \bar{\vartheta}^2) \quad . \quad . \quad . \quad . \quad (41)$$

$$\int h' \vartheta' = r \int \vartheta_e' \vartheta' - \vartheta'^2) \quad . \quad . \quad . \quad . \quad (42)$$

and finally Eq. 30, which is $-\frac{g^2 D^2}{f_c^2} \int \hat{\psi} J(\vartheta, \nabla_h^2 \vartheta) + \frac{gl\nu}{f_c} \int \vartheta\, \nabla_h \times \mathbf{V}^\circ \cdot \mathbf{k} = \nu \int \mathbf{V}^{\circ 2}$ splits into :

$$\frac{g^2 D^2}{f_c^2} \int \nabla_h^2 \vartheta\, J(\bar{\hat{\psi}}, \vartheta) + \frac{gl\nu}{f_c} \int \bar{\vartheta}\, \nabla_h \times \bar{\mathbf{V}}^\circ \cdot \mathbf{k} + [\hat{\mathbf{V}}'^2 \to \bar{\hat{\mathbf{V}}}^2] = \nu \int \bar{\mathbf{V}}^{\circ 2} \,. \quad (43)$$

$$\frac{g^2 D^2}{f_c^2} \int \nabla_h^2 \vartheta\, J(\hat{\psi}', \vartheta) + \frac{gl\nu}{f_c} \int \vartheta' \nabla_h \times \mathbf{V}'^\circ \cdot \mathbf{k} - [\hat{\mathbf{V}}'^2 \to \bar{\hat{\mathbf{V}}}^2] = \nu \int \mathbf{V}'^{\circ 2} \,. \quad (44)$$

We now make three simplifications as follows :

Simplification 1.

$$\frac{g^2 D^2}{f_c^2} \int \nabla_h^2 \vartheta\, J(\bar{\hat{\psi}}, \vartheta),\ [\mathbf{V}'^2 \to \bar{\mathbf{V}}^2],\ \text{and}\ [\hat{\mathbf{V}}'^2 \to \bar{\hat{\mathbf{V}}}^2]\ \text{are negligible} \quad . \quad (45a)$$

No theoretical explanation is attempted for their justification; instead, reference is merely made to the observable atmosphere.

From (45a) it follows that Eq. (43) simplifies to :

$$\frac{gl\nu}{f_c}\int \overline{\vartheta}\,\nabla_h \times \overline{\mathbf{V}}^\circ \cdot \mathbf{k} = \nu \int \overline{\mathbf{V}}^{\circ 2} \quad . \quad . \quad . \quad (43)'$$

There are two solutions of this equation for $\overline{\mathbf{V}}^\circ$:

$$\overline{\mathbf{V}}^\circ = 0 \quad \text{and} \quad \overline{\mathbf{V}}^\circ \neq 0. \quad . \quad . \quad . \quad . \quad (43)''$$

Here we choose the first expression in order to obtain results which more closely resemble the observed atmosphere.

Using (43)'' and (45a) in Eq. (37) we obtain :

$$\int \overline{\vartheta}\,\overline{w} = 0 \quad . \quad . \quad . \quad . \quad . \quad (37)'$$

By substitution of this, and from Eq. (41) into Eq. (39), we get :

$$r\int (\vartheta_e\,\overline{\vartheta} - \overline{\vartheta}^2) + \int \frac{d\overline{\vartheta}}{dy}\,\vartheta'\,v'^\circ = 0 \quad . \quad . \quad . \quad (39)'$$

Using (45a) in Eq. (38) we obtain :

$$\int g\vartheta'\,w' = \nu \int \mathbf{V}'^{\circ 2} \quad . \quad . \quad . \quad . \quad (38)'$$

Substituting Eq. (38)', and from Eq. (42), into Eq. (40) we arrive at :

$$r\int (\vartheta_e'\,\vartheta' - \vartheta'^2) - \int \frac{d\overline{\vartheta}}{dy}\,v'^\circ\,\vartheta' = \frac{S\nu}{g}\int \mathbf{V}'^{\circ 2} \quad . \quad . \quad (40)'$$

Simplification 2.

$$\vartheta_e' = 0 \quad . \quad . \quad . \quad . \quad . \quad (45b)$$

This is made because the external horizontal differential heating is basically a zonal field. Hence Eq. (40)' simplifies to :

$$-r\int \vartheta'^2 - \int \frac{d\overline{\vartheta}}{dy}\,v'^\circ\,\vartheta' = \frac{S\nu}{g}\int \mathbf{V}'^{\circ 2} \quad . \quad . \quad . \quad (40)''$$

Further, the first of the simplifications in (45a) implies that the first term in Eq. (30)'' is used nearly fully for the eddy motion. Using also the last of the simplifications in (45a), Eq. (44) can therefore now be written :

$$-\frac{g^2D^2}{f_c^2}(a' - a)\int \frac{d\overline{\vartheta}}{dy}\,v'^\circ\,\vartheta' + \frac{gl\nu}{f_c}\int \vartheta'\,\nabla_h \times \mathbf{V}'^\circ \cdot \mathbf{k} = \nu \int \mathbf{V}'^{\circ 2} \quad . \quad (44)'$$

Simplification 3.

$$\frac{gl\nu}{f_c}\int \vartheta'\,\nabla_h \times \mathbf{V}'^\circ \cdot \mathbf{k} \text{ is negligible} \quad . \quad . \quad . \quad (45c)$$

Again, for justification, we may confine ourselves to reference to the atmosphere where it is observed that $\frac{gl\nu}{f_c}\int \vartheta'\,\nabla_h \times \mathbf{V}'^\circ \cdot \mathbf{k} = (10^{-1} - 10^{-2})\,\nu \int \mathbf{V}'^{\circ 2}$. In addition it is also understood that the two l.h.s.-terms in Eq. (44)' tend to counterbalance each other mutually since $\int v'^\circ\,\vartheta'$ is large when $\int \vartheta'\,\nabla_h \times \mathbf{V}'^\circ \cdot \mathbf{k}$ is small, and vice versa. We have therefore made the most realistic choice between two possibilities.

With (45c), Eq. (44)' becomes :

$$-\frac{g^2D^2}{f_c^2}(a' - a)\int \frac{d\overline{\vartheta}}{dy}\,v'^\circ\,\vartheta' = \nu \int \mathbf{V}'^{\circ 2} \quad . \quad . \quad . \quad (44)''$$

Eqs. (39)′, (40)″, and (44)″ (as in the *Simplifications*), together with Eq. (13)′ for S, which can now be written as

$$S = S_e + \frac{\kappa\nu}{g}\int \mathbf{V}'^{\circ 2} \quad . \quad . \quad . \quad . \quad . \quad (13)''$$

are dealt with as follows. Dependent variables are considered $\int \mathbf{V}'^{\circ 2}$, $\int \vartheta'^2$, $\int \overline{\vartheta}'^2$ and S. Since the equations contain a function $\int \frac{d\overline{\vartheta}}{dy} v'^{\circ}\vartheta'$, we must express this in terms of the dependent variables. Let σ denote the triple coefficient

$$\sigma = \frac{\int \frac{d\overline{\vartheta}}{dy} v'^{\circ}\vartheta'}{\left(\int \left(\frac{d\overline{\vartheta}}{dy}\right)^2 \int v'^{\circ 2} \int \vartheta'^2\right)^{\frac{1}{2}}} \quad . \quad . \quad . \quad (46)$$

We have

$$|\sigma| \leqslant 1 \quad . \quad . \quad . \quad . \quad . \quad . \quad (47)$$

The actual value of σ depends upon the geometry of the fields $\frac{d\overline{\vartheta}}{dy}$, v'°, and ϑ', or what could be called the general ' kinematics.' This again depends upon what is dynamically possible. The ratio b given by

$$b = \int v'^{\circ 2} \Big/ \int \mathbf{V}'^{\circ 2} \quad . \quad . \quad . \quad . \quad . \quad (48)$$

is another parameter whose value depends upon the kinematics. Obviously

$$0 < b < 1$$

It is clear that b is smaller the more extended the eddy velocity field is in zonal direction relative to meridional direction. We define σ_2 by

$$\sigma_2 = \sigma b. \quad . \quad . \quad . \quad . \quad . \quad . \quad (49)$$

Further σ_1 is the correlation coefficient between ϑ_e and $\overline{\vartheta}$:

$$\sigma_1 = \frac{\int \vartheta_e \overline{\vartheta}}{\left(\int \vartheta_e^{\,2} \int \overline{\vartheta}^2\right)^{\frac{1}{2}}} \quad . \quad . \quad . \quad . \quad . \quad (50)$$

and a_2 is given by

$$\int (\nabla_h \overline{\vartheta})^2 = a_2 \int \overline{\vartheta}^2 \quad . \quad . \quad . \quad . \quad . \quad (51)$$

We therefore have *two* scale characteristics for the zonally averaged temperature field $\overline{\vartheta}$: one is the quantity, a, defined earlier in Eq. (35), and the other is a_2 defined above. Clearly, if $\overline{\vartheta}$ is represented by a single spherical harmonics, then a and a_2 become equal. In the winter, spring, and autumn seasons $\overline{\vartheta} \approx \overline{\vartheta}_2$ where $\overline{\vartheta}_2$ is a second zonal harmonics. Except in summer, we may therefore write for the atmosphere that

$$a \approx a_2 = \frac{2 \times 3}{R^2} \quad . \quad . \quad . \quad . \quad . \quad (52)$$

In summer, however, a higher value for a_2 should be taken, because most of the variance $\int \overline{\vartheta}^2$ is then concentrated to a more restricted region.

By substitutions into $\int \frac{d\bar{\vartheta}}{dy} v'^{\circ} \vartheta'$ in Eqs. (39)', (40)' and (44)'', we obtain after elimination :

$$\int \mathbf{V}'^{\circ 2} = \frac{g\gamma}{\nu} l_q \left[\left(\int \sigma_1^2 \vartheta_e^2 \right)^{\frac{1}{2}} \left(\frac{\gamma\nu}{g a_2 \sigma_2^2} \right)^{\frac{1}{2}} \left(\frac{1}{l_q(1 - S l_q)} \right)^{\frac{1}{2}} - \frac{\gamma\nu}{g a_2 \sigma_2^2} \frac{1}{l_q(1 - S l_q)} \right] \quad . \quad (53)$$

$$\left(l_q \equiv \frac{gD^2}{f_c^2} (a' - a) \right)$$

$$\int \bar{\vartheta}^2 = \frac{\gamma\nu}{g a_2 \sigma_2^2} \cdot \frac{1}{l_q(1 - S l_q)} \quad . \quad . \quad . \quad . \quad (54)$$

$$\int \vartheta'^2 = \frac{1}{l_q^2} \frac{\nu}{g\gamma} \cdot \frac{\gamma\nu}{g \sigma_2^2 a_2} \cdot \frac{\int \mathbf{V}'^{\circ 2}}{\int \bar{\vartheta}^2} \quad . \quad . \quad . \quad . \quad (55)$$

To this comes the earlier equation for overall vertical stability

$$S = S_e + \frac{\kappa\nu}{g} \int \mathbf{V}'^{\circ 2} \quad . \quad . \quad . \quad . \quad (13)''$$

6. Theoretical discussion

As a general remark it appears from the above equations that the solution depends on the one hand on ' external ' parameters as ϑ_e and S_e, and on the heating and friction coefficients r, k, and ν. On the other hand, however, it also depends upon the kinematics, as for instance on the horizontal scale parameter, a', characterizing an average scale of the eddy temperature field ϑ'. The latter fact is the same as saying that for given external parameters most likely a whole system of different steady solutions is possible. This in itself is a quite important result. In fact it may contribute to explaining why the atmosphere can have a number of quasipermanent dynamical regimes for seemingly constant external conditions, for, although the different solutions most certainly are not equally likely, for reasons which cannot be found by merely studying the stationary solutions, there is no *a priori* reason why the atmosphere should entirely prefer a single one of these solutions.*

From Eq. (53) follows :

$$\int \mathbf{V}'^{\circ 2} > 0 \text{ only when } \sigma_1^2 \int \vartheta_e^2 > \frac{\gamma\nu}{g a_2 \sigma_2^2 l_q (1 - S l_q)} \quad . \quad . \quad (56)$$

Since

$$[l_q (1 - S l_q)]_{\max} = \frac{1}{4 S_e},$$

we obtain

$$\left(\int \vartheta_e^2 \right)_{\min} = \frac{4\gamma\nu S_e}{g a_2 \sigma_2^2} > \frac{4\gamma\nu S_e}{g a_2} \quad . \quad . \quad . \quad (57)$$

Accordingly, if the horizontal temperature field, ϑ_e, which is set up by external heating sources when there is heating balance, has a variance less than the one given by Eq. (57), the motion will be a purely zonal one.

* This view is supported to some extent by the experiments in rotating tanks.

A second result of importance follows from Eq. (56) using also the expression for l_q :

$$\left.\begin{aligned} a' &> a + \frac{f_c^2}{gD^2 S_e}\left(\tfrac{1}{2} - \tfrac{1}{2}\sqrt{1 - \frac{\left(\int \vartheta_e^2\right)_{\min}}{\int \vartheta_e^2}}\right) \\ a' &< a + \frac{f_c^2}{gD^2 S_e}\left(\tfrac{1}{2} + \tfrac{1}{2}\sqrt{1 - \frac{\left(\int \vartheta_e^2\right)_{\min}}{\int \vartheta_e^2}}\right) \end{aligned}\right\} \quad . \quad . \quad (58)$$

This shows that there is an upper and lower limit to a' outside which no eddy solutions are possible. At the limits themselves $\int \mathbf{V}'^{o2}$ becomes zero. In Fig. 1 a diagram is given showing these limits as a function of $\left(\int \vartheta_e^2\right) \Big/ \left(\int \vartheta_e^2\right)_{\min}$.

To understand this in terms of characteristic horizontal wavelengths, L', one should recall that $a' \sim 1/L'^2$.

It follows now further that for any given value satisfying $\int \vartheta_e^2 > \left(\int \vartheta_e^2\right)_{\min}$, $\int \mathbf{V}'^{o2}$ will obtain a maximum value for an a' between the lower and upper limits given above. What value of a' this is, depends upon σ_2. Since this quantity most likely also depends upon a', the exact value of a' for which $\int \mathbf{V}'^{o2}$ becomes a maximum will be difficult to determine in a straightforward way. However, we can find qualitatively how this value depends upon the magnitude of $\int \vartheta_e^2$ by the following method.

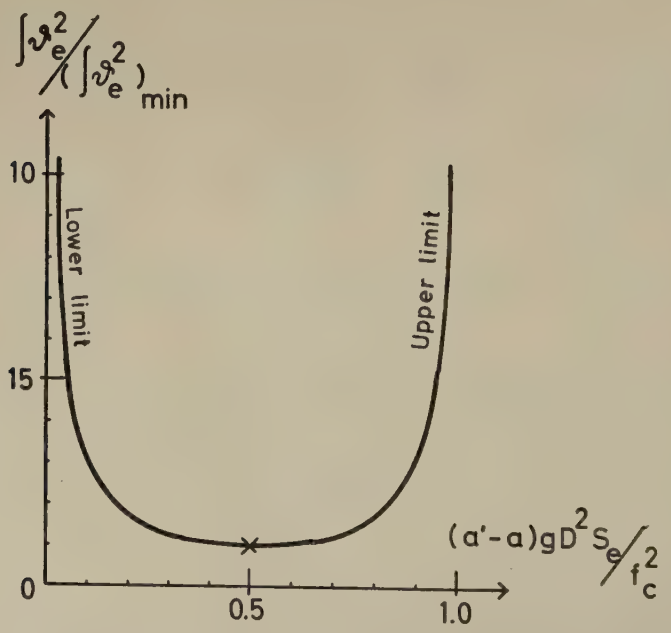

Figure 1. This figure illustrates the limits to the horizontal scales of the eddy motion as function of vertical scale (D) and the external parameters.

At first it is noted that we must have

$$1 - Sl_q > 0 \quad . \quad . \quad . \quad . \quad . \quad (59)$$

Inserting here the values for S given in (13)'' and the expression for l_q in Eq. (53), we obtain :

$$\int \mathbf{V}'^{o2} < \frac{gS_e}{\kappa\nu}\left(\frac{f_c^2}{S_e gD^2}\Big/(a'-a) - 1\right) \quad . \quad . \quad . \quad (60)$$

However large $\int \vartheta_e^2$ is, $\int \mathbf{V}'^{o2}$ is therefore bounded for any particular value of a'. This is illustrated in Fig. 2, where $\left(\int \mathbf{V}'^{o2}\right)_M$ denotes the above upper bound of $\int \mathbf{V}'^{o2}$.

It is now clear from an inspection of Eq. (53) that for any particular value of a', $\int \mathbf{V}'^{o2}$ will differ from the upper bound by an amount which can be made arbitrarily small if $\int \vartheta_e^2$ is taken sufficiently large. Further, as the upper bound $\left(\int \mathbf{V}'^{o2}\right)_M$ tends to infinity when a' tends to a, and as $\int \mathbf{V}'^{o2}$ is bounded for any particular value of $\int \vartheta_e^2$, it follows that $\int \mathbf{V}'^{o2}$ (for a particular value of $\int \vartheta_e^2$), is assuming its maximum value at horizontal scales ultimately increasing with $\int \vartheta_e^2$ to an upper limit L_U given by $L_U^2 \sim \frac{1}{a}$ This result is illustrated in Fig. 2 by idealized curves for $\int \mathbf{V}'^{o2}$ drawn for increasing values of $n \equiv \int \vartheta_e^2 \Big/ \left(\int \vartheta_e^2\right)_{\min}$.

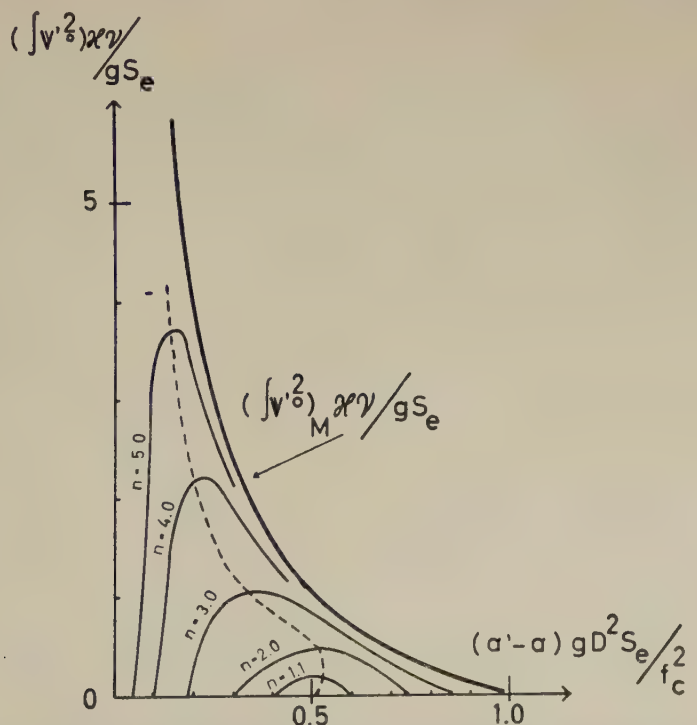

Figure 2. (a) A thin curve illustrates surface eddy kinetic energy in stationary solutions corresponding to different horizontal scales, a'; (b) System of thin lines correspond to different intensities of differential heating in the horizontal; (c) Heavy line gives the upper bound to surface eddy kinetic energy.

Next to $\int \mathbf{V}'^{o2}$, we should also consider the solutions for S, $\int \bar{\vartheta}^2$ and $\int \vartheta'^2$. As regards vertical stability this is proportional to $\int \mathbf{V}'^{o2}$. The variance $\int \bar{\vartheta}^2$ has, for any given value of $\int \vartheta_e^2$, a minimum for an intermediate value of a', and increases to $\sigma_1^2 \int \vartheta_e^2$ when a' goes to the critical limits on both sides. The eddy variance $\int \vartheta'^2$ on the other hand, has a maximum for an intermediate value of a', and decreases to zero when a' approaches the critical limits. It should be remarked that these extreme values are not obtained for the value of a' for which $\int \mathbf{V}'^{o2}$ becomes a maximum. The amplitudes of the temperature fields will therefore be more sensitive than surface kinetic energy against changes in the horizontal scale near the one where $\int \mathbf{V}'^{o2}$ obtains its maximum.

In particular we may also find how the overall Richardson number

$$R_i = \frac{gS}{\left(\frac{d\bar{\mathbf{V}}}{dz}\right)^2} = \frac{S f_c^2}{g a_2 \bar{\vartheta}^2}$$

depends upon the external parameters and on the horizontal scale characteristics. We shall then find the conditions when the dynamical stability criterion $R_i > 1$ is no longer fulfilled. In this case other types of solutions than those considered in this lecture will prevail. It is seen that R_i will *decrease* with increasing values of $\int \vartheta_e^2$ and ultimately become less than the critical value $R = 1$. This will first happen for the solutions having horizontal scales close to the critical limits.

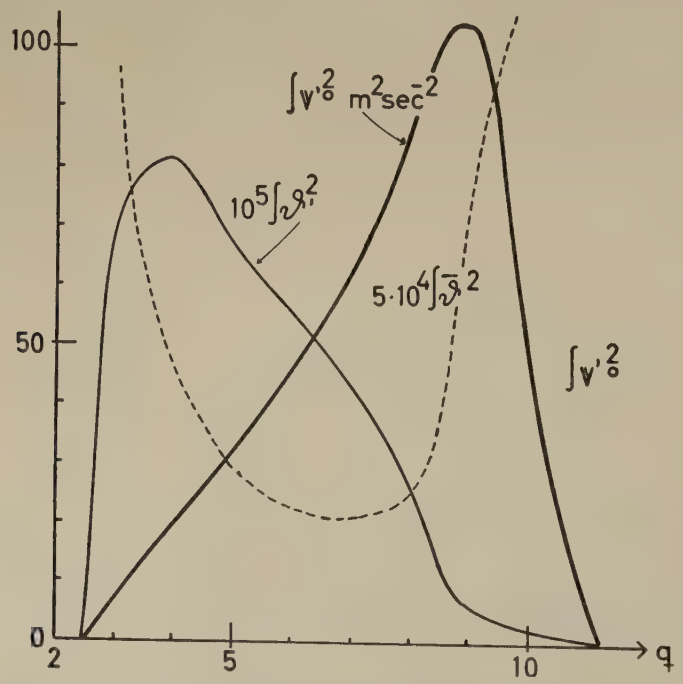

Figure 3. Surface eddy kinetic energy (heavy line), eddy 'temperature' variance (thin line) and zonal 'temperature' variance (broken line) in different stationary solutions corresponding to different horizontal scales (q). The curves are constructed on the bases of atmospheric winter conditions.

7. Comments on the possible application and further development of theory

The qualitative aspects of the results derived above should be studied in connexion with the experiments with rotating tanks and the observed behaviour of the atmosphere. Quantitative results should be derived for the atmosphere by assuming reasonable values for the parameters k, r, S_e, ϑ_e and ν as obtained from the proper heating and friction laws. Alternatively, some of these parameters could be determined by using the theoretical results diagnostically, as has been done, for instance, for S_e and k in Section 2. Using both these procedures in combination we have arrived at an adoption of the following values :

$$\left.\begin{aligned} k &= 5 \times 10^{-8}\ \text{sec}^{-1} \\ r &= 8 \times 10^{-7}\ \text{sec}^{-1} \\ \nu &= 2 \times 10^{-6}\ \text{sec}^{-1} \\ S_e &= 1{\cdot}9 \times 10^{-6}\ \text{m}^{-1} \end{aligned}\right\} \quad \text{all-year values}$$

$$\int \vartheta_e^{\,2} = 36 \times 10^{-4} \qquad \text{winter value.}$$

In Fig. 3 we have for the sake of illustration drawn curves showing the corresponding solutions for $\int \mathbf{V}'^{\circ 2}$, $\int \overline{\vartheta}^2$ and $\int \vartheta'^2$ as functions of the typical horizontal scale of eddy temperature. It has been assumed that

$$\text{(a)} \quad \sigma_2^{\,2} = \text{const} = 0{\cdot}25$$

$$\text{(b)} \quad a_2 = \frac{6}{R^2}$$

$$\text{(c)} \quad f_c^{\,2} = 10^{-8}\ \text{sec}^{-2}$$

$$\text{(d)} \quad D^2 = 17 \times 10^6\ \text{m}^2$$

The numbers q along the abscissa-axis are defined according to $a' = \dfrac{q\,(q+1)}{R^2}$.

It is outside the scope of this lecture to discuss further the atmosphere, as it is observed, in relation to the results derived above.

For further development of the considerations presented, it would be important, instead of considering a single, averaged horizontal scale for the eddy flow, to ask for steady-state solutions in which we want to know the spectral distribution of $\int \mathbf{V}'^{\circ 2}$ and $\int \vartheta'^2$. Examining the problem that way, it is likely that for given external conditions there will not be so much freedom in the number of possible steady-state solutions as in the case studied.

551.508.765 : 551.574.12 : 551.576.11

Some observations of drop-size distributions in low layer clouds

By F. SINGLETON and D. J. SMITH
Meteorological Research Flight, Farnborough

(Manuscript received 25 March 1960; in revised form 14 June 1960)

SUMMARY

125 drop samples in ten layers of low cloud of thickness 700-7,500 ft (210-2,300 m) have been obtained using the magnesium-oxide coated-slide technique. These observations are discussed in terms of the condensation-coalescence mechanism. Comparison has been made between these observations and a similar set, also obtained by the Meteorological Research Flight, Durbin (1959), for convective cloud, from which it is shown that the coalescence process is in greater evidence in the layer clouds. Values of water content deduced from the drop spectra are higher than those previously reported by other workers and correspond in magnitude to the full adiabatic values suitably modified by redistribution within the cloud.

Some measurements are also discussed relating to the effect of the aircraft on the representativeness of the drop samples. The extension of the magnesium-oxide calibration to drops larger than 100 μ diameter has also been examined experimentally.

1. INTRODUCTION

The results of repetitive drop sampling using the slide technique in 10 cumulus clouds varying in thickness from 750 ft (230 m) to 7,000 ft (2,100 m) have been reported by Durbin (1956; 1959). A similar volume of data has been obtained relating to 10 low layer clouds with thicknesses in the same range. These enable examination to be made of the manner in which drop spectra vary with height in any one cloud and also of the variation of average spectra from cloud to cloud. Considered as an extension of the cumulus work of Durbin, the observations presented here may be used also to investigate the differing effects of the drop-growth processes in convective and layer clouds under similar conditions of base heights and temperatures, although this must be undertaken with some reservation owing to different drop impactors being used.

When making any measurements from aircraft it is essential to ensure that these are representative of free-air conditions; if this is not possible then either one must be able to apply corrections or be able to express the limitations of the observations in a quantitative manner. In the case of drop sampling this involves, primarily, the conversion of the impression size to the drop size, the collection efficiency and design of the impactor (to avoid extraneous effects such as splashing), and the siting of the impacting position on the aircraft. Before proceeding with the presentation and discussion of the results obtained in this paper the precautions taken and, where possible, the corrections made to account for the factors mentioned above, are described.

2. IMPACTOR DESIGN, COLLECTION EFFICIENCY AND DROP IMPRESSION CORRECTION FACTOR

The slides used on these flights were made of perspex measuring 0·5 cm by 4·0 cm and were coated with a layer of magnesium oxide, the preparation of the slides being similar to that described by Levine and Kleinknecht (1951); the lower limit of detection of the method is generally believed to be for drops of about 4 μ diameter. The thickness of the coating was small compared to the size of the drops.

On flights prior to 1959 the slides were exposed in an impactor of which the head consisted of a flat plate with a shutter. The opening and closing of the shutter, by a manually operated handle, caused the slide, previously shielded by the plate, to be exposed

to the airstream. During 1959 the head of the impactor was in the form of two parallel tubes some 3 cm apart, the slide being mounted on the end of a rod and moved rapidly from inside one tube into the other, the exposure being effected as the slide traversed the gap. In each case the exposure was timed electronically. It was considered that the second impactor was less liable to splash effects although as a general rule impactions were made immediately the instrument was pushed outside the aircraft so as to avoid an accumulation of water on the leading parts. A moving trolley on a specially stressed ramp was used for the purpose of pushing the impactor out into the airstream. Both these impactors have been illustrated elsewhere (Durbin 1958).

Drop concentrations were corrected for the collection efficiency of the slide; the values used, obtained from the work of Langmuir and Blodgett (1946), are shown in Table 1.

TABLE 1. EFFICIENCY OF CATCH (PER CENT) FOR A SLIDE OF WIDTH 0·5 cm FOR DROPS OF DIAMETER 2-40 μ AND AIRSPEEDS 60-80 m sec^{-1}.

Drop diameter μ	Airspeeds m sec^{-1} 60	70	80
2	7	10	13
4	52	58	61
6	70	73	74
8	78	80	81
10	83	85	86
12	87	88	89
14	89	90	91
18	93	93	93
20	94	94	94
40	99	99	99

It will be noticed that the effective minimum drop size which would be expected to be caught by the slides (i.e., 3-4 μ) also corresponds to the minimum size detectable by the magnesium-oxide coating.

For thin layers of magnesium oxide, such as were used in this work, and speeds typical of aircraft, Levine and Kleinknecht have obtained a value of 0·713 for the ratio of drop diameter to impression size. This value was obtained for drops up to 30-40 μ diameter and compares with a value of 0·85, derived by May (1950) for magnesium-oxide layers of thickness comparable with the drop size.

In the present work, as drops larger than 30 μ were often impacted, it was considered advisable to obtain a calibration for larger drops. For this purpose use was made of a gun firing a brass projectile at known speeds aimed at drops suspended on an artificial web. The equipment used has been described by Jenkins (1954). The nose of the projectile held a circular slide which was coated with magnesium oxide. Since small drops of water evaporate quickly the liquid used was dibutyl-phthalate, this having a very low vapour pressure and unit density (also May showed that its behaviour on impaction with magnesium oxide is very similar to that of water). The smallest drop size for which it was possible to perform the experiment was 100 μ diameter, it being difficult to produce a single drop smaller than this. Altogether 12 impactions were made each with one drop on the web (at speeds similar to the airborne experiments) for which the average ratio of drop size to impression size was 0·727 with probable error 0·018. The value of 0·713 due to Levine and Kleinknecht, being within the experimental limits of the determination described above, consequently was considered applicable for all drop sizes encountered.

3. The impactor positions

Because of structural and other considerations it is frequently not possible to choose a suitable sampling position on an aircraft. The basic requirements are that such a position should be devoid of any boundary layer or turbulent effects around the aircraft and should also be ahead of the propellers or well clear of the propeller wash. This, in practice, is as far forward and as far out as is compatible with the design of the aircraft, the weight of the instrument and the strength of the instrument support. Of the ten flights, the results of which are presented in this paper, five were made using a Hastings aircraft and five using a Varsity aircraft, the samples being taken $1\frac{1}{2}$ ft (0·46 m) outside the skin of the aircraft. The position on the Hastings was to the side of, and just to the rear of, the first pilot, slightly farther back than the position used by Durbin. On the Varsity aircraft the samples were taken out of the top of the fuselage, about 6 ft (1·83 m) to the rear of the pilots. The position was forward of the propellers on the Hastings and slightly to the rear on the Varsity (but well clear of the propeller wash). In order to examine the representativeness of these positions measurements were made of the total head and differential pressures using a pitot static tube mounted on a boom in the impacting position at distances of 6 in. to 3 ft (0·15 to 0·91 m) outside the aircraft. Comparisons were then made with the free stream values as measured by the standard aircraft system.

The results for the Hastings showed, except at near-stalling speeds, that there was no difference in differential pressures at distances of 1 ft (0·30 m) or more of the pitot head outside the aircraft. Measurements of total head pressures showed that the value at the impacting position was less than the free stream value by 0·3-0·6 mb at 6 in. (0·15 m) outside the aircraft and by 0·1 mb at distances of 1 ft (0·30 m) or more. (At an indicated airspeed of 140 kt (70 m sec^{-1}) the total head pressure at 10,000 ft (3,000 m) is about 732 mb). At near-stalling speeds total head pressure differences were 1·9 mb at 6 in. (0·15 m) decreasing to 0·9 mb at 2 ft (0·61 m). When the engine immediately to the rear was feathered the result was a slight decrease in total head pressure at the impacting position for speeds of 105-120 kt (53-60 m sec^{-1}) but negligible effect otherwise on total head or differential pressures.

From these measurements it would appear that for the Hastings there is little effect, in terms of total energy, at the impacting position due to the propellers or to the shape of the aircraft. The slight decrease in total energy relative to the free airstream was presumably due to the pitot head on the boom not quite being in correct alignment with the air deflected around the aircraft, the deflection varying inversely with speed accounting for the greater difference in total head pressures at the lower speeds.

On the Varsity similar measurements were made except that differences in static pressure were measured between impacting position and aircraft system as it was not possible for technical reasons to obtain directly the differences in total head pressure. It was found that at all speeds of flight the differential pressure in the impacting position was high by values between 10 and 7 mb at 6 in. (0·15 m) outside the aircraft for speeds of 180 to 120 kt (90-60 m sec^{-1}) decreasing to about 5 mb at 3 ft (0·91 m) at all speeds. These figures correspond to a 10-20 kt (5-10 m sec^{-1}) speeding up of the air as it flows over the aircraft.

It would appear from these measurements that whilst the impacting position on the Hastings is probably satisfactory, that on the Varsity is liable to produce doubtful observations. The observations from the two aircraft have, accordingly, been treated separately and although the Varsity results are not directly comparable with those of the Hastings they should be self-consistent and the qualitative deductions discussed later are equally valid for both aircraft. In order to obtain a quantitative estimate of the likely errors in the Varsity observations as well as to confirm the veracity of those obtained from the Hastings, reference was made to work by Dorsch and Brun (1954). From this it is possible to obtain concentration factors (i.e. the ratio of the observed concentration to the actual concentration in the cloud) for drops of various sizes at different distances from the aircraft skin at positions along an aircraft fuselage on the assumption that this approximates to an ellipsoid

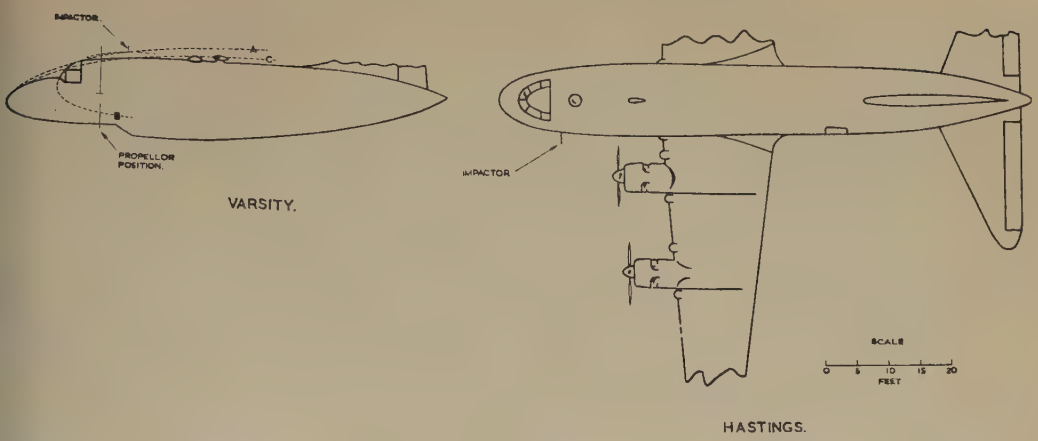

Figure 1. Profiles of the two aircraft drawn through the plane of the impactor. Dotted lines A, B and C superimposed on the Varsity show the ellipsoids to which the results of Dorsch and Brun (1954) were applied.

of fineness ratio 5. For the case of the smooth profile of the Hastings (see Fig. 1) it is possible to construct an ellipsoid in a reasonably satisfactory manner and, to this, apply their results. These showed that for drop sizes up to 140 μ diameter the increase in drop concentration should be 5 per cent or less, whilst for drops between 160 and about 750 μ concentrations would be increased by about 10 per cent at most; for drops of 1 mm there would be no measurable effect. On the other hand, owing to the sudden step in its profile just ahead of the impactor, the fitting of an ellipsoid to the Varsity is not possible. The results of Dorsch and Brun as applied to three ellipses, parts of which are shown superimposed on the outline of the Varsity, on Fig. 1, are, however, given in Table 2; these figures are necessarily only approximate, because of the peculiar relations between airspeed, position of drop sample, drop size and concentration factor.

TABLE 2. Drop concentration factors for the three ellipsoids used to represent the shape of the Varsity fuselage moving at 140 kt

	Drop diameters μ										
Ellipse	< 10	40	60	80	100	120	140	160	200	500	1,000
Curve A	1	1·05	1·1-1·2	1·6	1·8	2-4	0	0	0	1·4	1·2
Curve B	1	< 1·05	1·1	1·2	1·2	1·3	1·3	1·4	1·5	1·4	1·2
Curve C	1	< 1·05	< 1·05	1·1	1·1	1·1	1·2	1·2	1·3	1·1	1·0

From Table 2 it is seen that, for drops up to 60 μ diameter, concentrations would be correct certainly to within 10 per cent but, that for sizes larger than this, concentrations for some drop-size ranges could be too large by 100 per cent to 300 per cent, whilst for some drop-sizes, conditions might be such that none is caught. The applicability of these results to the Varsity aircraft will be mentioned later in relation to the observations made by both aircraft. It is relevant to note that the theoretical speeding-up of the air for cases A and B is in the range 7-10 kt as opposed to the measured 10-20 kt.

It is, perhaps, of interest to discuss, in the light of the above remarks, previous sampling work carried out by the Meteorological Research Flight. The droplet sampling work of Durbin was carried out in the Hastings aircraft and, except that no correction was made for collection efficiency, his results should not include errors of a larger magnitude than those encountered in any random sampling technique. In nucleus sampling work, e.g., Durbin (1959) in which both Hastings and Varsity were used the particles caught

were small (relative to cloud drops) and their concentrations would not be affected. On flights measuring large drops (100 μ diameter and larger) as described by Murgatroyd and Garrod (1960) for cumulus clouds and Singleton (1960) for layer clouds using both aircraft, large natural variations of drop concentrations were observed and no effect of the different aircraft used was evident. In the two latter papers, none of the drop concentrations reported should be in error by a factor larger than 1·5-1·8.

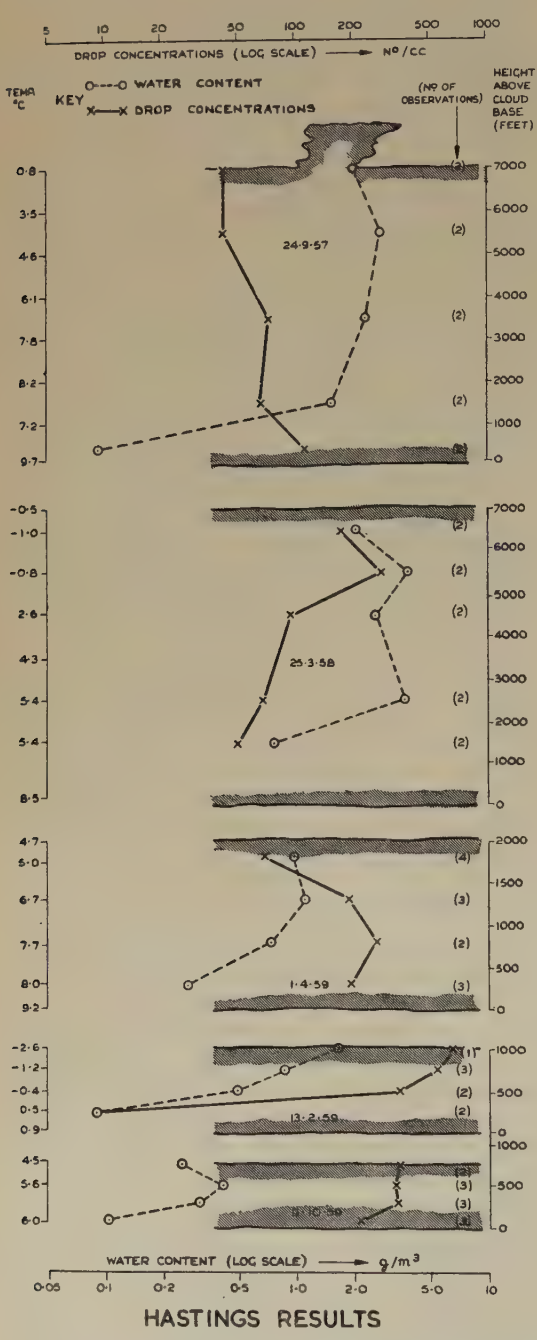

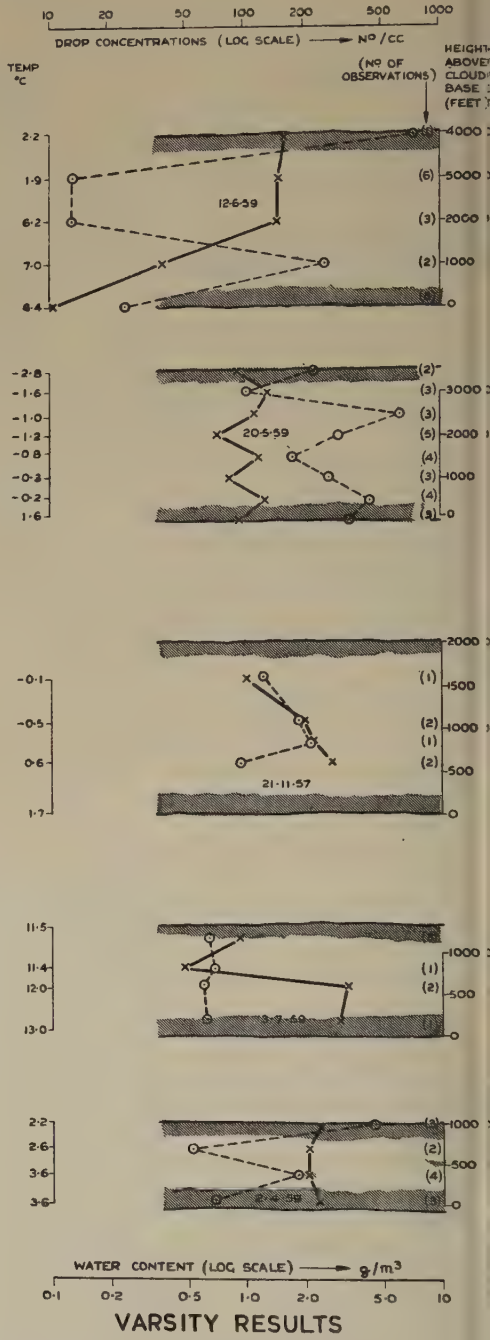

Figure 2. Variations with height of observed drop concentrations (×——×) and water content (⊙ · · · · ⊙). Also shown are temperatures and number of observations at each level.

4. Experimental procedure and presentation of results

In addition to visual notes of cloud types, observations were also made of pressure altitude and indicated airspeeds, the latter being corrected for height and temperature using readings of temperature from a standard Meteorological Office flat-plate resistance thermometer. (The corrections to be made, for kinetic heating and evaporational cooling, to temperatures measured with this instrument in cloud are not readily determinable, and consequently the corrections applicable to dry-air conditions were used. The largest correction made on these flights was 2·5°C. Following Murgatroyd (1955) it is suggested that the temperatures might be up to 0·75°C too low at 9,000 ft (2,700 m) and up to 0·5° too low at 2,000 ft (600 m)).

The flight plan was to select days when there existed an 8/8 layer of low cloud with little or no other cloud and then to fly at suitable height intervals on reciprocal headings, taking several samples at each level in rapid succession, the aim being to obtain representative measurements of mean drop-size distributions at various heights throughout the cloud in as small an area as possible. Altogether ten cloud layers of thickness 700 ft (210 m) to 7,000 ft (2,100 m) were examined, a total of 125 usable drop samples being obtained. All the flights were made in the vicinity of Farnborough except when stated in the summary of results.

For each metre flown (about 0·015 sec at 70 m sec^{-1}) a slide samples about 200 cm^3 of air, exposure times being generally between 0·005 and 0·025 sec. In order to minimize the laborious task of sizing and counting the drops a representative portion of each slide was microphotographed and enlarged to 100 times total magnification. Consequently the average volume of air for which counts were actually made was about 2·5 cm^3. Frith (1951), using a similar selective technique, considered that his samples were always quite representative of the whole slide; occasionally in the present work more than one photograph was taken of a slide and the representativeness of the small portions verified. In order to reduce the random element in the single shot-sampling technique described above all the usable samples obtained at any one level were averaged.

On the enlarged photographs the drop impressions were counted in 10 μ steps up to about 50 μ and somewhat larger steps above, the size correction being applied after the counting. Water contents were evaluated by assuming that for each size range the mid-diameter and mean volume diameter were equal. The validity of this assumption within a given drop-size range depends on the drop-size distribution within the range; the observations not being sufficiently detailed to produce this information in individual cases it has been estimated from the mean spectra that this assumption should not produce errors greater than 5-10 per cent in water content. The drop concentrations and water contents in the various size ranges were then corrected for collection efficiency from the values given in Table 1.

A summary of cloud heights, temperatures, synoptic conditions and aircraft used, together with drop concentrations and water contents averaged for all the samples taken in each cloud is given in Table 3. Variations, in each layer, of observed total water content and drop concentration with height above cloud base are shown in Fig. 2 together with corrected temperatures and number of samples. The average water content and drop concentrations measured in each cloud are shown in Fig. 3 plotted against cloud thickness, differentiation being made between Hastings and Varsity results. Similarly formed averages for cumulus clouds observed by Durbin are shown also. Fig. 3 also shows for direct comparison theoretical average cloud-water contents plotted against thickness calculated on the adiabatic assumption for clouds of thickness up to 8,000 ft (2,400 m) with bases of 950 mb and temperatures of 10°C and 0°C (AA′ and BB′ respectively). The lines AA′ and BB′ give the expected *average* water content assuming that the water to be found in any cloud is the integrated total of the water released as the air at each level ascends to that level from cloud-base cooling at the saturated adiabatic lapse rate with no entrainment of unsaturated air.

TABLE 3. SUMMARY OF RESULTS

Date and aircraft	Time GMT	(a) Height (ft) (b) Pressure (mb) (c) Temperature (°C) Cloud base	Cloud top	Cloud thickness (ft)	Water contents (gm^{-3})	Average drop concentrations (cm^{-3})	Remarks
9 October 1957 Hastings	1100	(a) 2,350 (b) 939 (c) 6·0	3,050 912 4·5	700	0·27	315·8	No cloud above. High centred over NW. Europe. Winds SE., light. No precipitation at the ground.
13 February 1959 Hastings	1100	(a) 750 (b) 1,007 (c) 0·9	1,750 971 − 2·6	1,000	0·78	391·7	No upper cloud. Ridge extending from high over S. Europe giving light SW. winds. No precipitation at ground. Sampling over sea near Beachy Head.
2 April 1959 Varsity	1100	(a) 3,900 (b) 895 (c) 3·6	4,900 863 2·2	1,000	1·88	225·5	$\frac{1}{8}$ cirrus. Anticyclonic centre over SE. England inside wide, open, warm sector. Winds light and variable. No precipitation at ground.
3 July 1959 Varsity	1300	(a) 2,600 (b) 926 (c) 13·0	3,900 882 11·5	1,300	0·65	194·8	Small amounts upper cloud. Low pressure troughs moving across England with anticyclone to SW. Winds NW., light to moderate. Sampling over Salisbury Plain.
1 April 1959 Hastings	1300	(a) 1,400 (b) 977 (c) 9·2	3,400 908 4·7	2,000	0·78	180·3	No upper cloud. Cold front moving SE. was to NW of Farnborough. Winds SW.–W., light. No precipitation at ground.

TABLE 3 (continued)

Date and aircraft	Time GMT	(a) Height (ft) (b) Pressure (mb) (c) Temperature (°C) Cloud base	Cloud top	Cloud thickness (ft)	Water contents (gm^{-3})	Average drop concentrations (cm^{-3})	Remarks
21 November 1957 Varsity	1200	(a) 1,400 (b) 980 (c) 1·7	3,400 912 − 0·1	2,000	1·56	198·3	Little upper cloud. Warm front over Irish Sea preceded by weak ridge. Winds SW.–W. No precipitation at ground. Both base and top of this layer were varying very considerably. The values given refer to the heights at time of sampling.
20 May 1959 Varsity	1000	(a) 5,500 (b) 831 (c) 1·6	9,000 727 − 2·8	3,500	3·15	105·8	Small amounts cirrus. Indeterminate low-pressure area over NW. Europe. Winds E.–NE., light to moderate. No precipitation during flight, slight rain at 1200 GMT.
12 June 1959 Varsity	1000	(a) 3,000 (b) 926 (c) 8·4	7,000 797 2·2	4,000	2·12	103·3	Broken altocumulus above. Quasi-stationary front over S. England, high pressure centres to NE. and SW. Winds light and variable. Intermittent slight drizzle at 1000 GMT.
25 March 1958 Hastings	1100	(a) 500 (b) 982 (c) 8·5	7,000 770 − 0·5	6,500	2·64	135·0	Broken altocumulus and cirrus above. Low-pressure area over Bay of Biscay with an occlusion lying NW.–SE. over E. Anglia. Winds light SE. Intermittent rain and drizzle.
24 September 1957 Hastings	1400	(a) 1,000 (b) 977 (c) 9·7	8,000-9,000 753-722 0·8 to − 1·0	7,000-8,000	1·95	68·3	Nil or little upper cloud. Sampling area just to rear of slow-moving, warm front. Winds E. becoming SW. light. Continuous slight rain at the ground.

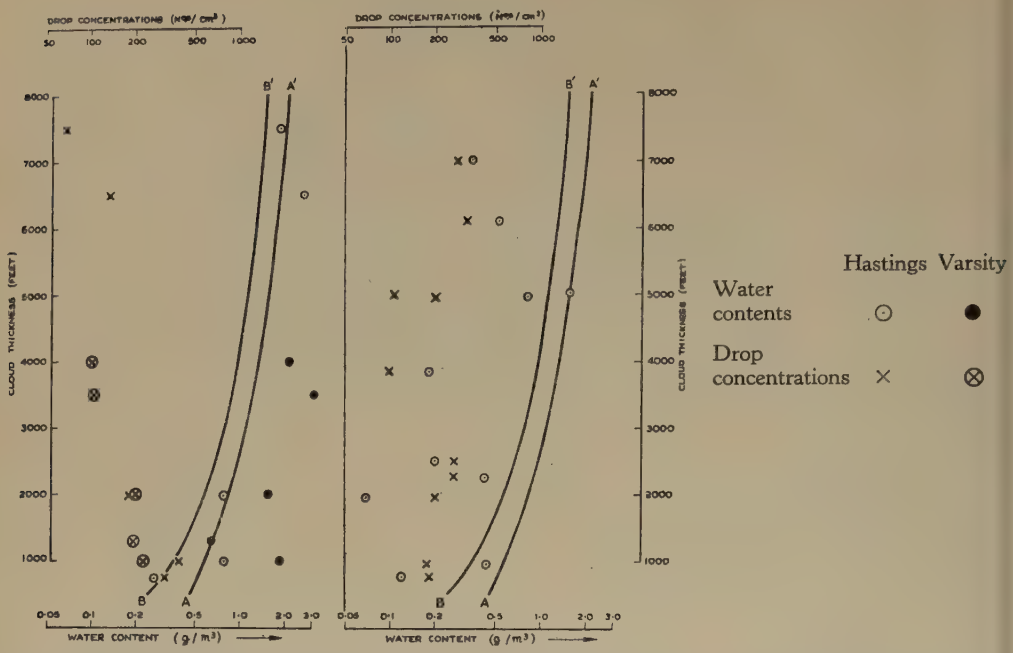

Figure 3. Average drop concentrations and water contents plotted against cloud thickness for layer and convective clouds. Theoretical average water contents are indicated by lines AA′ and BB′.

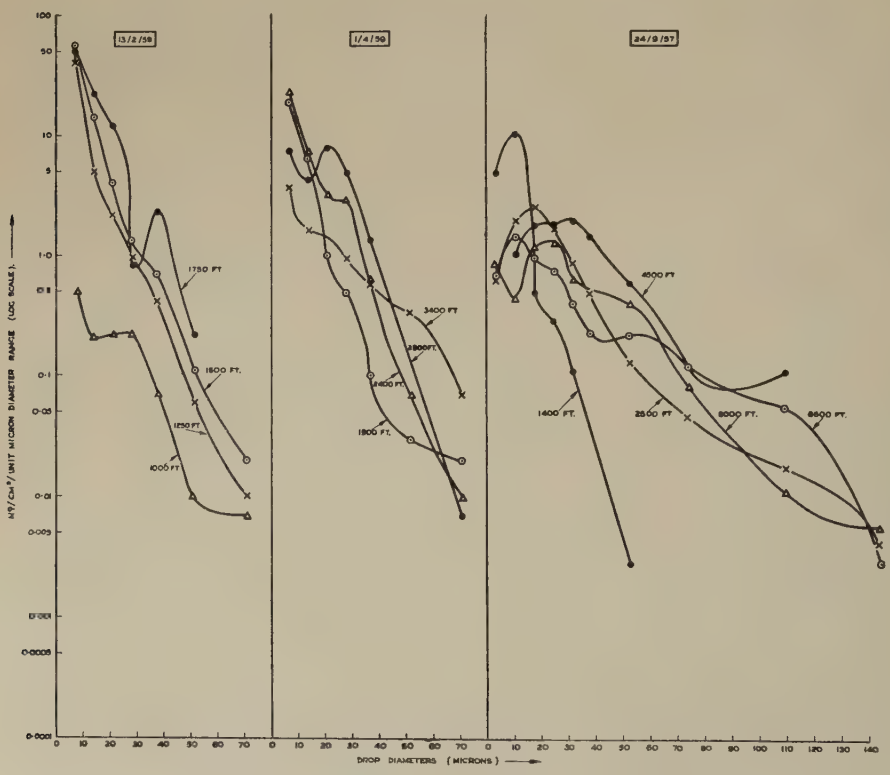

Figure 4. Some typical drop spectra for various heights above cloud base.

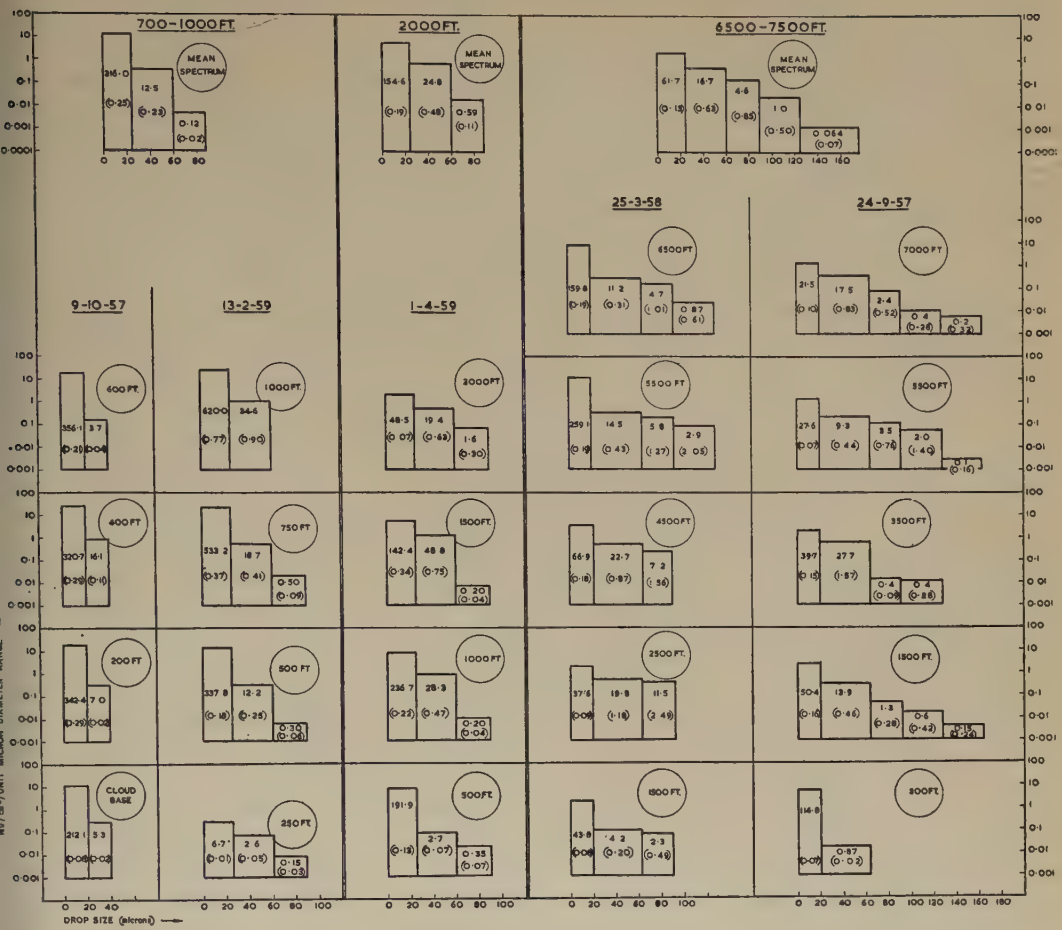

Figure 5. Observed drop spectra throughout all the clouds investigated in the Hastings aircraft. The figures in the blocks of each histogram are drop concentrations and water contents (in brackets) within the size range. Sampling heights above cloud base are indicated in the circles.

Detailed drop spectra for three layers of cloud, as observed at each level, are shown in Fig. 4; these are fairly typical of the ten layers. The system of plotting is concentration (no. cm^{-3}) per unit micron diameter range, i.e., the number of drops in the size range $d - \frac{1}{2}\Delta d$ to $d + \frac{1}{2}\Delta d$ is $N_d \Delta d$ where N_d is the number read off on the ordinate corresponding to size d on the abscissa. Fig. 5, using the same representation in a less detailed histogram form, shows the broad features of the transition from the shallow clouds to the deeper ones. Total drop numbers and water content for each drop-size range are also shown.

Mean spectra relating only to Hastings observations, are shown on Fig. 5 in the groups 700-1,000 ft (210-300 m), 2,000 ft (600 m), 6,500-7,500 ft (2,000-2,300 m).

For purposes of comparison with spectra obtained for cumulus clouds by Durbin, Fig. 6 shows detailed mean spectra for these groups. When the mean spectra for each cumulus cloud observed by Durbin were plotted on a composite diagram it was found that they formed two groups, the first consisting of eight clouds of thickness 750-7,000 ft (230-2,100 m) (with a mean shown as type I on Fig. 6), and the second group composed of two clouds of thickness approximately 5,000 ft (1,500 m) (with a mean shown as type II). In the first group there was no obvious variation of mean spectrum with cloud depth, all the mean spectra being narrower than any average spectrum of the layer-cloud groups

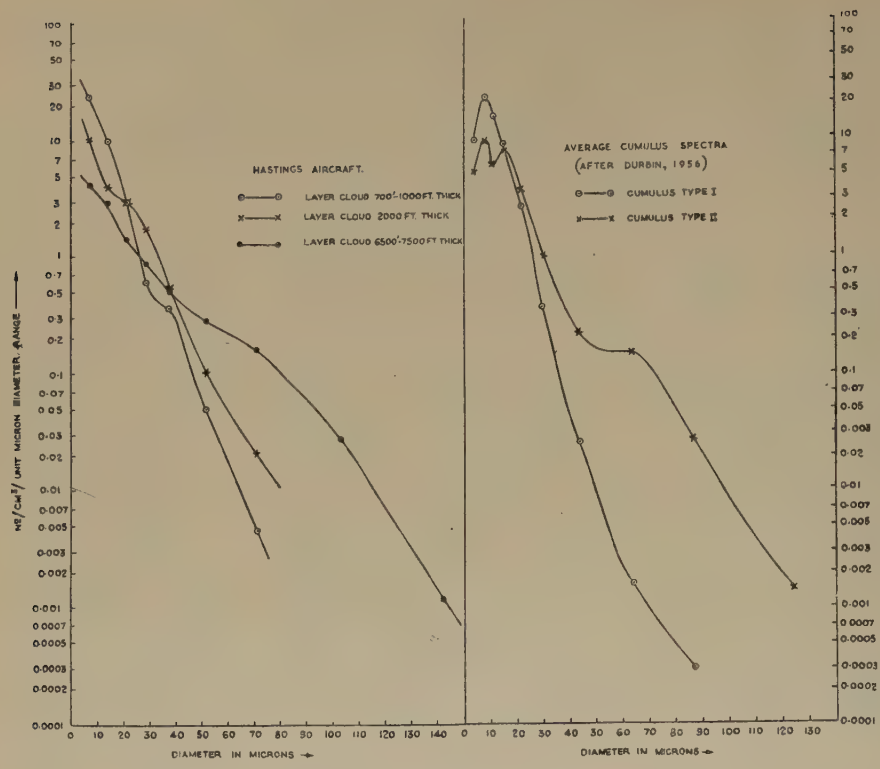

Figure 6. Average spectra for layer and convective clouds.

above. The two remaining cumulus clouds had spectra very like those of layer clouds of similar thickness.

Because of shortcomings in the Varsity results these are not presented in such great detail as are those from the Hastings results.

5. Discussion

Of the clouds which were sampled in this experiment five were entirely non-freezing and none of the remainder had temperatures below — 3°C at any level. At such temperatures it is unlikely that any drops would be frozen and consequently the results presented here will be discussed mainly in terms of the condensation-coalescence process of drop growth. Even if ice particles were present the small difference between the saturation vapour pressure over ice and water in this temperature range is such that the frozen particles would not grow appreciably faster, owing to the Bergeron-Findeisen process, than supercooled drops of similar size.

Variations with height above cloud base of water content and drop concentration as shown in Fig. 2 exhibit great variability in most of these clouds. There appears to be no consistent pattern when individual clouds are compared. In the thin cloud regions of high water content are apparently due to increases in the total drop concentrations, whilst in the thicker clouds such regions are due to increases in the large-drop concentrations only. The exact causes of these apparently localized variations in water content are not readily determinable. Possible reasons are variations of vertical motion and the age of the part of the cloud chosen for sampling; the first of these by

determining the largest drop size capable of being supported, and the second since the older regions of the cloud are likely to be precipitating, can greatly influence water contents. As far as is known orographic influences were not present in these layers and local variations of vertical motion would only result from the eddy motions which exist in layer clouds.

Comparing the average measured water contents with the theoretical values (Fig. 3) it is seen that the results from the Varsity are all, with one exception, apparently high, by a factor of approximately two. If it is valid to apply the results of Dorsch and Brun, to the Varsity profile (as above), then the high water contents measured should arise from drops larger than about 80-100 μ diameter being concentrated in the region of the impactor. Examination of the Varsity results showed, in fact, that the large water contents were probably due to drops larger than about 50 μ, all being concentrated at the impactor position by a factor of about two; the inapplicability in a fully quantitative manner of the results of Dorsch and Brun is presumably due to the sharp discontinuity in the profile of the aircraft.

Examining Fig. 3, and bearing in mind the reservations concerning the measured water contents from the Varsity, it is seen that the average water contents are all similar to the values to be expected as a result of adiabatic ascent. The results of sampling of precipitating particles, reported elsewhere, showed that large (100 μ) drops were frequently found falling below layer clouds of thickness greater than 1,000 ft (300 m). It seems likely that, since little water can be lost from base or top by evaporation (James 1959), the loss of water in the form of precipitating drops must be more or less balanced by production of water by continued condensation within the cloud. This must, presumably, be the case in many warm-sector situations where there is continuous steady drizzle lasting many hours over large areas.

Values of water contents in similar types of cloud, measured by other workers, have usually been less by up to an order of magnitude than those reported here on the average, although they are often comparable as regards maximum values. However, their reported values have many uncertainties associated with calibration and sampling position on the aircraft and further independent and careful verification is needed – possibly a technique in which a volume of water is caught and measured in preference to the more indirect methods.

Although it was not usually possible to detect a consistent pattern of the development of the drop spectra in individual clouds it was found possible to do so when examining the mean spectra in Fig. 6. From this it is seen that the thicker a layer cloud, then the broader the spectrum, and the fewer the drops. This implies that in the deeper clouds there is more time available for the coalescence mechanism to modify the drop spectrum, the individual drops having a longer time of residence than in the thinner clouds. The differences in the lifetime of drops are made apparent in the large drops having more time to coalesce with smaller drops and the small drops decreasing in concentration accordingly. In eight of the cumulus clouds sampled by Durbin such differences between shallow and deep clouds were not apparent; the mean spectrum of each of these clouds was narrower than the average spectrum of the thinnest layer cloud group. The implication here is that the coalescence process has considerably less time to affect the shape of drop spectrum in the cumulus cloud as compared with the layer cloud. It is not clear why the two cumulus clouds of thickness 5,000 ft (1,500 m) shown as type II in Fig. 6 should have produced so dissimilar spectra from the rest of the population. A possible explanation would be that the updraughts in these clouds were considerably less than in the other eight and possibly there was a tendency to stratification. It has been reported by Murgatroyd and Garrod (1960) that under such conditions the number of precipitation particles within cumulus clouds can increase markedly and approach concentrations typical of layer clouds. Similarly, considering the differences between the water contents of convective and layer clouds as shown in Fig. 3, it is suggested that mixing of cloud air with entrained drier air is an important factor in lowering the average water contents of cumulus cloud as

opposed to the layer clouds. In the latter, mixing can only take place at base and top, whereas mixing around the sides and also overturning motions are important in the former.

The total drop concentrations reported in this paper are for drops larger than about 3 to 4 μ diameter, the lower limit resulting from the limit of detection of the magnesium-oxide coating and also the collection efficiency characteristics of the slides. Whether there are drops smaller than this size existing in clouds is uncertain. The theoretical work of Howell (1949) indicates that, after the very early stages of condensation, drops which have not reached their critical size should decrease to sizes of less than about 1·5 μ diameter, while according to Mordy (1959) they should decrease to sizes of the order of 0·1 μ. The existence, or otherwise, of these small drops needs further investigation using an instrument capable of finer resolution than those developed so far. Ground-based measurements (Todsen 1958) indicate that drops of 1 to 2 μ diameter are present near the bases of layer clouds.

Because of the comparative crudeness of the aluminium-foil method of detecting large drops (Murgatroyd and Garrod 1960) by which the accurate sizing of drops of about 100 μ diameter is not possible, and also because of the greatly differing volumes of air sampled, direct comparison of individual samples can only be made in a general qualitative fashion. Comparison of the concentrations of the larger drops measured here with those presented elsewhere (Singleton 1960) for layer clouds using aluminium foil suggests that the lower limit of detection of the foil is probably nearer 100 to 120 μ as opposed to the 80 to 100 μ diameter previously suggested. Comparing the aluminium-foil results for layer clouds with the drop spectra presented here, it is seen that the broadening of the drop spectrum with cloud depth is analogous to the increase in drizzle-drop concentrations.

6. Conclusions

Repetitive measurements of drop-size distributions in layer clouds have shown that, even though samples in any one cloud are of a random nature, presumably due to the eddy motions characteristic of such clouds, there is a distinct trend for spectra to become broader as cloud thickness increases. This is in contrast with cumulus clouds in which no such variation with thickness is readily apparent. Drop spectra are also broader in the layer cloud and water contents higher than in cumulus clouds of comparable thickness. It is suggested that longer drop-life times in the layer clouds, together with less mixing with the environment, lead to the observed differences between the two cloud types and that the coalescence mechanism is often, but not always (cf. the cumulus type II spectra on Fig. 6) more in evidence in layer clouds than in convective clouds of similar depth. The water contents derived from the drop spectra are consistently higher than those previously measured by indirect methods such as hot-wire, wetted paper, etc., and it is suggested that work directed at the problem of measuring water content directly would be rewarding.

Comparison between results derived from two different aircraft illustrates the uncertainties of making this type of measurement from aircraft.

Acknowledgments

This paper is published by permission of the Director-General of the Meteorological Office. Acknowledgments are also due to Mr. D. C. Jenkins and Mr. J. D. Booker of the Mechanical Engineering Dept., Royal Aircraft Establishment, Farnborough, for assistance with the calibration procedure, and to staff and aircrew of the Meteorological Research Flight, Farnborough, without whose help and co-operation this work would not have been possible.

References

Dorsch, R. G. and Brun, R. J.	1954	*Tech. Note*, 3153, N.A.C.A., Washington.
Durbin, W. G.	1956	*Air Ministry Met. Res. Cttee. M.R.P.*, No. 991.
	1958	*Weather*, **13**, p. 143.
	1959	*Tellus*, **11**, No. 2, p. 202.
	1959	*Geofis. Pura é Appl.*, Milano, **42** (1959/1).
Frith, R.	1951	*Quart. J. R. Met. Soc.*, **78**, p. 333.
Howell, W. E.	1949	*J. Met.*, **6**, p. 134.
James, D. G.	1959	*Quart. J. R. Met. Soc.*, **85**, p. 120.
Jenkins, D. C.	1954	*R.A.E. Tech. Note Mech. Eng.*, No. 193.
Langmuir, I. and Blodgett, K. B.	1946	*U.S.A.F. Tech. Rep.*, No. 5418.
Levine, J. and Kleinknecht, K. S.	1951	*Res. Memo. E.*51G0.5, N.A.C.A., Washington.
May, K. R.	1950	*J. Sci. Instr.*, **27**, No. 5, p. 128.
Mordy, W. A.	1959	*Tellus*, **11**, No. 1, p. 16.
Murgatroyd, R. J.	1955	*Arch. Met. Geophys, Biokl*; A., **8**, p. 246.
Murgatroyd, R. J. and Garrod, M. P.	1960	*Quart. J. R. Met. Soc.*, **86**, p. 167.
Singleton, F.	1960	*Ibid.*, **86**, p. 195.
Todsen, M.	1958	*Rapport*, No. 1, Inst. Weather and Climate Res., Oslo.

551.501.81 : 551.578.71

Radar scatter by large hail

By D. ATLAS*, *Imperial College, London*
W. G. HARPER, *Meteorological Office, London*
F. H. LUDLAM and W. C. MACKLIN, *Imperial College, London*

(Manuscript received 26 February 1960)

Summary

Radars with wavelengths of 3·3 and 4·67 cm have been used to measure the back-scatter cross-sections of individual artificial hailstones and their variations as melting occurs. The measurements confirm the cross-sections computed theoretically. An ice sphere is a better scatterer than a liquid water sphere of equal size when its diameter exceeds 0·8 wavelengths; when the diameter lies between 1·2 and 2·3 wavelengths it is better by a factor of 10 or more. This behaviour of ice is supported by scatter measurements on a set of plexiglass (perspex) spheres with refractive index close to that of ice.

When melting begins, the 3·3 cm cross-sections drop sharply toward the all-liquid values; those at 4·67 cm decrease gradually, and sometimes not at all. The rate of decrease of the cross-sections during melting is also more variable at 4·67 cm than at 3·3 cm. Most of the 3·3 cm change appears to occur during the initial growth of the liquid coat to a maximum thickness of about 0·01 cm, while the major drop in 4·67 cm cross-sections occurs well beyond this stage of melting. The implications are that : (1) a water coat of 0·01 cm thickness has a major effect at 3·3 cm and a minor one at 4·67 cm; (2) liquid continues to collect in sub-surface cracks and cavities in the ice and causes a further decrease in the cross-sections after the maximum thickness of water coat has formed. The final cross-sections are generally within 2 db of the all-liquid value after 7 to 10 minutes of melting at 3·3 cm and after 15 to 20 minutes at 4·67 cm. Possible reasons for these results are discussed.

1. Introduction

Recent studies have shown that quantitative measurement of the radar back-scatter from a convective storm provides a useful indication of the presence of hail (Donaldson 1958, 1959). However, the interpretation of such measurements has been restricted by the lack of adequate data on the back-scatter cross-sections of large hail. Until recently, the only available data were theoretical values calculated by Ryde (1946) from the rigorous Mie theory. These were restricted to ice spheres of diameter D less than 1·25 times the wavelength, λ; i.e., to hail smaller than 3·75 cm at a wavelength of 3 cm. Moreover, some authors (Atlas and Donaldson 1954) had expressed intuitive doubt of their validity since ice with diameter to wavelength ratios D/λ in excess of 0·8 were indicated to scatter significantly better than liquid-water spheres of equal size, while the reverse is true for both smaller and much larger spheres. The back-scatter measurements reported here were therefore undertaken to check and to extend empirically Ryde's theoretical computations, and to determine how the cross-section of a large ice particle varies during the melting process.

After the experimental phase of this study was completed, the desirability of further theoretical computations became apparent. It was coincidental that Herman and Battan (1959) at the University of Arizona were already established to make these on an electronic computer. This work has now been completed and the authors have graciously made the results available to us in advance of their publication. We include a brief comparison with our measurements.

The apparently anomalous behaviour of the back-scatter cross-section of ice with respect to that of water is indicated by the crossing of their scattering curves in Figure 5. Indeed, since the scattering by metal spheres is represented essentially by an upward displacement of the water curve in Figure 5, until it oscillates around a ratio of radar to geometric cross-sections of $\sigma/(\pi D^2/4) = 1$, it is evident also that moderately large ice spheres have larger back-scatter cross-sections than metal spheres of the same size. To

* National Science Foundation Senior Post-Doctoral Fellow on detached duty from the Geophysics Research Directorate, Air Force Cambridge Research Center, Bedford, Massachusetts.

make a comparison, we examine the situation in the regions defined by $D/\lambda \ll 1$, the so-called Rayleigh region, and $D/\lambda \gg 1$, the geometric optics region. Writing $\sigma/(\pi D^2/4) = f_s$, in the Rayleigh region we have

$$f_s = 4\pi^4 |K|^2 D^4/\lambda^4 \quad . \quad . \quad . \quad . \quad . \quad (1)$$

where $K = (m^2 - 1)/(m^2 + 2)$, and m is the complex refractive index. For metal spheres with $m = \infty$ and $|K|^2 = 1$, the cross-section given by (1) is enhanced by 9/4 (Kerr 1951, p. 452). For very large values of D/λ it is well known that

$$f_s = (m - 1)^2/(m + 1)^2 \quad . \quad . \quad . \quad . \quad (2)$$

This is simply the power reflection coefficient of a plane surface. Gunn and East (1954) give values of m and $|K|^2$ for water and ice at various wavelengths. For example at 3·21 cm : $m = 7{\cdot}14 - 2{\cdot}89\,i$ and $|K|^2 = 0{\cdot}93$ for water at 0°C; $m = 1{\cdot}78$ and $|K|^2 = 0{\cdot}197$ for ice. The ratios of the back-scatter from water and metal spheres to those from ice spheres of equal size are then as given in Table 1. The superiority of metal and water to ice in both regions is notable. Confirmation of the theoretical calculations which show the reverse for the intermediate size range is therefore desirable.

TABLE 1. RATIOS OF BACK-SCATTER CROSS-SECTION OF METAL- AND WATER- TO THOSE FROM EQUAL-SIZED ICE SPHERES FOR THE RAYLEIGH REGION ($D/\lambda \ll 1$) AND GEOMETRIC OPTICS REGION ($D/\lambda \gg 1$) (AT 0°C AND FOR $\lambda = 3{\cdot}21$ cm).

	$D/\lambda \ll 1$	$D/\lambda \gg 1$
metal/ice	11·4	12·7
water/ice	4·72	7·81

2. EXPERIMENTAL PROCEDURE

Two radars were used in the experiment, the 3·31 cm TPS-10 and the 4·67 cm MPS-4. The targets were raised by a 500 g balloon (tethered by a nylon fishing line) at a range of 1·4 to 1·5 mi, until their echoes could readily be distinguished from ground clutter; their elevations varied between 4° and 13°. Special care had been taken in selecting the balloon launching site to ensure that at these angles there were no detectable ground echoes at the target range.

The targets were placed in fine nylon hair nets and tied to the balloon line. The balloon itself gave a measurable echo, and so the targets were suspended at least 150 ft below the balloon. Since the vertical beam-widths of the TPS-10 and the MPS-4 are 0·7° and 0·8°, or 97 and 111 ft respectively at a range of 1·5 mi, the balloon and target echoes could readily be distinguished, particularly as the former was subject to fading. On occasion as many as 3 targets could be suspended from the balloon simultaneously, with separations of about 150 ft.

A 12-in. diameter metal sphere, whose cross-section is equal to its geometric cross-sectional area, was used as a reference in all the measurements. Initially the reference sphere was raised at the start and end of a series of measurements on test targets. However, it was found that during a protracted series of measurements the intensity of the echo from the standard target varied by as much as a factor of 2, partly because of changes of range due to wind fluctuations. In later measurements the reference target was therefore suspended from the balloon simultaneously with the test target and measurements of its echo power were made immediately before and after, and even during, a series of measurements on the test target. These usually agreed to within $\pm$ 0·4 db, or even less if the wind was steady. If the test and standard targets were at equal ranges, the cross-section of the

test target was simply related to that of the standard target in the ratio of their echo powers. Thus, in principle, the accuracy of the measurements depends mainly on the relative accuracy of the attenuator of the microwave signal generators with which the radars were calibrated. Unfortunately, however, there were other sources of error in the 4·67 cm measurements.

On the TPS-10 radar, the target echo was displayed on an A-scope and the receiver gain adjusted to bring the echo amplitude below saturation. An artificial signal from a calibrated signal generator was displayed immediately beside the true echo and the attenuator adjusted to match the two signals in amplitude. This matching could be reproduced to within about $\pm$ 0·2 db, the remaining spread ($\pm$ 0·2 db) in the measurements being attributable to actual echo changes associated with small displacements of the target. Variations in echo power due to motion of the target away from the beam axis were kept very small by manually orientating the antenna to obtain maximum signal on the A-scope prior to each measurement. Since the mean of a series of measurements could be determined reliably the overall measurement accuracy on the TPS-10 was indeed determined almost solely by the accuracy of the test-set attenuator.

On the MPS-4, the echo intensity was determined by reducing the receiver gain control (I.F. bias) until the echo just broke the base line on the A-scope. This threshold gain setting or I.F. bias was always calibrated in terms of echo power before and after a test series, and frequently at intervals during the test, using a TS-620 microwave signal generator. In order to obtain better accuracy than that of the attenuator incorporated in the test set, a precision attenuator was inserted at the output of the signal generator. This attenuator was precisely calibrated by the manufacturer to an accuracy of $\pm$ 0·1 db over a range of 45 db.

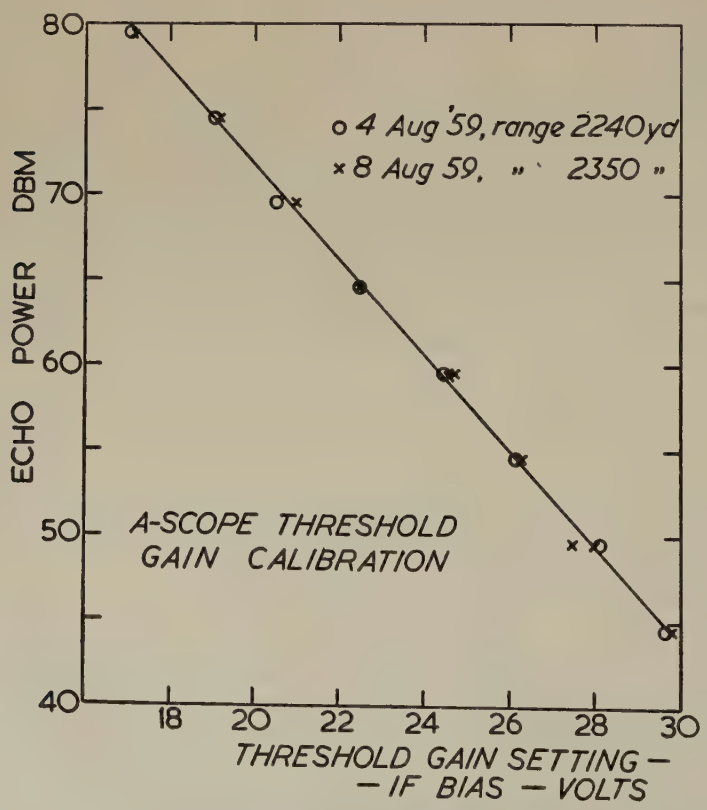

Figure 1. MPS-4 A-scope threshold gain calibration representing the echo power in decibels below 1 milliwatt which is required for detectability.

The threshold gain calibration curve for 4 and 8 August 1959 is reproduced in Fig. 1. The standard error of estimate of the observed points from the smooth curve is ± 0·53 db. Since the technique for obtaining the threshold gain setting for the artificial calibration signal is identical to that for true echoes, this is also the accuracy with which we may expect to reproduce readings from a perfectly steady target echo.

There were, however, two other more significant sources of error in the MPS-4 measurements. The first is that due to the motion of the target. The signal could be maximized readily in azimuth by slight adjustment of the manual slewing control. However, elevation could be controlled only by a switch which directed the elevation motor to drive upwards or downwards. With the narrow vertical beam (0·8°) it was difficult to stop the antenna exactly where desired. The result was a much broader spread in echo intensities than was the case with the TPS-10. Fig. 2 shows two typical series of measurements. The spread in the measured echo power is rather large, but most of the low values must be regarded as ' off-axis ' measurements. Since proper orientation of the beam will provide the maximum possible echo, the best estimate of the true echo power must be close to the maximum observed values. However, allowance must be made for possible over-estimation, due to random errors in adjustment and reading of the threshold gain setting, with the standard error of about ± 0·5 db indicated above. It is unlikely, therefore, that a measurement will exceed the true maximum by more than 1 db. Similarly, all values more than 1 db below the true maximum are probably due to orientation errors; some of these may cause the values to be as much as 6 db too low. It is evident from the measurements in Fig. 2 that the extreme orientation errors are not usually successive. Since the observer watched the A-scope for maximum signal as he varied the elevation angle, the first few measurements after an elevation change tend to occur near the maximum. The signal may then decrease as the target drifts away from the beam axis. Since the change in signal strength was quite obvious, a new elevation adjustment was then made. The points in Fig. 2 therefore tend to cluster within 2 db of the maximum *measured* value. We estimate the true echo-power level by drawing a line through this cluster in such a manner that out of a total of 10-20 measurements, 1 point falls approximately 1 db above and 2 or 3 points fall within 0·5 db above the line. While there is some judgement involved in drawing the line, the same estimate can be repeated by independent analysts to about ± 0·5 db.

The other source of difficulty in the MPS-4 measurements was a severe oscillation in the system response at short ranges, resulting from a faulty component which could not be replaced until the last working day (8 August), and which caused the receiver response to vary by as much as 7 db as the range changed by only 150 yd. The peaks in

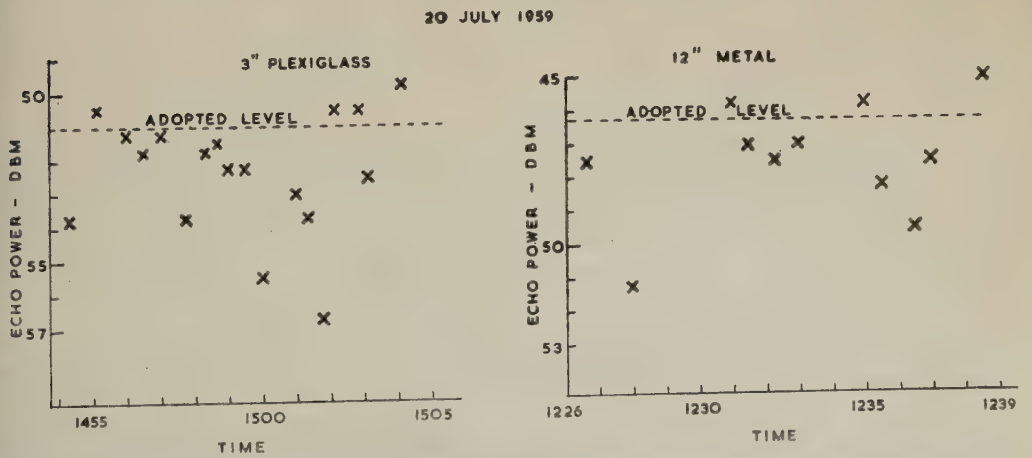

Figure 2. Sample MPS-4 measurements of echo intensity from the indicated targets in decibels below 1 milliwatt. The dashed lines indicate the levels adopted as the true echo intensities. See text for details.

the response curve were spaced about 300 yd. apart in range. Since the echo pulses were approximately 250 yd. wide, the strongest portion of the echo would appear at that range at which the receiver response was a maximum within the 250 yd pulse width. Thus it was not possible to use a series of measurements unless we were reasonably sure that the echoes from both the reference sphere and the unknown target occurred at identical ranges, and preferably on the same peak in receiver response. Roughly half the MPS-4 measurements were discarded on this basis. The oscillation in the receiver sensitivity is probably responsible for part of the scatter in the MPS-4 measurements. However, by using maximum signals for both the unknown and reference targets, the accuracy of the measurements which we have selected as valid is not seriously affected.

3. Results

(a) *Metal spheres*

Perhaps the best test of the overall accuracy of our methods arises from the results obtained with a set of accurately machined aluminium spheres 1, 2 and 3 in. in diameter. The cross-sections of such spheres are well established. The data from the TPS-10 are listed in Table 2. The MPS-4 measurements on the metal spheres were unacceptable because when these heavy targets were flown with the reference sphere even a light wind drew the balloon so far from the tethering point that the awkard range fluctuations. mentioned above were unavoidable. Individual measurements of the cross-section and their means are listed as an indication of their reproducibility. The theoretical cross-sections were obtained from Kerr (1951, p. 453, Fig. 6.1). The last column gives the decibel ratio of the average measured cross-section (σ_m) to that indicated by theory (σ_t).

TABLE 2. Measured and theoretical radar cross-sections of metal spheres (TPS-10, 3·31 cm)

Sphere Diameter D (in.)	Sphere Area πr^2 (cm^2)	Cross-sections (cm^2) Measured Individual data			Mean	Theory	10 log σ_m/σ_t (db)
3	45·6	77·7	76·5	73·3	75·8	55·2	+ 1·37
2	20·7	45·8			45·8	26·5	+ 2·38
1	5·07	10·1	10·2	9·6	9·97	9·28	+ 0·30

There appears to be a definite tendency for the measured cross-sections to exceed those indicated by theory. In Fig. 3, we have plotted the measured cross-sections against the theoretical values. Since all measurements were made with respect to the 12 in. sphere with $\sigma = 730$ cm^2, this point is established on the curve with zero error. If there were no systematic errors in our measurements we should expect the values to fall along the solid curve. The reproducibility of the measurements indicated in Table 2 does suggest some sort of systematic error, although the single measurement on the 2 in. sphere leaves this point in doubt. The dashed curve in Fig. 3 may, therefore, be used as an approximate calibration curve to indicate the true cross-section corresponding to any measured value. Since it is difficult to see how systematic errors of this sort can arise except as a result of an error in the test-set attenuator, we have placed scales of true and measured attenuation on the top and right side of Fig. 3. We shall use this calibration curve later to correct our results.

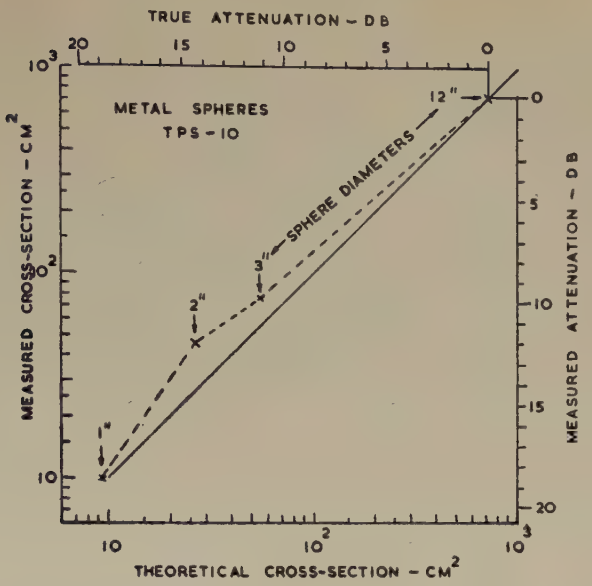

Figure 3. Measured versus theoretical cross-sections for metal spheres with the 3·31 cm TPS-10.

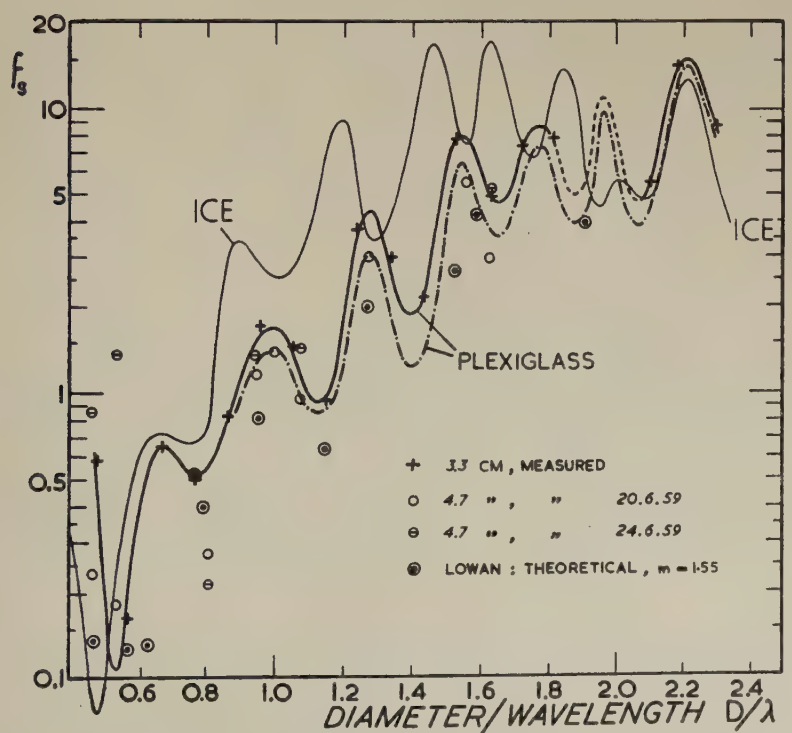

Figure 4. Normalized back-scatter cross-section f_s of plexiglass spheres ($m = 1{\cdot}6$) as measured by the TPS-10 and MPS-4. Heavy solid curve is based on TPS-10 measurements before correction. Dot-dash curve is corrected according to ' calibration ' of Fig. 3. The thin solid curve is that for ice taken from Fig. 5 while the circled dots are theoretical values for $m = 1{\cdot}55$ according to Lowan (1949).

(*b*) *Plexiglass (perspex) spheres*

Plexiglass (perspex) has an index of refraction $m = 1{\cdot}60$. Because this is so close to that of ice, we used a set of machined plexiglass spheres as a control. 20 such spheres were manufactured with diameters ranging from $\frac{5}{8}$ to 3 in. in $\frac{1}{8}$ in. steps. The results of measurements with these targets are shown in Fig. 4.

Most of the points in Fig. 4 represent individual measurements. In the case of the TPS-10 (3·31 cm) an 'individual' measurement is the mean of a series of perhaps 10 observations made in a period of about 15 min. The MPS-4 measurements were obtained in the manner already described. The 3·31 cm points for $D/\lambda = 1{\cdot}53$ and 2·30, corresponding to the 2 and 3 in. diameter spheres, represent the means of 4 and 5 measurements respectively, made during the month of tests. In both cases the individual values fell within $\pm$ 0·6 db of the means, indicating good reproducibility. Where there were two measurements made at 4·67 cm, both are plotted. These fall within $\pm$ 1·2 db of the mean, except for the two smallest values of D/λ, where the small signal strengths made the measurements rather more inaccurate.

The ringed dots in Fig. 4 represent theoretical values of f_s computed from Lowan's tables (1949) for $m = 1{\cdot}55$. These generally fall slightly below the measured values for plexiglass, as might be expected in this region of D/λ. For comparison we have also superimposed the ice ($m = 1{\cdot}78$) scattering curve taken from Fig. 5. The portion of the ice curve for $D/\lambda < 1{\cdot}25$ is due to Ryde (1946). The remainder of the curve is based on our measurements. By reference to both the ice-scattering curve and the theoretical values for $m = 1{\cdot}55$, we have been able to fit quite a reasonable curve to the plexiglass measurements. The dotted portion of the curve in the vicinity of $D/\lambda = 2$ is in doubt because of the lack of data there. However, it seems reasonable to expect another peak of about the indicated magnitude and position in this region.

The back-scatter curve has been drawn to fit the uncorrected TPS-10 data quite closely. However, we have seen in Fig. 3 that the measured cross-sections of the metal spheres tended to be slightly too high. We have therefore used the 'calibration' curve in Fig. 3 to reduce the measured cross-sections of the plexiglass spheres accordingly. The portion of the curve which has been corrected in this manner is shown by the dot-dash curve in Fig. 4. This modification of the curve brings it in closer accord with the 4·67 cm measurements, and is in slightly better agreement with the theoretical values for $m = 1{\cdot}55$. Except for the minimum at $D/\lambda = 1{\cdot}4$ which seems rather too low, possibly as a result of over-correction, we must assume that the corrected curve is closely representative of the true values of f_s for plexiglass.

Note that the plexiglass scatter curve crosses the ice curve in the vicinity of $D/\lambda = 2$; beyond this point it appears that plexiglass, with smaller refractive index, is a better scatterer than ice. We shall later see a similar cross-over for particles of $m = 2{\cdot}0$ and 1·78 (Fig. 5). Also of interest is the phase shift of the peaks and minima on the plexiglass curve from those for ice, the peaks of one corresponding closely to the minima of the other.

It is striking that the scattering curve reaches a peak value $f_s = 13{\cdot}9$ at $D/\lambda = 2{\cdot}22$. This implies that a plexiglass sphere of diameter 7·35 cm at $\lambda = 3{\cdot}31$ cm has a cross-section of 590 cm^2, equivalent to that of a metal sphere of diameter 27·4 cm.

(*c*) *Ice spheres, dry*

The ice spheres were manufactured by freezing water in hollow rubber balls of several centimetres internal diameter, and then cutting the ball away from the ice. Intermediate sizes were obtained by melting larger spheres in a warm-water bath. The shapes were not perfectly spherical, but in no case did the diameters of a single stone vary initially by as much as 5 per cent. The spheres were stored in a deep-freeze box and transferred on the day of use to a portable cold box containing dry ice. When they were brought into the open air, a thin coating of frost formed on them, which persisted without melting

for periods of up to about 15 min, so that scattering measurements could readily be made while they were completely dry.

The complete results for ice spheres with a dry surface are presented in Fig. 5. The TPS-10 measurements have been corrected according to the calibration curve in Fig. 3. For comparison, we have plotted the theoretical scattering curve for ice computed by Ryde (1946) for values of D/λ up to 1·25, and the theoretical values furnished by Herman and Battan (1959). A few theoretical values for $m = 2{\cdot}0$, taken from Lowan's tables, are also shown. The measurements are generally in remarkably good accord with the theoretical values. Before receiving the data of Herman and Battan we had sketched in a reasonable (dashed) curve which was based solely on the measurements (the portion drawn as a dotted line was in doubt because of absence of measurements). This empirical back-scatter curve is in excellent agreement with the calculations of Herman and Battan, excepting only those at $D/\lambda = 2{\cdot}04$ and 2·36, and we have not altered it. For $D/\lambda < 1{\cdot}0$, the measured values are generally too high, approaching the theoretical ones for $m = 2{\cdot}0$. In view of the possible experimental errors, especially for the small values of σ associated

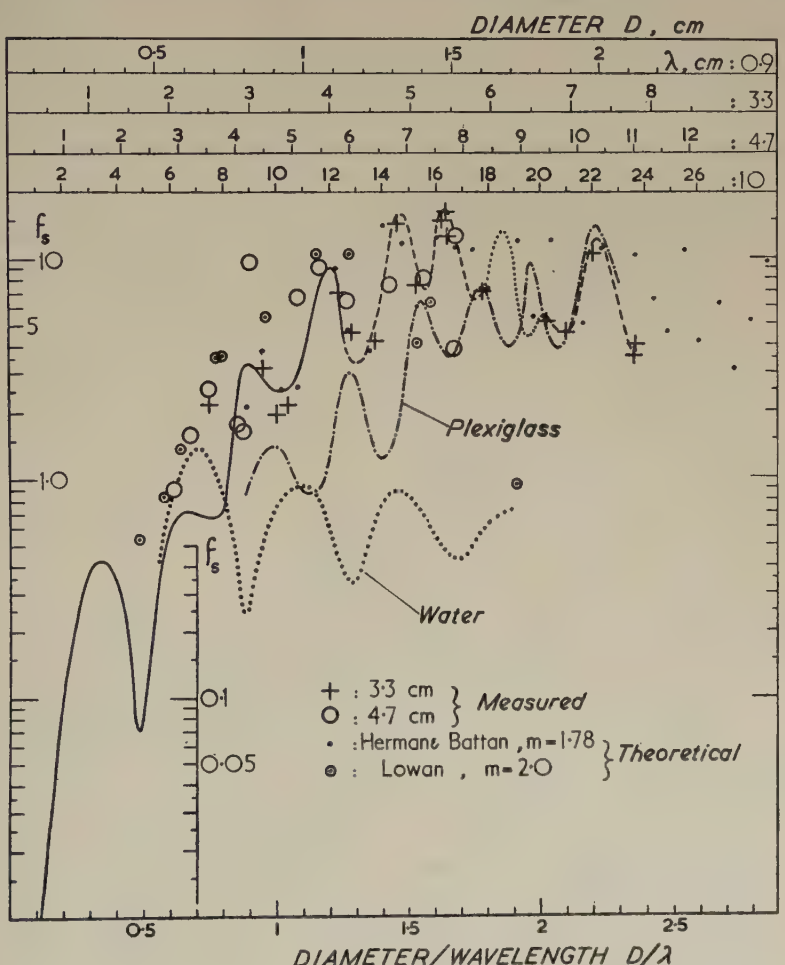

Figure 5. Normalized back-scatter cross-sections $f_s = \sigma/(\pi D^2/4)$ of ice spheres with $m = 1{\cdot}78$ as measured by the TPS-10 and MPS-4. The solid part is based on theoretical computations by Ryde (1946). The dashed part is based entirely on the measurements; dotted portion in doubt. Theoretical values computed for ice by Herman and Battan (1959) are shown by dots while corresponding values for $m = 2{\cdot}0$ are taken from Lowan (1949). Scales at top represent sphere diameters at indicated wavelengths. Scattering curves for plexiglass and liquid water spheres are also shown.

with low echo intensities not far above the receiver noise level, there is no evidence to indicate any significant discrepancy between theory and measurement. Rather, we consider the measurements as a good confirmation of the theoretical calculations. Where they differ, we must accept the theoretical values.

It is to be noted that the theoretical scattering cross-sections for $m = 2{\cdot}0$ exceed those for ice for values of D/λ up to about 1·4, where they suddenly fall below the ice cross-sections. This behaviour is to be expected from existing knowledge of the total extinction cross-sections for non-absorbing spheres. Since, in this case, the extinction is due entirely to scattering, we may expect the total scattering cross-section and the back-scatter to vary in roughly the same manner with D/λ. However, this is only qualitatively true since the distribution of scattered energy with scattering angle is also a function of D/λ, i.e. the fraction of the energy scattered back per unit solid angle is not constant. Nevertheless, it is interesting that the extinction curves presented by Van de Hulst (1957, p. 151) show similar crossings, although at smaller values of D/λ. Indeed, the general behaviour of the back-scatter curves for $m = 2{\cdot}0$, 1·78, 1·6 and 1·55 which are shown in Figs. 4 and 5, is qualitatively similar to that of the total extinction curves for a similar range of refractive indices.

(*d*) *Melting ice spheres*

In the portable cold chamber the ice spheres attained a uniform temperature which varied from about − 30°C to − 60°C. After one has been brought into the open and weighed a frost coat forms (equivalent to a melt-water shell 1 or 2 × 10^{-2} cm thick), and 10-15 min later melting begins. From wind-tunnel experiments we find that even at the centre of a sphere the temperature reaches within several degrees of 0°C before the first

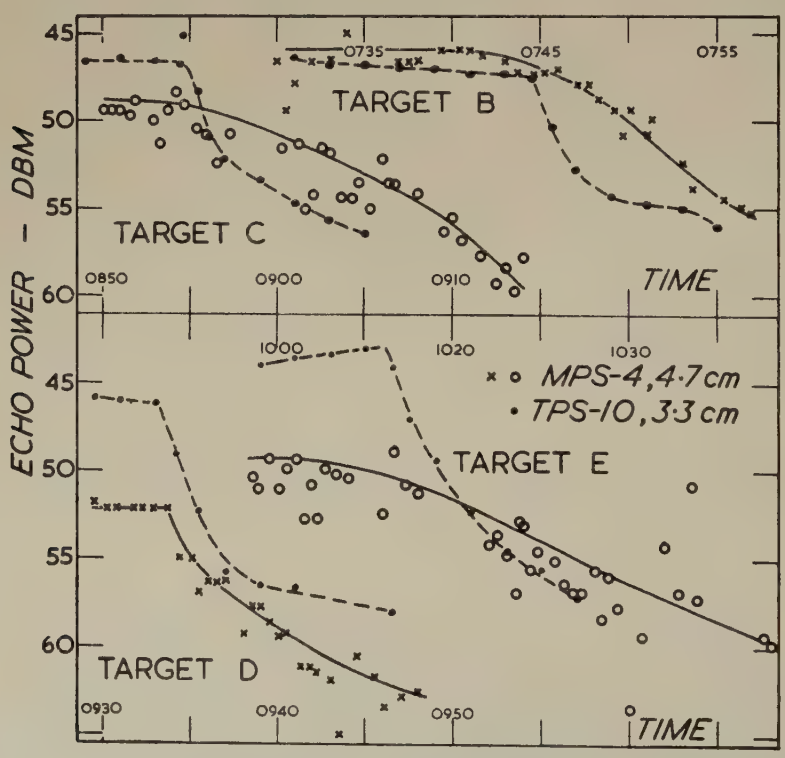

Figure 6. Simultaneous echo intensity measurements with the TPS-10 and MPS-4 from four large melting ice spheres on 8 August, 1959. Initial radii are B – 3·90 cm; C – 3·33 cm; D – 2·95 cm; E – 3·63 cm. These targets correspond to those similarly marked in Figs. 7 and 9.

drip of melt-water forms, irrespective of the initial temperature in the range — 30 to — 60°C. Consequently the melting fairly closely obeys the simple relation

$$a_0^2 - a^2 = kt \quad . \quad . \quad . \quad . \quad . \quad (3)$$

(where a is the radius of the ice sphere at time t after the start of the melting, a_0 is the initial radius, and k is a constant), except during the melting-away of an outermost shell of thickness about 3×10^{-2} cm during the first several minutes : the initial melting rate is only about one-third that indicated by the equation when k is determined from a change of size during a longer period. Further, we find in the laboratory that the thickness of the liquid film on an unventilated melting (and dripping) ice sphere is only $1{\cdot}0 \times 10^{-2}$ cm.

Fig. 6 contains selected back-scattering measurements, which show that after an initial period of fairly consistent measurements the signals decrease : abruptly at 3·3 cm, more slowly but more persistently at 4·67 cm. This decrease is associated with the onset of melting.

The spheres were weighed before they were raised as targets, and again when they were lowered 20-30 min later. Measuring values of the average radii and assuming the melting commences when the 3·3 cm signals begin to decrease, we obtain values of k in Eq. (3) varying from 0·07 to 0·17 cm^2 min^{-1}. The period for the formation of the complete water coat would then be 20-60 sec using the equation, but probably 1-3 min in practice.

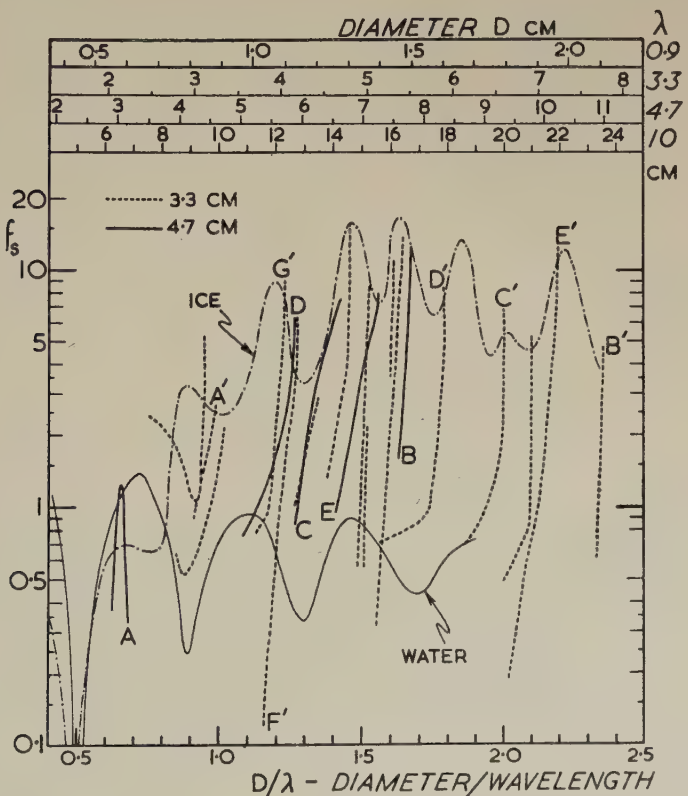

Figure 7. Variations of the normalized back-scatter cross-sections $f_s = \sigma/(\pi D^2/4)$ during melting at 3·3 and 4·67 cm. The ice curve (dot-dash) is taken from Fig. 5. The water curve is after Aden (1951). Curves marked by symbols are those referenced in text. Primed and unprimed symbols are measurements for the same particle at 3·3 and 4·67 cm respectively. Scales at top represent sphere diameters at indicated wavelengths. The water curve is not accurate at a wavelength of 0·9 cm.

In Fig. 7 all the scattering measurements made during meltings are plotted as values of f_s against D/λ, together with the scattering curves for ice spheres (from Fig. 5) and all-liquid spheres (Aden 1951*). The scattering cross-sections fall sharply from values near the all-ice curve to final values close to the all-water curve. Since Eq. (3) was used to compute D, the steepness of the curves should be even greater initially, but the final values are accurate.

There are two interesting features where $D/\lambda < 1$. First, two of the 3·3 cm curves show an initial fall, but then *rise* parallel to the all-water curve which rises as D/λ further decreases. Secondly, the one 4·67 cm curve shown† *rises*, as could be anticipated, from rather below the ice curve to a peak on the all-water curve, and then falls in sympathy with the all-water curve (the actual measurements are shown in Fig. 8; at 3·3 cm the signal falls steadily, because the same sphere lies in a different D/λ region – at both wavelengths the change as melting begins is towards the all-water value). Clearly, in this region of D/λ the development of a liquid coat can *increase* the scattering cross-section.

In the region where $D/\lambda > 1$ the cross-sections continue to decrease even after the time required to establish a complete melt-water coat. Moreover, in Fig. 7 there are five spheres whose final cross-sections fall below the all-water curve : two spheres (E', F') are so far below that the difference must be considered significant. This might be because a certain thickness of coat acts as a resonant shell or interference filter, trapping the entering radiation, because of liquid-filled cracks and cavities in the ice, or to irregularities of shape (one diameter of particle E' was 14 per cent smaller than the other two on its return to the ground).

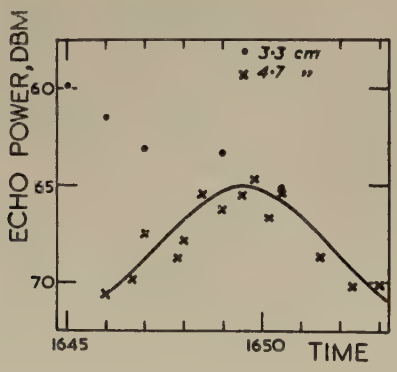

Figure 8. Basic measurements at 3·3 and 4·67 cm for melting ice sphere *A* in Fig. 7.

To improve the demonstration of the effect of progressive melting and compare the 3·3 and 4·67 cm observations, the data for the four particles of Fig. 6 have been re-plotted in Fig. 9; here the ordinate σ/σ_0 is the fraction of the initial or dry-state cross-section, and the abscissa Δa is the change in radius according to Eq. (3). We see that at 3·3 cm there is a substantial decrease in the cross-section during the growth of the melt-water coat (thickness 1×10^{-2} cm, corresponding, for reasons already given, to $\Delta a \approx 3 \times 10^{-2}$ cm). In all cases the 3·3 cm signal decreased by 6 db or more, whereas at 4·67 cm the corresponding decrease in two of the four cases was only 2-3 db. The measurements at 3·3 cm are more consistent, and overlooking the peculiar results for E' (on Fig. 7 this is a particle whose final cross-section lies well below the all-water curve) we have drawn around them a reasonable envelope.

* Aden's curve was computed for a wavelength of 16·23 cm and a temperature of 20°C, but is sufficiently accurate for all wavelengths down to 3 cm and temperatures of 0°C, if $D \geqslant 0{\cdot}3\ \lambda$. The ratio of Aden's cross-sections to those at 3·2 cm and 0°C is approximately the ratio of the asymptotic values given by Eq. (2), or 0·64/0·614 = 1·04.

† In general the changes at 4·67 cm were erratic, the scatter in the measurements usually exceeding the greatest difference – 3 db – between the ice and all-water curves for $D/\lambda < 0{\cdot}8$.

When the cross-sections have decreased to approximately the all-water values, we should expect further melting to change the cross-section in agreement with the trend of the all-water curve in Fig. 7. Neglecting the fluctuations, σ is roughly proportional to (πa^2); when, therefore, the radius of an ice sphere becomes 3·3 cm, about the average size of the particles in Fig. 9 when $\Delta a = 0{\cdot}3$ cm, a further decrease of 0·1 cm should produce a decrease of about 0·2 db in σ. We see from the figure that the 3·3 cm curves do tend eventually to this slope.

Nevertheless, over most of their length the curves are much too steep for their trend to be explained simply by the shrinking of the particles. Similarly the 4·67 cm measurements, although less consistent, also show a total change in cross-section of about 10 db, spread over a much longer time than is required to establish a liquid coat. In other words, the particles look more and more like water although no water can accumulate on the surface to a depth greater than 10^{-2} cm. We conclude that somehow liquid is accumulating in greater amount than is needed to form the coat, probably in sub-surface cracks or cavities, either by percolation from the surface or by internal melting. Minute cracks are almost certainly produced in our artificial hailstones during their production because of strains set up by the expansion of the interior, which was the last part to freeze. Their presence may also be inferred from the ' cracking ' noises which were sometimes heard

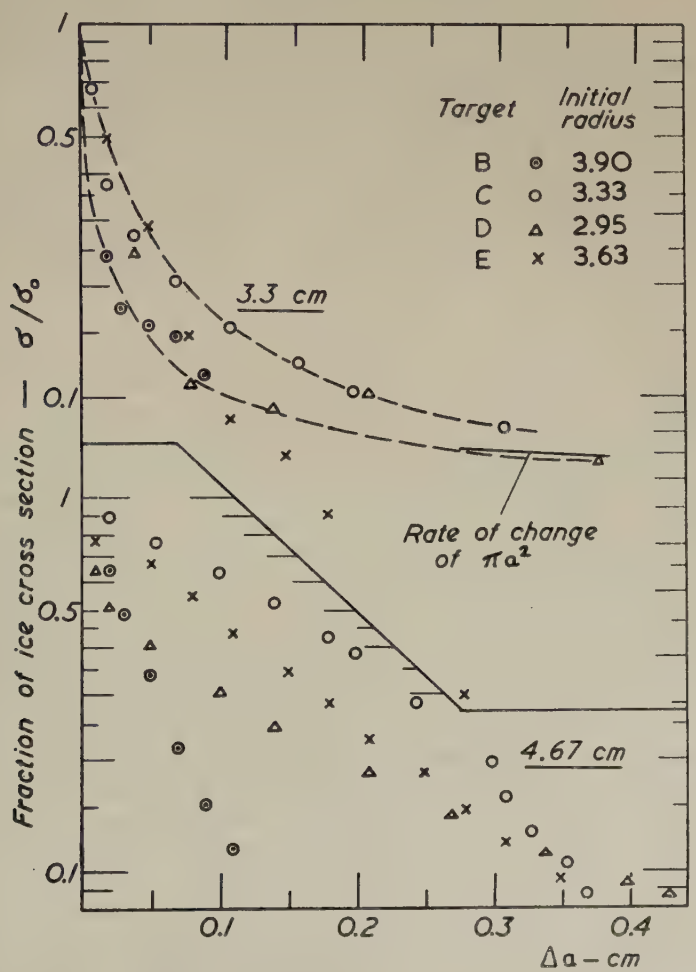

Figure 9. Measured fractional decrease in the initial (dry) cross-section of a melting ice sphere versus calculated change in its radius. Symbols correspond to particles in Figs. 6 and 7.

when the artificial hail was placed in a warm-water bath for the purpose of reducing their size. On one occasion a water-filled cavity was found near the top of a large ice sphere when it was brought to the ground.

This is the only reasonable explanation which we can offer for the rather odd and inconsistent behaviour of the 4·67 cm scattering cross-sections and their differences from those at 3·3 cm. First of all, since the absorption coefficient of water is greater at 3·3 cm than at 4·67 cm, we expect radiation of the shorter wavelength to be affected the more strongly by a thin water coat. This is apparent from the relative changes in σ at the two wavelengths as a function of time in Fig. 6 and as a function of change of size due to melting in Fig. 9. At 3·3 cm the building of the water shell to a maximum thickness of about 10^{-2} cm appears to account for the major reduction (approximately 6 db) in cross-section, while this thickness of coat has a rather small effect at 4·67 cm. At 3·3 cm therefore, what happens below this water shell is of substantially less importance than at 4·67 cm. At the latter wavelength the rate of change of σ appears to depend largely on how fast water is accumulating in sub-surface cracks or cavities below the outer shell of water. Thus the variations in the number and size of cracks or cavities from one particle to the next could readily account for the wide variations in the 4·67 cm σ/σ_0 curves in Fig. 9, which occur despite the similarity in size of the original ice spheres. Indeed, this may also explain why some of the smaller ice particles showed no significant change in scattering cross-section as melting progressed : these may not have contained cracks.

This is not to say that the effect of cracks is negligible at 3·3 cm. In fact, it is the only reasonable means of explaining the continued fall in σ in Fig. 9, at a rate substantially in excess of the rate of decrease in particle sectional area, after the water coat has reached its maximum thickness. This is evidenced also by the 3·3 cm melting curves marked F′ and G′ in Fig. 7. When the associated spheres diminish to a size such that $D/\lambda = 1{\cdot}2$, and presumably have acquired a water coat of maximum thickness, G′ shows a cross-section 5·6 db greater than F′. This could occur only if sphere F′ did in fact contain the greater amount of liquid water. Perhaps extensive liquid-filled cracks or cavities in this sphere are responsible for its cross-section falling so far below the all-water curve.

4. Discussion

Experience has shown that it is hazardous to attempt to apply a simple physical picture to the scattering mechanism. Certainly the rigorous Mie scatter theory is so complex as to defy a simple physical representation. On the other hand, while the theory of geometric optics lends itself to reasonable physical models, it does not provide exact solutions to the scattering problem in the region of $D \simeq \lambda$. In the case of metal spheres, the solutions given by geometric optics and the Mie theory converge with increasing D/λ so that the former is sufficiently accurate for $D/\lambda \geqslant 6$. Thus, it is not unreasonable to use geometric optics to provide some physical insight into the cause of the large back-scatter cross-section for ice when $D/\lambda > 1$.

Consider first a large metal sphere. Its cross-section is determined essentially by the specular reflection from the first Fresnel zone; i.e. the surface area intercepted by cutting a plane perpendicular to the sphere diameter (along the direction of propagation) a distance $\lambda/4$ in from the surface. The reflection is entirely a surface phenomenon; it is of no consequence whether the sphere is hollow or solid. This is due to its large conductivity, which manifests itself as an extremely large absorption coefficient; i.e., imaginary part of the refractive index. Furthermore, for a large sphere we may remove the half of the sphere obscured from the radar without affecting its cross-section.

Although the absorption coefficient of water in the microwave region is much smaller than that of metal, we find that the back-scatter curve for water spheres is essentially a downward displacement of that for metal by an amount given by Eq. (2). It appears, therefore, that the absorption coefficient of water is sufficiently large to make the reflection essentially a surface phenomenon. Our radar measurements of melting ice spheres confirm this, although the water surface must have some finite thickness. The shorter the

wavelength, the higher the absorption coefficient and the thinner the water shell required. Eq. (2) indicates that at 3·2 cm 61 per cent of the incident power is reflected from the front surface (where that surface is perpendicular to the direction of propagation). At other angles the reflected energy is even greater. The 39 per cent of the incident power which enters the surface is rapidly absorbed. At 3·2 cm, the power decays to 10 per cent in a water depth of only 2 mm. Thus only 3·9 per cent of the power incident on the surface penetrates to a depth greater than 2 mm. We must infer from this and especially from our 3·3 cm measurements that it matters little what is contained within the water shell, at least for the larger spheres with which we are concerned. It is apparent also, as with metal, that we could remove the back-half of the sphere without reducing its radar cross-section. It is the front surface which largely determines the reflection.

On the other hand, ice has a negligible absorption coefficient. The reflection from the front surface of a large ice sphere is one-eighth of that from an equal water sphere and one-thirteenth of that from an equal metal sphere. Thus a major part of the incident energy enters the sphere. None of this energy is absorbed in penetrating the ice. Instead it is partially focused as in a lens and reaches the back surface with an increased power density. The energy partially reflected from the back surface is concentrated further due to its concavity toward the radar. Thus in the case of ice we conclude that the reflection from the back surface is significantly greater than that from the front. Indeed, it is greater by an order of magnitude than the reflection from the convex front surface of a metal sphere. Interference of the phase-shifted large reflection from the back surface with the smaller reflection from the front may be responsible for the humps in the scatter curve. In addition, with larger real refractive index (and no absorption) optimum focusing on the back surface will be attained with smaller spheres, thus accounting for the shift in the peak of the scatter curve toward lower D/λ which was noted for the refractive indices of 1·55, 1·60, 1·78 and 2·0.

It is of special interest to compare the ice cross-sections to that of a dielectric Luneberg lens (Peeler and Coleman 1958). By tapering the refractive index with radial distance r in the sphere according to the law $m = [2 - (r/R)^2]^{\frac{1}{2}}$ where R is the radius of the lens, a plane wave incident on the front surface is brought to a perfect focus on the back surface. A small spherical segment of metal placed at the focal point on the back surface then ensures that all the energy is reflected along reciprocal paths. Practical radar targets have been built on this principle whose radar cross-sections are phenomenally greater than their geometric sizes. For example a 3 in. (7·62 cm) diameter Luneberg lens has a radar cross-section of 3 ft^2 (2,800 cm^2) while a 1 ft diameter lens has a cross-section of 700 ft^2 at 3·2 cm*. By comparison, our results indicate that a 3 in. ice sphere has a 3·3 cm cross-section of 270 cm^2. While the analogy between an ice sphere and the Luneberg lens is not rigorous, it does demonstrate the effects of partial focusing in the ice and reflection by the back surface. Since the power reflection from the ice surface is 1/12·7 (Eq. 2), the cross-section of our 3 in. ice sphere might be enhanced by somewhat less than a factor of 12·7 if we were to place a metal cap at the back surface. Then its cross-section would approach that of the 3 in. Luneberg lens mentioned above, an indication of the efficiency of focusing by the ice.

If our qualitative interpretation is correct, it may be noted that the partially focused energy escaping from the back surface is 12·7 times that reflected. Thus if this surface were largely responsible for the back scatter, we might expect the forward scatter cross-section to be slightly less than 12·7 times the back scatter cross-section. This is supported by reference to Lowan's (1949) computations for refractive indices of $m = 1{\cdot}55$ and 2·0, which bracket that of ice. These indicate that a 3 in. ice sphere would have a forward scatter cross-section of about 3,000 cm^2.

The large back-scatter cross-sections of ice spheres with dry surfaces and the effects of wetting which have been reported here have interesting implications in the interpretation of radar observations of hailstorms. However, these are so extensive as to be appropriately left to a future paper.

* Emerson and Cumming, Inc., Canton, Massachusetts.

Note : Since completion of this paper, Herman and Battan of the University of Arizona have extended their theoretical computations on the electronic computer to the case of water-coated ice. Preliminary results for just two hail diameters, 2·87 cm and 6·6 cm, have been forwarded to us privately. An 0·01 cm thick water-coat decreases the 3 cm dry cross-sections of these stones by about 6 db and 4 db respectively, in very satisfactory accord with our deductions.

Acknowledgments

We are pleased to thank the Director-General of the Meteorological Office for the provision of staff and facilities at the East Hill Radar Station. The research on severe storms of which this work is a part is also supported by the Geophysics Research Directorate, Air Force Cambridge Research Center of the Air Research and Development Command, United States Air Force, through its European Office. W. C. Macklin is indebted to the Commonwealth Scientific and Industrial Research Organization of Australia for the support of studies including this work. The authors are especially grateful to Dr. S. C. Mossop of the South African Council for Scientific and Industrial Research for his contributions to both the experiments and their analysis, and to the following personnel who participated in the experiments : Messrs. N. Coupe, A. E. Denham, and J. G. D. Beimers of the East Hill Radar Station; Messrs. P. Petrocchi and P. J. Harney of the U.S. Air Force Cambridge Research Center, and Mr. K. Browning of Imperial College. Mr. P. Thompson of Imperial College made the wind-tunnel experiments.

References

Aden, A. L. 1951 'Electromagnetic scattering from metal and water spheres,' *J. Appl. Phys.*, **22**, p. 601.

Atlas, D. and R. J. Donaldson 1954 'The feasibility of the identification of hail and severe storms,' *Air Force Surveys in Geophysics, No. 65*, A.F.C.R.C., pp. 91.

Donaldson, R. J. 1958 'Vertical profiles of radar reflectivity in thunderstorms,' *Proc. 7th Wea. Radar Conf.*, Univ. of Miami, p. 8. (Amer. Met. Soc., Boston.).

1959 'Analysis of severe convective storms observed by radar – II,' *J. Met.*, **16**, p. 281.

Gunn, K. L. S. and T. W. R. East 1954 'The microwave properties of precipitation particles,' *Quart. J. R. Met. Soc.*, **80**, p. 522.

Herman, B. M. and L. J. Battan 1959 'Calculations of Mie back-scattering of microwaves from ice spheres,' *Sci. Rep. No. 12, Inst. Atmos. Phys.*, Univ. Arizona

Kerr, D. E. 1951 *Propagation of short radio waves, M.I.T. Radiation Lab. Series*, **13**, (McGraw-Hill, New York), p. 452.

Lowan, A. N. 1949 *Tables of scattering functions for spherical particles, Appl. Math. Series*, **4**. Nat. Bureau Standards, Washington.

Peeler, G. D. M. and H. D. Coleman 1958 'Microwave stepped-index Luneberg lens,' *Trans. Inst. Radio Engs., Antennas and Propagation*, **AP-6**, p. 202.

Ryde, J. W. 1946 'The attenuation and radar echoes produced at centimetre wavelengths by various meteorological phenomena,' *Meteorological factors in radio-wave propagation*, (Phys. Soc., London).

Van de Hulst, H. C. 1957 *Light scattering by small particles*, (John Wiley, New York).

551.511.6 : 551.524.4 : 551.551.8 : 551.558.1

Control of inversion height by surface heating

By F. K. BALL

C.S.I.R.O. Division of Meteorological Physics, Aspendale, Victoria, Australia

(Manuscript received 1 February 1960)

SUMMARY

Viscous dissipation is inadequate to account for the destruction of all the thermal turbulence generated by upward transfer of heat in a deep convection layer. It is suggested that the surplus turbulent kinetic energy is destroyed by buoyancy forces in a region of *downward* transfer of heat in the upper part of the convection layer. This process is associated with mass transfer downwards through the convection (or subsidence) inversion and also with an upward movement of the inversion, though the latter may be overcome by sufficiently strong subsidence. A simple theory of the process is developed and the results deduced thereby agree well with observations of the diurnal variation of inversion height in Central Australia.

1. INTRODUCTION

When the ground is strongly heated by solar radiation, convective mixing occurs in the lower part of the atmosphere. The mixed layer may be several kilometres deep and within it the vertical temperature gradient is very close to dry adiabatic, provided condensation does not take place. Next to the ground, while the heating is in process, there is a shallow layer (often less than 30 m deep) which is markedly superadiabatic. The mixed layer is frequently surmounted by a sharp inversion or a well defined stable layer, which may have been formed solely by the convective mixing of the layers below, or, more frequently, results from the sharpening of a pre-existing inversion which has limited the vertical extent of the convection columns. Winter and summer examples of such convection layers are shown in Fig. 1. These soundings were made in the early evening when the nocturnal inversion is already evident.

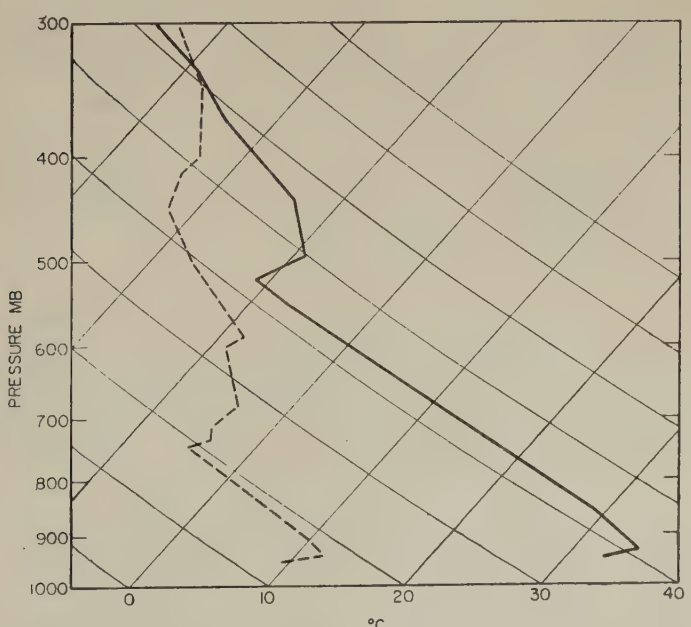

Figure 1. Examples of convection layers at Giles, Central Australia.
——— 1130 GMT 8 Jan. 1958 (Summer example).
– – – – – 1135 GMT 9 July 1957 (Winter example).

A similar situation occurs in oceans and lakes where an almost isothermal layer extends from near the water surface to the beginning of the thermocline. This layer is usually assumed to be maintained by the mechanical mixing action of the wind. It seems probable that in many locations convection currents caused by nocturnal and evaporational cooling of the water surface play a significant part.

Experiments which have a direct bearing on these phenomena were carried out by Rouse and Dodu (1955). Their experimental liquid consisted of saline water underlying pure water, the two layers being each of constant density and separated by a sharp 'inversion.' When turbulent kinetic energy was generated mechanically in the upper layer by means of an oscillating wire grid, the inversion surface migrated downwards through the water. Tests showed that the underlying salt water remained undiluted, whereas the fresh water became increasingly saline throughout its depth by the mixing of entrained salt water from the lower layer. The entrainment appeared to take place by filaments drawn out from the sharp tops of waves in the inversion surface.

It seems likely that generation of turbulent kinetic energy in the saline water would have resulted in the *upward* migration of the inversion and the dilution of the saline layer, the fresh water remaining uncontaminated. It can be shown that the equations determining the motion are unchanged if the system is inverted and the sign of the density anomaly reversed, provided this anomaly is everwhere small. It is also likely that the results would be similar if the turbulent kinetic energy were generated thermally by the vertical convective transfer of heat rather than mechanically by an oscillating wire grid. In fact it will be indicated subsequently that thermal turbulence is likely to be more effective in this respect than mechanical turbulence (at least in the atmosphere).

2. The generation of turbulence

Consider now the generation of turbulence within a dry adiabatic layer surmounted by a sharp inversion. In the lower atmosphere turbulent kinetic energy is mostly generated either by wind shear (mechanical turbulence) or by upward transfer of heat (thermal turbulence). The rate of generation per unit volume by wind shear can be written $\tau_x \partial u/\partial z + \tau_y \partial v/\partial z$. Thus most of the mechanical turbulence is generated close to the ground where the vertical velocity gradients are large. Furthermore, the spectrum of eddy sizes which are created in this way is proportional to the spectrum of eddies which contribute to the shearing stress. Near the ground these eddies are small, i.e. a few metres or tens of metres in characteristic size.

If we assume that, in the planetary boundary layer, geostrophic and pressure-gradient forces are balanced by internal friction, then the relevant form of the equations of motion is:

$$\rho f (v - v_g) = -\frac{\partial}{\partial z}\tau_x \qquad (1)$$

$$\rho f (u - u_g) = \frac{\partial}{\partial z}\tau_y \qquad (2)$$

Where u_g, v_g are the components of the geostrophic wind and f is the Coriolis parameter. When the geostrophic wind is independent of height the rate of generation of mechanical turbulence per unit volume can be written:

$$G = \tau_x \frac{\partial}{\partial z}(u - u_g) + \tau_y \frac{\partial}{\partial z}(v - v_g)$$

which by virtue of Eqs. (1) and (2) reduces to:

$$G = \frac{\partial}{\partial z}(\boldsymbol{\tau} \cdot (\mathbf{V} - \mathbf{V}_g)) \qquad (3)$$

Thus, by integration of Eq. (3) the total generation of mechanical turbulence in a layer

can be expressed in terms of the values of wind and shearing stress at the upper and lower boundaries.

Integrating from the surface upwards we find

$$\int_0^z G\,dz = \boldsymbol{\tau} \,.\, (\mathbf{V} - \mathbf{V}_g) + \boldsymbol{\tau}_0 \,.\, \mathbf{V}_g \quad . \quad . \quad . \quad (4)$$

and if at a height h *either* τ is negligible *or* the wind is close to geostrophic, then the total generation of mechanical turbulent kinetic energy below that height is given by

$$\int_0^h G\,dz = \boldsymbol{\tau}_0 \,.\, \mathbf{V}_g \quad . \quad . \quad . \quad . \quad . \quad (5)$$

Typical daytime values, in the conditions of strong convection with which we shall mainly be concerned, are $V_g = 10$ m sec^{-1} and $\tau_0 = 1$ dyne cm^{-2}, whence $\boldsymbol{\tau}_0 \,.\, \mathbf{V}_g$ is about 10^3 g sec^{-3}.

The rate of generation of turbulent kinetic energy by vertical heat transfer in the atmosphere is given by $H\,g/C_p\,T$ where H is the upward turbulent flux of heat (Richardson 1920). It can be shown that this expression is valid when the turbulence is ' buoyant,' i.e. when the inequality $S \geqslant 0{\cdot}27\,E/p$ is satisfied, where E is the turbulent kinetic energy per unit volume, p is the pressure and S^2 is the mean square percentage deviation of density (or temperature), given by $S^2 = \overline{(\rho'/\bar{\rho})^2}$. This inequality is always satisfied in the lower atmosphere. In a convection layer of the type under discussion, H probably decreases roughly linearly with height to zero near the inversion and the rate of generation is therefore still appreciable near the middle of the layer. Furthermore, the spectrum of eddies created by heat transfer is proportional to the spectrum of eddies which contribute to the flux. These eddies, particularly near the middle of a deep convection layer, are much larger than those generated by mechanical turbulence near the earth's surface.

The rate at which thermal turbulence is generated throughout the layer is :

$$\int_0^h \frac{H\,g}{C_p\,T}\,dz \simeq \tfrac{1}{2}\,\frac{H_0\,gh}{C_p\,\theta_0}$$

where H_0 is the vertical turbulent flux of sensible heat at the surface and θ_0 is the potential temperature (assumed independent of height) in the convection zone. A typical summer daytime value for H_0 in clear weather, over dry ground, is 20 mw cm^{-2}. If we take h equal to 3 km then we have $H_0\,gh/2C_p\,\theta_0 = 10^4$ g sec^{-3}.

It is clear from the preceding discussion that there are at least three important differences between the generation of mechanical turbulence and the generation of thermal turbulence *in a deep convection layer*. These are summarized below :

(i) There is a difference in location. Mechanical turbulence is generated mainly in the surface layers whereas thermal turbulence is generated throughout a much deeper layer.

(ii) There is a difference in quality. Mechanical turbulence is small scale (metres to tens of metres) whereas thermal turbulence is large scale (hundreds of metres to kilometres).

(iii) There is a difference in quantity. The total rate of generation of mechanical turbulence is typically only about one-tenth of the total rate of generation of thermal turbulence.

3. The dissipation of turbulence

The two processes of most importance in the destruction of turbulent kinetic energy, are molecular viscous dissipation and downward turbulent transfer of heat. Viscous dissipation operates appreciably only on very small eddies; large eddies must be broken down into sufficiently small eddies before being dissipated by viscous forces. The small-scale mechanical turbulence near the earth's surface is therefore more readily destroyed by this process than is the larger-scale convective or thermal turbulence which occurs

throughout most of the convection layer. Indeed, there is evidence to support the view that the bulk of the turbulence generated mechanically near the earth's surface is destroyed *locally* by viscous forces (Taylor 1952).

During the night a surface inversion usually develops. Such inversions are formed largely by the turbulent transfer of heat down towards the ground which is being cooled radiatively, though direct radiative cooling of the air layers themselves also plays a part (Rider and Robinson 1951). The downward turbulent transfer of heat must be accompanied by the destruction of turbulent kinetic energy. Thus buoyancy forces and viscous forces combine to destroy mechanical turbulence generated at night in the surface layers, and *local* destruction of turbulent kinetic energy is more completely assured than it is during the day. If it is assumed that kinetic energy is handed down the scale of eddy sizes, it follows that the eddies destroyed by buoyancy at night cannot be larger, and are probably appreciably smaller, than those created by wind shear. This conclusion agrees with the observed large contribution of rapid fluctuations to the nocturnal heat flux (see, for example, Priestley 1959).

It still remains to explain the means by which the large-scale thermal turbulence is dissipated. If this energy were largely dissipated by molecular viscosity then the molecular viscous dissipation per unit mass would be about 30 erg g^{-1} sec^{-1}, implying fairly intense small-scale turbulence throughout the convection layer. Because the energy is being supplied to large eddies and there is little or no geometrical constraint on the turbulent motions (except in the surface layers) it is to be expected that the inertial subrange will be broad. The velocity structure function should obey the two-thirds power law up to separations of about 100 m or more, i.e.

$$\overline{[w(x) - w(x+r)]^2} = \tfrac{4}{3}(2\epsilon r)^{\frac{2}{3}}$$

(see, for instance, Batchelor 1950) where ϵ is the viscous dissipation and r the separation. The autocorrelation of Jones (1957) does in fact indicate a two-thirds power law up to a separation of about 140 m at a height of 2,000 ft. The viscous dissipation estimated from this autocorrelation is about 5 erg g^{-1} sec^{-1}. Furthermore, Charnock (1951) gives values of ϵ as low as 0·3 and 0·4 erg g^{-1} sec^{-1} between 1 and 2 km on a clear summer afternoon with a windspeed of 3·6 m sec^{-1}.

The remarks in the preceding paragraph suggest, though they do not prove, that viscous dissipation is only responsible for the destruction of a small part of the kinetic energy of thermal turbulence. The experiments of Rouse and Dodu (1955) indicate another way in which turbulent kinetic energy can be destroyed; namely by buoyancy forces associated with the turbulent mixing accompanying the migration of an inversion. In the simple incompressible case the kinetic energy that is lost appears as the increase of gravitational potential energy implied by the change in inversion height. If a similar process occurs in a larger scale in the atmosphere, then warm air from above the inversion is entrained by the convection circulations. The mixing of this warm air results in a *downward* transfer of heat in the upper part of the convection layer. Thus turbulent kinetic energy is created by the upward transfer of heat in the lower part of the convection layer and destroyed by the downward transfer of heat in the upper part of the convection layer.

The changes in temperature and inversion height implied by these processes are considered in detail in the following sections. There are also implications concerning the turbulent structure, two of which will be briefly mentioned here.

Firstly, as a consequence of the continuous transfer of energy down the scale of eddy sizes, the turbulence which is being destroyed in the upper part of the convection layer will have a smaller scale than that which is being created beneath. One is therefore led to expect a slightly stable layer containing relatively small-scale turbulence beneath the inversion. Certainly slight stability in the upper part of a convection layer is frequently observed though there appear to have been no measurements of the scale of turbulence in this region.

Secondly, as a consequence of the spatial separation of the layers of creation and destruction of turbulent kinetic energy there must be a considerable upward flux of turbulent kinetic energy near the middle of the convection layer. That this is indeed the case has long been known to sailplane pilots and balloonists, who have usually found marked turbulence in the ascending air of thermals and relatively smooth conditions elsewhere. These conclusions are also supported by the observations of Jones and Butler (1958).

4. Simple theory

We can now formulate a simple theory which predicts, among other things, the rate at which an inversion will rise in dry convection conditions. The lapse rate in the convection layer is assumed to be dry adiabatic; a convenient though not an essential assumption which is in close accord with observation. We have seen that in a typical case the rate of generation of mechanical turbulence (i.e. by wind shear) is only about one-tenth of the rate of generation of thermal turbulence and that a high percentage of this mechanical turbulence is dissipated by viscosity. We therefore assume that mechanically generated turbulence is negligible or is completely destroyed by viscous forces. Furthermore, in order to avoid confusing the physical picture and increasing the complexity of the mathematical equations, radiative absorption and emission within the convection layer and viscous dissipation of thermal turbulence are neglected. The qualitative effects of these processes are mentioned briefly where they are thought to be of importance. They will be considered in detail elsewhere. Finally it is assumed that the inversion is a perfect discontinuity of temperature separating the dry adiabatic convection layer from the more stable region above.

In the absence of viscous dissipation and radiative transfer, the principle of conservation of potential heat (Ball 1956) states that the rate of increase of potential heat is equal to the convergence of the turbulent flux of potential heat, i.e.

$$\frac{C_p}{g}\frac{d\theta}{dt} = \frac{\partial F}{\partial p} \quad . \quad . \quad . \quad . \quad . \quad (6)$$

where F is the upward vertical turbulent flux of potential heat. This equation depends on the neglect of pressure fluctuations and the conditions for its validity are similar to, though not identical with, the conditions for the validity of Richardson's equation mentioned in Section 2.

At a similar level of approximation we also have

$$F = H\left(\frac{p_0}{p}\right)^{\frac{\gamma-1}{\gamma}} \quad . \quad . \quad . \quad . \quad (7)$$

where H is the vertical flux of sensible heat. Integration of Eq. (6) from p to p_0 and substitution for F using Eq. (7) yields :

$$H = \left[H_0 - (p_0 - p)\frac{C_p}{g}\frac{d\theta}{dt}\right]\left(\frac{p}{p_0}\right)^{\frac{\gamma-1}{\gamma}} \quad . \quad . \quad . \quad (8)$$

This equation is important since it enables one to determine (using Richardson's equation) not only the total generation of thermal turbulent kinetic energy but also the way in which the rate of production is distributed vertically throughout the layer. We leave this last consideration aside for the moment and determine the total generation of turbulent kinetic energy in the convection layer :

$$\int_{p_1}^{p_0}\frac{H}{C_p\rho T}\,dp = H_0\left\{1 - \left(\frac{p_1}{p_0}\right)^{\frac{\gamma-1}{\gamma}}\right\} + \frac{C_p p_0}{g}\frac{d\theta}{dt}\left[\left(\frac{\gamma-1}{2\gamma-1}\right)\left\{1 - \left(\frac{p_1}{p_0}\right)^{\frac{2\gamma-1}{\gamma}}\right\} - \left\{1 - \left(\frac{p_1}{p_0}\right)^{\frac{\gamma-1}{\gamma}}\right\}\right] \quad . \quad (9)$$

where p_1 is the pressure at the inversion at the top of the convection layer. Returning to Eq. (8) we see that the heat flux at the top of the layer is

$$H_1 = \left[H_0 - (p_0 - p_1)\frac{C_p}{g}\frac{d\theta}{dt}\right]\left(\frac{p_1}{p_0}\right)^{\frac{\gamma-1}{\gamma}} \quad . \quad . \quad . \quad (10)$$

and Eq. (9) can be written :

$$H_0 - H_1 - \frac{C_p}{g}\int_{p_1}^{p_0}\frac{dT}{dt}\,dp = \int_{p_1}^{p_0}\frac{H}{C_p\rho T}\,dp \quad . \quad . \quad . \quad (11)$$

Therefore the gain in kinetic energy is equal to the loss in total heat as shown by Normand (1946). The corresponding equation for potential heat is readily derived by integrating Eq. (6) throughout the depth of the convection layer or by consideration of the potential heat balance of the whole convection layer. The result is :

$$F_0 - F_1 - \frac{C_p}{g}\int_{p_1}^{p_0}\frac{d\theta}{dt}\,dp = 0 \quad . \quad . \quad . \quad (12)$$

Eqs. (11) and (12) are not essential to the main argument and have merely been introduced to show firstly that the present analysis is not inconsistent with Normand's equation and secondly that total heat is not conserved in the same sense as is potential heat.

The heat flux at the top of the convection layer is related to the rate of entrainment of warm air, i.e.

$$H_1 = \frac{C_p\,\Delta\theta}{g}\frac{dp_1}{dt}\left(\frac{p_1}{p_0}\right)^{\frac{\gamma-1}{\gamma}} \quad . \quad . \quad . \quad . \quad (13)$$

where $\Delta\theta$ is the inversion strength. Both H_1 and dp_1/dt are negative. The quantity $-g^{-1}\,dp_1/dt$ is the rate at which mass is being added to the convection layer by entrainment.

The rate of generation of thermal kinetic energy per unit mass is $gH/C_p\rho T$. During one hour at this rate (with $H = 20$ mw cm^{-2}), 25×10^4 cm^2 sec^{-2} would be generated corresponding to a root mean square turbulent velocity of 5 m sec^{-1}. This value considerably exceeds the typical turbulent intensity in a convection layer. In fact, of course, the turbulence reaches quasi-equilibrium at a lower intensity and the kinetic energy changes are small. Furthermore, we shall largely be concerned in subsequent applications with the change from morning to late evening, the thermal turbulence being small at both these times and the difference being even smaller. It is therefore assumed that the changes in kinetic energy are negligible and consequently that the left-hand sides of Eqs. (9) and (11) are zero.

We now have the two Eqs. (9) and (10) relating the three quantities H_0, H_1 and $d\theta/dt$; H_1 as we have seen being proportional to the entrainment. Either H_1 or $d\theta/dt$ can be eliminated, thus expressing $d\theta/dt$ or H_1, in terms of H_0 the heat input at the base. Results derived by manipulating these equations in their exact form are rather cumbrous. The essential features of the physical process are indicated with sufficient accuracy by much simpler approximate forms of the equations. Let us put p_1/p_0 equal to $1 - \Delta p/p_0$ (where Δp equals $p_0 - p_1$). The quantity $\Delta p/p_0$ is rarely as great as one-half and usually appreciably less. By expanding various terms in powers of $\Delta p/p_0$ and approximating we find :

$$\frac{C_p\,\Delta p}{2g}\frac{d\theta}{dt} \simeq H_0 \simeq -H_1 = -\frac{C_p\,\Delta\theta}{g}\frac{dp_1}{dt} \quad . \quad . \quad . \quad (14)$$

and from Eq. (8)

$$H \simeq H_0\left[1 - \frac{2(p_0 - p)}{\Delta p}\right] \simeq H_0\left(1 - \frac{2z}{h}\right) \quad . \quad . \quad (15)$$

where z is the height above the ground and h is the height of the convection layer.

On the basis of this simple model the heat gained by entrainment from above is equal to the heat supplied at the base. Also the heat flux diminishes linearly to zero at a height $h/2$ at variance with the assumption made in the initial qualitative discussion. In reality a part of the kinetic energy generated by buoyancy is destroyed by viscous forces. The depth of the layer of upward heat transfer, in which kinetic energy is generated, is therefore greater than $h/2$ and the heat flux vanishes at a height somewhere between h and $h/2$.

The more important qualitative implications of the preceding analysis can be summarized as follows. Surface heating causes convection currents which rise roughly to the height of the inversion and, broadly speaking, maintain a completely mixed state beneath the inversion. The turbulent convection columns spread out laterally beneath the inversion, these motions resulting in a continuous entrainment of warmer air into the circulating air in the convection layer. The effect of surface heating is therefore twofold :

(i) The air beneath the inversion increases in potential temperature because of the heating at the base and of the entrainment of warm air at the top.

(ii) The entrainment of upper air causes the inversion to *rise* relative to the air, i.e. there will be a mean transfer of mass *downward* through the inversion.

On the basis of the foregoing reasoning one would expect a continuous warming of the air beneath the inversion at an appreciably greater rate than is implied by direct surface heating. This warming is always partly, and sometimes largely, offset by longwave radiative cooling. For instance in midsummer a flux of 20 mw cm^{-2} for 12 hr would raise the temperature of a 450 mb layer (corresponding to a mean inversion height of 550 mb in Central Australia) by less than 2°C. If warming by entrainment is included this gives a total increase in temperature of about 3 to 4°C per day compared with a typical long-wave radiation loss of about 1°C per day. Both these quantities are variable and the latter is not known accurately. The cooling has little effect on the entrainment, except perhaps when the convection layer is shallow, but of course reduces the rate of increase of temperature by an amount corresponding to the loss of heat by longwave radiation. It is therefore difficult to compare theory with observation by using temperature measurements.

The tendency of entrainment and heating to cause the inversion to rise, weaken and finally disappear is countered by several processes. Firstly, the air above the inversion is nearly always stably stratified throughout a considerable depth and the entrainment process will therefore result in an apparent increase in the potential temperature of the air immediately above the inversion, thus tending to keep pace with the increase in potential temperature beneath and so maintain inversion strength. Secondly, horizontal divergence in the lower layers, accompanied by subsidence at inversion level, may be sufficient to counteract the rise by entrainment. Finally, the dry convection inversion usually slopes upward along the trajectories and thus advection tends to lower the inversion at a fixed point.

The last two points can be illustrated by a numerical example. If we take typical values $H_0 = 20$ mw cm^{-2}, $\Delta\theta = 5°C$, then we find that dp_1/dt is about -15 mb hr^{-1} corresponding to an upward movement of the inversion of about 150 m hr^{-1}. A mean horizontal divergence of 10^{-5} sec^{-1} in the lowest 3 km of the atmosphere would be associated with a *downward* movement of the same magnitude. Similarly a slope of one in 250 of the inversion surface with a wind of 10 m sec^{-1} directed upslope could entirely mask the effect of convection. A comparison between theory and observation must therefore either :

(i) make use of routine observations in a region where radiosoundings are combined with a sufficiently dense network of upper-wind measurements for horizontal divergences and inversion slopes to be estimated;

(ii) make use of special observations, e.g., ' inversion hopping ' by aircraft combined with special pilot-balloon ascents;

(iii) make use of routine observations and attempt to eliminate undesired effects statistically, e.g., perhaps by consideration of diurnal variations.

In the next section method (iii) is adopted to provide some comparison between observation and theory.

5. Diurnal variation of inversion height

During clear weather in summertime the net incoming radiation at the earth's surface is about 10^3 joules $cm^{-2} day^{-1}$, which, on the basis of Eq. (14), in regions where evaporation is small, would cause a decrease in pressure at the inversion of about 200 mb. Surface-wind variations and observations of small cumulus clouds suggest that large-scale convection activity becomes vigorous by late morning and starts to decrease rapidly an hour or two before sunset, i.e. roughly when the net radiation changes sign. Convection columns (' thermals ') are also useful for sailplanes for about the same period. Thus the vigour of convectional activity, even on a fairly large scale, closely follows the course of diurnal heating. The rise of 200 mb should therefore occur largely while the heating is taking place. If the processes which are tending to lower the inversion (notably subsidence and advection) operate uniformly throughout day and night and if this descent on the average compensates for the rise caused by convection, then there would be a diurnal variation in inversion pressure of about 100 mb.

An observation station suitable for the purpose of investigating such a diurnal variation must satisfy the following conditions :

(i) There must be a morning and evening radiosonde flight.

(ii) It must be in an arid zone with a high percentage of clear days.

(iii) There must be comparative freedom from ' synoptic disturbances.'

(iv) Not only must the station itself satisfy conditions (ii) and (iii) but so must the surrounding area for a distance of about 500 km (approximately the distance an air particle moves in 12 hr) particularly in the directions whence the air more frequently comes.

(v) A convection layer and convection inversion must be present sufficiently often.

The radiosonde station at Giles, Central Australia (lat. 25·02 S, long. 128·18 E) satisfies all the above requirements and is therefore particularly well situated for the study of dry convection. Radiosonde flights are made at 1130 and 2330 GMT. Diurnal variation is immediately apparent from casual inspection of the radiosonde data. Some examples from both winter and summer are shown in Figs. (2) and (3). Successive observations are

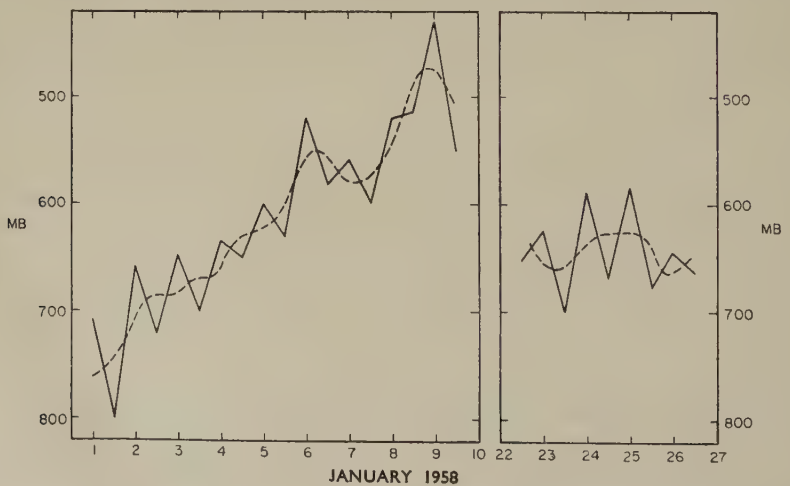

Figure 2. Examples of the diurnal variation of inversion pressure, midsummer at Giles, Central Australia.

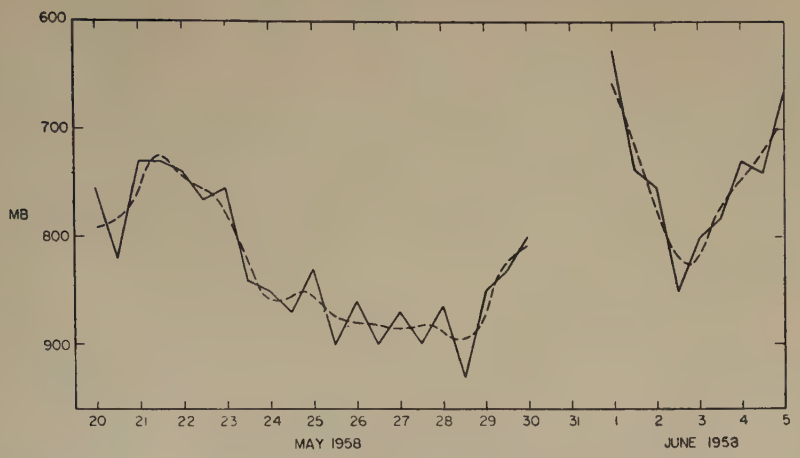

Figure 3. Examples of the diurnal variation of inversion pressure, late autumn and winter at Giles, Central Australia.

plotted and joined by straight lines, the dotted curves being drawn smoothly through the midpoints of the straight line segments in an attempt to illustrate the continuous movement of the inversion with the diurnal variation suppressed. Sequences such as these can be found for almost every month of the year. They are usually terminated either by the occurrence of cloud or the disappearance of the inversion.

Monthly means of the pressure at the inversion for the period July 1957 to July 1959 inclusive are shown in Fig. (4). There is a marked annual variation and the separation of the curves also indicates an appreciable diurnal variation throughout the year. All available dry convection data were used in calculating these means. This is probably satisfactory for determining the annual variation but introduces a considerable random element into the estimates of diurnal variation. Accordingly, the diurnal variation was recalculated considering only pairs of observations, both morning-evening and evening-morning pairs being used. This procedure gives double weight to observations that occur within a sequence by comparison with those that occur at the beginning or end of a sequence and isolated observations are discounted completely. The annual variation of the amplitude of the diurnal variation calculated in this way is shown in Fig. 5.

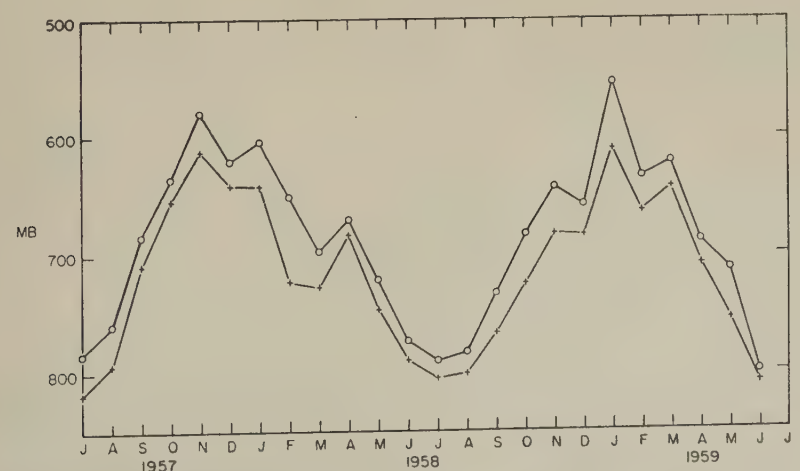

Figure 4. Mean monthly pressures at the dry convection inversion at Giles. ○ = 1130 Z, + = 2330 Z.

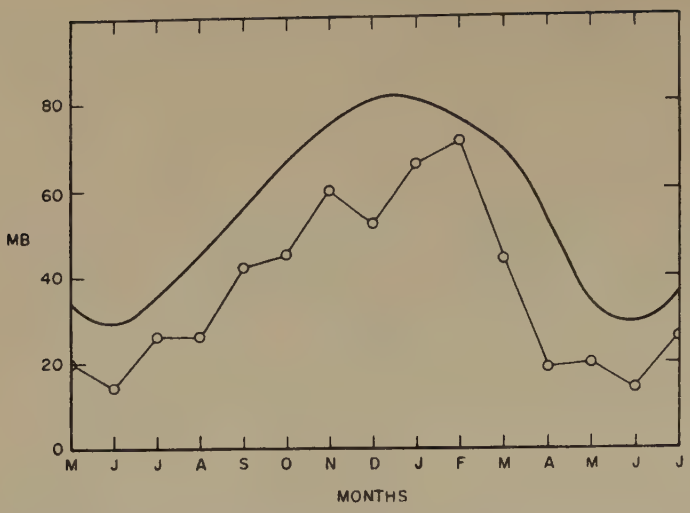

Figure 5. Annual variation of the amplitude of the diurnal variation of inversion pressure at Giles (○). The smooth curve represents the theoretical estimate based on Budyko's values for the net incoming radiation.

The upper smooth curve gives the theoretical estimate of the diurnal variation (using Eq. (14)) based on four-fifths of Budyko's (1955) values for the net incoming radiation and assuming $\Delta\theta = 5°C$. The remaining one-fifth of the incoming radiation is used in evaporation. This factor was derived from Albrecht's (1950) estimates of the natural evaporation. If one considers the uncertainties which are involved in the estimates of both curves then the agreement in form is surprisingly good. The observed diurnal variation is generally about 10 to 30 mb less than the predicted. Differences of this magnitude between the two curves are to be expected for various reasons, four of the more important reasons being :

(i) Viscous dissipation of thermal turbulence of 5 erg g^{-1} sec^{-1} could reduce the diurnal variation by 10 to 20 mb.

(ii) Uncertainties of one or two degrees centigrade in the value of $\Delta\theta$ could cause errors of 10 to 20 mb in either direction.

(iii) There is no reason to suppose that the morning and evening soundings at Giles exactly coincide with minimum and maximum inversion height. It is also probable that the degree of coincidence varies throughout the year.

(iv) The mean net incoming radiation (less heat used in evaporation) is not the most appropriate quantity to use in this connection. The observed values of the diurnal variation are strongly biased towards undisturbed sunny conditions, this bias being particularly important in spring and early summer when disturbed conditions are more frequent.

We can conclude from these observations that the air is being entrained through the convection inversion at a rate equivalent to a maximum rise of about 140 mb day^{-1} in summertime at Giles. If this convectional rise were nullified solely by subsidence then there would be descending velocities of about 2·5 km day^{-1} or 3 cm sec^{-1}. This value is rather larger than one would expect for a monthly average rate of descent and indeed, as we shall see, horizontal advection also lowers the inversion at Giles and we have no need to invoke such large subsidence rates.

Where the air crosses the Australian coast moving from sea to land, the inversion pressures are about 900 mb (Melbourne), 880 mb (Adelaide), 820 mb (Sydney) and 800 mb (Brisbane), whereas at Giles (Central Australia) the mean pressure at the inversion is 540 mb (the figures quoted here are means for January 1959). There must therefore be a typical gradient of about 200 mb in 1,000 km along the trajectories. It is probable that the steepest slopes occur in the first few hundred km after the air has crossed the coast

nd that, as a result, the gradient at Giles is rather less than the average along the trajectory - perhaps about 100 mb in 1,000 km. This magnitude of slope is also suggested by the Alice Springs observations (500 km from Giles) which give a mean pressure of 600 mb compared with the Giles mean of 565 mb (in the morning). On this basis advection would lower the inversion by about 90 mb day^{-1} when the wind speed at inversion height is about 10 m sec^{-1}. Thus on the quantitatively reasonable estimates of an advection lowering of 90 mb day^{-1} and a subsidence lowering of 50 mb day^{-1} a quasi-equilibrium would exist with a daily convection rise of 140 mb.

6. Extension to moist convection

The preceding theory can be applied directly and quantitatively to the dry convection layers which occur frequently over tropical and sub-tropical land areas. The process of entrainment will still occur in moist convection and the qualitative behaviour will presumably be similar. A shallow moist convection layer beneath the trade wind inversion is usually present over the tropical and sub-tropical oceans. It has already been suggested by J. Wyman (unpublished, but see Riehl *et al.*, 1951, p. 619) that continuous mass transfer (i.e., entrainment) occurs across the trade-wind inversion. Indeed such a transfer is necessary to account for the observed rise of the inversion along the trade-wind trajectories (horizontal convergence is inadequate). Wyman considers that clouds play an essential part in the entrainment process, whereas it is maintained here that the presence of moisture is by no means essential. It is also possible that the entrainment process occurs on a rather larger scale when there is deep convection up to the tropopause.

It is not proposed to develop, at present, a quantitative theory of moist convection. We will, however, consider the relative orders of magnitude of the contributions of latent and sensible heat transfer to the production of turbulent kinetic energy. Consider a small volume of moist air with vapour pressure e and absolute humidity ξ. The water-vapour density is $ape/p = ae/RT$, where a is the ratio of the specific gravity of water vapour to that of air ($a = 0{\cdot}622$). The density of the mixture (air at pressure $p - e$) is :

$$\rho = \frac{p-e}{RT} + \frac{ae}{RT} = \frac{p}{RT}\left[1 - \left(\frac{1-a}{p}\right)e\right].$$

Now the absolute humidity is $\xi = ae/p$ whence

$$\rho = \frac{p}{RT}(1 - b\xi)$$

where $b = (1 - a)/a = 0{\cdot}608$. If pressure variations are neglected then

$$\rho' = -\bar{\rho}\left(\frac{T'}{\bar{T}} + b\xi'\right)$$

and the rate of generation of kinetic energy is

$$-g\overline{\rho' w'} = g\bar{\rho}\left(\frac{\overline{w'T'}}{\bar{T}} + \overline{bw'\xi'}\right)$$

$$= \frac{gH}{C_p\bar{T}} + \frac{gbQ}{L} \quad . \quad . \quad . \quad . \quad (16)$$

where H and Q are the vertical turbulent fluxes of sensible and latent heat respectively. The relative importance of these two heat fluxes in the generation of kinetic energy depends on the dimensionless number $L/bC_p\bar{T}$ which has a value of about 15 when $\bar{T}$ is about 20°C. *Therefore the fluxes of latent and sensible heat are of comparable importance in the production of turbulent kinetic energy when the former is about 15 times the latter.*

According to Riehl *et al.* (1951) the mean values of the transfers for the months July to October 1945 inclusive at Pearl harbour in the North Pacific Trades are : latent heat 250 cal cm^{-2} day^{-1} and sensible heat 8 cal cm^{-2} day^{-1}. We see therefore that below condensation level in the Trades, the transfer of latent heat can be more than twice as effective as the transfer of sensible heat in creating turbulent kinetic energy. It might be expected that below cloud base, under these conditions, the convection columns consist of air moister rather than warmer than their surrounding and should perhaps be called ' moistals,' not ' thermals.'

7. Conclusions

An interesting and important feature of the theory presented in Section 4 is its freedom from semi-empirical concepts. The theory is greatly concerned with turbulent transfers yet no use whatever is made of ' K,' the eddy conductivity. Most of the assumptions are not essential to the theory but are merely made to reduce the complexity and make the results more clear cut. The analysis is readily extended to take account of viscous dissipation, radiative transfer, etc. In spite of (or perhaps because of) the simplicity and generality of the theory we have been able to make definite quantitative predictions, which agree well with observation, concerning the important phenomenon of mass transfer through the inversion. We have also made other predictions, the validity of which is as yet inadequately tested, concerning the characteristics of the turbulence in a convection layer.

The meteorological implications of the mass transfer or entrainment are considerable. For example, any dynamical study of the air motion beneath an inversion when surface heating is occurring, should take account of the transfer of mass and momentum through the inversion. It is possible that dynamic behaviour which is qualitatively, as well as quantitatively different, can occur in an ' entraining system.'

A further example which is perhaps of direct practical importance concerns the spread of pollutants. The entrainment mechanism acts as a ' valve ' as far as the movement of pollutants (or water vapour) is concerned. Thus material *beneath* the inversion cannot penetrate through it, whereas material *above* the inversion readily passes through and affects the whole convection layer. That this is generally true is shown by the frequent sharp ' cut-off ' of water vapour at the convection inversion. It is, however, probably not always true. There are occasions when middle tropospheric inversions appear to be associated with mechanical mixing *above* the inversion in which case the inversion will migrate downwards and pollutants will be able to pass upwards through the inversion but not downwards.

References

Albrecht, F. H. W.	1950	*Arch. Met. Geophys. Biokl.*, B, **2**, p. 23.
Ball, F. K.	1956	*Quart. J. R. Met. Soc.*, **82**, p. 15.
Batchelor, G. K.	1950	*Ibid.*, **76**, p. 133.
Budyko, M. I.	1955	' Atlas of heat balance,' Ministerial Council, U.S.S.R., Central Geophys. Observatory, Leningrad, p. 41.
Charnock, H.	1951	*Quart. J. R. Met. Soc.*, **77**, p. 654.
Jones, R. A.	1957	*Air Ministry Met. Res. Cttee., M.R.P.* No. 1044.
Jones, J. J. P. and Butler, H. E.	1958	*Quart. J. R. Met. Soc.*, **84**, p. 359.
Normand, C. W.	1946	*Ibid.*, **72**, p. 145.
Priestley, C. H. B.	1959	' Turbulent transfer in the lower atmosphere,' Chicago Univ. Press, p. 54 and p. 65.
Richardson, L. F.	1920	*Proc. Roy. Soc.*, A, **97**, p. 373.
Rider, N. E. and Robinson, G. D.	1951	*Quart. J. R. Met. Soc.*, **77**, p. 375.
Riehl, H., Yeh, T. C., Malkus, J. S. and La Seur, N. A.	1951	*Ibid.*, **77**, p. 598.
Rouse, H. and Dodu, J.	1955	*Houille Blanche*, J. Hydraulic Eng., No. 4, p. 530.
Taylor, R. J.	1952	*Quart. J. R. Met. Soc.*, **78**, p. 179.

551.551.2

The spectrum of vertical velocity near the surface

By H. A. PANOFSKY and R. A. McCORMICK
*Pennsylvania State University** *U.S. Weather Bureau*

(Manuscript received 8 February 1960)

Summary

Observations of a considerable number of vertical-velocity spectra are combined to show that under near-neutral and unstable conditions, the shape of the spectrum is essentially invariant up to heights of order 100 m, and the ' scale ' of turbulence is proportional to height within this régime.

A semi-empirical working hypothesis is suggested which relates the spectrum to wind speed, lapse rate, height and roughness.

1. Introduction

The spectrum of vertical velocity is of considerable interest owing both to its influence on air-borne structures, and its effect on diffusion of impurities in the atmosphere. Unfortunately, most of the observations refer to the spectrum of locally varying wind components, whereas space spectra are required for aircraft design, and Lagrangian spectra for diffusion calculations. In homogeneous turbulence, it is often satisfactory to identify spectra of time series with space spectra along the mean wind direction, subject to the condition that $k = n/V$, where V is the mean wind speed, k the wave number, and n the frequency. Recent evidence (see for example, Panofsky, Cramer and Rao 1958) has shown that this assumption is adequate over uniform, smooth ground for distances up to at least 90 m, although observations reported elsewhere (Lappe, Davidson and Notess 1959) show that the time spectra underestimate the magnitude of the spectra at low frequencies under less uniform conditions. Some experimental comparisons between Lagrangian and Eulerian spectra have also been made, but with less clear-out results (Hay and Pasquill 1959).

The remainder of this paper will combine observations of vertical velocity spectra in space and time. The ratio V/n will be considered as a ' wave length,' in accordance with the discussion above.

2. The shape of the spectra

Fig. 1 summarizes spectra observed at six widely different locations at heights ranging from 20 cm to 600 m. The observations at 15 m or below were made under conditions of varying stability; the observations above that level all refer to conditions of unstable stratification only.

Table 1 summarizes sources, observing conditions, sensing equipment and analysis techniques applied in the derivation of the data displayed in Fig. 1.

The ordinate in Fig. 1 is the product of spectral estimate and frequency, or the variance produced per unit logarithmic frequency increment. The abscissa is $f = nz/V$, where z is the height. This quantity can be interpreted as the ratio of height to wave length.

The most remarkable feature of Fig. 1 is that the shape of the spectra seems to be independent of stability, roughness, and wind speed. The position of the maximum on the f-scale shows no systematic shift with height, from 0·2 m to several hundred meters in unstable atmospheres. In other words, the wavelength domain of the turbulence contributing most strongly to the product of frequency and spectrum intensity of the vertical velocities is about four times the height above the surface. In stable air, this statement seems to be adequate up to about 15 m.

* College of Mineral Industries, Contribution No. 59-54.

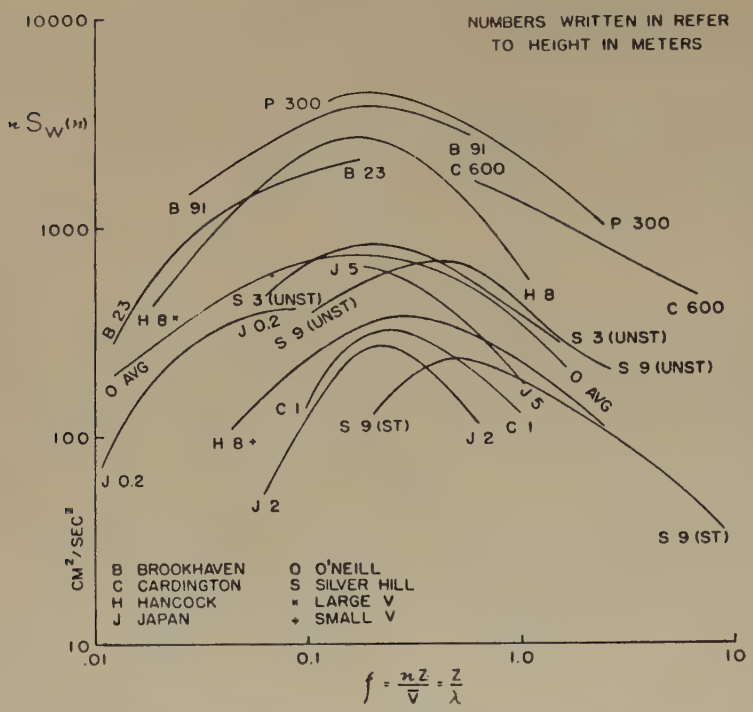

Figure 1. Product of frequency and spectrum estimates from many sources as function of reduced frequency f.

TABLE 1. SUMMARY OF CONDITIONS FOR FIG. 1

Location	Source	Instrumentation	Analysis technique
Brookhaven	Panofsky and Van der Hoven (1956)	Vanes	Digital
Cardington	Jones (1958)	Vanes on balloons	Digital
Cardington	Charnock and Robinson (1957)	Hot wire	Digital
Japan	Shiotani (1956)	Hot wire	Digital
Silver Hill	Unpublished	Sonic	Digital
O'Neill	Lettau and Davidson (1957)	Sonic	Analogue
Hancock	Unpublished	Sonic	Analogue

Location	Height m	Stability	Surface	Wind speed m sec^{-1}	Remarks
Brookhaven	23	unstable	brush and clearing	6	average of 3
Brookhaven	91	unstable	brush and clearing	8	average of 5
Cardington	300	unstable	grass land	7	average of 2
Cardington	600	unstable	grass land	7	average of 2
Cardington	1·2	unstable	grass land	2·5	relative magnitudes only
Japan	0·2	near-neutral	beach	4	5 pts. only
Japan	2	near-neutral	beach	5	5 pts. only
Japan	5	near-neutral	beach	5	5 pts. only
Silver Hill	9	unstable	city park	2	average of 4
Silver Hill	9	stable	city park	1	
Silver Hill	3	unstable	city park	2	average of 2
O'Neill	3-12	various	flat grass land	8	average of 9
Hancock	8	unstable	alfalfa	7	
Hancock	8	unstable	alfalfa	3	

Also, under these conditions, the general *shape* of the spectra seems to be about the same at all heights and all sites. The reason for this similarity is presumably that the low-frequency portion of the spectra is determined by the influence of the ground, whereas the high-frequency portion is governed by the energy input and the minus five-third power law of the inertial subrange.

The exact height up to which this simple structure of the vertical velocity spectrum is likely to persist probably depends on the degree of instability. Fig. 2 from Lappe, Davidson and Notess (1959) shows a series of spectra obtained in quite unstable air. The hypothesis that the spectrum as function of f is of invariant shape seems to hold up to somewhere between 150 and 250 m; above that level, the ' scale ' of turbulence appears more or less independent of height, the ' maximum ' occurring at a wavelength of about 1,000 m.

On the other hand, spectra determined from observations collected by Bunker from a slow plane in the tropics show that the simple model is adequate only up to 80 m; beyond that level, the scale seems to be independent of height.

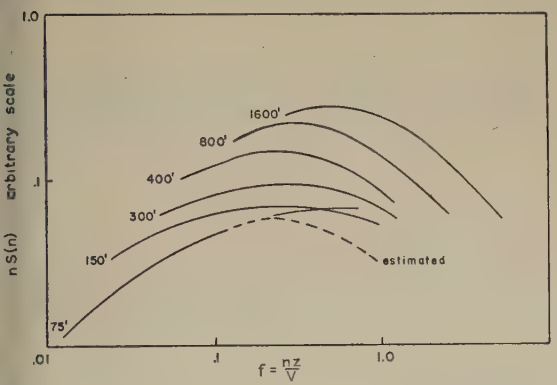

Figure 2. Product of frequency and spectrum estimates as function of reduced frequency at Brookhaven at various heights.

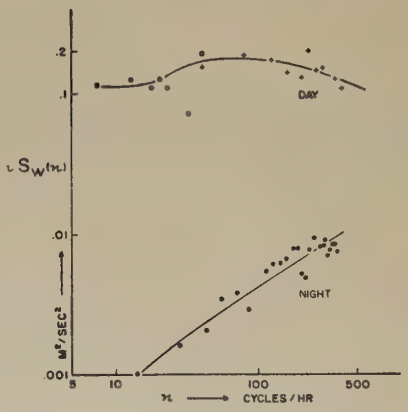

Figure 3. Product of frequency and spectrum estimates as function of frequency in stable and unstable air at 91 m at Brookhaven, Long Island.

From the few observations available in unstable air it seems that the layer in which the scale of vertical motions is proportional to height is the same layer in which the variance of vertical velocity increases upward. Bunker (1956) has shown that this layer extends from the ground up to 100 m in moderate instability, but may extend to 600 m in cold air over quite warm water, and, as shown by Fig. 1, may extend to 600 m also in an unstable airmass over land.

Above about 15 m, there exists a distinct difference between the energy distribution in stable and unstable air. This effect is demonstrated by Fig. 3 which contrasts two spectra at the same height, 91 m, with the same wind speed at that level, 7 m sec^{-1}. The figure demonstrates two important differences : firstly the total energy is much greater in unstable air (mainly because turbulent intensity decreases rapidly upward in stable air), and secondly, the energy in stable air is concentrated at greater frequencies than in unstable air. The reason for this is possibly that in stable air it is not the ground that limits the shape of the spectrum; rather the effect of stability is to compress the largest eddies vertically, as shown by the observation that the variance of vertical velocity is only one twentieth of that of the horizontal velocity. Thus, it is the absence of convection rather than the presence of the ground which determines the shape of the spectra at low frequencies.

3. Spectrum shape near the ground, and under unstable conditions

From the foregoing observational material, it is reasonable to describe the spectrum of vertical velocity, close to the ground, and higher up in unstable air, by :

$$n\,S_w(n) = \overline{w^2}\,g(f) \qquad . \quad . \quad . \quad . \quad (1)$$

Here, $\overline{w^2}$ is the total variance of vertical motion, n is the frequency and $S_w(n)$ the spectrum of vertical motion. $g(f)$ is a ' universal ' function of f such that $\int_0^\infty g(f)\,dh \ln f = 1$.

At least five different functions have already been suggested for $g(f)$, by Charnock and Robinson (1957), Inoue (1956), Deland and Panofsky (1957), Press (1957) and by Henry (1959). All these functions were found empirically, as interpolation formulae, to fit the known or assumed properties of spectra at high frequencies, low frequencies, or both.

Here, it will be assumed that $g(f)$ is of the form :

$$g(f) = \frac{4f}{(1+4f)^2} \qquad . \quad . \quad . \quad . \quad (2)$$

This function closely resembles that suggested by Charnock and Robinson, but is much simpler, and yields as good a fit to the data as the more complex expressions. Thus $S_w(n)$ the spectrum function, is given by :

$$S_w(n) = \frac{4\,\overline{w^2}\,z}{V\left(1+4\,\frac{nz}{V}\right)^2} \qquad . \quad . \quad . \quad . \quad (3)$$

At heights above the region of ground-controlled turbulence, Eq. (2) may still be adequate with $f = n\lambda/V$, where λ is a constant and equal to the height of the top of this region.

In order to estimate the vertical-velocity spectrum, it remains to study the variation of $\overline{w^2}$ with wind speed, stability, roughness and height.

4. The relation of variance to known parameters

A working hypothesis for the variance of vertical motion will be derived under the assumption that the variance is determined by height and by the rate at which turbulent energy is added to the system by convection and mechanical turbulence. Given these assumptions, the relation is developed by dimensional analysis, with the undetermined constants obtained by comparison with observations.

Let $\sigma_w = \sqrt{\overline{w^2}}$ be the standard deviation of vertical velocity. Then, under the assumptions, it can be of the form :

$$\sigma_w = A\,[z\,(\epsilon_1 + \delta\,\epsilon_2)]^{\frac{1}{3}} \qquad . \quad . \quad . \quad . \quad (4)$$

Here, A and δ are arbitrary dimensionless constants. ϵ_1 is the rate at which mechanical energy is added, $u_*^2\,\partial V/\partial z$, where u_* is the friction velocity, $\sqrt{\tau/\rho}$; τ is the surface stress and ρ the air density. ϵ_2 is the energy added by convection, $gH/c_p\,\rho T$ where g is the acceleration of gravity, T the absolute temperature, H the vertical heat flux and c_p the specific heat at constant pressure. The dimensionless quantity δ is introduced to allow for the possibility that convection is more efficient than wind shear in producing a vertical component of turbulence. There is no a priori reason why δ should be a constant; but the empirical results do not contradict this possibility over the range covered by the observations.

Substitution of the expressions for ϵ_1 and ϵ_2 into Eq. (4) yields, after some algebraic manipulations

$$\sigma_w = B\, u_* \left[S + \delta \frac{z}{L}\right]^{\frac{1}{3}} \quad . \quad . \quad . \quad . \quad (5)$$

Here, S is defined by: $(kz/u_*)\, \partial V/\partial z$, L is Monin's length, given by: $L = kgH/u_*^3\, c_p\, \rho T$ (independent of height), and B is the constant $Ak^{-1/3}$, where k is von Kármán's constant.

Under neutral conditions, L is infinite and S is unity, so that σ_w becomes equal to $B\, u_*$ and therefore independent of height. The constant B was determined from observations near the surface, or with large L, to be about 1·25.

The conclusion that the r.m.s. vertical velocity is proportional to the friction velocity is not new; it follows, for example, from similarity theory (Monin 1959a), and also from Businger's treatment (1959). However, Monin concludes from Perepelkina's data that B is 0·86, and Businger infers a value of unity. In view of the observations presented later, these estimates are believed to be too low.

As pointed out by Monin and Obukhov (1954), S is a universal function of z/L, say $\phi\,(z/L)$. Therefore:

$$\sigma_w = 1{\cdot}25\, u_* \left[\phi\left(\frac{z}{L}\right) + \delta \frac{z}{L}\right]^{\frac{1}{3}} \quad . \quad . \quad . \quad (6)$$

For practical purposes, u_* can most conveniently be determined from the fact that the logarithmic wind profile is valid at low levels even in non-neutral atmospheres. We can then write:

$$\sigma_w = 0{\cdot}51 \frac{V_1}{\ln \dfrac{z_1}{z_0}}\, h\left(\frac{z}{L}\right) \quad . \quad . \quad . \quad . \quad (7)$$

Here V_1 is the wind speed at a low height z_1 and $h\,(z/L)$ is the ' universal ' function $h\,(z/L) = [\phi\,(z/L) + \delta\, z/L]^{\frac{1}{3}}$. It has the property of being unity in a neutral atmosphere, or close to the ground.

In practice, measurements of L are rarely available, because they imply measured values of heat flux. Instead, it is convenient to introduce a quantity L' which is related to L by the condition that:

$$L = L'/P \quad . \quad . \quad . \quad . \quad . \quad (8)$$

where P is the turbulent Prandtl number, the ratio of the exchange coefficients for heat conduction to the eddy viscosity. L' is easily observable and is given by:

$$\frac{1}{L'} = \frac{kg\,(\gamma - \gamma_d)}{T\, u_*\, \dfrac{\partial V}{\partial z}} = \frac{g\,(\gamma - \gamma_d)}{T\, V_1\, \dfrac{\partial V}{\partial z}} \ln \frac{z_1}{z_0} \quad . \quad . \quad . \quad (9)$$

where γ is the lapse rate and γ_d the adiabatic lapse rate.

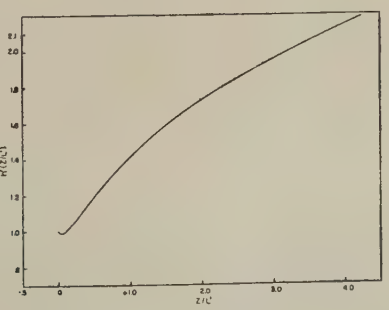

Figure 4. The function $h'\,(z/L')$.

In terms of L', we have :

$$\sigma_w = 1{\cdot}25\, u_* \left[\phi'\left(\frac{z}{L'}\right) + \frac{\delta P z}{L'}\right]^{\frac{1}{3}} = 0{\cdot}51\, \frac{V_1}{\ln \frac{z_1}{z_0}}\, h'\left(\frac{z}{L'}\right) \quad . \quad . \quad (10)$$

Fig. 4 shows the function $h'(z/L')$, making use of $\phi'(z/L')$ suggested by Panofsky, Blackadar and McVehil (1960), and taking $\delta P = 2{\cdot}4$. This numerical value was chosen to give the best fit to observations of variance at large z/L' obtained by Swinbank (1955) in Victoria. The slight decrease of $h'(z/L')$ in near-neutral unstable layers is almost certainly unreal. It is caused by the fact that according to the theory, the decrease of wind shear overbalances the increase in convective turbulence for small positive z/L'. At large z/L', of course, the convective effect predominates.

Figs. 5 and 6 show the variation of standard deviation of vertical velocity, σ_w, as function of the wind at 2 m in Victoria (see Swinbank 1955). Fig. 5 contains standard deviations at 1·5, 1·9 and 2 m, and Fig. 6, variances at 23 m and 29 m. On both figures, the theoretical equation for neutral conditions is entered : $\sigma_w = 0{\cdot}51\, V_1/\ln z_1/z_0$. z_0 was determined from wind profiles to be 1·5 cm. V_1 was taken as the wind at 2 m. In Figs. 5 and 6, situations with different Richardson numbers are indicated by different symbols.

It is clear that there is little effect of stability on standard deviations at low levels, as, indeed, is to be expected. The amount by which the theoretical standard deviations exceed the observed ones can be shown to be of the right order of magnitude to be caused by underestimates of the observed σ_w; at these low levels, a large fraction of high energy turbulence was smoothed out by the recording technique (Priestley 1959). At 29 m, on the other hand, the theoretical line fits well, on the average, the points with small convection; further, the points with large convection are consistent with the full Eq. (10), as indeed they should be in view of the fact that δ was determined to fit these data.

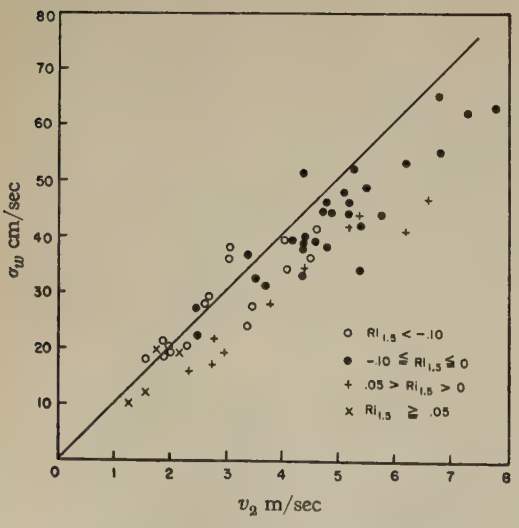

Figure 5. Standard deviation of vertical velocity at 2 m and below as function of wind speed at 2 m in Victoria, Australia. Richardson numbers estimated at 1·5 m. Solid line gives theoretical relation for neutral conditions.

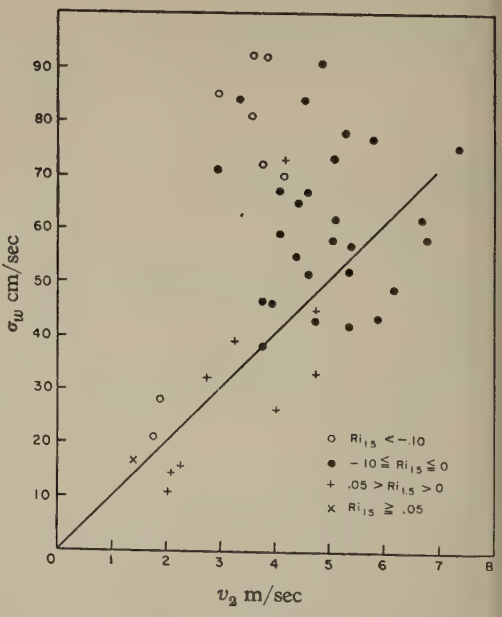

Figure 6. Standard deviation of vertical velocity at 23 m and 29 m as function of wind speed at 2 m in Victoria, Australia. Richardson numbers estimated at 1·5 m. Solid line line gives theoretical relation for neutral conditions.

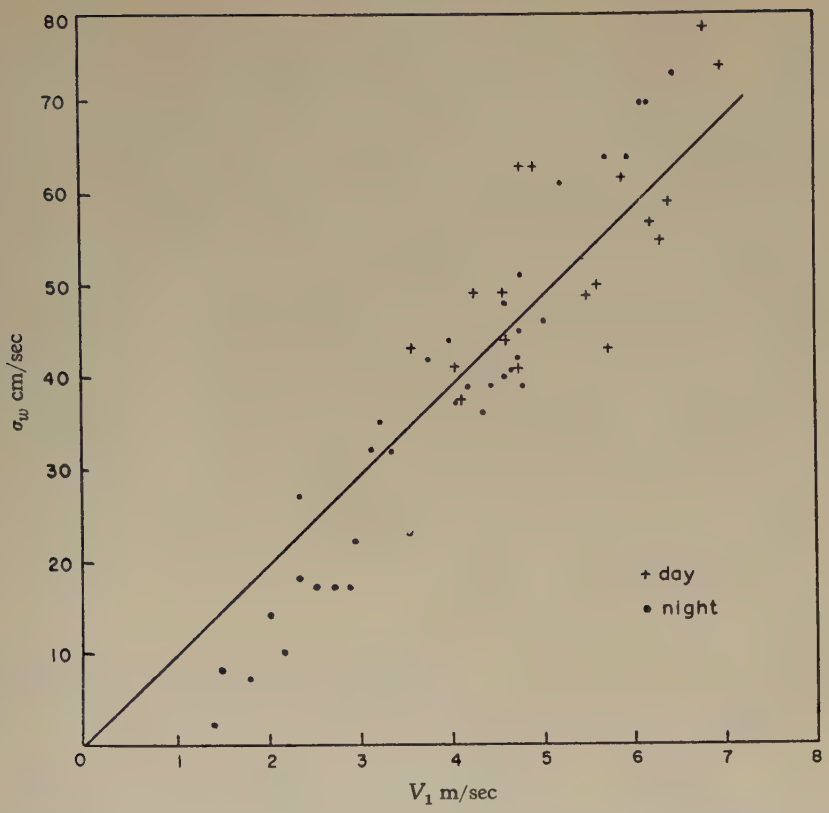

Figure 7. Standard deviation of vertical velocity at 12 m as function of wind speed at 1 m at O'Neill, Nebraska. Solid line gives theoretical relation for neutral conditions.

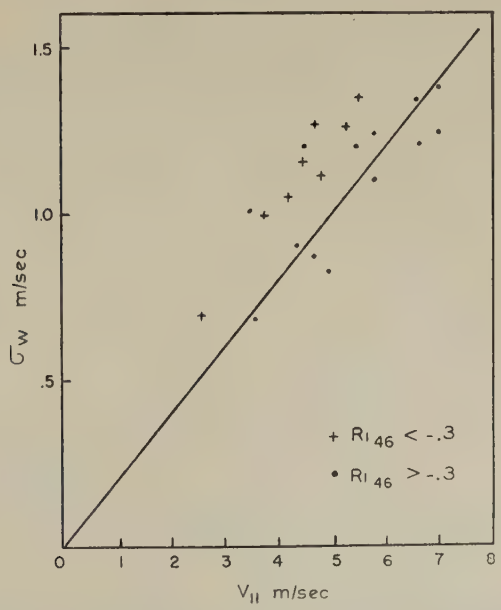

Figure 8. Standard deviation of vertical velocity at 91 m as function of wind speed at 11 m at Brookhaven, Long Island. Richardson numbers estimated at 46 m. Solid line gives theoretical relation for neutral conditions.

Fig. 7 shows the relation between standard deviations of vertical velocity at 12 m at O'Neill as function of the wind speed at 2 m height. At 12 m, the scale of turbulence is sufficiently large so that there should be no important underestimate of the observed σ_w. Apparently, a straight line of the form $\sigma_w = 0{\cdot}51\ V_1/\ln z_1/z_0$ with $z_0 = 1$ cm fits the data well, except at very low wind speeds, where the response of the bi-directional vanes is poor. There is little systematic scatter about the line, since no cases of extreme Richardson number are included in this set of observations (taken from Lettau and Davidson 1957).

Fig. 8 shows standard deviations of vertical velocity at 91 m at Brookhaven as function of the wind speed at 11 m. The roughness length here is large, 1 m. Here, the equation : $\sigma_w = 0{\cdot}51\ V_1/\ln (z_1 + z_0)/z_0$ is entered with V_1 the wind at 11 m. It fits well for the cases of small convection, and the deviations for the most convective periods is consistent with the complete Eq. (10). Eq. (10) also agrees with conditions of very smooth ground (beach) reported by Shiotani (1956). In summary, it appears that Eq. (10) is capable of accounting for the behaviour of variances of vertical motion under neutral and unstable conditions up to heights of over 100 m, and perhaps to higher levels in cases of large instability.

5. The complete spectrum

Combining Eqs. (10) and (3) we arrive at a semi-empirical expression for the spectrum of vertical velocity, in terms of u_*,

$$S_w(n) = \frac{6{\cdot}25\ {u_*}^2\, z}{V}\, h'^2\left(\frac{z}{L'}\right)\frac{1}{\left(1 + 4\,\frac{nz}{V}\right)^2} \quad . \quad . \quad . \quad (11)$$

or in terms of wind at a low level z_1 :

$$S_w(n) = 1{\cdot}1\,\frac{z\,{V_1}^2}{V \ln^2 \frac{z_1}{z_0}}\, h'^2\left(\frac{z}{L'}\right)\frac{1}{\left(1 + 4\,\frac{nz}{V}\right)^2} \quad . \quad . \quad (12)$$

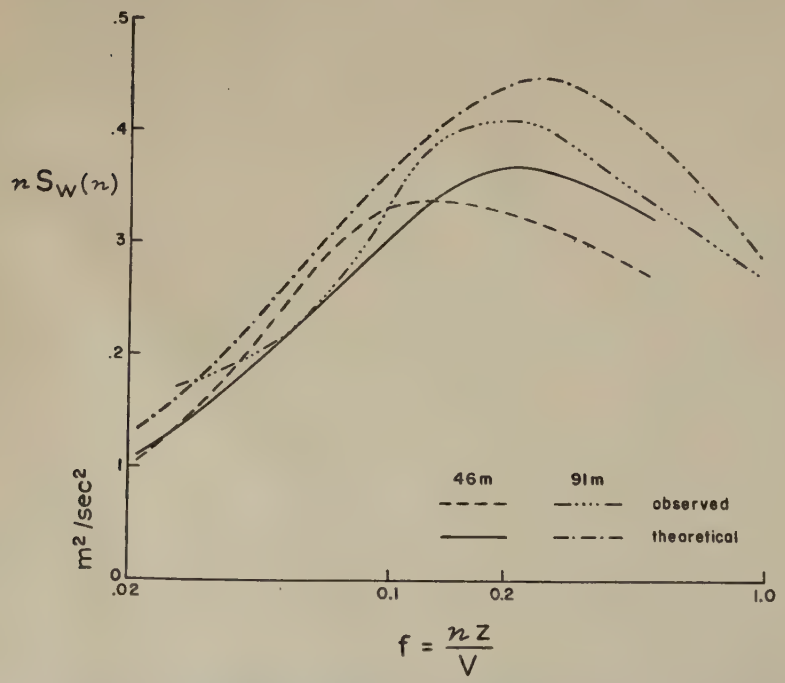

Figure 9. Vertical-velocity spectra at Brookhaven, 46 m and 91 m, on a day with considerable radiation, observed and according to Eq. (11).

It is to be noted that Eq. (11) is of the form :

$$S_w(n) = \frac{u_*^2 z}{V} \psi\left(\frac{nz}{V}, \frac{z}{L}\right) \quad . \quad . \quad . \quad . \quad (13)$$

which was predicted by Monin (1959b). This agreement is not too surprising because the treatment given here as well as Monin's are based on dimensional analysis.

Of course, Eq. (12) cannot be considered to apply at high frequencies where the $n^{-5/3}$ law is valid. Further, it does not fit observations in stable air.

A test of the question whether the effect of stratification on spectra is correctly described by Eq. (11) or Eq. (12) is difficult; on the one hand, the spectra must be obtained under condition of large z/L; on the other, the winds must be known at low levels so that u_* can be inferred. Fig. 9 shows a comparison of theory and observation on a day with strong solar heating at Brookhaven, when the conditions seem to be satisfied. The data cover three separate hours on the same day, and values of z/L and u_* were averaged to form the ' theoretical ' curve. In view of the large scatter of the observations, to which the ' observed ' curves were drawn by eye, the fit is not bad. In particular, the difference between the magnitude of the spectral estimates at 46 m and 91 m, which is largely due to the difference in z/L' is well represented.

Acknowledgments

The authors are grateful for the support of the Geophysics Research Directorate of the United States Air Force, Cambridge Research Center, which made some of this research possible. They also would like to thank the Meteorology Group at Brookhaven National Laboratory for making available their tower observations.

Finally, the authors would like to acknowledge the assistance of Dr. Joost Businger for making available unpublished observations obtained by staff members of the Department of Meteorology, University of Wisconsin.

References

Bunker, Andrew F. 1956 *Woods Hole Oceanog. Inst., Rep.* 56-65.
Businger, J. A. 1959 *J. Met.*, **16**, p. 515.
Charnock, H. and Robinson, G. D. 1957 *Air Ministry, Met. Res. Cttee., M.R.P.*, No. 1062.
Deland, R. J. and Panofsky, H. A. 1957 *Sci. Rep.*, **2**, U.S.A.F. Project 19 (604) 1027, AFCRC-TN-57-262.
Hay, J. S. and Pasquill, F. 1959 *Advances in Geophysics*, **6**, p. 345.
Henry, R. M. 1959 *Inst. Aero Sci.*, IAS Rep. No. 59-43.
Inoue, E. 1956 *Proc. 6th Jap. Nat. Cong. Appl. Math.*, p. 315.
Jones, R. A. 1958 *Porton Tech. Pap.* No. 635.
Lappe, O., Davidson, B., and Notess, D. B. 1959 *Task. Rept. Bull. Aer.*, U.S. Navy Proj. No. 59-517-d.
Lettau, H. and Davidson, B. 1957 *Exploring the atmosphere's first mile*, Vol. 2 (Pergamon Press, London).
Monin, A. S. and Obukhov, A. M. 1954 *Acad. Nauk. SSSR, Leningrad, Geofizi. Inst.*, Trudy, No. 24 (151), p. 163.
Monin, A. S. 1959a *Advances in Geophysics*, **6**, p. 331.
1959b *J. Geophys. Res.*, **64**, p. 2196.
Panofsky, H. A., Blackadar, A. and McVehil, G. 1960 *Quart. J. R. Met. Soc.*, **86**, p. 390.
Panofsky, H. A., Cramer, H. E. and Rao, V. R. K. 1958 *Ibid.*, **84**, p. 270.
Panofsky, H. A. and Van der Hoven, I. 1956 *Sci. Rep.*, **1**, USAF Project AF 19 (604) 1027 AFCRC-TN-56-254.
Press, Harry 1957 *NATO Advis. Grp. Aero. Res. and Dev. Rep. 115.*
Priestley, C. H. B. 1959 *Turbulent transfer in the lower atmosphere*, (University Chicago Press).
Shiotani, M. 1956 *Proc. 6th Jap. Nat. Cong. Appl. Math.*, p. 311.
Swinbank, W. C. 1955 *C.S.I.R.O., Div. Met. Phys. Tech. Pap.*, No. 2.

551.509.313 : 551.511.33

A report on some experiments in numerical prediction using a stream function

By E. KNIGHTING and MAVIS K. HINDS

Meteorological Office, Dunstable

(Manuscript received 25 January 1960)

SUMMARY

A series of experiments is described in numerical forecasting in which the wind field at mid-tropospheric level is derived from a stream function, but the wind shear in the lower troposphere is computed in a variety of ways. The results show that the overestimation of the pressures in the region of anticyclones, which is inherent in models in which the mid-tropospheric wind field is assumed to be geostrophic, is significantly reduced.

1. INTRODUCTION

During the early months of 1959 about 50 numerical forecasts were made using the Sawyer-Bushby (1953) system of prognostic equations applied to initial data relating to 0001GMT on the day the forecast was made. Both these numerical forecasts and the forecasts made by the Central Forecasting Office were compared statistically with the actual situation at the time for which the forecast was made and the results will be reported in *Meteorological Office Scientific Paper* No. 5. It was clear from the statistics that the root-mean-square error in the contour-height field was larger in the case of the numerical forecasts than for the forecasts issued by the Central Forecasting Office. Visual inspection of the charts showed that anticyclogenesis had frequently been overestimated and that this spurious anticyclogenesis was probably the main factor contributing to the errors in the contour-height field.

The so-called barotropic vorticity equation gives rise to a forecasting equation which asserts that the absolute vorticity of a parcel of air is conserved. Shuman (1957) pointed out further that the procedure of computing the wind geostrophically contradicts the conservation of absolute vorticity and implies that vorticity is destroyed in a wind flow from the south and created in a wind flow from the north. The important factor here is the variation with latitude of that part of the absolute vorticity which arises owing to the rotation of the earth. The effect is often more noticeable in the flow around relatively slow-moving anticyclones and gives rise to overestimated anticyclogenesis in forecasts based on the barotropic equation. The spurious anticyclogenesis noted above was probably due, at least in part, to this effect. The depressions, which have northerly airstreams in their rear, are usually more mobile and the corresponding overestimation of cyclogenesis is not so marked because the effect is rarely applied to the same region for a long period.

Shuman also contended that barotropic forecasts made by assuming that the wind field was obtainable from a stream function, and therefore strictly non-divergent, should be superior to those made assuming that the wind is geostropic, in that the spurious anticyclogenesis should not be so important an error; subsequent experience has shown that this is so and barotropic forecasts made by the Joint Numerical Weather Prediction Unit at Washington D.C. make use of a stream function. Bushby and Huckle (1956) had already shown that there was an improvement in baroclinic forecasts when the computations proceeded from a field closely allied to the stream-function field. Accordingly, some of the cases, in which the integrations made on the basis of the Sawyer-Bushby model showed marked height errors, were selected for re-computation with winds derived from stream-function fields in place of the contour-height fields.

2. The introduction of a stream function

The divergence of the equations of motion of a frictionless fluid yields an equation which, with the assumption of a non-divergent wind field, relates the stream function to the contour heights. This equation is the so-called balance equation which has been extensively reported in the literature (e.g. Charney (1955)) and can be used to derive a stream function corresponding to a geopotential distribution. The incorporation of a stream function into barotropic forecasting equations presents no difficulty, since a single stream function represents the motion at all levels and the vorticity equation provides a predictive equation for the changes in the stream function with time. The forecasting equations are then

$$\mathbf{V} = \mathbf{k}_\Lambda \nabla \psi, \qquad \zeta = \nabla^2 \psi \quad . \quad . \quad . \quad . \quad (1)$$

$$2\left\{\frac{\partial^2\psi}{\partial x^2}\frac{\partial^2\psi}{\partial y^2} - \left(\frac{\partial^2\psi}{\partial x\,\partial y}\right)^2\right\} + f\nabla^2\psi + \frac{\partial\psi}{\partial x}\frac{\partial f}{\partial x} + \frac{\partial\psi}{\partial y}\frac{\partial f}{\partial y} = g\nabla^2 h\,. \quad . \quad (2)$$

$$\frac{\partial\zeta}{\partial t} + J(\psi, \zeta + f) = 0 \quad . \quad . \quad . \quad . \quad (3)$$

The first of these states how the horizontal velocity $\mathbf{V}$ and the vertical component of vorticity ζ are to be computed when ψ is known. The second is the balance equation; given h, the contour height of the isobaric surface in which the wind is non-divergent, it may be solved under suitable conditions to give ψ, the stream function. The third is the barotropic vorticity equation, which when written in terms of ψ shows how ψ varies in time. These equations are usually applied at a mid-tropospheric level, so that h is the contour height of the 500 or 600 mb isobaric surface.

When the motion is baroclinic the temperature field has a controlling effect upon the development which may be expressed by the equation

$$\frac{\partial h'}{\partial t} + \mathbf{V}\,.\,\nabla h' + \Gamma\varpi = Q \quad . \quad . \quad . \quad . \quad (4)$$

where h' is the thickness between two isobaric surfaces, ϖ is the vertical velocity dp/dt, Γ is a measure of the stability and Q is a non-adiabatic heating term. If we now seek to preserve the strict non-divergence at the mid-tropospheric level, expressed by the use of a stream function ψ_m to compute velocities at that level, and also to account for the baroclinity through Eq. (4) a difficulty arises. The two-level baroclinic model (see e.g., Sawyer and Bushby (1953)) involves an equation for the rate of change of relative vorticity ζ'. When the geostrophic assumption is made this relative vorticity equation may be directly interpreted in terms of h' and combined with Eq. (4). However, when the wind field at the upper level is obtained from a stream function the relative vorticity ζ' is no longer easily expressed in terms of h'. The predictive equations are of the form

$$\nabla^2\frac{\partial\psi_m}{\partial t} = F(\psi_m, \psi', \varpi) \quad . \quad . \quad . \quad . \quad (5)$$

$$\nabla^2\frac{\partial\psi'}{\partial t} = G(\psi_m, \psi', \varpi) \quad . \quad . \quad . \quad . \quad (6)$$

$$\frac{\partial h'}{\partial t} = -J(\psi_m, h') - \Gamma\varpi + Q \quad . \quad . \quad . \quad (7)$$

where ψ_m is the stream function at mid-tropospheric level, ψ' the difference between the stream functions at mid-level and near the surface, and F and G are known functional forms. If now h' can be simply expressed in terms of ψ_m and ψ' the integrations may readily be carried out. From a mathematical point of view we may note that Eqs. (5), (6) and (7) contain 4 unknowns, ψ_m, ψ', h' and ϖ and a further equation is required to close the system. In the series of experimental calculations of 24 hr changes in the geopotential field the following linkages between stream functions and thickness fields were used :

MODEL A

At time $t = 0$ the balance equation was solved at the mid-level (600 mb) and at the lower level (1,000 mb), yielding respectively ψ_m and ψ_0. The difference between these, ψ', was equated to gh'/f. Thus Eq. (7) was written

$$\frac{\partial \psi'}{\partial t} + J(\psi_m, \psi') + \frac{\Gamma \varpi}{f} = Q^* \quad . \quad . \quad . \quad (8)$$

where Q^* is an adjusted value of Q. There is the implication that at time $t = 0$ near the surface the divergence terms which are omitted to give the balance equation are small compared with the terms which arise in the balance equation (say $f\zeta$ where ζ is the vorticity), but the motion is not subsequently treated as non-divergent. The forecast values of h_m and h_0 are obtained from the forecast values ψ_m, $\psi_m - \psi'$ through the balance equation.

MODEL B

At time $t = 0$, the balance equation was solved to give ψ_m at the mid-level. ψ' was related to h' through the equation

$$\psi' = \frac{gh'}{\bar{f}} \quad . \quad . \quad . \quad . \quad . \quad (9)$$

where $\bar{f}$ is a mean value of f over the forecast area. Before we were able to report this work Phillips (1958) had described an experiment under similar conditions with similar assumptions.

MODEL C

Similar to Model B except that the terms involving ψ' in Eq. (5) were suppressed to make this equation the same as for barotropic flow, the equation being applied as in Model A and B to flow at the 600 mb level.

MODEL D

Similar to Model B except that the thermal wind $\mathbf{V}'$ was computed directly from

$$\mathbf{V}' = \mathbf{k}_\Lambda \frac{g}{f} \nabla h' \quad . \quad . \quad . \quad . \quad (10)$$

MODEL E

Similar to Model D, barotropic at the 500 mb level (and not at the mid-level, 600 mb). The thickness used to obtain thermal winds was the 1,000-500 mb thickness.

MODEL F

The model suggested by Bushby and Huckle (1956) in which velocities are computed from the formula

$$\mathbf{V} = \mathbf{k}_\Lambda \frac{g}{f} \nabla \psi \quad . \quad . \quad . \quad . \quad (11)$$

and a modified form of the balance equation is used.

3. THE RESULTS OF THE TIME-INTEGRATIONS

The statistics which have been computed for each time integration using the unmodified Sawyer-Bushby model include the correlations between the forecast and actual 24 hr changes in contour height at 1,000 mb and 500 mb and between the changes in thickness between these levels, the correlations between the contour heights and thicknesses of

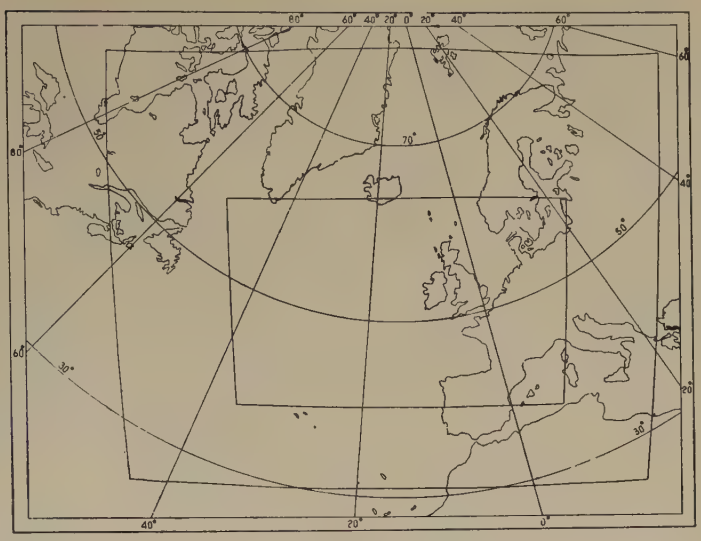

Figure 1. The forecast and verification areas. The inner boundary shows the verification area, the outer the forecast area.

TABLE 1. MEAN STATISTICS RELATING TO NUMERICAL FORECASTS MADE BY VARIOUS MODELS
(The statistics relate to 24 hr forecasts, and are computed over 150 grid points in each of 15 cases)

Model	r_c	ϵ (*m*)	τ	V (kt)
		(1,000 mb)		
Sawyer-Bushby	0.58	110	0·81	29
A	0·65	87	0·82	30
B	0·63	86	0·80	30
C	0·63	85	0·81	28
D	0·64	88	0·81	30
E	0·65	83	0·79	30
F	0·61	88	0·81	31
C.F.O.	0·57	78	0·78	31
		(1,000-500 mb thickness)		
Sawyer-Bushby	0·71	64	0·85	27
A	0·67	83	0·81	30
B	0·69	66	0·84	28
C	0·70	62	0·84	27
D	0·69	65	0·84	28
E	0·71	63	0·86	28
F	0·68	64	0·83	28
C.F.O.	0·63	73	0·84	29
		(500 mb)		
Sawyer-Bushby	0·58	109	0·90	30
A	0·59	101	0·90	31
B	0·59	100	0·90	31
C	0·59	100	0·87	30
D	0·58	101	0·89	32
E	0·58	96	0·90	30
F	0·55	103	0·89	33
C.F.O.	0·60	90	0·91	32

r_c = correlation coefficient between actual and forecast 24 hr contour height changes.
ϵ = root-mean-square height error in 24 hr forecast (metres).
τ = correlation between 24 hr forecast and actual contour heights.
V = root-mean-square vector error in 24 hr forecast wind (knots).

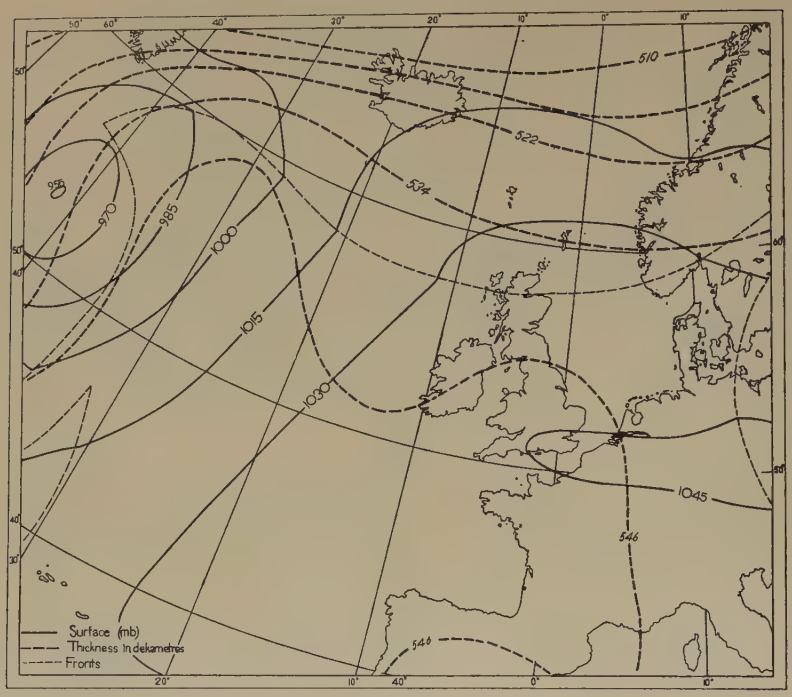

Figure 2. The surface and 1,000-500 mb thickness charts, 0000 GMT, 17 Feb. 1959.

the forecast and verifying charts, the root-mean-square differences in height between the forecast and verifying charts; the computations were made using the values at all grid points. Geostrophic winds were computed from the height values at adjacent grid points and the root-mean-square difference between the forecast and verifying geostrophic winds was obtained; this is termed the root-mean-square vector error.

The numerical forecasts were carried out over a grid of 24 × 20 points, the grid length being approximately 170 mi, and the statistics refer to an inner area of 15 × 10 points (Fig. 1). Similar computations of statistics have been made for each of the forecasts made by the various models detailed in the previous paragraph. The mean values for the 15 days are given in Table 1. All of the numerical forecasts used an objective analysis for initial data. Similar statistics have been computed for the forecasts made by the Central Forecasting Office (C.F.O.).

From Table 1 it is clear that the primary object of reducing ϵ at 500 mb and at 1,000 mb from its values given by the Sawyer-Bushby model is achieved by each of the models. At 500 mb Model E appears to reduce ϵ by rather more than half the difference found between the C.F.O. and the Sawyer-Bushby forecasts. The other models give slightly larger values of ϵ differing little among themselves. At 1,000 mb the values of ϵ are all considerably reduced from that given by the Sawyer-Bushby model and are more comparable with that given by the C.F.O. forecasts. Model E appears to give a smaller root-mean-square height error than the others.

The mean statistics relating to the thickness forecasts show that for these 15 cases ϵ was smaller for the forecasts made using the Sawyer-Bushby model than for the C.F.O. forecasts and that the 24 hr changes in thickness were correspondingly better forecast; both these results are shown also by the mean statistics of all forecasts made during the early months of 1959. It is also evident that in the mean the numerical forecasts of thickness are superior to those at 500 mb and to the derived 1,000 mb forecasts. The results of using Model A, which assumes that the thickness is proportional to the difference in stream function values at 500 mb and 1,000 mb, show that this model leads to a much

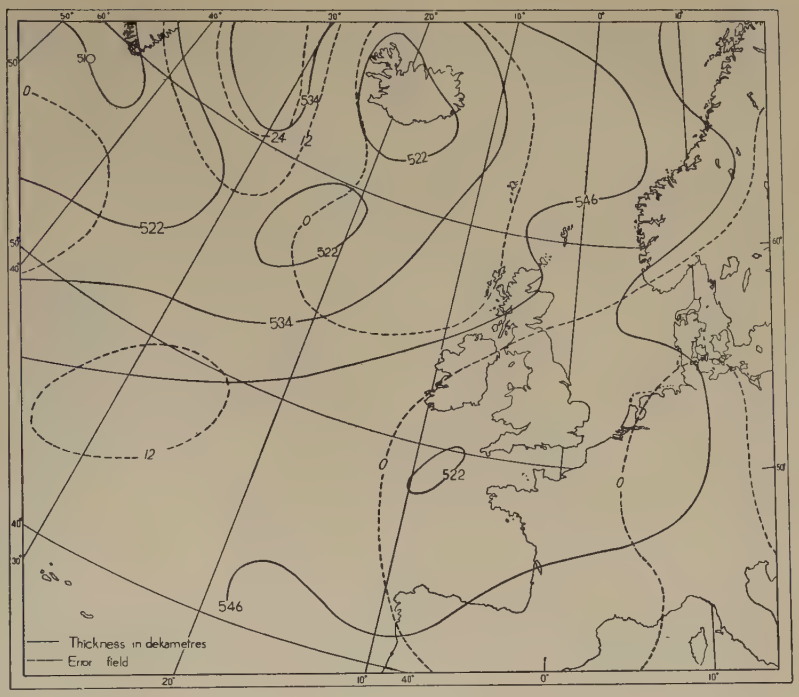

Figure 3 (a) Thickness forecast and error field, using Sawyer-Bushby model, 0000 GMT, 18 Feb. 1959.

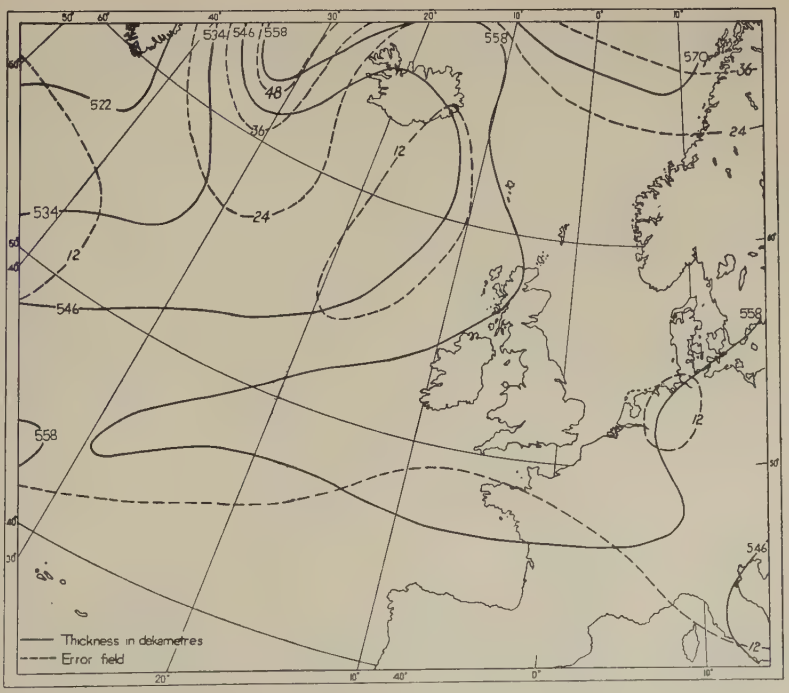

Figure 3 (b) Thickness forecast and error field, using Model A, 0000 GMT, 18 Feb. 1959.

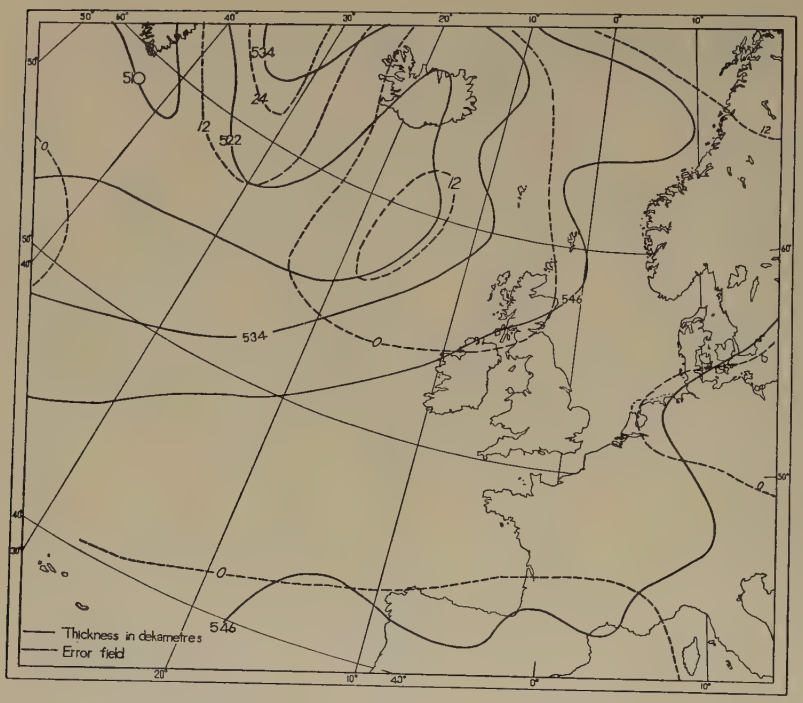

Figure 3 (c) Thickness forecast and error field, using Model B, 0000 GMT, 18 Feb. 1959.

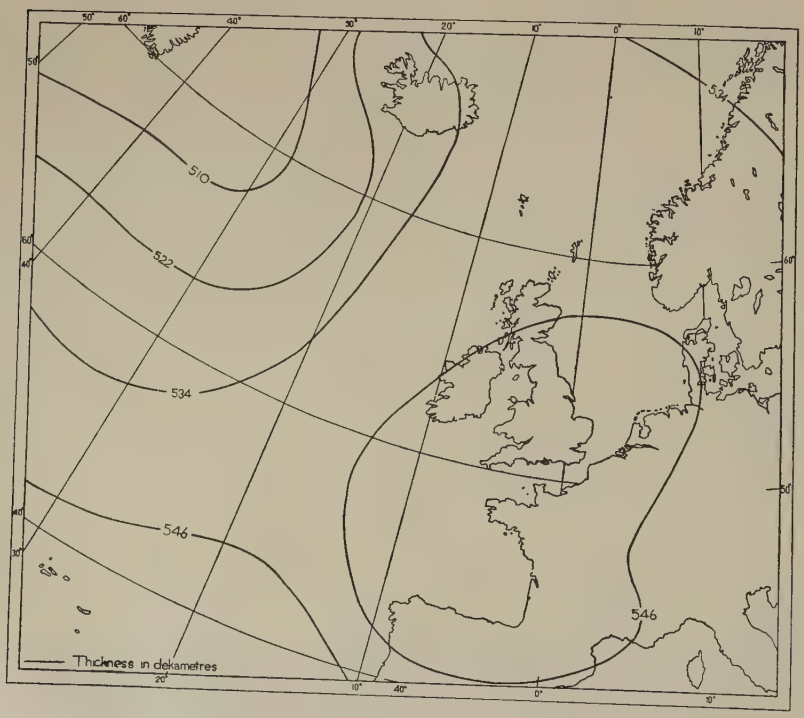

Figure 3 (d) Thickness chart, 0000 GMT, 18 Feb. 1959.

poorer forecast of thickness than does the Sawyer-Bushby model. There is little difference between the results obtained in regard to thickness by using the Models B-G and the Sawyer-Bushby model. The implication is that in regard to the average performance of the models it matters little whether the variation of Coriolis parameter is taken into account when thermal winds are computed from thicknesses, with a slight indication that it is preferable to include it.

Models C and E are barotropic at a mid-tropospheric level. There appears to be a slight advantage in using these models as far as the root-mean-square errors are concerned. However, an examination of the forecasts showed that upon two occasions these models had failed to indicate important baroclinic developments at the mid-tropospheric level, and it may be that it is preferable to accept a poorer overall forecast in order to be able to detect such developments.

The forecasts made using as initial data the charts referring to 0001 GMT 17 February 1959, illustrate the differences that arise in the thickness forecasts. Fig. 2 shows the surface and 1,000 mb-500 mb thickness charts for the time of commencement of the forecast. The principal change in the succeeding 24 hr was the rapid movement of the deep Atlantic depression in a north-easterly direction. Figs. 3 (a) to 3 (d) show the forecasts of thickness made using the Sawyer-Bushby model, Models A and B and the verifying thickness chart for 0001 GMT 18 February 1959. The results relating to the other models are similar to those using model B and are not shown. The forecast made using Model A has carried the warm air too far north and too far around the depression so that the air between Iceland and Greenland is much too warm. It has also failed to carry cold air into the rear of the depression. Each of the other numerical forecasts has to some extent carried the warm air around the depression, but not to the extent that the Model A forecast did, whereas in fact a cold trough lay to the west of the depression. Model A was also less successful in bringing cold air into the rear of the depression, and in this respect the forecast made using the Sawyer-Bushby model was more successful.

Acknowledgment

This paper is published by permission of the Director-General of the Meteorological Office.

References

Bushby, F. H. and Huckle, V. H. 1956 'The use of a stream function in a two-parameter model of the atmosphere,' *Quart. J. R. Met. Soc.*, **82**, p. 409.

Charney, J. G. 1955 'The use of the primitive equations in numerical prediction,' *Tellus*, **7**, p. 22.

Phillips, N. A. 1958 'Geostrophic errors in predicting the Appalachian storm of November 1950,' *Geophisica*, Helsinki, **6** : 3-4, p. 389.

Sawyer, J. S. and Bushby, F. H. 1953 'A baroclinic model atmosphere suitable for numerical integration,' *J. Met.*, **10**, p. 54.

Shuman, F. 1957 'Predictive consequences of certain physical inconsistencies in the geostrophic barotropic model,' *Monthly Weather Review*, **85**, p. 229.

551.510.533

The vertical distribution of atmospheric ozone over Canadian stations from *umkehr* observations

By C. L. MATEER and W. L. GODSON
Meteorological Service of Canada, Toronto

(Manuscript received 1 March 1960)

SUMMARY

The vertical distribution of ozone is estimated from *umkehr* observations at the Canadian ozone stations at Edmonton, Moosonee and Resolute. Average seasonal vertical distributions are presented and compared with European and Indian results. The Canadian results indicate the existence of two levels of maximum ozone density, one at about 27 km and a lower one at about 15 km. During the spring, summer and autumn seasons the higher-level maximum is slightly more predominant than the lower. However, during the winter months, the lower-level maximum becomes much more pronounced. As a result, there is an extremely good correlation between ozone amount between 12 and 24 km and total ozone, three-quarters of the seasonal changes in total ozone being attributable to changes in this layer.

1. INTRODUCTION

Vertical distributions of ozone (see Appendix) have been estimated from 27 *umkehr* series at Moosonee (51° 16′ N, 80° 39′ W), 7 series at Edmonton (53° 34′ N, 113° 31′ W), and 4 series at Resolute (74° 43′ N, 94° 59′W). The calculations have been made with the standard method B recommended for the I.G.Y. (Ramanathan and Dave 1957), using the C wavelength pair (3114·5/3324 A.U.) and a short-cut linearized method of solution (Mateer 1960). The recommended (provisional) corrections for secondary scattering have been applied.

2. THE VERTICAL DISTRIBUTION OF OZONE

Fig. 1 shows the average of 4 autumn distributions for Resolute. The distributions must be considered as quite tentative because of difficulties with the optical wedge at Resolute. The distribution has a centre of gravity at 20·7 km, a rather broad main maximum just below 20 km, and a secondary maximum at about 37 km. The secondary maximum appears not because of the large amount of ozone in the 36-42 km layer, but because of the small amount of ozone in the 30-36 km layer. Note the large amount of ozone in the 48-54 km layer, amounting to $0{\cdot}8 \times 10^{-3}$ cm km^{-1}. The dashed lines represent the largest and smallest ozone densities calculated in the four separate distributions. There are two levels of maximum mixing ratio, one at 28 km (8·9 mg kg^{-1}) and one at 47 km (20·7 mg kg^{-1}).

Fig. 2 shows average curves for various seasons of the year at Moosonee and Edmonton. The results from the two stations were combined since there appeared to be no significant difference with the small sample available.

The autumn curve corresponds to 0·297 cm* ozone and has a centre of gravity at 23·3 km. There appears to be one broad maximum of ozone density between 20 and 30 km although the smooth curve could just as easily be drawn with a main maximum at about 27 km and a secondary maximum about 20. There is a single maximum of ozone mixing ratio at about 42 km (15·7 mg kg^{-1}).

* All ozone values quoted in this paper are based on the Vigroux values for the ozone absorption coefficients. Units are cm at STP.

Figure 1. Average vertical distribution of ozone at Resolute from four *umkehr* series.

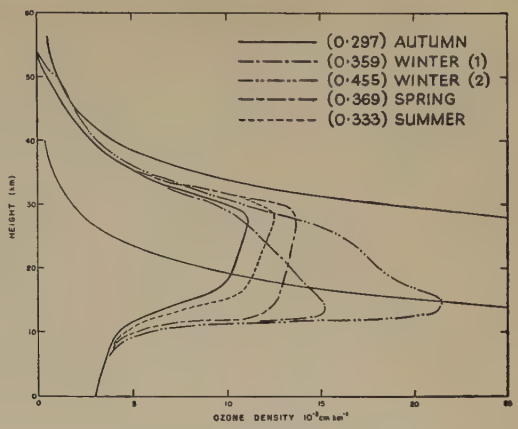

Figure 2. Average vertical distribution of ozone at Moosonee/Edmonton for various seasons of the year. The two fine lines running from upper left to lower right are lines of constant ozone mixing ratio, based on the pressure-height data used by Ramanathan and Dave (1957), and correspond to 21 mg kg^{-1} (top line) and 2·1 mg kg^{-1} (bottom line).

As we progress into early winter, we find an increase in total ozone with virtually the entire change occurring between 12 and 24 km. The centre of gravity drops to 21·0 km. Although we still have a rather broad maximum of ozone density, the emphasis has shifted. A double maximum could still be shown, but now the maximum below 20 km would be the main one and the higher maximum near 27 km would assume a secondary role. Once again there is a single maximum of ozone mixing ratio at 42 km (15·7 mg kg^{-1}). It is appropriate to note here that no significant differences were found above 36 km except in the case of the late winter curve.

As we proceed further into winter, following the abrupt increase in total ozone, we find the centre of gravity is still at about 21 km. Increases in ozone density have occurred throughout the atmosphere above about 12 km, with the amount of the increase most marked between 12 and 30 km. However, a secondary maximum could still be drawn somewhere between 24 and 27 km.

Also of interest in this second winter curve is the small hump near 50 km. It is not clear whether this small hump arises from the mathematical analysis or is physically real. If recent *umkehr* data for Arosa (Dütsch 1957) are examined and a smooth curve drawn through the block distribution, there is a tendency for a small hump to appear at a somewhat lower level (see Figs. 3 and 4). The small hump on the Moosonee-Edmonton curve corresponds to a maximum of mixing ratio of 22·4 mg kg^{-1}. It is possible that this feature is associated with the three-body collision of atomic oxygen, which results in a more rapid rate of decrease in the equilibrium concentration of ozone with height above about 50 km (Johnson 1953).

Following the late-winter maximum of total ozone, we find the spring curve resembles the autumn curve very closely, but with more ozone at all levels between 10 and 35 km. If the two maxima are now drawn in, the main one will have to be at the higher level. The centre of gravity of the spring distribution is 22·6 km. Once again, the maximum of mixing ratio is at about 42 km and is 15·7 mg kg^{-1}. However, the general maximum is very broad since a mixing ratio of 14·9 mg kg^{-1} is achieved at about 30 km.

The summer curve lies between the spring and fall curves and appears to pretty well coincide with the spring curve above about 32 km. Therefore, the same comments regarding mixing ratio apply. The centre of gravity of the summer curve is 23·1 km.

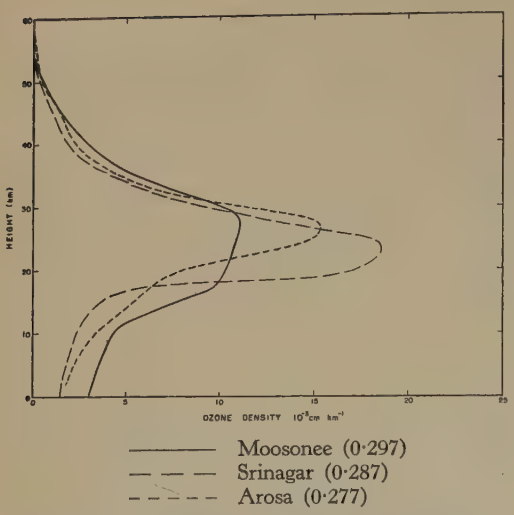

Figure 3. Comparison of vertical distribution of ozone at Moosonee, Srinagar and Arosa for total ozone 0·275 to 0·300 cm.

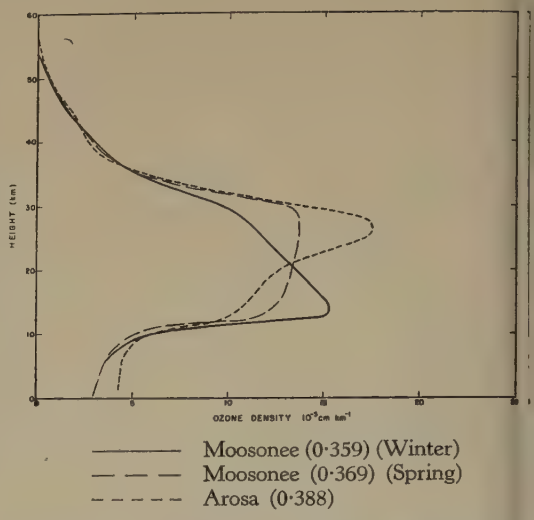

Figure 4. Comparison of vertical distribution of ozone at Moosonee and Arosa for total ozone 0·35 to 0·40 cm.

3. Comparison with vertical distributions over Europe and India

Fig. 3 shows curves for Moosonee (autumn average curve), Srinagar (Ramanathan *et al.* 1956) and Arosa (Dütsch 1957), all corresponding to about the same total ozone. Secondary scattering corrections were applied in the solutions for Moosonee and Srinagar but not in that for Arosa. The solution at Srinagar divided the atmosphere into only 6 ozone-bearing layers, whereas the Moosonee solution utilized 9 and the Arosa solution 30 (gathered into 9 groups).

While the Srinagar and Arosa solutions show only the one main maximum, the Moosonee solution gives evidence of a secondary maximum below 20 km. The Moosonee curve shows a greater ozone density between about 30 and 45 km, with the Arosa curve catching up above 45 km. Note the small hump on the Arosa curve at 46-47 km. It corresponds to an ozone mixing ration of 16·9 mg kg^{-1}.

Fig. 4 compares the early winter and spring curves for Moosonee-Edmonton with a winter-spring curve for Arosa (Dütsch 1957). The interesting point here is the continuing preponderance at Arosa of the high-level main maximum with the lower-level maximum retaining a distinctly secondary role. At Moosonee, even in the spring curves, the lower maximum appears to retain a role of importance nearly equal to that of the higher maximum. Note again the small hump on the Arosa curve near the 45 km level corresponding to a mixing ratio of 20·2 mg kg^{-1}.

4. Discussion of results

(*a*) *Seasonal variations of the vertical distribution*

The averaged seasonal data used in the construction of Fig. 2 are presented in Table 1. It is instructive to examine these data for seasonal fluctuations in the individual 6 km layers. In Fig. 2, the seasonal curves are run into a single curve in the 0-6 km layer because of the low confidence normally assigned to tropospheric ozone densities calculated by the *umkehr* method. Despite this low confidence, it is interesting to note the small annual cycle with maximum in summer and minimum in winter early. This cycle may be related to tropospheric photochemical reactions involving oxides of nitrogen (Cadle and Johnston 1952). Such reactions would be in phase with the sun. However, the seasonal cycle of

TABLE 1. AVERAGE SEASONAL VERTICAL DISTRIBUTION

(Each layer is 6 km thick. Layer 1 is 0-6 km, layer 2 is 6-12 km, etc.)

	Ozone density in the various layers (10^{-3} cm km^{-1})									Total (cm)
	1	2	3	4	5	6	7	8	9	
Summer	4·1	4·8	9·0	11·6	12·3	8·5	3·2	1·6	0·5	0·332
Autumn	3·8	4·3	7·6	10·4	10·9	7·2	3·4	1·6	0·5	0·297
Winter (1)	2·8	5·8	14·8	13·1	11·1	6·8	3·3	1·7	0·5	0·359
Winter (2)	3·0	5·7	20·4	17·9	14·5	7·9	3·8	2·0	0·8	0·455
Spring	3·4	5·2	12·4	13·2	13·6	8·4	3·4	1·7	0·6	0·369

tropospheric ozone must also depend on such factors as cross-tropopause transfer, local tropospheric sources (thunderstorms in summer, silent discharge in blowing snow in winter), and rate of ground-level destruction (minimum in winter with snow cover, but also depending on tropospheric vertical diffusion).

The 6-12 km layer (upper troposphere) has a minimum in autumn and a maximum in winter, although the changes are relatively small. Since the layer contains some of the lower stratosphere on many occasions, its general behaviour is intermediate between that of the two domains : troposphere and lower stratosphere.

The 12-18 km layer (lower stratosphere) is the most important 6-km layer with regard to changes in ozone. This layer has a minimum of ozone in autumn and a maximum after the rapid temperature and ozone increases of late winter. The early winter values are roughly twice the autumn values and the late winter amounts almost three times as great. Since the atmospheric processes that produce ozone changes in this layer are essentially those important for temperature changes (horizontal advection and vertical motion), one would expect a positive correlation between total ozone and temperature at 15 km (Meetham 1937). The correlation will be best for long-period changes, since the lower stratosphere is closely linked to the troposphere for short-period changes, and for regions of great stratospheric stability, for which the effects of vertical motions are large.

The 18-24 km layer (middle stratosphere) is very similar to the lower stratosphere, although the seasonal changes are less intense, with a minimum ozone density in autumn and a maximum in late winter. The 24-30 km layer shows a broader minimum, covering autumn and early winter, and a maximum in late winter. The phase shift increases with height, with the 30-36 km layer having a broad spring-summer maximum and a minimum in early winter. This is crudely in phase with what one might expect from photochemical calculations. However, the three layers between 36 and 54 km do not follow this pattern, showing only very minor seasonal fluctuations, except for slightly greater densities at the time of maximum total ozone.

(b) *Variations in layer concentrations with total ozone*

Figs. 5-9, inclusive, are scatter diagrams of absolute or fractional ozone amounts in various broad layers against total ozone. Fig. 5 is for the 0-12 km layer (troposphere) and shows fractional ozone versus total. There is some evidence of a negative correlation, although the scatter is large. The equation and calculations were based on the Moosonee data only. The correlation coefficient is $-0{\cdot}36$ and the standard error of estimate 0·037. Perhaps the safest conclusion is that the average amount of ozone in the troposphere is about 14 per cent of the total, with a standard deviation of 4 per cent (of the total). This figure may be compared with the 8·5 per cent (± 3 per cent) reported from aircraft measurements (Kay *et al.* 1954).

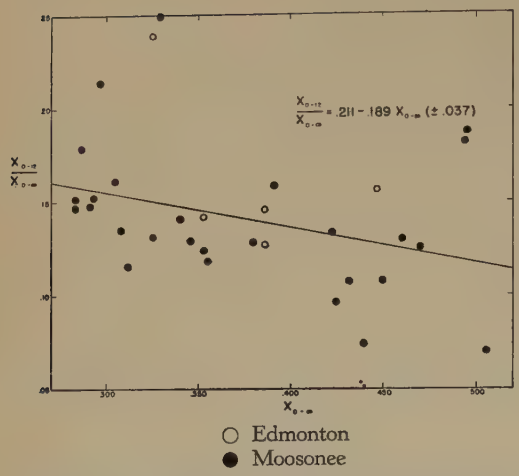

Figure 5. Scatter diagram of fractional zone amount in the 0-12 km layer against total ozone.

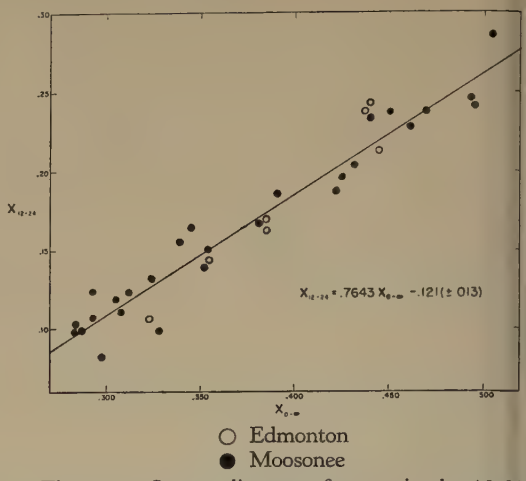

Figure 6. Scatter diagram of ozone in the 12-24 km layer against total ozone.

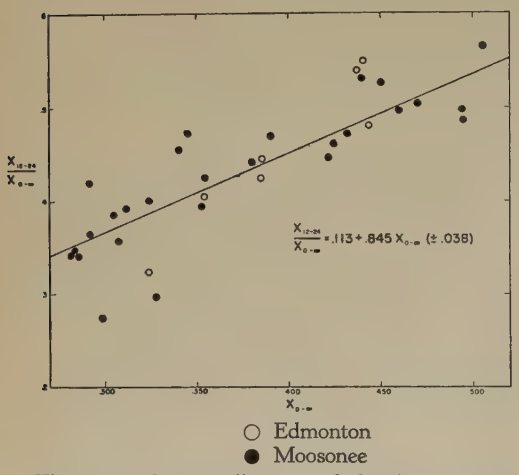

Figure 7. Scatter diagram of fractional ozone amount in the 12-24 km layer against total ozone.

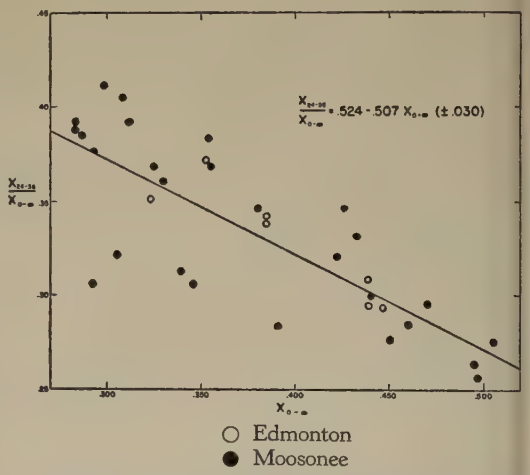

Figure 8. Scatter diagram of fractional ozone amount in the 24-36 km layer against total ozone.

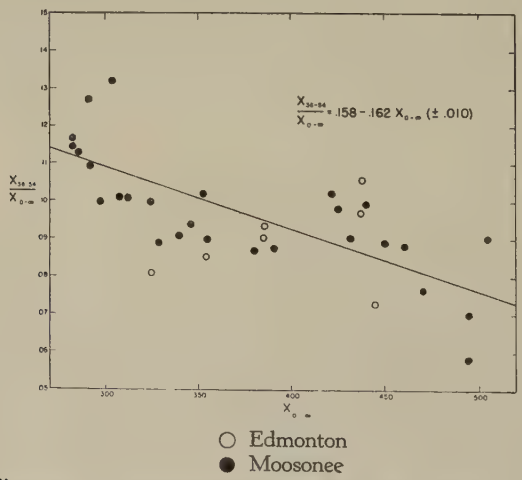

Figure 9. Scatter diagram of fractional ozone amount in the 36-54 km layer against total ozone.

Fig. 6 shows the remarkably good correlation between the amount of ozone in the 12-24 km layer and total ozone. The straight line, which was derived from the Moosonee data only, predicts the amount of ozone in this layer, as a function of total ozone, with a standard error of estimate of only $\pm$ 0·013 cm. The coefficient of correlation is 0·97. Changes of the ozone in this layer account for three-quarters of the total change, on a daily or seasonal basis.

Fig. 7 shows the fractional amount of ozone in this lower stratospheric layer plotted against the total. The correlation coefficient here is 0·86 and the standard error of estimate $\pm$ 0·038. This diagram indicates that not only does the amount of ozone in the lower stratosphere increase with total ozone but that the percentage in this layer increases with total. Thus the relation in Fig. 6 is actually a parabolic one, although the effect is masked by the general scatter. For very large ozone amounts, over half of the total ozone is contained between 12 and 24 km.

Fig. 8 shows the fractional amount of ozone in the 24-36 km layer, plotted against total ozone. The correlation is negative, the correlation coefficient being $-$ 0·79, and the standard error of estimate $\pm$ 0·030.

Fig. 9 shows the fractional amount of ozone in the 36-54 km layer. The correlation is negative with a correlation coefficient of $-$ 0·76 and a standard error of estimate of $\pm$ 0·010.

In summary, when the total amount of ozone increases, the major change appears to take place in the 12-24 km layer where not only the actual amount of ozone increases but the percentage of the total increases as well. Thus, for a total ozone amount of 0·300 cm, we find 11 per cent between 36 and 54 km, 37 per cent between 24 and 36, 37 per cent between 12 and 24 km, and 15 per cent between 0 and 12. At a total ozone of 0·500 cm, only 8 per cent is found between 36 and 54, 27 per cent between 24 and 36, and 12 per cent between 0 and 12, whereas we now find 53 per cent between 12 and 24.

Acknowledgments

Acknowledgment is given to the Director, Meteorological Branch, Department of Transport, Canada, for permission to publish this paper. Acknowledgments are due also to Mr. W. D. Komhyr in charge of I.G.Y. ozone work at Moosonee; to Mr. J. J. Kinisky, in charge at Edmonton; and to Mr. H. M. Sullivan, in charge at Resolute, for taking the *umkehr* observations reported on in this paper.

References

Cadle, R. D. and Johnston, H. S. 1952 *Proc. Second Nat. Air Pollution Symposium*, Stanford Res. Inst., p. 28.

Dütsch, H. U. 1957 'Evaluation of the *umkehr* effect by means of a digital electronic computer,' *Sci. Rep.* No. 1, U.S.A.F. Contract No. AF (514)-905.

Johnson, F. S. 1953 *Proc. Toronto Met. Conf.*, R. Met. Soc., p. 17.

Kay, R. H., Brewer, A. W. and Dobson, G. M. B. 1954 *Sci. Proc. Int. Assoc. Met.*, Rome, p. 189.

Mateer, C. L. 1960 Met. Branch, Toronto, Circ. No. 3291.

Meetham, A. R. 1937 *Quart. J.R. Met. Soc.*, **63**, p. 289.

Ramanathan, K. R., Kulkarni, R. N. and Degaonkar, J. S. 1956 'Further results on the vertical distribution of ozone in India obtained by the *umkehr* method.' Unpublished paper presented at International Ozone Conference, Weissenau, 1956.

Ramanathan, K. R. and Dave, J. V. 1957 *Annals of the I.G.Y.*, **5**, Pt. 1, p. 23, Pergamon Press, London.

Appendix

As the results for the individual days may be of considerable interest to meteorologists the estimated vertical distributions for each of the 38 *umkehr* series are tabulated below.

(Each layer is 6 km thick. Layer 1 is 0-6 km, layer 2 is 6-12 km, etc.)

Date	Amount of ozone in the various layers (10^{-3} cm km^{-1})									Total ozone (10^{-3} cm)
	1	2	3	4	5	6	7	8	9	
RESOLUTE										
9 Oct. 1958	5·1	6·2	13·6	13·6	12·2	1·4	3·3	1·8	0·8	348
3 Oct. 1958	2·8	5·4	15·0	15·0	9·5	2·7	2·7	1·9	0·8	335
22 Sept. 1958	2·7	4·6	13·6	10·9	9·5	5·4	3·7	2·1	0·8	320
21 Sept. 1958	1·4	2·1	13·6	13·6	9·5	4·8	4·1	2·4	0·8	314
EDMONTON										
14 May 1959	4·5	4·4	11·6	12·2	13·6	8·2	3·1	1·5	0·4	354
11 April 1959 p.m.	2·9	6·8	13·6	13·6	13·6	8·2	3·3	1·8	0·7	385
11 April 1959 a.m.	2·8	5·6	14·7	13·6	13·6	8·2	3·4	1·9	0·7	385
24 Mar. 1959	1·4	2·7	21·8	17·7	14·3	8·2	4·4	1·9	0·8	438
22 Mar. 1959	3·7	8·3	20·4	15·0	13·6	8·2	3·3	1·6	0·5	445
9 Mar 1959	1·4	2·3	21·8	18·4	13·6	8·2	4·5	2·3	1·0	440
9 Oct. 1958	7·0	6·8	9·5	8·2	10·9	8·2	2·7	1·4	0·3	325
MOOSONEE										
25 Feb. 1959	2·7	2·7	21·2	17·7	13·6	8·2	3·8	2·4	1·0	440
23 Feb. 1959	2·7	5·4	21·8	17·7	13·1	7·6	3·3	2·4	1·0	450
19 Feb. 1959 p.m.	2·9	3·0	25·8	21·8	15·0	8·2	4·1	2·4	1·0	505
19 Feb. 1959 a.m.	4·5	10·9	21·8	18·4	13·6	7·5	3·7	1·6	0·5	495
25 Jan. 1959	2·9	7·5	17·1	13·6	11·6	6·8	3·3	1·9	0·5	391
7 Oct. 1958	1·9	4·1	9·5	10·9	12·2	8·2	3·1	1·6	0·5	312
5 Sept. 1958	3·0	4·1	9·5	12·2	11·8	8·2	3·1	1·6	0·7	325
4 Aug. 1958	2·9	4·0	7·5	10·9	11·6	9·2	3·3	1·5	0·4	308
20 July 1958	2·7	5·4	13·6	14·4	13·6	8·2	3·3	1·6	0·5	380
4 July 1958	3·5	3·5	12·2	12·9	13·6	8·2	3·3	1·6	0·4	355
3 June 1958	3·2	4·1	9·5	13·6	13·6	8·8	3·7	1·6	0·7	353
7 Mar. 1958	4·0	5·3	13·6	17·7	14·3	8·2	4·2	2·2	0·8	422
22 Feb. 1958	1·4	5·4	16·3	16·3	17·7	6·8	3·7	2·3	1·0	425
19 Feb. 1958	4·0	6·0	20.4	17·7	13·6	8·2	4·1	1·9	0·8	460
15 Feb. 1958	4·1	10·9	21·8	19·0	15·0	6·8	3·0	1·4	0·4	494
14 Feb. 1958	3·0	6·8	21·8	17·7	16·3	6·8	3·3	1·9	0·8	470
12 Feb. 1958	3·6	4·1	16·3	17·7	14·3	9·5	3·7	2·0	0·8	432
25 Jan. 1958	2·7	5·3	13·6	12·2	9·5	8·2	3·3	1·5	0·4	340
4 Jan. 1958	2·8	4·7	13·6	13·6	12·2	5·4	3·3	1·6	0·5	346
26 Oct. 1957	3·1	4·1	6·8	13·6	9·5	5·4	3·7	1·8	0·7	292
20 Oct. 1957	2·8	5·4	6·8	12·8	10·9	5·4	4·1	1·9	0·7	305
6 Oct. 1957	3·5	3·5	6·8	9·5	10·9	7·5	3·3	1·6	0·5	283
5 Oct. 1957	4·1	3·0	6·8	9·5	10·9	7·5	3·3	1·6	0·5	283
4 Oct. 1957	3·5	4·1	6·8	9·5	10·9	7·5	3·3	1·6	0·5	286
28 Sept. 1957	4·1	3·3	8·2	9·5	10·9	7·5	3·3	1·6	0·5	293
24 Aug. 1957	8·4	5·5	6·8	9·5	10·9	8·8	3·0	1·6	0·3	329
20 July 1957	4·1	6·5	4·1	9·5	12·2	8·2	2·9	1·6	0·5	298

551.510.534

The accuracy of determination of the vertical distribution of atmospheric ozone from emission spectrophotometry in the 1,043 cm^{-1} band at high resolution

By C. D. WALSHAW
Cavendish Laboratory, Cambridge

(Manuscript received 12 February 1960)

SUMMARY

A method is outlined for obtaining the vertical distribution of atmospheric ozone from ground-level measurements of the downcoming thermal radiation in the region of the 1,043 cm^{-1} (9·6 μ) band. The emission measurements are such as may be made with a grating spectrometer of the Goody type; the slit width is about 2·5 cm^{-1}, enabling interference from water vapour and carbon-dioxide lines to be eliminated.

Estimates are made of the various sources of error, using a model atmosphere having three ozone variables (which are the ozone contents of the layers 1,000-600, 600-300 and 300-50 mb), and basing the analysis on four combinations of wave number and zenith angle of observation.

It is concluded that results of useful accuracy may be obtained for the two tropospheric layers, but that the method is not sufficiently sensitive to give significant information on the upper layer. The continuous absorption over the region lowers the accuracy appreciably but does not affect the main conclusion.

1. INTRODUCTION

The purpose of this paper is to make an objective estimate of the accuracy of determination of the vertical distribution of ozone from ground-level observations of the atmospheric emission spectrum in the region of the 1,043 cm^{-1} (9·6 μ) band. Observations of this type are obviously unable to show fine details in the ozone profile; for this purpose, sondes, whether chemical or optical, are naturally preferable. But for many synoptic studies where a relatively coarse distribution suffices, the infra-red method may well be able to provide useful information together with the attendant advantages of working from a ground station. The observations are simple and the necessary equipment relatively inexpensive, while the interpretation of the measurements, though involving considerable computation, is fundamentally straightforward. The ' continuous ' absorption over this spectral region is indeed a serious complication, but its origin has now been almost certainly identified with the absorption caused by the accumulated wings of distant lines in the water-vapour rotation and ν_2 bands (Roach and Goody 1958; Saiedy 1959). Against this may be set the very great advantage over the ultra-violet region in that atmospheric haze is virtually negligible at these wavelengths.

The type of observation considered here is such as may be made with a grating spectrometer of the kind described by Goody (1957). This enables one to measure, in absolute energy units, the intensity $I(\nu, \eta)$ of the radiation arriving at the ground at wave number ν from a direction in the atmosphere with zenith angle $\sec^{-1}\eta$ (η is termed the air mass). So great is the light-gathering power of the diffraction grating compared with the prism instruments used up till now for this type of work (Epstein, Osterberg, and Adel 1956; Goody and Roach 1956, 1958; Vigroux 1959) that a single value of $I(\nu, \eta)$ may be measured with a standard error of about $\pm$ 2 per cent using as small a slit width as 2·5 cm^{-1}. This fact sharpens the point of the infra-red probe in three important ways :

(a) spectral regions may be selected where ozone is the only active component and there are no water-vapour or carbon-dioxide lines to interfere;
(b) advantage may be taken of the variation of ozone absorption across the band;
(c) the ' continuum ' may be observed by itself at certain ' window ' wave numbers; if these can be chosen on each side of the 1,043 cm^{-1} band, its influence should be accurately calculable.

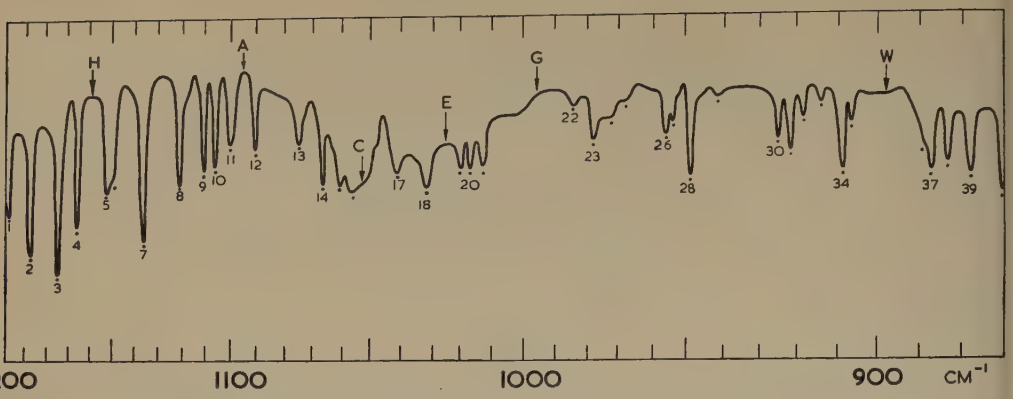

Figure 1. Typical emission spectrum (obtained with the Goody instrument) in the region of the 1,043 cm^{-1} ozone band. (29 August 1957 : 3 air masses, slit width approx. 1·2 cm^{-1} at 1,000 cm^{-1}).
The vertical deflection is proportional to energy leaving the detector, the lower boundary of the diagram representing zero. The letters indicate wave numbers selected for ozone measurements (only C, G, and the 'window' W are referred to in this paper). A table of identifications of the numbered features is available on request from the author.

A series of observations was made at Ascot, Berkshire (the field station of the Department of Meteorology, Imperial College) from March to September 1958. Unfortunately trouble was encountered as a result of reflection of radiation from the surface of the liquid-air black body, and other methods which were adopted to estimate the zero-air-mass deflection, which is needed for the conversion ofrecorder deflections to radiation intensities, were only partially successful. As a result, not much confidence can be placed in the ozone distributions which were fitted to these observations.

A new observing programme has now been started in which steps have been taken to overcome these difficulties. In this paper a careful assessment will be made of the theoretical possibilities of the method.

2. Aim of calculations

We wish to consider the accuracy with which suitable parameters of the ozone vertical distribution can be measured by this infra-red technique.

The atmospheric model used for computation is basically the one proposed by the International Ozone Commission (1956) and described by Goody and Roach (1958). (For these papers we use the abbreviations GR and IOC). It has been adapted as described in the Appendix. We take three ozone variables, x_1, x_2, x_3, giving the amounts of ozone in the layers 1,000-600, 600-300 and 300-50 mb respectively. The total amount of ozone is assumed known from the network of Dobson instruments, but no *a priori* value is assumed for the spectroscopic mean pressure of the ozone. Temperatures up to 50 mb are taken from routine radiosonde ascents. Above this level the IOC conventions and procedures are followed.

A departure from the GR treatment of the continuum has been made (see Appendix). It should be emphasized that the physical cause of the continuum is not important for this problem, since we only require to interpolate the continuum effects between measurements on each side of the ozone band. It is only necessary that the model employed should be free from serious systematic error as between regions of strong and weak ozone absorption. In fact it now appears from the extensive study of the continuum by Saiedy (1959) and by Dr. S. D. Smith at Ascot and also from the work of Vigroux (1959) at Arosa that it can be almost entirely ascribed to water vapour. In this case the radiosonde humidity measurements could be used and all arbitrary models discarded. Desirable as this would be for the interpretation of actual observations, it would have negligible effect on the results presented here.

The ozone transmission is assumed to be given by the transmission function and parameters published by the author (Walshaw 1954a; 1954b). The calculation of transmission along a path of varying pressure is effected with the help of the Curtis-Godson approximation (see Walshaw 1959).

This model enables $I(\nu, \eta)$ to be calculated from the known values of total ozone, the continuum extinction coefficient $\beta(\nu)$, and the radiosonde temperatures, and assumed values of the ozone variables x_i $(i = 1, 2, 3)$. The calculation was programmed for EDSAC 2, the Cambridge University electronic computer; the steps are outlined in the Appendix. The method of obtaining an ozone distribution from the radiation observations consists in the systematic adjustment of the x_i so as to obtain the best fit between the observed and computed $I(\nu, \eta)$.

The x_i thus determined are subject to errors arising from the following distinct sources :

(i) errors of observation of the $I(\nu, \eta)$;
(ii) errors in the radiosonde temperatures (instrumental; together with separation in space and time);
(iii) errors in $\beta(\nu)$ (observational error at the ' window ' wave number combined with interpolation errors);
(iv) errors in the conventional ozone and temperature values of the upper layers;
(v) errors in the calculation of ozone transmission (failure of Curtis-Godson approximation, inaccuracy of ozone transmission function);
(vi) failure of the ozone to be distributed in the ideal manner assumed in the model;
(vii) general rounding and other errors of computation.

No attempt is made here to assess the items (v), (vi), and (vii). This is not to say that they are negligible; but it will be evident that, unless they are so large as to preclude altogether a fit between observed and computed $I(\nu, \eta)$, (and the preliminary observations suggest that this is not the case), they will affect the deduced x_i in a systematic manner which is not likely to obscure the changes in ozone distribution of meteorological origin. Of these errors, failure of the Curtis-Godson approximation may well be the worst, since it is least accurate, as Curtis (1952) showed, when the gradients of concentration and pressure are opposed. An attempt to assess these errors is in progress.

3. Method

In order to investigate the effects of the other sources of error, (i) to (v), the following method has been employed. First, a set of combinations (ν, η) of wave number and air mass is chosen on which to base the analysis. Preliminary work indicated that this selection is not critical, provided a wide range of ozone transmission is covered. It was therefore decided to use the four combinations of the wave-numbers 996·5 and 1,053·2 cm^{-1} and the air-mass values 2 and 5. These air-mass values were chosen as being rather better determined by observation than the extreme values 1 and 6 actually measured. 1,053·2 cm^{-1} is at the R-branch ozone absorption maximum; at 996·5 cm^{-1} occurs about the lowest absorption that can conveniently be distinguished from the background. Both wave-numbers are suitable for observation with the slit width used (2·5 cm^{-1}), being effectively free of lines of other gases.

Next, a standard temperature distribution is assumed, corresponding to the summer average at Larkhill, the summer conventional values for the upper layers are taken and the total ozone is taken as 350 units (1 unit = 10^{-3} cm STP)*. Finally, consideration is restricted to a set of possible ozone distributions for which the x_i take discrete values whose upper and lower limits embrace the range of variation found in the atmosphere by other methods (*umkehr*, sondes, rockets) and whose spacing is determined partly by the desirable and partly by the anticipated accuracy. The values chosen are $x_1 = 0\ (5)\ 30$,

* All ozone values in this paper are in the new Vigroux scale.

$x_2 = 0\ (5)\ 30$, $x_3 = 20\ (60)\ 140$ units, giving altogether $7 \times 7 \times 3 = 147$ different ozone distributions. EDSAC is now used to compute systematically the values of $I(\nu, \eta)$ at the four (ν, η) values given above for each distribution. It will be convenient to denote by the vector $\mathbf{x}$ the set of three quantities $\{x_1, x_2, x_3\}$ characterizing the distribution, and by the vector $\mathbf{I}$ the set of four quantities $\{I_1 = I(996{\cdot}5, 2), I_2 = I(996{\cdot}5, 5), I_3 = I(1{,}053{\cdot}2,2), I_4 = I(1{,}053{\cdot}2, 5)\}$. We shall also use the term *radiation table* to denote the complete table $\mathbf{I}(\mathbf{x})$.

Radiation tables have been computed for the above assumptions and for two continuum conditions: (i) with the continuum absent, $\beta(\nu) = 0$; this will enable us to assess the maximum accuracy which may be approached in a very dry atmosphere at a high-altitude station; and (ii) with continuum conditions broadly representative of the Ascot measurements, taking $\beta(996{\cdot}5) = \beta(1{,}053{\cdot}2) = 0{\cdot}125$ (air mass)$^{-1}$ (base e). These radiation tables form the basis of the assessment of the various sources of error in the ways now to be described.

4. Results

We consider the errors listed under the headings (i) to (iv) in Section 2.

4·1 *Errors of observation of* $I(\nu, \eta)$

The effects of random errors in the observations themselves will first be considered. The following procedure is used. Choose a distribution $\mathbf{x}$ and perturb its $\mathbf{I}$ by a suitable random vector $\delta\mathbf{I}$, giving $\mathbf{I}' = \mathbf{I} + \delta\mathbf{I}$. Now compare $\mathbf{I}'$ with all the $\mathbf{I}$ in the radiation table and select the distribution $\mathbf{x}'$ which gives the ' best fit ' on the least squares criterion, i.e., which makes $\sum_{i=1}^{4} (I_i - I_i')^2$ a minimum. Then the difference between $\mathbf{x}$ and $\mathbf{x}'$ is a measure of the ' error ' in the ozone distribution arising from the ' error ' $\delta\mathbf{I}$ in $\mathbf{I}$. The process may be repeated with further random vectors $\delta\mathbf{I}$ (drawn from the same population) until a statistically significant number has been taken. The distribution of the resulting $\mathbf{x}'$ then gives the information we require.

Various types of random error may be simulated, but we have only considered the type corresponding to the observational limitation of signal-to-noise ratio. This gives rise to an absolute error in each I_i which is some constant fraction f of the maximum I_i measured. Specifically we take

$$\mathbf{I}' = \{I_1 + u_1 f I_4,\ I_2 + u_2 f I_4,\ I_3 + u_3 f I_4,\ I_4 + u_4 f I_4\}$$

where the u_i are normally distributed random numbers with zero mean and unit variance.

This process enables a very realistic estimate of the effects of this type of error to be obtained, and is well suited to electronic computation owing to the simplicity of the arithmetical operations. A sample of 50 trials has been found satisfactory, taking approximately 15 sec machine time. Random numbers in the range (0, 1) with a uniform distribution are easily generated by well known digital processes and the correction to a normal distribution may be made by a numerical factor.

The general trend of the results is illustrated by frequency diagrams in isometric projection (Fig. 2). Each cell on the base plane represents a combination (x_1, x_2); the height of each column rising from this plane is proportional to the number of times, in a total of 50, with which each combination has been selected as the best fit. The columns are subdivided according to the frequencies of x_3. The initial distribution in each diagram has x_1 and x_2 indicated by a distinctive shading of the top of the appropriate column; the initial value of x_3 was always 80 units. In the cases illustrated the random error, as defined above, was taken as 1·15 per cent ($f = 0{\cdot}0115$).

These diagrams illustrate clearly the deterioration in accuracy caused by the screening effects both of increasing ozone amounts in the lower layers and also of the continuum. Accuracy in the 300-50 mb layer quickly degenerates (cf (a) and (b), (a) and (d)). After this, errors in x_1 and x_2 begin to occur; it will be seen that as soon as the results begin to

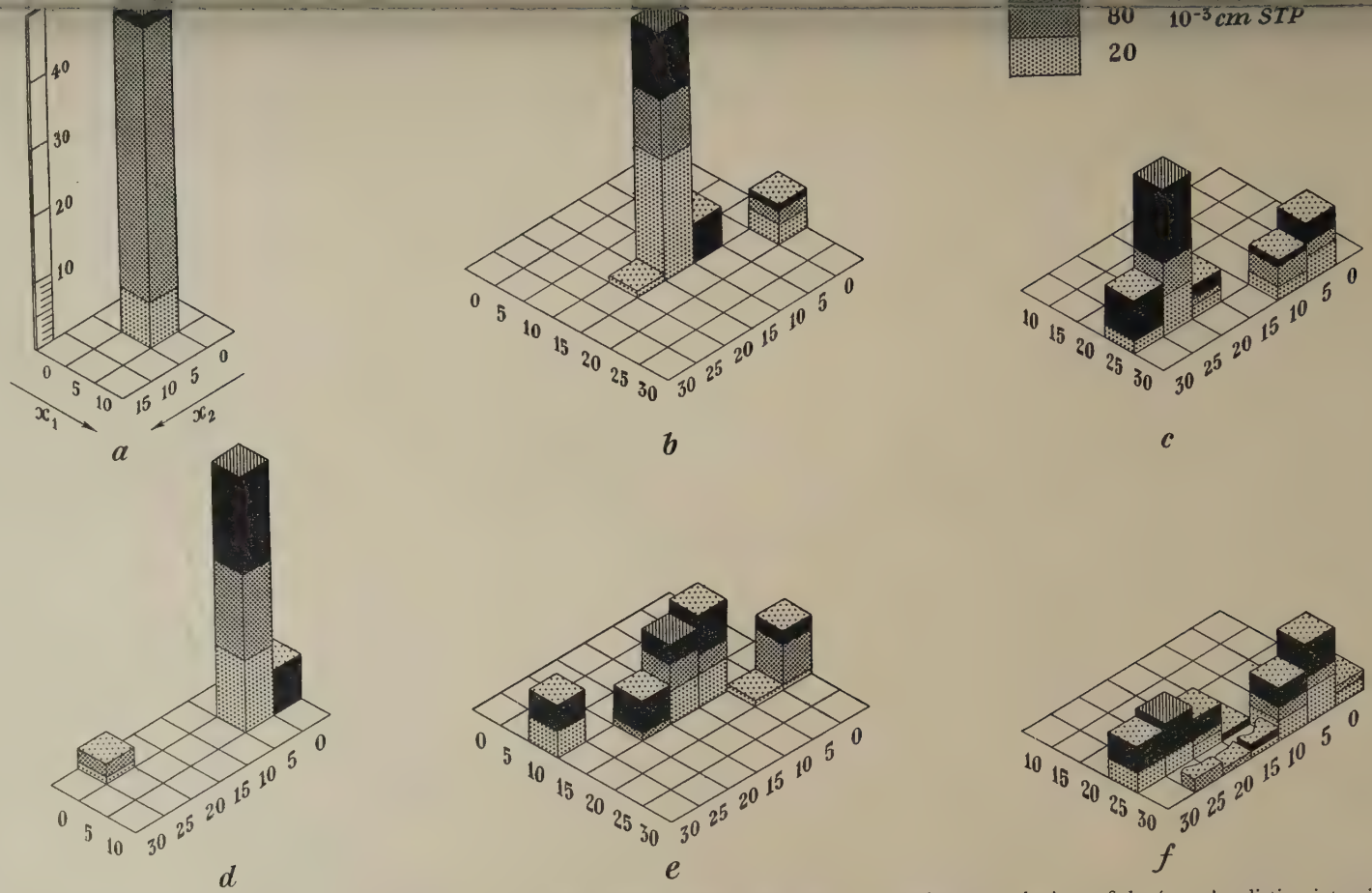

Figure 2. Effect of random errors on the observations of $I(\nu, \eta)$. Each diagram shows the effect of 50 random perturbations of the 'true' radiation intensities. The number of times any particular distribution was selected as the best fit to the perturbed intensities is represented by the heights of the columns, the distribution being indicated by the co-ordinates on the base plane (x_1, x_2) and the shading of the columns (x_3). The (x_1, x_2) values of the initial ('true') distribution are those for the column whose top is shaded differently from the others; the x_3 value in this distribution was always 80 units (1 unit = 10^{-3} cm STP). For all these cases the percentage random error (for definition see text) was 1·15 per cent. In (a), (b), (c) the continuum was absent; going from (a) to (c) shows an increase in errors due to the 'blanket effect' of increasing ozone amount in the lower layers. (d), (e) and (f) correspond to (a), (b), and (c) but with the addition of a grey continuum with extinction coefficient 0·125 (air mass)$^{-1}$ (base e) broadly representative of Ascot conditions.

be distributed in x_2 along a line of constant x_1, some also begin to appear with a higher x_2 and reduced x_1 or vice versa. It is also apparent that no useful information on x_3 is obtained once this condition has been reached.

While Fig. 2 illustrates the general effects of random radiation errors, we wish to know the standard errors of the ozone contents of the three layers which will arise from a given standard error in the radiation measurements. These may be found to an adequate degree of accuracy by taking the number of times the ' correct ' (i.e., initial) value of x_0 say x_0, for a particular layer was selected, and assuming this to be a sample from a normal distribution. The standard deviation of the distribution giving this number between the limits $x_0 \pm 2{\cdot}5$ units is then found from a table of the probability function. The number of ' correct ' values must of course be greater than the number expected by pure chance. This can be secured by a suitable choice of the perturbing error f for each initial distribution.

TABLE 1. EFFECTS OF RANDOM ERRORS IN RADIATION MEASUREMENTS

Initial distribution			Without continuum			With continuum		
x_1	x_2	x_3	1	2	3	1	2	3
0	5	80	–	–	25	–	–	85
0	15	80	1·8	1·8	34	2·2	2·8 ± 0·2 (2)	95
5	5	80	1·6	1·8	38	2·3 ± 0·1 (2)	3·0 ± 0 (2)	–
15	0	80	–	–	–	5·0 ± 0 (2)	6·3 ± 0·5 (2)	–
15	15	80	2·8	3·8	178	6·3 ± 0·6 (7)	9·0 ± 0· (5)	–
25	15	80	3·9 ± 0·3 (2)	6·1 ± 0·3 (2)	–	6·3 ± 0·6 (3)	–	–
25	25	80	3·8 ± 0·2 (3)	7·4	–	7·4	–	–

Numbers in the body of the table are the standard deviations in the ozone contents (unit : 10^{-3} cm STP) of each layer (1 : 1,000-600 mb, 2 : 600-300 mb, 3 : 300-50 mb) caused by random errors in radiation intensities $I(\nu, \eta)$ having a standard deviation ± 2 per cent of I (1,053·2, 5). Where more than one estimate has been obtained, the value given is the mean with its standard error, and the number of estimates in brackets.

Standard deviations obtained in this way are given in Table 1. These have all been scaled to refer to a standard error of ± 2 per cent in the radiation measurements, in the sense already defined. They should therefore correspond to experimental conditions. It will be seen from the results obtained with the same initial distribution but different f-values and different sets of random numbers that the method gives quite adequate statistical accuracy.

Table 1 indicates that the level of observational accuracy that can be realized in practice will permit quite useful accuracy in the determination of the ozone contents of the layers 1,000-600 and 600-300 mb, but will hardly ever be sufficient to give useful information on the 300-50 mb layer. The influence of the continuum on this type of error, however, is somewhat less than was initially expected.

4·2 *Errors in radiosonde temperatures*

A similar procedure is used to that just described. For an initial ozone distribution $\mathbf{x}$, $\mathbf{I}$ is recalculated with the perturbed temperatures. The result, $\mathbf{I}'$, is then compared with the radiation table values exactly as described above to find the distribution $\mathbf{x}'$ of best fit, and the difference between $\mathbf{x}$ and $\mathbf{x}'$ is a measure of the ' error.'

This calculation has been carried out with a temperature increase of 1°K throughout each of the three layers in turn for a range of initial **x**, both with and without the continuum. The detailed results show in all cases a progressive deterioration in accuracy from the top layer downwards; if an error occurs in layer 2, for example, it is very unlikely that any significance can be attached to the result obtained for layer 3; similarly an error in layer 1 prevents useful information being obtained on layers 2 and 3. The essential features of these results can therefore be concisely indicated, as has been done in Table 2, by stating the lowest layer whose ozone content is wrongly determined; ozone contents of the layers below this one are always recovered correctly, while above it they bear little relation to the true value. The sense of the error is that if the radiosonde temperatures are higher than the true temperatures, the ozone amounts will be underestimated.

TABLE 2. INFLUENCE OF RADIOSONDE TEMPERATURES

x_2	x_1		
	5	15	25
5	000	303	203
	300	203	203
15	000	333	133
	100	203	133
25	033	333	133
	233	233	133

The cells in the table correspond to the x_1 and x_2 values of the initial distribution; the initial x_3 was always 80 units (unit : 10^{-3} cm STP). The first digit of each number indicates the error in distribution when the temperatures throughout layer 1 are increased by 1°K; the second and third digits give the corresponding errors when the same change is applied to layers 2 and 3 respectively. The meaning of the digits is : 0 : no error, 1 : layer 1 in error by 5 units, 2 : layer 2 in error by 5 units (no error in layer 1), 3 : layer 3 in error by 60 units (no errors in layers 1 and 2). In each cell the upper number is for continuum absent, the lower for continuum present.

4.3 *Effect of errors in continuum extinction coefficient*

We have already indicated that two types of error in the continuum extinction coefficient $\beta(\nu)$ must be considered. First, the observational errors at the ozone-free frequencies must be taken into account; these can readily be estimated from the observational data. Secondly, the values of $\beta(\nu)$ at these frequencies must be put into some kind of interpolation formula to obtain $\beta(996{\cdot}5)$ and $\beta(1053{\cdot}2)$. This process will involve further errors. At present there does not seem to be sufficient experimental material for a useful discussion of these interpolation errors. The 1958 observations were treated with a purely empirical interpolation formula, but the large variations found in the spectral form of the continuum are almost certainly of instrumental origin. Since then it would appear from the Ascot work that a continuum spectrum based on line wing absorption may be practicable. It may prove necessary, however, to retain a small empirical component to allow for variations in the small contribution from haze.

In order to estimate the effects of both kinds of error calculations similar to those of Section 4·2 were made using ' errors ' of 0·5, 1, 2 and 5 per cent in $\beta(\nu)$. The calculations were done first with the same error applied to both frequencies, and then repeated with the error applied only at 996·5 cm^{-1}. These may be regarded as errors in *level* and in *spectral form* respectively, and correspond broadly to the two types of error discussed above.

The results, summarized in Table 3, show no marked difference between the two types of error. To obtain the ozone amounts of the 1,000-600 and 600-300 mb layers to within 5 units, errors in $\beta(\nu)$ must be less than 2 per cent. This level of error is certainly

realizable on the 'window' frequencies, and does not appear unrealistic for the ozone-absorbing frequencies. But to avoid ozone errors greater than 60 units in the 300-50 mb layer requires the $\beta(\nu)$ errors to be less than 0·5 per cent in some cases, and this is unlikely to be achieved in practice. We must therefore not expect to obtain ozone values in this layer with a useful level of accuracy in the presence of the continuum normal to this climate.

TABLE 3. INFLUENCE OF ERRORS IN THE CONTINUUM EXTINCTION COEFFICIENT

x_2	x_1		
	5	15	25
5	0033	0332	3332
	0033	0033	0331
15	0332	0332	3332
	0033	0332	0333
25	0332	3332	3332
	0033	0333	333–

The arrangement is similar to that of Table 2 and the digits have the same meaning. The four digits of each number refer, from left to right, to errors of 0·5, 1, 2 and 5 per cent in continuum extinction coefficient $\beta(\nu)$. In each cell the upper number applies when the error occurs at both frequencies, the lower when it occurs at 996·5 cm^{-1} only.

4.4 *Errors in conventional ozone and temperature values of the upper layers and in total ozone*

The procedure of Section 4.2 has been repeated with variation of these quantities, the effects of which are summarized in Table 4. It will be seen that the method is quite insensitive to them as far as concerns layers 1 and 2, but a useful level of accuracy for layer 3 requires that their values should be known rather precisely.

TABLE 4. EFFECT OF VARIATIONS IN CONVENTIONAL DATA FOR UPPER LEVELS AND IN TOTAL OZONE AMOUNT

		Initial x_1		
		0	15	25
(1). Ozone content of 0-10 mb layer	(a) reduced by 10 per cent	*Z*	*Z*	*Z**
	(b) replaced by winter value	*Z*	*N*	*N*
(2). Temperature of 0-10 mb layer	reduced by 5°K	*Z*	*N*	*N*
(3). Temperature at 45 mb level (affecting assumed emission temperature of 10-50 mb layer)	reduced by 5°K	*N*	*N*	*N*
(4). Total ozone amount increased	(a) by 5 per cent	*Z*	*Z*	*Z*
	(b) by 10 per cent	*Z*	*P*	*P*
	(c) by 25 per cent	*P*	*P*	*P*

Each column on the right represents an initial distribution; the initial values of x_2 and x_3 were always 15 and 80 units respectively. The variations listed had no effect on layers 1 and 2. The effect on layer 3 was either zero, + 60, or − 60 units, indicated respectively by the symbols *Z*, *P* or *N*. The calculations gave the same results with and without the continuum, except for the case marked *, where the calculation with continuum gave an *N*.

5. Conclusions

We have now examined the accuracy with which we might expect to obtain the vertical distribution of ozone from high-resolution measurements of atmospheric emission from the ground. The broad conclusion is that results of meteorologically significant accuracy should be obtainable for the ozone contents of two layers between the ground and the tropopause. This is based on the assumption of ± 2 per cent accuracy in the radiation measurements and $\pm 1°K$ in radiosonde temperatures. The former figure is a rather conservative estimate of the accuracy at present achieved with the Goody instrument with slits of constant geometrical width. In principle it is desirable to use a different slit width for each spectral region, so as to obtain the maximum amount of energy without including H_2O or CO_2 lines, but against this must be set the time taken to adjust the slits and the possibility of undetectable erroneous settings being made. The somewhat radical redesign of the instrument necessary to permit the use of optimum pass bands and rapid changes of zenith angle may, however, be justified, because the 2 per cent accuracy quoted is limited by detector noise and not by sky unsteadiness.

The 1°K accuracy assumed for radiosonde temperatures is also rather conservative in the ordinary sense of random errors, but it must be remembered that the radiosonde station may be some distance away and inversions are often present when the sky is clear.

For the determination of the ozone contents in the two tropospheric layers no accurate knowledge is required of total ozone, nor of conditions in the upper layers. Rather accurate information about the continuum is necessary; it is hoped that this will be acquired from the work in progress.

Significant ozone information above the tropopause is difficult to obtain by this technique, because the region of low temperatures makes but little contribution to the radiation arriving at the ground. Very much better observational accuracy than we have considered would be necessary, together with rather precise information on the upper-air conditions and the total ozone; its achievement seems rather unlikely.

Finally, the possibility of combining this type of observation with scattering observations in the ultra-violet (*umkehr* method or a modification of it) may be mentioned as likely to give a reasonably accurate measurement of the complete ozone distribution from a ground station.

Acknowledgments

Professor R. M. Goody and Professor P. A. Sheppard have greatly stimulated and encouraged this work at many points. To them, and to the United States Air Force, who provided financial assistance, I am most grateful. The Director and Staff of the Cambridge University Mathematical Laboratory have given much helpful advice in the use of EDSAC 2, and I also wish to acknowledge with thanks the help of the Department of Mathematics, Northampton College, where preliminary calculations were made on the Pegasus computer.

References

Curtis, A. R.	1952	*Quart. J. R. Met. Soc.*, **78**, pp. 638-640.
Epstein, E. S., Osterberg, C. and Adel, A.	1956	*J. Met.*, **13**, pp. 319-334.
Goody, R. M.	1957	*Quart. J. R. Met. Soc.*, **83**, pp. 517-521.
Goody, R. M. and Roach, W. T.	1956	*Ibid.*, **82**, pp. 217-221.
	1958	*Ibid.*, **84**, pp. 108-117.
International Ozone Commission	1956	Report of Conference of Infra-Red Panel. Unpublished.
Roach, W. T. and Goody, R. M.	1958	*Quart. J. R. Met. Soc.*, **84**, pp. 319-333.
Saiedy, F.	1959	I.A.M. Radiation Symposium, Oxford, Summary No. 30 (in course of publication).
Vigroux, E.	1959	*Annales de Géophys.*, **15**, pp. 453-460 and pp. 516-538.
Walshaw, C. D.	1954a	*Proc. Toronto Met. Conf. 1953*, pp. 49-52.
	1954b	Dissertation, Cambridge University.
	1959	*Science Progress*, **47**, pp. 67-79.

Appendix

(a) *The atmospheric model*

The basic IOC model is given in Table 2 of GR. The numbers 45 and 27 in the last two rows of column 5 should read 61 and 36 respectively in the new (Vigroux) ozone scale used in these calculations; the rest of columns 5 and 6 are not used here. Our x_1, x_2, x_3 represent the ozone contents of the layers there called 1a, 1b, 2. For computation a further subdivision is made according to the scheme 1,000 (− 50) 600 (− 50) 300 (− 30) 120 (− 14) 50 (− 40) 10 (− 10) 0 mb. This choice of intervals enables the 50 to 300 mb layer to be divided at 120 mb if desired, although this has not been done here.

A rather close spacing of levels has been chosen in order to be able to calculate the emission by direct use of the trapezium integration rule, without having to use the GR approximation of a mean emission temperature for fairly thick atmospheric layers. Some preliminary investigations of this approximation were carried out. The effective radiation temperature was computed for a model atmosphere in a spectral region with weak ozone absorption, and this temperature was then used to calculate the emitted intensity in a strongly absorbing region. The result was found to be in error by about 5 per cent compared with the results of direct numerical integration. Since in the present work we aim at keeping such systematic errors to a minimum, the GR approximation has not been used. For purposes of hand calculation it may be essential, but its errors will require careful assessment if a fairly wide range of ozone absorption coefficients is to be employed.

The GR procedure for the 10-50 mb layer, based on the empirical fact that its temperature structure is effectively determined by the temperature at the 45 mb level, is adapted to our requirements by converting the GR black-body intensites computed for the centre of the 1043 cm^{-1} band (their Table 3) to radiation temperatures T_e by means of the Planck function. This gives as a working formula $T_e = T(45\text{ mb}) + \Delta T$, with $\Delta T = -2{\cdot}1, -1{\cdot}8, -1{\cdot}2, +0{\cdot}1, +2{\cdot}3, +4{\cdot}6$°C for $T(45\text{ mb}) = -70\ (5) -45$°C. For the 0-10 mb layer the IOC conventional temperatures, 258·0°K for summer and 224·6°K for winter, are used.

GR treated the continuum as a thin layer close to the ground but with the temperature of the 950 mb level. This was found to be unsatisfactory for the range of ozone absorptions employed here, so an attempt has been made to set up a more realistic model. This assumes the material responsible for the continuum to have an exponential distribution with height, and the scale height h is an arbitrarily chosen parameter equivalent to the choice of the 950 mb level in the GR model. In principle the observed variation of $I(\nu, \eta)$ with η should yield the two parameters, h and the continuum extinction coefficient $\beta(\nu)$. But in practice this is found to require enormously greater observational accuracy than can be realized. h must therefore be arbitrarily assumed and the observations used to determine the value of $\beta(\nu)$. To represent the distribution of the continuum material with height it is convenient and sufficiently accurate to use a formula based on an isothermal atmosphere. This gives for the continuum extinction coefficient $\beta_p(\nu)$ for the layer bounded by pressure level p and the ground (p_0)

$$\beta_p(\nu) = \beta(\nu)\,[1 - (p/p_0)^{H/h}] \quad . \quad . \quad . \quad . \quad (1)$$

where H is the scale height of the isothermal atmosphere. We have used throughout the values $H = 8$ km, $h = 1$ km.

(b) *The calculation of* $I(\nu, \eta)$

The first stage is to calculate, from the given ozone values x_1, x_2, x_3, the total ozone amount, and the conventional 0-10 mb amount, the vertical ozone amounts m_j ($j = 0, 1, 2 \ldots n$, $n = 27$) between the ground and each level j from the IOC model

formulae. These are stored. Next the Curtis-Godson mean pressure p_j^* are calculated from $m_j p_j^* = \frac{1}{2} \sum_{i=1}^{j} (p_i + p_{i-1})(m_i - m_{i-1})$. These are also stored. The first wave number value ν_1 is now taken and the Planck functions $B_j = B(\nu_1, T_j)$ are calculated and stored for each level; also the values of parameters for the ozone transmission function and the continuum extinction coefficient $\beta(\nu)$ are set in the appropriate registers. The first air mass value η_1 is now taken and the summation

$$I(\nu_1, \eta_1) = \int B \, d\tau = \tfrac{1}{2} \sum_{j=1}^{n} (B_j + B_{j-1})(\tau_{j-1} - \tau_j)$$

is started. Here τ_j is the combined transmission of ozone and continuum between ground and level j.

Allowance for earth curvature is made by the approximate procedure developed by GR. This consists in adjusting the value of η by a fractional amount depending on η itself and on the p_j^* value of the level considered. The GR data for this correction were put into the following form, purely for convenience in electronic calculation :

$$\eta_j^* = \eta \left[1 - 10^{-3} (107{\cdot}88 - 0{\cdot}108\, p_j^*)(100 + 0{\cdot}68\, p_j^*)^{-1} (3{\cdot}17\, \eta^2 + 5{\cdot}83\, \eta - 9{\cdot}00)\right]$$

where η_j^* is the corrected value of η and p_j^* is in mb. The appropriate value of $\beta_j(\nu_1)$ is then calculated from Eq. (1). The ozone transmission along the slant path from ground to level j is calculated from the transmission function, using $m = m_j$. η_j^* and $p = p_j^*$; this is multiplied by the corresponding continuum transmission $\exp(-\eta_j^* \beta_j)$ to give τ_j. Other air-mass values at the same ν_1 are next taken, and then the next ν with its air-mass values, and so on.

551.594.253

Measurements on the electricity of precipitation

By M. W. RAMSAY and J. ALAN CHALMERS
Physics Department, University of Durham

(Manuscript received 18 February 1960)

SUMMARY

Measurements have been made of the electricity of precipitation, the potential gradient and the rate of rainfall. The results for the winter of 1957/58 show general agreement with those of earlier workers, in giving a linear relation between potential gradient and precipitation current, but those of the summer of 1958 are less ordered. Comparisons have been made of the currents to open and shielded receivers, and show general agreement. The ' mirror-image effect ' and time delays connected with it have also been studied, without any complete explanation.

1. INTRODUCTION

Measurements of the electricity of precipitation are of importance in atmospheric electricity in two respects; first, precipitation must play some part in the total transfer of charge between clouds and earth; and second, a study of the charge on precipitation and its relation to other factors may provide useful information which will help to elucidate the charge-generating processes in clouds, processes which are often considered to be very closely associated with precipitation.

There are several reasons why it is considered desirable to concentrate attention on conditions of continuous non-stormy precipitation; in the first place it seems quite certain that precipitation plays only a very small part in the transfer of charge between storm clouds and earth, while it must play the major part in the much smaller transfer in continuous precipitation, since there is no lightning and no point discharge; also, conditions are so much steadier during continuous precipitation that it is likely to be much more easy to recognize relations between the factors concerned; and, finally, continuous precipitation is much more frequent than storms and so, in a limited period of work, more observations are possible.

Recent measurements on the electricity of continuous precipitation include those of Simpson (1949) and Chalmers (1956). Simpson used a receiver which was partly shielded from the direct action of the atmospheric field and so missed some of the precipitation which would fall on an open area of ground. He was concerned mainly with average values over one-minute intervals, and since his electrometer was earthed every minute, it was difficult to notice changes in conditions over periods of the order of a few minutes.

Chalmers (1956) used a fully-exposed area of ground, but measured only the total effect over a period of $4\frac{1}{2}$ minutes, correcting for potential-gradient changes; he was therefore not able to examine any alterations of current during the $4\frac{1}{2}$-minute period. He also did not measure the rate of rainfall.

Simpson found that, for all his results for potential gradients between $\pm$ 1,000 v/m, the best formula was :

$$q = -4{\cdot}8 \times 10^{-8}\,(F - 400)$$

where q is the charge in C m^{-3} and F is the potential gradient in v m^{-1}. His results may also be expressed as :

$$I = -1{\cdot}33 \times 10^{-14}\,R\,(F - 400)$$

where I is the current in a m^{-2} and R is the rate of rainfall in mm hr^{-1}.

Chalmers's results for rain gave :

$$I_1 = -1{\cdot}18 \times 10^{-14}\,(F - 150)$$

which is the average for all rates of rainfall and includes the conduction current as well as the precipitation current.

The objects of the present investigation were to repeat Simpson's work, but with the following modifications : an exposed receiver was used as well as a shielded receiver, and the results for the two receivers compared; with a continuous recording of the current instead of earthing every minute, variations of the current over periods of minutes can be recognized; and a specific investigation of the variation of the current with rate of rainfall was undertaken, not just Simpson's test that q, rather than I, showed a linear relation with F.

2. Measurement of current

The measurement of the current and the way in which compensation for the effect of potential-gradient changes is achieved has been described in detail by Adamson (1960). The general principle is that the current to the exposed surface flows through a high resistance and the potential developed across this is applied to one grid of a double electrometer valve. The potential gradient close by is measured by means of a field mill; the output from this is differentiated by a condenser and the resulting signal is applied to the second grid of the valve. By a suitable adjustment of the condenser, the effects of potential-gradient changes are eliminated.

For the electronics of the circuits and the consideration of time constants, the reader is referred to Adamson's (1960) paper. This apparatus was used for the measurement of the current to an exposed receiver.

For the measurement of the current to a shielded receiver, apparatus was constructed similar to that of Scrase (1938) and the current measured by an Ekco vibrating-reed electrometer, with the head unit firmly fixed to the receiver funnel, to avoid piezo-electric effects in the cable.

3. Measurement of rate of rainfall

Scrase (1938) and Simpson (1949) measured the rate of rainfall from the filling of a small tilting bucket incorporated in the receiver. This gave no indication of the actual rate of rainfall but only the average rate between two tippings. In addition there was a possibility that the dripping of the water into the bucket might introduce charging even though the point of dripping was well shielded.

As an alternative the rate of rainfall was measured independently at a point close to the place where the other quantities were measured. The method used is described by Ramsay (1960) and consists of the measurement of the capacity of a condenser, which is filled by the rain water and siphons out when full. This provides an electrical measurement which acts continuously and can be recorded in the same way as the other results. Even though the analysis used average rates of rainfall, these were over shorter periods than in the earlier work, and it was possible to detect alterations of rate.

The galvanometer deflections were recorded by the photographic trace on a drum camera; on each record, lasting for about 90 min, there were traces for current to open receiver (2 sensitivities recorded by 2 galvanometers in series), current to shielded receiver, potential gradient and rainfall. A timing circuit, triggered by half-minute pulses from a standard clock, switched off a fogging lamp for 30 sec every 5 min, providing a time scale. A transparent scale in front of the recording drum was illuminated by the fogging lamp and provided a scale on the record. On each record, at each end, zeros and calibrations, where necessary, were recorded.

The records were analysed by taking the average values of the deflections over every one-minute interval during which the records were satisfactory. Analysis was confined to periods during which the potential gradient remained within the range $\pm$ 500 v m^{-1}, so as to ensure that there were no periods when point discharge would be occurring. No restrictions were imposed as to the duration of precipitation but cases of obviously 'showery' conditions were excluded.

The results were divided according to the rate of rainfall into the classes : $< 0{\cdot}003$ mm min^{-1}, $0{\cdot}003 - 0{\cdot}01$; $0{\cdot}01 - 0{\cdot}02$; $0{\cdot}02 - 0{\cdot}03$; $0{\cdot}03 - 0{\cdot}04$ and $< 0{\cdot}04$,

and for each rate of rainfall it was possible, by statistical methods, to obtain the ' best straight line ' relating current and potential gradient, as the regression of I on F.

The results were divided into 3 periods, winter 1957-58, summer 1958 and 1959; the division was first made because the shielded receiver was not in action until the summer of 1958, but differences between the results for the open collector were apparent as between winter and summer.

5. Relation between precipitation current, potential gradient and rate of rainfall

The results obtained between 5 November 1957 and 30 April 1958 were recorded on 20 different days, with a total of 51 records, each record giving up to 75 min useful recording time. From these records, 3,144 one-minute average values of precipitation current, potential gradient and rate of rainfall were obtained and analysed as described in the previous section.

The results are shown in Table 1 where a and C are the constants in :

$$I = a\,(F + C).$$

For the intermediate rates of rainfall, the results for each group fitted a straight line reasonably well (see e.g. Fig. 1) but for high and low rates, there appeared a tendency for the points to follow a curve concave upwards (see Fig. 2).

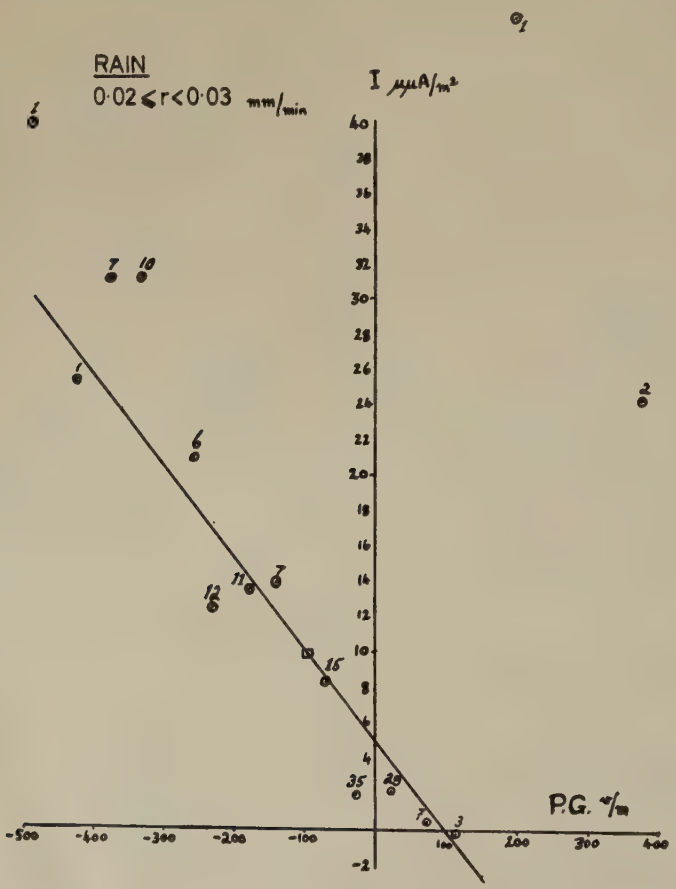

Figure 1. Variation of current with potential gradient showing good linearity.

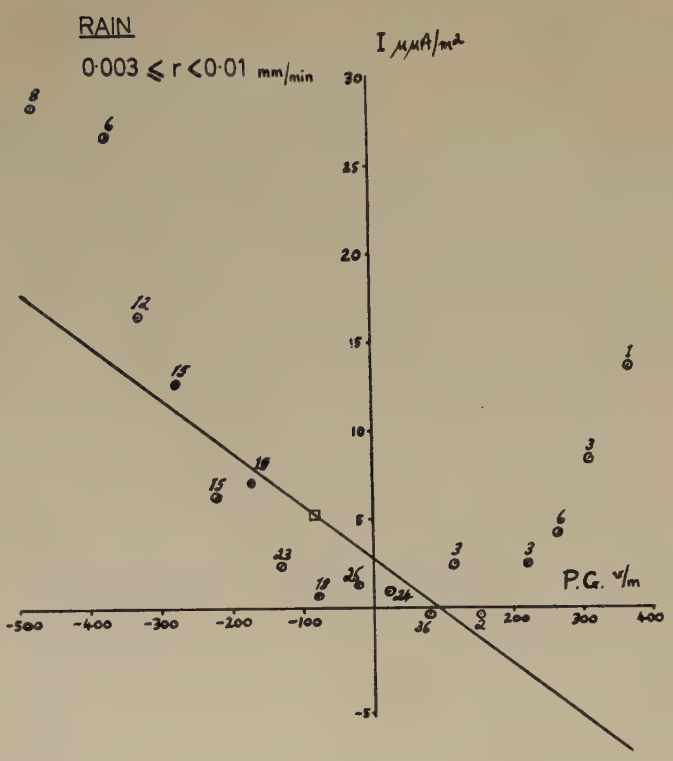

Figure 2. Variation of current with potential showing tendency to curvature.

For those cases where the straight line is a good fit, the values of C are nearly the same and agree fairly well with the guess of Simpson (1949) that C represents the fine-weather potential gradient. Also it is seen that $-a$ increases with the rate of rainfall, in general agreement with Simpson's results, although Simpson gave a direct proportionality. If $-a$ is plotted against r, the rate of rainfall, it is found to fit closer to $a^2 = r/10$ than to a straight line.

TABLE 1. WINTER 1957/58

Type of precipitation	R (mm min^{-1})	$-a$ $\frac{\mu\mu a\ m^{-2}}{v\ m^{-1}}$	$-C$ v m^{-1}	Total points
Rain	< 0·003	$0{\cdot}32 \times 10^2$	31·1	962
Rain	0·003-0·01	$3{\cdot}00 \times 10^2$	94·7	219
Rain	0·01-0·02	3·93	99·8	267
Rain	0·02-0·03	5·18	95·7	147
Rain	0·03-0·04	7·09	16·3	46
Rain	> 0·04	6·53	− 6·3	37
Rain	Average	2·19	64·8	1,677
Rain	Chalmers (1956)	1·18	140	1,418
Sleet		1·19	− 124	472
'Wet snow' *		17·8	12	133
Snow		0·94	− 176	862
Snow	Chalmers (1956)	0·92	− 440	990

* one day only 10 December 1957

On one occasion (6 January 1958) there was a quite sudden change from sleet to snow and, simultaneously (to within $\frac{1}{4}$ minute), there was a change from positive I and negative F to negative I and positive F.

In the summer of 1958, results were obtained on 11 days from 5 May to 3 October, giving 31 records, from which 1,345 one-minute average values were obtained of the same data as before, together with the current to the shielded receiver. These results showed much wider divergence from a linear relation (see Fig. 3) and though the ' best straight lines ' were obtained statistically as for the winter results, the lines and their slopes have little meaning. The comparison of results for the open and shielded receivers are considered in Section 7 of this paper. Average values of potential gradient and current and the slopes of the best lines are given in Table 2 with the winter results for comparison. From these results we see that the potential gradient shows no correlation with the rate of rainfall; the current appears to increase with the rate of rainfall and the ' slope ' gets more negative as the rate of rainfall increases.

TABLE 2. AVERAGE VALUES AND COMPARISONS

	Winter 1957/58				Summer 1958					
mm min^{-1}	Total	mean F v m^{-1}	mean I $\mu\mu a\ m^{-2}$	slope $10^{-2}\ \mu\mu a\ m^{-2}$	Total	mean F	mean I	mean I_s	slope I	slope I_s
< 0·003	962	− 89	0·34	− 0·32	692	− 49	2·3	2·9	1·42	1·24
0·003-0·01	219	− 83	5·33	− 3·00	193	− 49	5·9	6·5	0·04	0·26
0·01-0·02	267	− 116	8·48	− 3·93	167	− 83	7·5	7·1	0·46	1·12
0·02-0·03	147	− 95	9·88	− 5·18	140	− 79	8·7	8·0	− 2·29	− 1·67
0·03-0·04	46	− 103	8·49	− 7·09	84	− 73	6·5	6·0	− 2·62	− 1·31
> 0·04	36	− 78	4·71	− 6·53	69	− 78	14·3	7·9	− 4·94	− 3·72
All	1,677	− 93	3·46	− 2·19	1,345	− 59	5·03	4·97		
Chalmers (1956)	1,418	− 176	3·8	− 1·18						

A few results were obtained during the early part of 1959, but they were mostly in conditions of low rate of rainfall and low potential gradient. On two occasions of very fine drizzle the potential gradient was about -25 v m^{-1} and the current around $-3\ \mu\mu a\ m^{-2}$, both remaining negative throughout the records.

6. Discussion of results

The winter results show general agreement with the earlier results of Simpson (1949) using a shielded receiver and of Chalmers (1956) using an open receiver, although there is not detailed numerical agreement. The general agreement also extends to snow, although here there is a marked difference in the intercept. For the summer results, the agreement is much less marked.

The winter results give support to the conclusions of Chalmers (1956; 1959) that in nimbostratus clouds the precipitation, when in the form of snow, receives a negative charge, leaving a positive charge behind in the cloud; but when it melts, a positive charge is acquired, leaving negative charge behind. Sleet, as a mixture of snow and rain, gives results intermediate between the two. If melting takes place close to the ground, then we should expect the relation between the charge on the precipitation and the potential gradient caused by the charge left behind to be closer then when it takes place higher up and such effects as turbulent diffusion, convection currents, etc., would be more prominent. In agreement with this, it is found that the linear relation between I and F is closest for sleet and ' wet snow ' and least obvious in the summer.

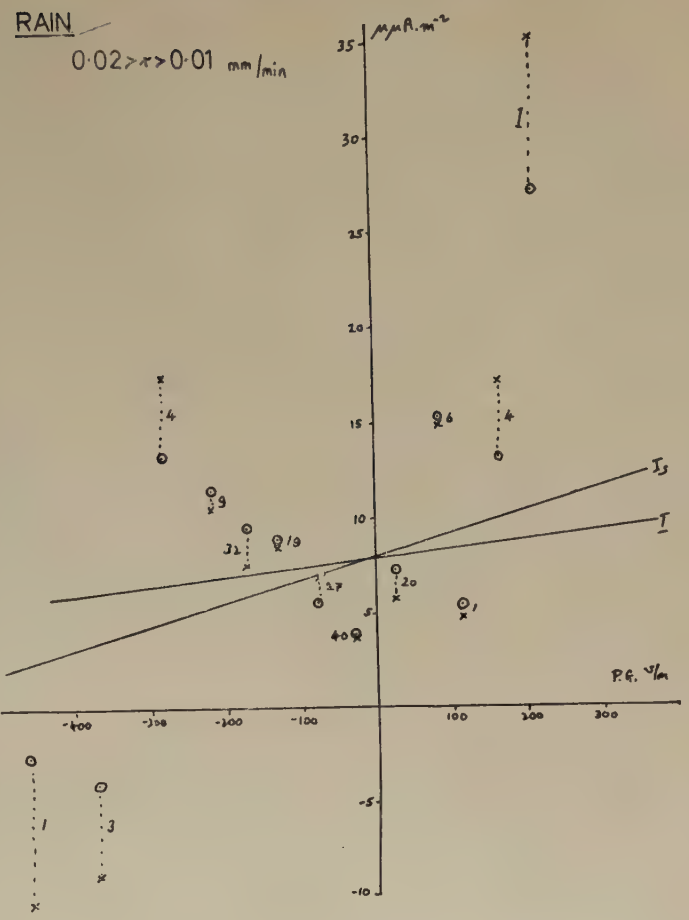

Figure 3. Variation of current with potential gradient showing little correlation.

In summer, too, there may be cases in which the rain has never been snow, but has been produced by the coalescence mechanism. It is not to be expected that such rain would show the same relation between I and F as holds for rain which has received a charge when snow, and another when melting.

The connection between the I/F relation and the ' mirror-image effect ' is considered in Section 8.

7. Comparison of open and shielded receivers

Measurements of the current to open and shielded receivers showed that values were usually nearly equal, showing similar variations with time. Differences between I, the current to the open receiver, and I_s, the current to the shielded receiver, were seldom more than 1 $\mu\mu$a m^{-2} and showed no definite correlation either with the potential gradient or with the rate of rainfall.

When the results were considered in groups according to the rate of rainfall, there appeared to be a definite tendency for I_s to be greater than I for all rates of rainfall when F is positive, and for low rates of rainfall when F is negative, but I_s is less than I for high rates of rainfall with F negative.

It might be expected that the conduction current would produce a difference between I_s and I; this would make I greater than I_s for F positive and less for F negative, agreeing only with the results for F negative with low rates of rainfall. Also it would be expected

that $I - I_s$ would vary with the rate of rainfall, which is not found. Measurements of the conduction current in fine weather showed that it had the very small value of 0·8 $\mu\mu$a m^{-2} in a potential gradient of 100 v m^{-1}, so that a similar value in rainy weather might well give little noticeable effect, except in the cases of the lowest currents.

Another possible contribution to the difference between I and I_s might be the effect of splashing. The results of Smiddy and Chalmers (1960) suggest that splashing is unlikely to be important until the rate of rainfall is higher than that reached in most of the cases here considered and their results would suggest $I > I_s$ if splashing gives a positive charge to the rain; Adkins (1959) found a charging due to splashing and depending on the potential gradient, but effective only for potential gradients beyond $\pm$ 700 v m^{-1} and therefore not in evidence for the measurements considered here.

Another cause for the difference between I and I_s might be the fact that, in windy weather, some of the smallest drops will not reach the shielded receiver. The technique of recording drop sizes by means of filter paper impregnated with dye, originating with Weissner (1895) and used by Hutchinson and Chalmers (1951), was employed to compare the drops reaching the open and shielded receivers. On one day, with very little wind, the numbers of drops and their distribution with size were identical to within observational error, but on a second day, with more wind, there was a very distinct difference in the smallest drops, the shielded receiver obtaining less than half the number of drops of diameter below 0·05 mm reaching the open receiver. If then the smallest drops carry a negative charge we should have an explanation of the difference between I and I_s except in heavy rain with negative F. The results for drizzle, when all the drops are small, agree with this idea.

8. The mirror-image effect

Simpson (1949) first drew attention to the ' mirror-image effect ' that, when curves are drawn of the variations with time of the precipitation current and of the potential gradient, these curves often appear almost as the mirror images of one another. Since then, the term has been misunderstood by some workers and has sometimes been used to refer to the general inverse relation of positive precipitation current and negative potential gradient; some workers too, have used the term to refer to the cases when the precipitation current decreases to zero and the increases with opposite sign in a symmetrical way.

In many of Simpson's examples, the precipitation current and the potential gradient crossed the zero lines simultaneously in opposite directions; in Simpson's observations the mirror-image effect was observed mainly when the potential gradient was high enough to give point discharge.

In the present observations it was frequently found that the current and the potential gradient had maxima in opposite directions at or close to the same time. This will still be termed the ' mirror-image effect ' although the ' mirrors ' would not be the zero lines and although there is sometimes a time delay.

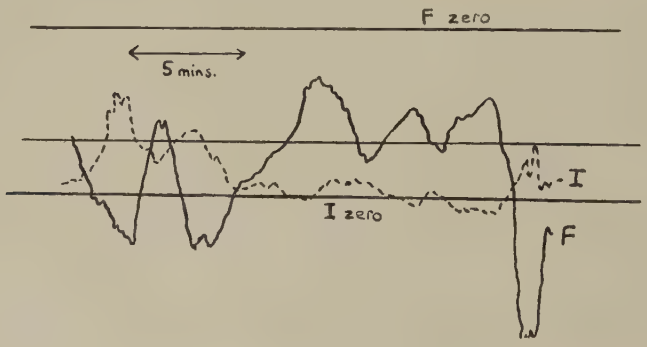

Figure 4. Mirror-image effect.

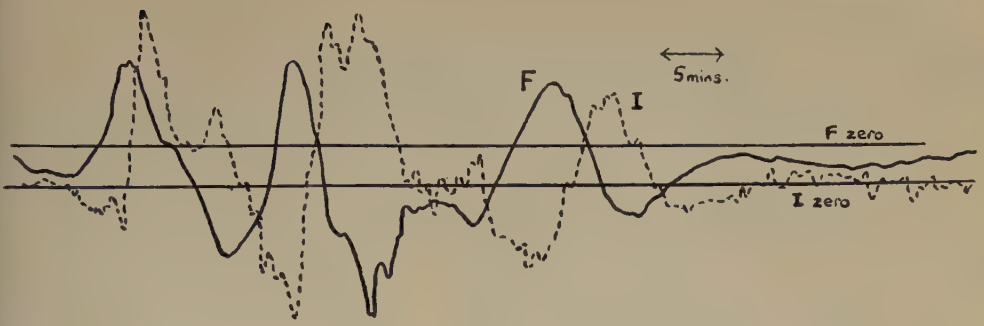

Figure 5. Mirror-image effect with delay.

Fig. 4, comprising a period of about 20 min, shows a good example of a normal mirror-image effect with no time delay, but it will be seen that I crosses the zero though F does not. In Fig. 5, comprising a period of about 80 min, there is clearly a time delay between the maxima of I and F, amounting to 1 or 2 min. If, for this case, corresponding values of I and F are plotted, the successive points tend to lie on ellipses (Fig. 6).

In the idealized case where the variations of current and potential gradient with time are simple harmonic, it can be seen that the I/F curve is a straight line for the ' normal ' mirror-image effect and becomes an ellipse if there is a time delay; so long as the time delay is less than a quarter period, this same line remains the major axis of the ellipse, but does not remain the ' best straight line,' determined as the regression of I on F; for increasing time delay the points are less and less on a straight line and the best straight line gets a smaller slope, until for time delays of over a quarter period the slope changes sign.

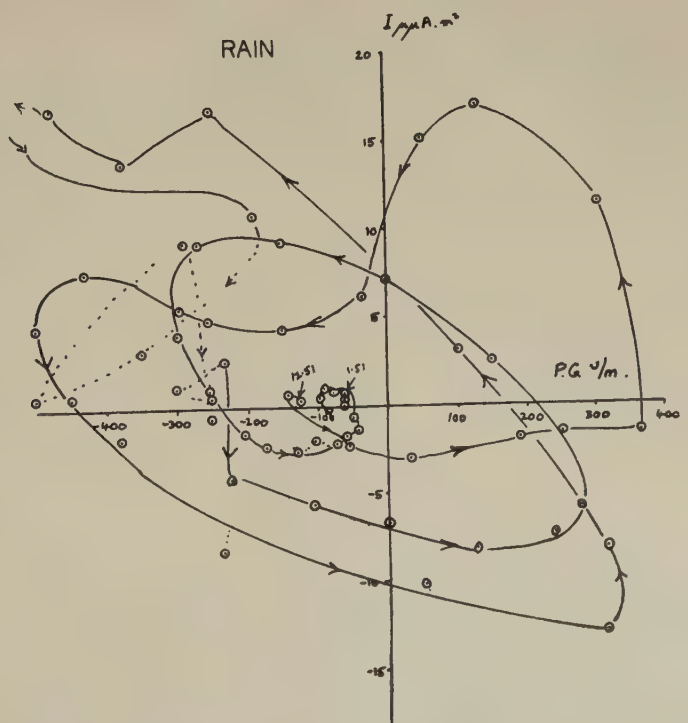

Figure 6. Variation of current with potential gradient showing ellipses (11 Jan. 1958, 1251 to 1351 GMT).

An anti-clockwise ellipse means that the current maximum occurs before the potential-gradient maximum (negative) and a clockwise ellipse the reverse.

Out of 40 days' recording, the mirror-image effect was observed on 21 days although not always as well defined as on the occasions illustrated. Table 3 shows the distribution.

TABLE 3. DISTRIBUTION OF MIRROR-IMAGE EFFECT

	Rain	Snow	Sleet	'Wet snow'	Total
No time delay	6	1	1	1	9
Current maximum first	3	3	1	0	7
Current maximum later	5	0	0	0	5
Total	14	4	2	1	21

The normal mirror-image effect could be explained in a general way if there is some process by which the precipitation obtains its charge of one sign, leaving the opposite charge behind somewhere above; this latter charge then gives rise to the potential gradient observed at the ground. If we now imagine that different portions of the cloud passing overhead give different precipitation currents and so carry different charges and if the whole system of cloud and precipitation moves horizontally at the same speed, then a normal mirror-image effect would result. A deviation from the normal mirror-image effect would be expected if (a) the precipitation reaches the ground at a different time from that at which the portion of the cloud from which it originates arrives above the observer, (b) if one portion of a cloud does not give a constant precipitation current or (c) if the space charge on the precipitation has an appreciable effect.

If the precipitation loses horizontal velocity in falling, from the usual decrease of wind speed with height, then the potential gradient maximum would occur before the current maximum, as is more usually the case with rain, and the same would occur for (b) above.

On the other hand, if the potential gradient is partly determined by the space charge in the precipitation, then this part of the potential gradient is of the same sign as the current which is due to arrive later and so the resultant potential gradient, of the opposite sign to the current, will have its maximum later than if there were no such effect and may thus be later than the maximum of the current, as is found for snow; since snow falls more slowly than rain, there will be a larger effect of space charge.

Thus no complete explanation of the phenomena is afforded, but the results for snow agree with what is to be expected.

ACKNOWLEDGMENTS

The geophysical research reported in this paper has been sponsored by the Geophysics Research Directorate of the Air Force Cambridge Research Center, United States Air Force, through the European Office, A.R.D.C.

The authors wish to acknowledge the assistance received from the technicians, Mr. C. Maclean and Mr. M. Binks, and from other members of the technical staff of the Physics Department, and also the assistance from members of the Atmospheric Electricity Research Group at Durham.

References

damson, J.	1960	'The compensation of the effects of potential-gradient variations in the measurement of the atmospheric air-earth current,' *Quart. J. R. Met. Soc.*, **86**, p. 252.
dkins, C. J.	1959	'The small ion concentration and space charge near the ground,' *Ibid.*, **85**, pp. 237-252.
halmers, J. A.	1956	'The vertical electric current during continuous rain and snow,' *J. Atmos. Terr. Phys.*, **9**, pp. 311-321.
	1959	*Recent advances in atmospheric electricity*, (Ed. L. G. Smith), (London, N.Y., Paris, Los A.; Pergamon Press), pp. 309-351.
utchinson, W. C. A. and Chalmers, J. A.	1951	'The electric charges and masses of single raindrops,' *Quart. J. R. Met. Soc.*, **77**, pp. 85-95.
crase, F. J.	1938	'Electricity on rain,' *Geophys. Mem.*, London, **75**.
mpson, G. C.	1949	'Atmospheric electricity during disturbed weather,' *Ibid.*, London, **84**.
middy, M. and Chalmers, J. A.	1960	'Measurements of space charge in the lower atmosphere,' *Quart. J. R. Met. Soc.*, **86**, pp. 85-90.
Veissner, J.	1895	'Beiträge zur Kenntnis des tropischen Regens,' S.B. Aked. Wiss., Wien, **104**B, pp. 1397-1434.

551.557.

Notes on the wind flow at 50 mb in tropical and sub-tropical regions in January 1957 and January 1958

By R. A. EBDON
Meteorological Office, Harrow

(Manuscript received 27 April 1960)

SUMMARY

In January 1957 the mean 50 mb flow pattern was persistently E'ly over large areas near the Equato and this is compared with the flow pattern of January 1958 which was predominantly W'ly over much th same area. The mean vector winds for Canton Island for six Januarys show a remarkable 2-yr periodicit and suggest that either an E'ly or W'ly flow is equally likely to occur.

1. INTRODUCTION

During the preparation of mean 50 mb contour and streamline isotach charts it was noticed that over large areas near the Equator the mean vector wind was close to easterly in January 195 (with the easterlies persisting throughout the month) and nearly westerly over the same area in January 1958 (with the westerlies persisting throughout the month). The daily values of the zonal wind component at 50 mb during these two Januarys are shown for Christmas Island (02° 00′ N 157° 23′ W) in Fig. 1 and for Canton Island (02° 46′ S, 171° 43′ W) in Fig. 2. The monthly mean vector winds for stations in the tropics and sub-tropics for January 1957 and January 195 are shown on the charts in Figs. 3 and 4 respectively.

50 mb corresponds approximately to a height of 67,000 ft or 21 km and, for some stations, radar winds at or near these heights have been used when no winds were available at 50 mb

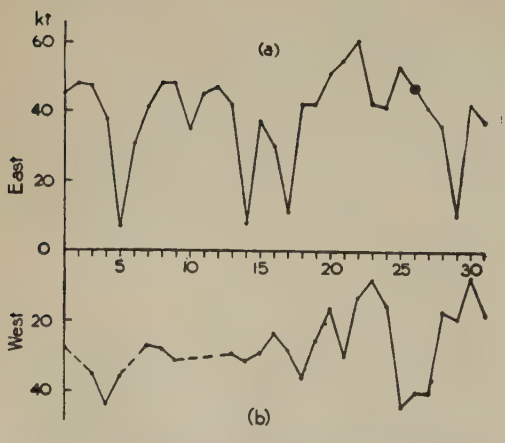

Figure 1. Daily values of zonal wind component at 50 mb for Christmas Island. (a) January 1957 (0200 GMT, but ● indicates 1400 GMT ascent used); (b) January 1958 (0001 GMT).

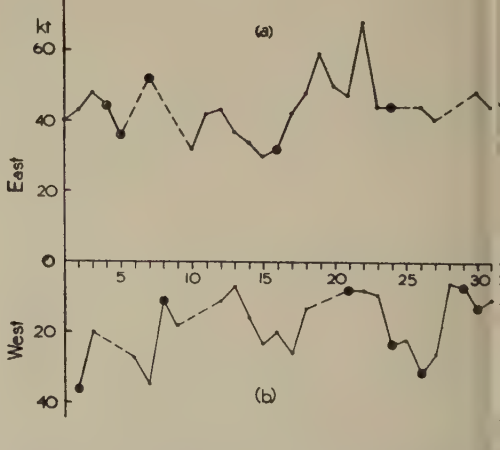

Figure 2. Daily values of zonal wind componen at 50 mb for Canton Island. (a) January 195 (0300 GMT, but ● indicates 1500 GMT ascent used) (b) January 1958 (0001 GMT, but ● indicate 1200 GMT ascent used).

2. Discussion

At this level near the Equator one might expect to find the ' Von Berson Westerlies ' (Palmer 1954) – at least over the Central Pacific if not over a greater part of the world. The Central Pacific is an area for which data were plentiful and it is considered that in both years the charts depict the flow quite accurately in that region.

It will be seen from Fig. 3 that in 1957 the easterlies (which, from such data as are available, appear to be a normal feature of the January circulation at this level from just south of the Equator to at least 20°S) cover the Central Pacific to about 20°N. In fact there appears to be a solid band of easterlies from 20°S to 20°N with a maximum of 40-50 kt near the Equator. Although only a few observations were available for the remainder of the chart there are indications that something similar occurred over other regions; for instance, a mean wind of 090 deg. 32 kt at Albrook Field (08° 58′ N, 79° 33′ W) and 100 deg. 16 kt at Kano (12° 03′ N, 08° 32′ E). Between approximately 25° N and 30° N there is a zone in which the easterlies and westerlies both occurred during the month. Daily values of the wind at this level for Kadena (26° 21′ N, 127° 45′ E), Iwojima (24° 47′ N, 141° 20′ E), Midway Island (28° 13′ N, 177° 22′ W), Coffin Hills (25° 16′ N, 76° 18′ W), Turks Island (21° 28′ N, 71° 08′ W) and Port Lyautey (34° 18′ N, 06° 36′ W) show this variation in direction during the month.

In January 1958 the flow pattern is very different (Fig. 4). Once again the easterlies are present south of the Equator but there is now a westerly flow over many areas in which the wind direction was easterly in January 1957. These westerlies extend to just south of the Equator with maxima at about 5° N over the Central Pacific and at a similar latitude over Africa with mean speeds of 25-35 kt in both areas. A feature of this chart is what appears to be a ' high ' cell at about latitude 20° N giving light easterly winds to the north of the westerly maximum over the Central Pacific.

The differences between the flow patterns in Figs. 3 and 4 can be variously interpreted – one interpretation being a latitudinal meandering of the boundary between the easterly and westerly regimes. On the other hand, the equatorial stream does seem to have its own maximum whether easterly or westerly and it may not be the mere fringe of a current belonging to one hemisphere or the other. In fact, the evidence suggests that, between the more or less regular westerlies north of 30° N and the easterlies south of 10° S, there exists a zone in which the wind flow is eastwards in some years and westwards in others.

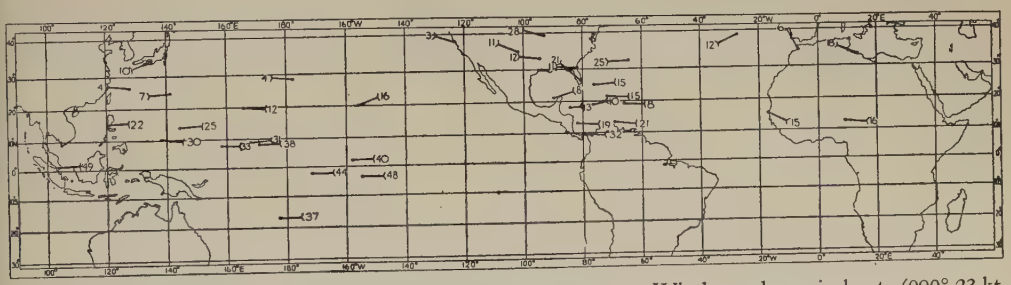

Figure 3. Monthly mean vector winds at 50 mb for January 1957. Wind speeds are in knots (090° 23 kt plotted as •—(23).

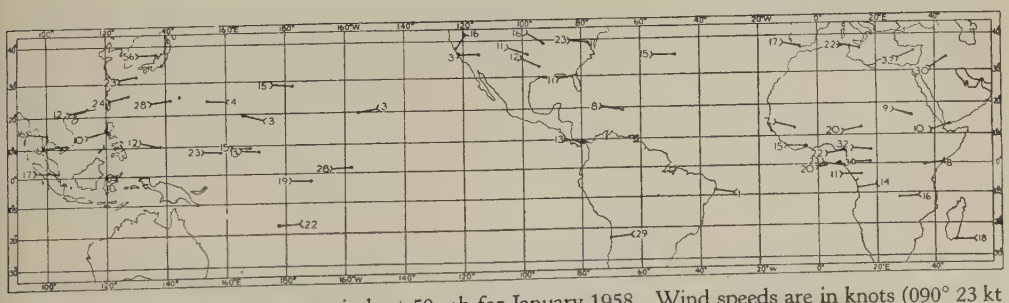

Figure 4. Monthly mean vector winds at 50 mb for January 1958. Wind speeds are in knots (090° 23 kt plotted as •—(23)

As the data show, over many tropical and sub-tropical areas the variation in wind direction at the 50 mb level in the month of January can be considerable from year to year, with wind speeds which are often greater than 40 kt : such variations must be important for practical purposes apart from the theoretical considerations. Attempts to obtain reliable winds at this level covering a long period have been unsuccessful, but Table 1 shows the mean winds for each January from 1954 to 1959 for Canton Island (02° 46′ S, 171° 43′ W) together with the maximum wind reported during each month and the number of occasions in the month when the zonal wind component was easterly or westerly. It is clear that in some Januarys, easterly winds, and in other Januarys westerly winds persisted throughout all or most of the month at the 50 mb level. On occasions when an ' anomalous ' wind direction occurred the speed was less than 12 kt and the value of the zonal wind component did not exceed 10 kt – indeed, of the three occasions in 1959, two were less than 1 kt.

As yet there are insufficient data to determine what the ' normal ' or long-period mean flow pattern at 50 mb is in January in tropical and sub-tropical areas. It might be inferred from Table 1 that neither the 50 mb flow pattern of January 1957 nor that of January 1958 is really exceptional and that either might occur with equal frequency. Although the years for which 50 mb data are available are very limited, the mean (and maximum) winds for Canton Island show a remarkable 2 yr periodicity. This phenomenon appears to extend at least some 14 deg. farther west to Christmas Island (02° 00′ N, 157° 23′ W) where the mean winds for three consecutive Januarys were : 1957 : 091 deg. 40 kt (52 observations); 1958 : 271 deg. 27 kt (29 observations); 1959 : 091 deg. 31 kt (3 observations).

TABLE 1. JANUARY MEAN AND MAXIMUM WINDS FOR CANTON ISLAND (1954-1959)

Year	Level or height	No. of ascents	No. of days with one observation or more	No. of occasions when zonal wind component was easterly or westerly		Mean wind		Maximum wind	
	feet			East	West	deg.	kt	deg.	kt
1954	65,000	10	10	0	10	270	14	290	46
1955	65,000	11	11	10	1	091	25	090	38
1956	50 mb	26	20	1	25	275	12	260	30
1957	50 mb	36	27	36	0	090	44	088	68
1958	50 mb	30	24	0	30	270	18	264	36
								282	36
1959	50 mb	51	31	48	3	095	22	085	56

ACKNOWLEDGMENT

This note is published by permission of the Director-General of the Meteorological Office.

REFERENCE

Palmer, C. E. 1954 ' The general circulation between 200 mb and 10 mb over the Equatorial Pacific,' *Weather*, **9**, p. 341.

551.501.75 : 551.557 : 519.2

The statistical variation of wind with distance

By C. S. DURST
formerly *Meteorological Office, London*

(Manuscript received 8 April 1960)

Summary

Correlation coefficients have been formed between the winds at pairs of points, the correlation being made between components *along* the line joining the points and also between components at right-angles. The original purpose was the derivation of the effective winds experienced by aircraft. However, certain results are found which appear to throw light on the application of turbulence theory to the large-scale pattern of winds and hence it is thought that the results may be of more general interest.

1. Introduction

In 1952 when examining the effect of wind on the operation of *Comet* aircraft, I calculated correlation coefficients between winds at Larkhill and Malta at the level of 200 mb and I reported (Durst 1952) that if wind components were taken *along* and *across* the line joining these two places, the correlation coefficients of components along the line was small, but that those across the line were negative in all seasons, and in spring attained to as much as $-0{\cdot}57$.

2. The data used

I have, since then, collected statistics of the variation of wind with distance between various points, taking in all cases the components along the line joining the correlated points and those across that line. The statistics are set out in the appendices to this paper. They comprise the following :

(a) correlation coefficients at 100, 150 and 200 mb between wind-observing stations along a parallel from Hanover to Ocean Weather Ship *C* (Appendix I);

(b) at 300 mb between geostrophic winds in a pattern of points over the North Atlantic (Appendix II) ;

(c) at 500 mb between wind observing stations at Gibraltar, Malta, Nicosia, Habbaniya, Bahrein and Aden (Appendix III);

(d) at 500 mb between five wind observing stations at Hanover, Hemsby, Valentia, Ocean Weather Ship *J* and Ocean Weather Ship *C* (Appendix IV).

These arrangements were chosen so as to test all levels from 100 to 500 mb and to examine whether the same features were reproduced in low latitudes as in high latitudes. Only in Appendix I and in Durst (1952) was the test made for summer as well as winter, i.e., at 200 mb or higher. In other examinations the data used referred to the winter half-year.

The results for 200, 300 and 500 mb are plotted on Figs. 1 and 2, with Fig. 1 showing the components along the track and Fig. 2 showing those across the track. Fair curves have been drawn among the points on the diagrams. There is a certain amount of scatter among the points of Fig. 1, but considerably less on Fig. 2. The points for different levels, different areas and different seasons have been given distinguishing symbols, but there does not appear to be any very decided trend except that in summer, at 200 mb, the tendency for the cross-track coefficient to become negative is not so marked as in winter.

3. The generalized result

It would seem that the general run of the fair curve is representative of levels in the troposphere and the lower regions of the stratosphere and also of lower latitudes as well as for latitudes 50° to 55°N. Values read off these fair curves are shown in Table 1.

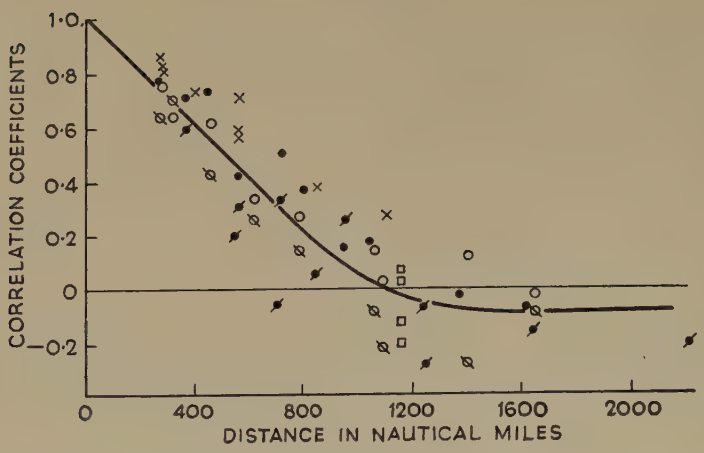

Figure 1. Variation of wind with distance – correlation coefficients of components along track.

● 500 mb, North Atlantic
◉ 300 mb, Middle East
× 500 mb
○ 200 mb, Winter
⊘ 200 mb, Summer
□ 200 mb, Larkhill to Malta.

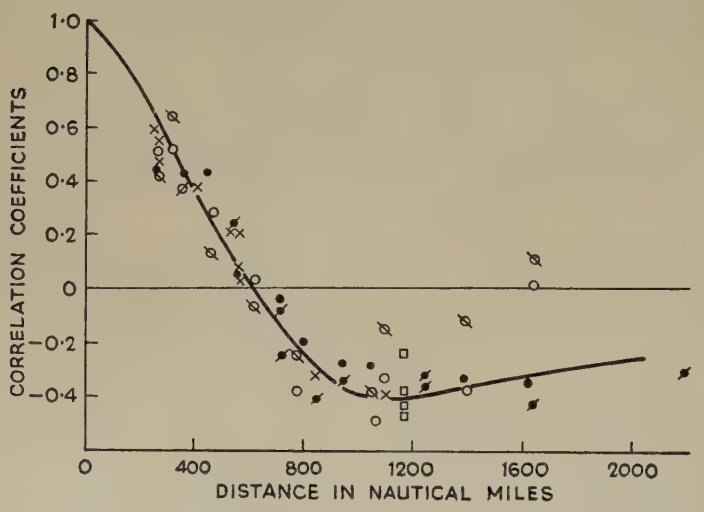

Figure 2. Variation of wind with distance – correlation coefficients of components across track.

● 500 mb, North Atlantic
◉ 500 mb, Middle East
× 300 mb
○ 200 mb, Winter
⊘ 200 mb, Summer
□ 200 mb, Larkhill to Malta.

TABLE 1. CORRELATION COEFFICIENTS OF WIND AT VARIOUS DISTANCES

	Naut. mi.									
Distance	0	200	400	600	800	1000	1200	1400	1600	1800
Along Line $f(r)$	1·00	0·83	0·64	0·44	0·21	0·04	− 0·06	− 0·11	− 0·10	− 0·08
Across Line $g(r)$	1·00	0·71	0·37	0·04	− 0·22	− 0·36	− 0·37	− 0·35	− 0·33	− 0·30
Ratio $(1-f)/(1-g)$		0·59	0·57	0·58	0·65	0·71	0·77	0·82	0·83	0·83

4. The theoretical relationship

After statistics given in the appendices had been completed and Table 1 had been prepared, my attention was drawn to Taylor's paper (1938) in which he points out Karman (1937) had shown that for isotropic turbulence there is a definite relationship between two correlation functions $f(r)$ and $g(r)$. The function $f(r)$ is the correlogram of velocity components along the line joining two points of distance r apart, and the function $g(r)$ is the correlogram of components at right-angles to this line. Theory shows that $f(r)$ should be greater than $g(r)$ and that the latter should become negative at some point. Taylor shows, moreover, that some laboratory experiments by Simmons (unpublished) very well verified Karman's relationship.

5. Comparison of observations with theory

Hutchings (1955) has expressed the expectation that the atmospheric turbulence should follow the same laws as turbulence on the laboratory scale and has obtained corroborative results by using autocorrelation coefficients at a single point and assuming that the general pattern of turbulence flows on with the general circulation. He deduces, on the same lines as Batchelor (1953) that :

$$1 - f(r) = a r^{\frac{2}{3}}$$

and

$$1 - g(r) = \tfrac{4}{3} a r^{\frac{2}{3}} \quad \text{or} \quad \tfrac{5}{3} a r^{\frac{2}{3}} \quad . \quad . \quad . \quad . \quad (1)$$

according as the turbulence is taken to be isotropic in three or two dimensions, i.e., the ratio $(1 - f(r))/(1 - g(r))$ should be 0·75 or 0·60 in the two cases. I have added as a third line to Table 1 the values of this ratio. It seems to be nearly 0·6 for distances up to 800 mi but to be larger thereafter.

Further, when $\log(1 - f)$ and $\log(1 - g)$ are plotted against $\log r$ (as in Fig. 3), the points up to 800 mi fall very nearly on two parallel lines, giving a relation

$$1 - f(r) = a r^{c}$$

$$1 - g(r) = \tfrac{5}{3} a r^{c}$$

where c would seem to be 0·90 rather than 0·67 as required by Eq. 1. The scatter of points in Figs. 1 and 2 precludes an exact estimation of the values of $f(r)$ and $g(r)$ in Table 1, but nevertheless, it is difficult to believe that the smoothed lines in Figs. 1 and 2 are so grossly in error as to produce an erroneous value of c of 0·90. Moreover, when the individual values of $\log(1 - f(r))$ from the

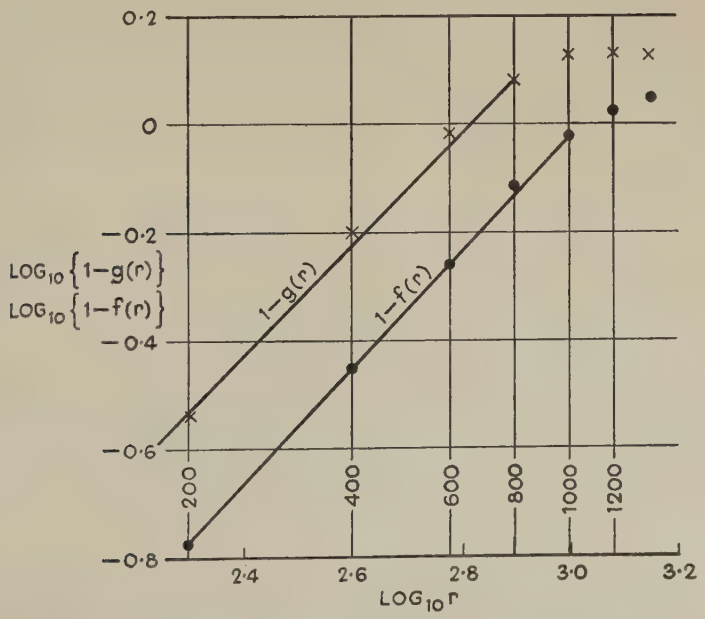

Figure 3. Plot of $\log\{1 - f(r)\}$ and $\log\{1 - g(r)\}$ against $\log r$.

appendices are plotted against log r and straight lines are drawn to fit the points, none give slopes approaching 0·67, but are, in general, considerably greater, although the fit of the points to straight lines is not at all close.

6. Deductions

In the cases I quote, the tendency to negative values of the correlation coefficients is more marked than in the laboratory experiments. This is probably due to the atmospheric turbulence not being isotropic and homogeneous. Indeed, one can understand that if there are a succession of eddies passing over two points separated by a distance L, there will be a strong tendency to a negative correlation of the wind component across the line joining the points when the distances between the centres of the eddies are predominantly of the magnitude L. Also, in such a scheme, there will not be the same tendency to negative correlation in the components along the line joining the two points. For this reason, there is probably a significance in the maximum negative correlation coefficient being at 600 to 1,200 mi, since that is the order of the distance between depressions in the day-to-day circulation, at any rate in the extra-tropical latitudes.

7. The effect on calculations of equivalent head-winds

The original purpose of the calculation of the correlation coefficients was to find out what would be the standard deviations of wind components along and across the tracks of aircraft and to check up the calculations of equivalent head-winds that have been made (e.g., Graystone 1958, and Meteorological Office 1950).

The calculation of the standard deviation of the mean component along track Σ is made by the formula :

$$\frac{\Sigma}{\sigma} = \frac{\sqrt{2}}{S}\sqrt{\int_0^S \int_0^x f(r)\, dr\, dx}$$

where σ can be taken as the mean standard deviation of the wind component along the track, length S. Similarly, the standard deviation of the mean component across the track Σ' is calculated from a similar formula but substituting the mean standard deviation of wind component across track σ' for σ and correlation function $g(r)$ for $f(r)$.

Using the values of $f(r)$ and $g(r)$ from Table 1, we obtain the results shown in Table 2.

TABLE 2. Ratio of the standard deviation of the mean wind component to the mean of standard deviations of components for various distances (L)

	Naut. mi.									
L	0	200	400	600	800	1000	1200	1400	1600	1800
Along track	1·0	0·97	0·94	0·91	0·87	0·83	0·79	0·75	0·72	0·69
Across track	1·0	0·95	0·90	0·83	0·77	0·70	0·63	0·56	0·50	0·45
From Graystone (1958)	1·0	0·94	0·90	0·86	0·80	0·76	0·72	0·68	0·65	0·62

In the last line of Table 2, are set down the corresponding values which were used by Graystone (1958). These values were derived from Durst (1954), using curve B of Fig. 6 of that publication. The correlation coefficients represented by curve B were stretch vector correlation coefficients; at the time when curve B was produced, it was believed that the linear correlation coefficient for the components would be the same along track as across it, and that in consequence the same as the stretch vector coefficient.

Since the effect of the beam-wind on the time of flight of an aeroplane is small in comparison with the effects of head-winds, the most important ratios in Table 2 are those along track. The difference between them and the last line shown in the Table is of the order of 10 per cent, but as the standard deviation of head-winds given by Graystone (1958) is seldom more than 20 to 25 kt (and is usually considerably smaller) it would seem that the errors involved are not more than 2 or 2½ kt.

Acknowledgments

I wish to express my thanks to the Director-General of the Meteorological Office for granting access to a considerable amount of unpublished data. I also wish to acknowledge the helpful advice I have received from Mr. A. F. Crossley and Dr. F. Pasquill.

References

Batchelor, G. K.	1953	*Homogeneous turbulence*, Cambridge Univ. Press.
Durst, C. S.	1952	*Air Ministry Met. Res. Cttee., M.R.P.*, No. 776.
	1954	*Geophys. Mem. Met. Off.*, No. 93.
Graystone, P.	1958	*Met. Rep.*, **20**, M.O. 621 d., H.M.S.O.
Hutchings, J. W.	1955	*J. Met.*, **12**, p. 263.
de Karman, T.	1937	*J. Aero. Sci.*, **4**, p. 131.
Meteorological Office (Anon.)	1950	*Met. Rep.*, **7**, M.O. 535 b., H.M.S.O.
Taylor. G. I.	1938	*Proc. Roy. Soc.*, p. 484.

Appendix I

Standard deviations and correlation coefficients of E-W and N-S components of observed winds in 1951 at points between Hanover and Ocean Weather Ship *C*.

		WINTER					SUMMER				
200 mb Stations	Distance	Standard deviations E-W	N-S	Correlation coefficients E-W	N-S	No. of Obs.	Standard deviations E-W	N-S	Correlation coefficients E-W	N-S	No. of Obs.
Hanover	1,650	31	27	− 0·02	+ 0·02	154	18	27	− 0·08	+ 0·12	215
O W S *C*		17	20				17	18			
Hemsby	1,370	30	31	+ 0·12	− 0·35	144	21	25	− 0·26	− 0·12	224
O W S *C*		21	20				17	18			
Aldergrove	1,100	29	27	+ 0·03	− 0·33	105	25	25	− 0·21	− 0·14	167
O W S *C*		18	19				16	18			
Hanover	1,070	27	27	+ 0·15	− 0·49	214	17	25	− 0·09	− 0·37	172
O W S *J*		33	39				26	37			
Hemsby	790	27	29	+ 0·27	− 0·37	203	22	30	+ 0·14	− 0·23	171
O W S *J*		31	40				26	37			
Hanover	620	27	28	+ 0·34	+ 0·04	215	19	26	+ 0·27	− 0·06	241
Aldergrove		27	29				25	25			
Hanover	450	28	29	+ 0·61	+ 0·28	281	19	27	+ 0·43	+ 0·13	280
Liverpool		26	30				25	28			
Hemsby	310	26	29	+ 0·64	+ 0·53	209	22	27	+ 0·70	+ 0·64	244
Aldergrove		25	29				25	23			
Hanover	280	26	28	+ 0·75	+ 0·51	295	19	23	+ 0·63	+ 0·42	333
Hemsby		27	29				21	28			
150 mb											
Hemsby	1,370	21	21	− 0·03	− 0·31	87	14	17	− 0·03	− 0·14	171
O W S *C*		12	18				12	12			
Hemsby	790	18	22	+ 0·32	− 0·32	162	15	19	+ 0·22	− 0·03	144
O W S *J*		24	30				17	24			
Hanover	280	19	19	+ 0·83	+ 0·61	253	12	17	+ 0·69	+ 0·55	300
Hemsby		19	20				14	18			
100 mb											
Hemsby	1,370	12	17	+ 0·03	− 0·04	32	9	11	− 0·08	+ 0·01	92
O W S *C*		16	15				9	14			
Hanover	1,070	17	11	+ 0·50	− 0·46	91	9	10	+ 0·14	− 0·08	86
O W S *J*		18	20				11	17			
Hemsby	790	17	16	+ 0·70	− 0·34	90	9	11	+ 0·27	+ 0·08	78
O W S *J*		17	19				11	17			
Hanover	620	15	13	− 0·59	+ 0·09	94	8	9	+ 0·45	+ 0·33	131
Aldergrove		15	13				9	12			
Hanover	450	16	14	+ 0·68	+ 0·35	152	8	11	+ 0·38	+ 0·51	201
Liverpool		13	13				10	11			
Hanover	280	16	13	+ 0·81	+ 0·65	155	8	12	+ 0·65	+ 0·58	204
Hemsby		15	14				9	11			

Appendix II

Standard deviations and correlation coefficients of geostrophic winds at 300 mb along and across lines joining various positions above the North Atlantic, November 1957 to February 1958; based on 120 comparisons.

Points Lat.	Points Long.	Direction	Distance naut. mi	Standard deviation Along	Standard deviation Across	Correlation coefficients Along	Correlation coefficients Across
52½	12½	W	280	36	38	+ 0·831	+ 0·549
52½	20			39	47		
52½	20	W	280	39	47	+ 0·827	+ 0·591
52½	27½			41	41		
57	27½	S	280	46	36	+ 0·873	+ 0·587
52½	27½			41	41		
52½	20	NW	400	42	43	+ 0·736	+ 0·374
57	27½			42	41		
52½	12½	W	560	36	47	+ 0·572	+ 0·037
52½	27			41	41		
52½	20	W	560	39	47	+ 0·583	+ 0·086
52½	35			43	47		
57	27½	S	560	46	36	+ 0·707	+ 0·210
47	27½			41	35		
52½	12½	W	840	36	38	+ 0·369	− 0·314
52½	35			43	47		
52½	12½	W	1,120	36	38	+ 0·239	− 0·390
52½	42½			41	46		

Appendix III

Standard deviations and correlation coefficients of observed wind components along and across track at 500 mb in the Middle East area. January, February, November and December 1955. Based on about 120 observations.

Stations	Direction and distance apart		Standard deviations Along	Standard deviations Across	Correlation coefficient Along	Correlation coefficient Across
Gibraltar	270°	950	21	22	+ 0·274	− 0·351
Malta			24	23		
Malta	270°	700	24	23	− 0·049	− 0·239
Nicosia			15	17		
Malta	310°	350	21	26	+ 0·600	+ 0·368
Benina			19	22		
Benina	255°	700	23	18	+ 0·330	− 0·060
Nicosia			17	16		
Nicosia	285°	560	14	19	+ 0·309	+ 0·230
Habbaniya			15	14		
Habbaniya	325°	550	11	17	+ 0·196	+ 0·219
Bahrain			12	18		
Bahrain	29°	850	15	16	+ 0·063	− 0·410
Aden			9	11		
Gibraltar	270°	1,650	21	22	− 0·175	− 0·435
Nicosia			15	17		
Malta	275°	1,250	24	23	− 0·267	− 0·304
Habbaniya			16	13		
Gibraltar	270°	2,200	21	22	− 0·200	− 0·304
Habbaniya			16	13		
Habbaniya	360°	1,250	13	16	− 0·073	− 0·364
Aden			8	11		

Appendix IV

Standard deviations and correlation coefficients of observed winds at 500 mb. November and December 1956, 1957, 1958 and January and February 1956, 1957, based on 153 comparisons.

Stations	Distance naut. mi	Standard deviation	Hanover 31·5	Hemsby 31·8	Valentia 29·6	O W S *J* 27·2	O W S *C* 34·8
Hanover	0	25·2	–	+ 0·793	+ 0·508	+ 0·174	− 0·059
Hemsby	280	27·8	+ 0·459	–	+ 0·724	+ 0·374	− 0·017
Valentia	710	32·2	− 0·053	+ 0·436	–	+ 0·704	+ 0·162
O W S *J*	1,070	31·2	− 0·268	− 0·188	+ 0·431	–	+ 0·429
O W S *C*	1,630	34·0	− 0·393	− 0·330	− 0·267	+ 0·066	–

The figures above and to the right give the standard deviations and correlation coefficients of wind components along the lines joining the various stations; those below and to the left across the lines joining the stations.

551.574.11

The variation in composition of sea-salt nuclei with mode of formation

By B. C. V. ODDIE
Meteorological Office, London

(Manuscript received 2 May 1960)

Summary

It is shown that at coastal stations, while the coarser spray has a composition close to that of sea water, the smaller droplets (diameters less than about 25 microns) have a much higher proportion of potassium. The rapid decrease in the Na : K ratio with increasing distance from the sea is principally due to the settling out of the coarser spray. The result is consistent with Wilson's hypothesis that salt nuclei are formed largely from an extremely thin surface layer very rich in organic matter, which contains a high proportion of potassium.

Wilson (1959) analysed samples of snow taken from the mountains of New Zealand at heights of 6,000 ft or more, and found that the ratio, amount of sodium : amount of potassium was generally only one-fifth to one-tenth of the corresponding ratio in sea water. This was remarkable since in those latitudes it was scarcely conceivable that there could be any appreciable source other than the sea. Wilson's explanation was that the salt nuclei brought down by the snow are derived from a surface film of the ocean, which is rich in organic material and, consequently, in potassium.

This explanation fits in well with the theory of Mason (1957) on the origin of salt nuclei. Mason considers that, of salt nuclei which are small enough to be carried up to cloud height and so take part in the processes of precipitation, the great majority originate as fine spray formed from the top film of bubbles bursting at the sea surface. Obviously spray so formed must consist very largely of any surface film which may cover the sea. Other mechanisms of spray formation produce mainly a coarser spray which may be expected to have a composition nearer to that of ordinary sea water. This applies particularly to the process of Woodcock *et al.* (1953) in which a few droplets are projected upwards in a jet when the crater left by a bursting bubble collapses. Such droplets originate at the bottom of the crater, i.e. slightly below the surface film.

Wilson (1960) appears to have been the first to suggest that there must be this considerable difference in composition between coarse and fine sea spray. The fact is, however, easily demonstrated from the data obtained by the chemical sampling stations. The observations are of two kinds. One method simply collects the precipitation and analyses it monthly. At an exposed coastal station such as Lerwick salts are mostly brought down as spray (Oddie 1959). It must be fairly coarse to be deposited in the collecting funnel, but it is not coarse enough to be noticeable on the face or visible as discrete drops on a window : probably most of it consists of droplets in the range of diameters 20-100 μ.

The second sampling procedure obtains monthly samples of air. In order to exclude precipitation, the orifice by which the air enters the sampling apparatus points downwards. Air flows in at a speed of about 3 cm sec^{-1}, so that droplets with terminal velocities appreciably less than this will be quite well represented in the sample. Indeed, it is evident that any *metals* in the air sample must enter as particles or droplets.

Table 1 shows the relative amounts of the three principal metals in the precipitation samples and in the air samples at Lerwick for the twelve months April 1958 to March 1959 – the first 12 months for which data are available. Corresponding figures for sea water are also shown.

TABLE 1. Values of ratio Na : K, Na : Mg. Lerwick, April 1958-March 1959

Precipitation	Na/K	Na/Mg
Precipitation	24	7·3
Air	6·2	4·8
Sea water	28	8·3

(by the ratio Na : K is meant mass of sodium in sample divided by mass of potassium)

These results clearly show that, as Wilson supposed, the coarse spray has very much the composition of sea water, whereas the fine spray has a much higher proportion of potassium – the Na : K ratio has more than four times its sea water value.

One would naturally expect that the coarse spray would all be deposited in the first few miles, so that at greater distances inland the fine spray would be dominant in both the air and precipitation samples. This does occur : as distance from the sea increases, the Na : K ratio falls still lower in the air sample, and the discrepancy between precipitation and air samples is much reduced. This is shown in Table 2.

TABLE 2. Na : K ratio in different localities, April 1958-March 1959

	Exposed coastal stations		Inland stations, Sweden		Inland stations, Finland	
	Lerwick	Stornoway	Flahult	Ultuna	Jyvaskyla	Kuopio
In precipitation	24	23	1·7	1·3	0·5	0·6
In air	6·2	3·1	0·9	0·9	1·0	0·8

This effect is, of course, well known, but has often been attributed to the transfer of potassium from the ground to the air. But the extraordinary speed with which the Na : K ratio in precipitation falls off, as distance from the sea increases, strongly suggests that it is mainly due to the deposition of the coarse spray (even at Eskdalemuir, which is scarcely a sheltered spot, the ratio is less than 7). There is little doubt, however, that transfer of potassium from the ground to the air does take place and is a contributary cause of the fall-off of the Na : K ratio inland.

Thus the average concentration of potassium in the air sample increases fairly consistently as one goes inland. For the twelve months under review, the concentrations are shown in Table 3.

TABLE 3. CONCENTRATION OF POTASSIUM IN AIR SAMPLES (g m^{-3}) APRIL 1958-MARCH 1959

Exposed coastal stations		Inland stations, Sweden		Inland stations, Finland	
Lerwick	Stornoway	Flahult	Ultuna	Jyvaskyla	Kuopio
0·7	0·9	1·6	0·9	1·9	2·4

Although these observations are compatible with Wilson's theory, it may be remarked that it is not impossible to imagine a purely physical process which would similarly decrease the Na : K ratio in spray. For example, the droplets released from the sea surface usually undergo evaporation. In a sufficiently dry atmosphere the result will be the formation of a crystal of sodium chloride, and the remaining liquid will contain sodium, potassium and magnesium in not greatly different amounts. It is known, moreover, that crystallization in a droplet does not readily occur until a considerable degree of supersaturation has been reached and that when it does occur, it is a sudden and quite violent process. It is conceivable that some part of the liquid is shaken off at this stage in the form of smaller droplets, which would have a composition much like that which has been found in fine spray. This hypothesis accounts satisfactorily for the low values in fine spray of both the Na : K and Na : Mg ratios. It ought to follow that the precipitation, which includes the residues of this separation process, should in favourable circumstances show abnormally *high* values of these two ratios. In fact, this can sometimes be observed at Lerwick. In June and July 1958 the Na : K ratios in precipitation were respectively 30 and 31 (well above the sea-water value) while the Na : Mg ratio in both months was 8·3 (equal to the sea-water value). In June 1959 both ratios were again high (Na : K 36, Na : Mg 19). It is suggestive that all three cases were in the height of summer, when evaporation is likely to have been high; but though there is some evidence to support this crystallization theory, it seems on the whole more likely that Wilson's is the correct explanation. It has the support of Ericsson (1960) who has given reasons for believing that precipitation collected near the sea always contains substantial amounts of organic material which, he suggests, must originate in the sea-surface film, probably by the mechanism suggested by Mason.

ACKNOWLEDGMENTS

I am indebted to the Director-General of the Meteorological Office for permission to publish this paper, and to Dr. A. T. Wilson for a very stimulating correspondence on this subject.

REFERENCES

Ericsson, E. 1960 *Tellus*, **12**, 1.
Mason, B. J. 1957 *The Physics of Clouds*, Clarendon Press, Oxford.
Oddie, B. C. V. 1959 *Quart. J. R. Met. Soc.*, **85**, 364, p. 163.
Wilson, A. T. 1959 *Nature*, **184**, p. 99.
1960 *Ibid.*, **186**, p. 785.
Woodcock, A. H., Kientzler, C. F., Arons, A. B. and Blanchard, D. C. 1953 *Nature*, **172**, p. 1,144.

551.574.11

Ice-nucleating properties of clay minerals and stony meteorites

By B. J. MASON
Imperial College, London

(Manuscript received 2 May 1960)

Summary

The ice-nucleating properties of clay minerals have been investigated in relation to their crystalline and surface structures. The kaolin minerals, the illites and halloysite are the most effective and important, their threshold temperatures for ice nucleation lying between — 9°C and — 12°C. Minerals of the montmorillonite group and related forms are active only below — 15°C. The relative contributions which the various clay minerals are likely to make to the ice-nucleus content of the atmosphere are discussed in relation to their natural abundance, wind-borne dispersion and particle size. Kaolinite is considered to be the most important source of highly efficient nuclei in confirmation of results obtained earlier by Mason and Maybank (1958).

Tests on three new specimens of stony meteorites showed them to be inactive at — 17°C.

Introduction

In a previous paper (hereafter referred to as MM), Mason and Maybank (1958) reported on the ice-nucleating ability of 30 naturally-occurring mineral dusts and found 21 of these, mainly silicate minerals of the clay and mica groups, to be effective to the extent of one particle in 10^4 producing an ice crystal when introduced into a supercooled cloud at temperatures above — 18°C. Eight substances showed this level of activity above — 10°C, the most abundant of these being kaolinite with a threshold temperature of — 9°C. On the other hand, small particles of three different samples of stony meteorites, produced both by grinding and vaporization by an electric spark, were inactive as ice nuclei at temperatures above — 17°C. These results suggested wind-borne mineral dusts and soil particles to be the main source of atmospheric ice nuclei, with the small, well-formed crystals of kaolinite being a particularly important constituent.

This paper records the results of some rather more extensive tests on the nucleating properties of the clay minerals and of three more different samples of stony meteorites.

2. Tests on clay minerals

During a recent stay at the University of California, Los Angeles, the writer was fortunate to obtain a number of standardized samples of clay minerals prepared and investigated under the auspices of the American Petroleum Institute (1949-50). These included four different samples of kaolinite taken from four different locations and the other minerals listed in Table 1. All these materials have been extensively studied by X-ray diffraction (crystal structure), chemical analysis, electron-microscopy (particle size and shape), differential thermal analysis and infra-red spectroscopy. A good deal is therefore known about their structure and properties.

The four samples of kaolinite and nine other minerals were tested for ice-nucleating ability by the methods described in MM. The particles were dispersed as a powder into a supercooled cloud formed in a mixing-cloud chamber and the appearance of ice crystals was detected by a very stable supercooled soap film.

The results, together with salient facts concerning the structure and properties of the tested substances, are summarized in Table 1.

The most effective nucleators were the kaolin minerals which include kaolinite, dickite, anauxite, halloysite and the illites, all these having threshold temperatures between — 9°C and — 12°C. Kaolinite was again the most efficient; the four samples from Pike County, Arkansas; Macon, Georgia; Bath, S. Carolina; and Mesa Alta, New Mexico, which were structurally identical although differing in their Al/Si ratios, showing no detectable differences in nucleating ability.

TABLE 1. PROPERTIES OF CLAY-MINERAL PARTICLES

Substance	Symmetry	Lattice parameters						Constitution	Good crystals?	Easily dispersed?	Atmospheric abundance	Threshold temp. (°C)
		a	b	c	α	β	γ					
Kaolinite	Triclinic	5·14 Å	8·93	7·37	91° 50′	104° 30′	90	$Al_2(OH)_4 . Si_2O_5$	Yes	Yes	H	− 9
Dickite	Monoclinic	5·14	8·94	14·42	90	96° 50′	90	$Al_2(OH)_4 . Si_2O_5$	Yes	No	R	− 12
Anauxite	Monoclinic	5·14	8·93	7·37				$Al_2(OH)_4 . Si_2O_5$	Yes	Yes	R	− 9
Halloysite	Monoclinic	5·14	8·93	variable				$Al_2(OH)_4 . Si_2O_5 . 2H_2O$	Yes	Yes	M	− 12
Illite	Monoclinic	5·18	9·02	20·04	90	~90	90	$(OH)_4K_y(Al_4 . Fe_4 . Mg_4 . Mg_6)(Si_{8-y}Al_y)O_{20}$	No	Yes	H	− 9
Metabentonite								Alternate layers of illite and montmorillonite	No	Yes	R	− 9
Montmorillonite	Monoclinic	5·15	8·95	variable	90	?	90	$5Al_2O_3 . 2MgO . 24SiO_2 . 6H_2O$ (Na_2O, CaO)	No	No	H	− 16
Nontronite	Monoclinic	5·23	9·06	?	90	?	90	$6Fe_2O_3 . Al_2O_3 . 22SiO_2 . 6H_2O$ (Na_2O, CaO)	No	No	L	− 15
Pyrophyllite	Monoclinic	5·14	8·90	18·55	90	99° 55′	90	$Al_2(OH)_2 . Si_4O_{10}$	No	No	R	− 10
Attapulgite	Monoclinic	12·9	18					$4H_2O . (OH)_2Mg_5Si_8O_{20} . 4H_2O$	No	No	R	− 14

Anauxite (− 9°C), dickite (− 12°C) and halloysite (− 12°C) had the threshold temperatures indicated in the brackets and were about ten times more effective when the temperature was lowered another two degrees.

The least effective group contained the montmorillonite minerals – montmorillonite itself, nontronite, and the chemically similar attapulgite. These showed little activity at temperatures above − 15°C but were definitely active at − 18°C.

3. Properties of clay minerals

All the minerals tested have monoclinic crystalline symmetry (except kaolinite which is strictly triclinic but very nearly monoclinic since $\alpha = 91{\cdot}8°$). The crystals are built up in layers whose planes are normal to the *c*-axis, the *a*- and *b*-lattice spacings on these planes being very nearly the same for all the substances except for attapulgite.

The kaolin minerals are built up of alternate layers of Si_2O_5 tetrahedra and $Al_2(OH)_4$ octahedra, so that OH groups are exposed on one surface and silica on the other. The difference between the various kaolin minerals lies mainly in the stacking, and separation of these layers parallel to the *c*-axis. Halloysite normally occurs in a hydrated form in which water molecules are interleaved between layers of the kaolinite structure.

The montmorillonite-type minerals, on the other hand, are 3-layer structures, with either aluminium, magnesium or iron hydroxide sandwiched between two layers of silica. Water molecules are strongly adsorbed between the layers to produce an expanding lattice in the *c*-direction which is typical of the swelling clays. But water is not strongly absorbed on the surfaces of the particles. As suggested in MM, the differences between the nucleating properties of kaolinite-type and montmorillonite-type minerals may probably be ascribed to fact that cleavage of kaolinite exposes an alumina layer whose OH^- ions will firmly bind arriving water molecules into an ice-like configuration, the degree of misfit between the OH^- configuration and the basal plane of ice being only 1·2 per cent and 1·5 per cent in two mutually perpendicular directions. On the other hand, the exposed surfaces of silica on montmorillonite are relatively poor for ice nucleation as tests with silica particles show.

The structures of the illites, and of metabentonite which is made up of irregularly alternating layers of illite and montmorillonite with illite predominating, are complex and not fully understood. Illite is similar but not identical in structure to muscovite mica but differs from it in its alkali and hydration content.

Attapulgite is chemically similar to montmorillonite but with a higher magnesium content and has a chain rather than a layer structure in which water molecules lie in tunnels between the chains and parallel to the *c*-axis.

Pyrophyllite is a hydrous aluminium silicate which resembles talc and is not generally considered a clay mineral though very closely related. It has a 3-layer structure of the montmorillonite type but differs from montmorillonite in that inter-layer water is apparently absent and it contains little or no Na or Ca or other exchangeable bases.

Another factor in the nucleation efficiency may be the crystallinity and size of the particles. Electron microscopy shows that the kaolinite specimens contain a high proportion of well-formed pseudo-hexagonal plates. The distribution of crystal sizes is rather different in the four different specimens but the smallest particles are less than 0·1 μ in diameter and about 30 per cent of the mass is composed of particles of $d < 0{\cdot}5\ \mu$. The dickite particles are coarse with diameters of up to 8 μ but they are often six-sided and well-formed crystals. The halloysite is composed mainly of small rods and tubes, often split, with median outer diameter 0·07 μ; again about 30 per cent of the mass is composed of particles smaller than 0·5 μ.

The montomorillonite particles are small, of about the same size as those of kaolinite, but they are in the form of thin flakes (0·002 to $> 0{\cdot}02\ \mu$ thick) with irregular outlines and little evidence of crystallinity. They strongly adsorb water and ' cake ' so that they are difficult to disperse in finely-divided form. The nontronite particles are similarly poorly crystallized in the form of small laths of average dimension $0{\cdot}06 \times 0{\cdot}01 \times 0{\cdot}001\ \mu$. These also tend to form large aggregates.

The illite particles have rather similar characteristics to those of montmorillonite but do not adsorb water strongly and form aggregates; they are easily dispersed.

Pyrophyllite is composed of coarsely crystalline flakes with only about 1 per cent having diameters less than 0·5 μ. Attapulgite is made up of fibres and bundles of fibres, a large proportion of which are smaller than 0·5 μ, but there are also well-developed rods which attain a maximum length of 4-5 μ and width 0·1 μ.

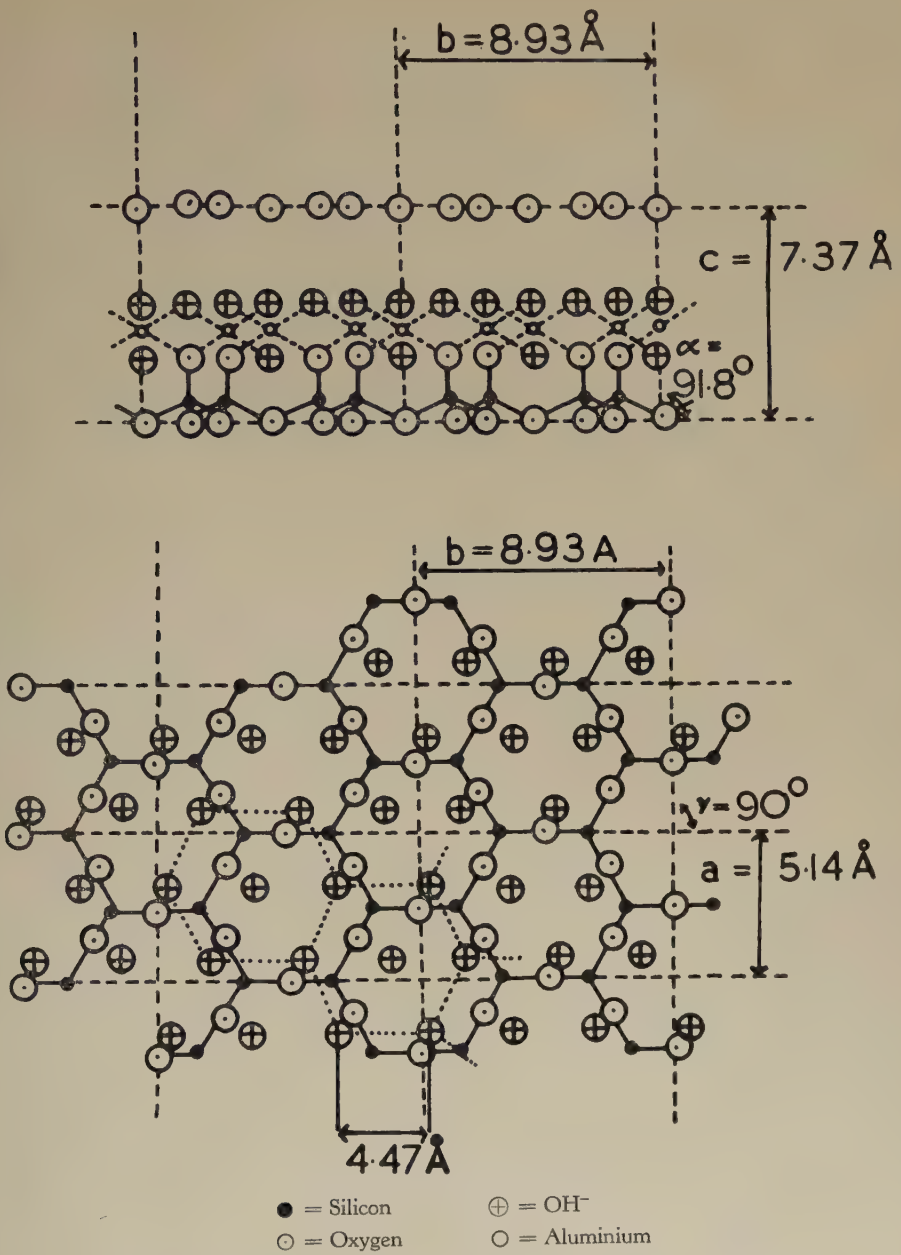

Figure 1. The crystal structure of kaolinite.

4. Abundance of clay particles in the atmosphere

The relative abundance of the various types of dust particles in the atmosphere will be determined by:

(i) their relative abundance in the soil, and the extent to which they are exposed to the winds will carry them aloft;

(ii) the ease with which the particles are dispersed, and

(iii) the particle size which will determine for how long they will remain suspended in the atmosphere.

Kaolinite and montmorillonite, followed by illite, are by far the most abundant of the mineral listed in Table 1. Kaolinite, which is probably the most stable of all the clay minerals, is formed by the weathering of feldspar under the influence of acidic water. It is therefore found mainly in warm, humid climates which favour rapid weathering; soils containing kaolinite are therefore usually covered with vegetation. Montmorillonite, on the other hand, is formed under alkaline conditions and is found mainly in arid regions. Illite may be formed by the weathering of feldspar, the disintegration in acid solutions of muscovite and the alteration of montmorillonite.

Probably the mass of kaolinite which becomes airborne is consideraly less than that of montmorillonite but this will be partly offset by the fact that kaolinite is composed of small particles which show little tendency to aggregate and are slow to settle out. Giving both kaolinite and montmorillonite a high relative abundance, those of the other tested substances are given on a scale of High (H), Medium (M), Low (L) and Rare (R) in Table 1.

5. The nucleating ability of stony meteorites

Through the courtesy of Dr. E. P. Henderson, the National Museum in Washington, D.C. kindly supplied the writer with specimens of the following meteorites : (i) Holbrook, Arizona, 1912 : a spherulite chondrite consisting mainly of olivine and pyroxene (both magnesium-iron silicates) with specks of nickel-iron; (i) Murray, Kentucky, 1950 : a carbonaceous chondrite consisting mainly of olivine, graphite and iron dust : and (iii) Ochansk, U.S.S.R., 1887 : a brecciated spherulite bronzite chondrite consisting mainly of magnesium-iron silicate and containing some nickel-iron grains.

Fine particles of the meteorites were produced both by grinding, and by the scraping off their surfaces and these were then introduced into a supercooled cloud formed in a mixing-cloud chamber, their nucleating efficiency being measured in the same manner as for the clay minerals. The specimens were also vaporized in a hydrogen-oxygen flame at 2,800°C which caused the material to boil, and the resulting smoke was introduced into the cloud chamber. In no case did the meteorite particles produce a detectable number of ice crystals at temperatures above − 17°C. The results were therefore very similar to those obtained with three other specimens of meteorites used in paper MM.

6. Conclusions

The present tests support those reported in MM in suggesting that kaolinite, aided mainly by illite and halloysite, are the most effective and important of the clay minerals for ice nucleation, while those of the montmorillonite group and related forms are relatively inactive. However, as shown in MM, montmorillonite particles may be pre-activated to act at considerably higher temperatures.

In the light of their natural abundance, these active clay-mineral particles probably constitute only a small proportion of atmospheric aerosols; this would account for the low concentrations of effective ice nuclei and the prevalence of supercooled clouds.

That the clay minerals, especially kaolinite, are probably the main source of atmospheric ice nuclei is also strongly supported by the latest results of the Japanese school who report that of the foreign particles found at the centres of snow crystals, 90 per cent have been identified as soil particles, 75 per cent of these being clay particles, most probably kaolinite (Isono 1959).

Acknowledgments

This work was carried out while the author was on leave as Visiting-Professor of Meteorology in the University of California at Los Angeles.

I am indebted to Dr. E. P. Henderson of the National Museum, Washington, D.C. for providing the meteorite samples and to Dr. H. Winterer of the Geology Department, University of California at Los Angeles for the samples of clay minerals. I also wish to thank Mr. Hans Pruppacher for his assistance in making the experiments.

References

American Petroleum Institute 1949-50 *Reports on Clay-Mineral Standards.*
Isono, K. 1959 *Jap. J. Geophys.*, **2**, No. 2, p. 1.
Mason, B. J. and Maybank, J. 1958 *Quart. J. R. Met. Soc.*, **84**, p. 235.

551.589.1

A note on the synoptic climatology of Labrador-Ungava

By R. G. BARRY
University of Liverpool

(Manuscript received 22 December 1959; in revised form 21 March 1960)

Summary

Aspects of the synoptic climatology of the Labrador-Ungava peninsula are investigated with reference to a classification of airflow pattern types, formulated on the basis of synoptic weather maps for November 1956 to February 1958. The winters 1956-57 and 1957-58 exhibit, respectively, marked negative and positive temperature departures and the temperature and precipitation characteristics of the airflow types are discussed for these two seasons. The validity of the airflow categories is statistically tested.

1. Introduction

Knowledge of the climatology of the Labrador-Ungava peninsula – the mainland lying north-east of a line drawn between the mouths of the Rupert and Saguenay rivers – has been greatly restricted by a paucity of observational records and there are no detailed studies of the area. Data from the Moravian Mission stations on the Labrador coast have been analysed by Döll (1937) and Tanner (1944); Hare (1950) has investigated the dynamic climatology of the eastern Canadian Arctic and Sub-Arctic.

This paper discusses synoptic situations over Labrador-Ungava in terms of some of their climatic characteristics, by means of a classification of airflow pattern types. The method provides a link between climatological statistics and synoptic reality.

2. Data and methods employed

The classification was formulated after initial examination of the movement of cyclones and anticyclones over the area. The categories are based upon the general trajectory of air currents near the surface for two or three days prior to their passage over Labrador-Ungava. The modification of an air current is particularly dependent upon the trajectory of the air, as Burbidge (1951) demonstrated in a study of polar continental air over Hudson Bay. The precise determination of trajectories is time-consuming and in the present investigation these are assessed subjectively. A basis for this assessment is provided by calculated trajectories for various synoptic patterns (Shaw and Lempfert 1906) and for an idealized depression (Sawyer 1954).

The study employs twice-daily synoptic analyses for November 1956 to February 1958 and the flow pattern over Labrador-Ungava is classified for each m.s.l. analysis for a six-fold regional subdivision of the peninsula (Fig. 1). The regions approximate to Hare's physiographic divisions (1950), but it is only in the case of the central Lake Plateau that the observing stations can be considered as representative for the whole region. Data on the airflow categories and daily climatological information (maximum and minimum temperatures, rainfall, snowfall and occurrences of fog and freezing precipitation) for the eleven stations shown on Fig 1, have been put on to punched cards and relationships between airflow type and climate examined using a card-sorter. Discussion of the results is here confined primarily to the two winter seasons.

3. Winters 1956-57 and 1957-58

The winter season is arbitrarily taken as November to February and, for convenience, winters 1956-57 and 1957-58 are referred to as winters I and II respectively. There are marked differences between the temperature characteristics of the two winters (See Table 1). The available averages are for variable periods of record and therefore values are not strictly comparable between stations, but the contrast between the negative departures of winter I and positive departures of winter II is evident. The precipitation figures (see Table 2) show less uniform patterns. Snowfall and rainfall are well below average over central and north-west Labrador-Ungava in winter I. In winter II snowfall is markedly above average at Great Whale River and Fort Chimo.

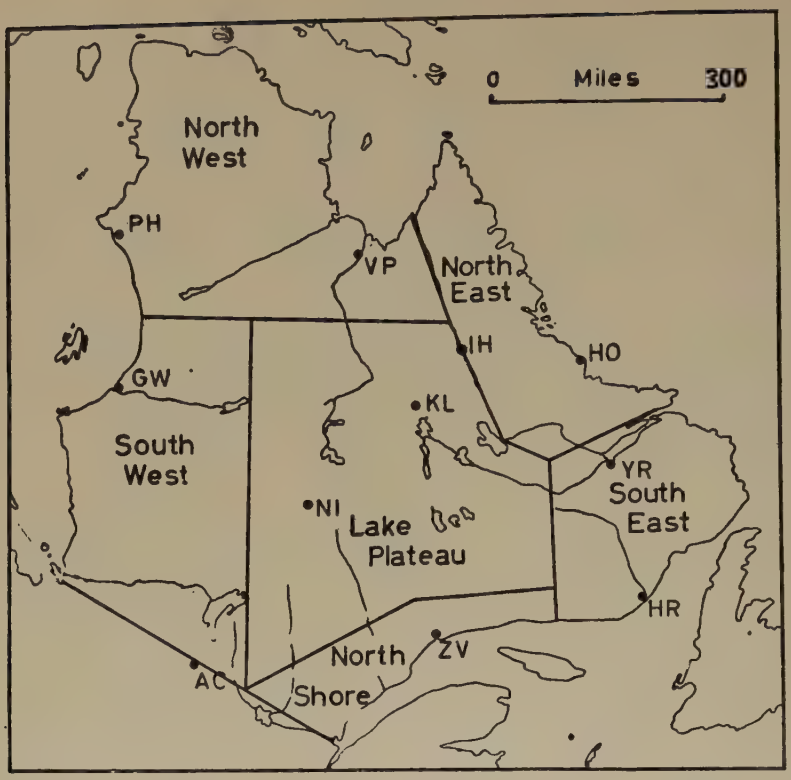

Figure 1. Weather stations and the regional subdivision of the peninsula.

TABLE 1. SELECTED TEMPERATURE DATA (°F)

Station	Period of record	January mean temp.	Departure of mean January temperature from average January 1957	January 1958
Harrington Harbour	1921-50	9·4	− 12·0	12·4
Goose Bay	1942-50	− 0·2	− 10.8	14·4
Knob Lake	1949-58	− 10·4	− 11·8	13·7
Hopedale	1942-50	0·2	− 11.3	12·6
Port Harrison	1921-50	− 14·8	− 7·2	8·6
Fort Chimo	1941-50	− 12·5	− 10·8	11·5
Great Whale River	1925-50	− 10·1	− 9·3	8·8

TABLE 2. SELECTED PRECIPITATION DATA (INCHES)

Station	Period of Record	Average winter snowfall	Average winter rainfall	Winter I Snowfall	Winter I Rainfall	Winter II Snowfall	Winter II Rainfall
Harrington Harbour	1921-50	139	5·77	166	4·74	82	8·66
Goose Bay	1942-50	90	·80	107	·24	66	1·63
Knob Lake	1949-58	66	·54	40	·10	82	1·77
Hopedale	1942-50	57	1·12	47	·15	73	·74
Port Harrison	1921-50	39	·11	24	·09	20	tr
Fort Chimo	1941-50	35	·10	24	·22	63	·37
Seven Islands	1944-57	125	3·48	122	1·33	152	6·34
Great Whale River	1925-50	66	·33	–	–	130	·38

The gross circulation features over north-eastern North America during winter II are of significance for this discussion. In January-February 1958, particularly, there was a general tendency for cyclones to pass northwards over Labrador-Ungava. Thomas and Titus (1958) show that warm air caused extreme surface maxima to reach 40°F in the eastern Canadian Arctic during a particular spell from 19 to 24 January 1958. Temperatures up to 500 mb were well above normal associated with a warm ridge aloft from Newfoundland to Baffin Island. Such warm advection would in turn affect the temperature characteristics of air moving out from the Arctic archipelago. During 9 to 14 February 1958 the surface flow type over most of Labrador-Ungava changed from Easterly (E) to north-westerly (NW), although the surface temperatures during the NW spell were considerably modified until 14 February. The 1,000-500 mb thickness chart for this period showed a pattern similar to that of 19 to 24 January, with an upper warm ridge over the peninsula.

A factor which would affect the temperature of air moving towards Labrador-Ungava from a general westerly direction is the extent of ice-coverage in Hudson Bay. Hare and Montgomery (1949) and Burbidge (1951) show that precipitation amounts over the east shore of the Bay normally decrease sharply at the end of December when, with the exception of small leads, the Bay freezes over. However, indications for winter II from precipitation data at Great Whale River are that ice was late in extending to the eastern section of Hudson Bay.

4. The airflow types

The classification is divided in the first instance into cyclonic or anticyclonic type. Anticyclonic types are defined arbitrarily as having m.s.l. pressure of 1,016 mb, or above, with neutral or anticyclonic curvature. These cases are subdivided according to the origin of the air, where possible, or termed indeterminate. Cyclonic cases, including transient ridges, are defined as having m.s.l. pressure below 1,016 mb or cyclonic curvature. There is no general ' cyclonic type,' since depressions on the ' arctic,' ' maritime ' or ' polar front ' (Anderson, Boville and McClellan 1955) may cross the area and there is a need to differentiate between cyclones with dissimilar air-current components. There are nine cyclonic types whose identifying synoptic features are described below, together with a discussion of related climatological data.

Climatological parameters have been determined for each station in Fig. 1 for individual airflow types in each season. The parameters are mean maximum and minimum temperatures and average precipitation amounts per day of a given flow type – referred to as ' precipitation indices.'

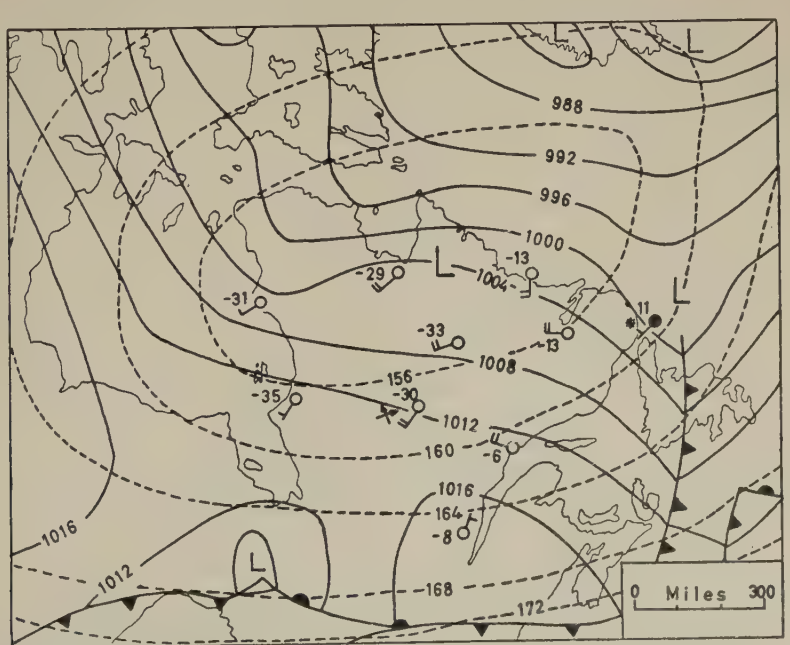

Figure 2. North-westerly (NW) type, 28 January 1957; m.s.l. 00 GMT isobars (solid); 500 mb 03 GMT contours (dashed) – hundreds of feet.

North-westerly (NW) is associated with an outflow of air from the Arctic archipelago or North West Territories. This may occur in the rear of a depression travelling eastwards along the arctic front, in which case the flow tends to affect only north-western Labrador-Ungava. More persistent NW flow, extending over the greater part of the peninsula, results from the development of high pressure over north-western Canada. The latter situation is typified by the example in Fig. 2.

Snowfall is generally light with NW flow, although the type makes an important contribution to the total snowfall of north-west Ungava in winter I by reason of its frequent occurrence. In winter II, the precipitation index is 0·10 in. at Cache Lake and Great Whale River, but elsewhere indices are low. This distribution, together with the higher temperatures in winter II (Table 3) can be ascribed to the dynamic and physical influences noted in Section 3. Nevertheless, the lowest average daily temperatures occur in both winters with NW type (disregarding anticyclonic cases which have not been subdivided in the determination of these parameters).

TABLE 3. AVERAGE MAXIMA AND MINIMA (°F) FOR SELECTED STATIONS AND AIRFLOW TYPES

WINTER I

	NW		W		Wm		SW		E	
Harrington Harbour	2·7	− 14·6	14·1	− 2·5	30·2	12·5	43·4	32·4	27·9	14·3
Seven Islands	− 0·2	− 17·8	20·6	1·2	24·0	1·0	35·8	20·0		
Knob Lake	− 15·6	− 29·9	− 3·1	− 18·8	14·0	− 9·5			(17·8	5·0)
Hopedale	− 3·9	− 14·5	5·0	− 4·5	19·3	4·2			24·4	15·4
Port Harrison	− 4·5	− 17·8	− 0·8	− 14·6	21·4	2·7				
Fort Chimo	− 6·0	− 15·9	− 4·2	− 20·1	− 13·4	− 0·7				

WINTER II

	NW		W		Wm		SW		E	
Harrington Harbour	14·5	0·0	28·5	14·7	38·1	27·1	40·6	24·2	34·2	27·3
Seven Islands	15·0	3·6	24·2	6·2	35·0	22·5	36·2	22·6	29·7	16·1
Knob Lake	0·3	− 12·2	12·6	− 1·0	25·3	7·1	(34·4	26·8)	26·2	15·3
Hopedale	4·1	− 5·8	20·2	9·8	33·5	17·5			32·1	21·6
Port Harrison	− 3·7	− 16·5	18·3	7·3	23·0	9·5			20·6	6·3
Fort Chimo	2·6	− 15·9	14·4	2·8	28·1	11·5			23·0	15·6

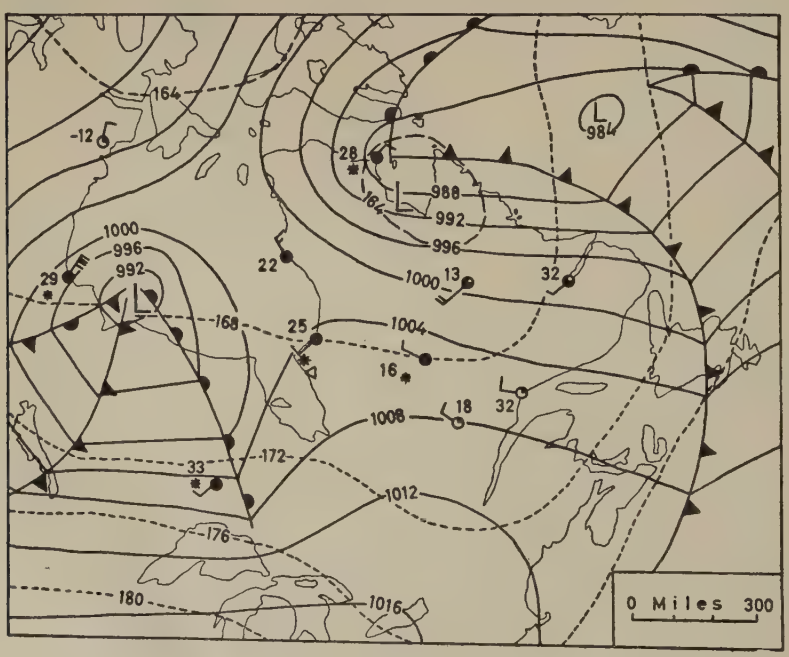

Figure 3. Westerly (W) type 6 November 1957, m.s.l. and 500 mb 12 GMT.

North-westerly modified (NWm) differs from the NW pattern mainly with regard to the longitudinal situation of the synoptic features. The anticyclone over north-west Canada lies farther west than in the NW case, leading to north-west to north flow across Keewatin, and zonal flow over Hudson Bay and Ungava. The climatological characteristics are intermediate between those of NW and W flow.

Westerly (W) type (Fig 3) occurs basically in situations with zonal flow. Two idealized cases for cyclones forming on the arctic or maritime fronts may be recognised. With the former, W may designate warm sector air associated with NW (or NWm) ahead of the warm front and in the rear of the cold front. With the maritime front, W may occur ahead of the warm front and/or to the rear of the depression.

Precipitation indices in winter I are 0·02 in. over much of the peninsula and there is a maximum value of 0·12 in. at Harrington Harbour. Values are much higher in winter II at Great Whale River (0·15 in.), Cache Lake (0·11 in.) and Knob Lake (0·10 in.), but not at Fort Chimo, Port Harrison and Goose Bay. Temperatures are higher in winter II at all stations.

Westerly modified (Wm) is differentiated from W type by the air swinging south-eastwards from western into central North America and later recurving north-eastwards across Labrador-Ungava. Wm and SW types are shown in Fig. 4.

Precipitation indices for both winters are high in the southern part of the peninsula, decreasing northwards. The index is 0·47 in. at Harrington Harbour and 0·24 in. at Seven Islands in winter I. The figures at these stations in winter II are 0·18 in. and 0·23 in. respectively, whilst an index of 0·19 in. at Great Whale River indicates a second area of higher values. Table 3 shows that temperatures with Wm are consistently higher than with W flow.

South-westerly (SW) occurs predominantly in warm sectors of cyclones moving north-eastwards from the Great Lakes area. The type is rather infrequent, but it is associated with high temperatures and high precipitation amounts in southern parts of the peninsula.

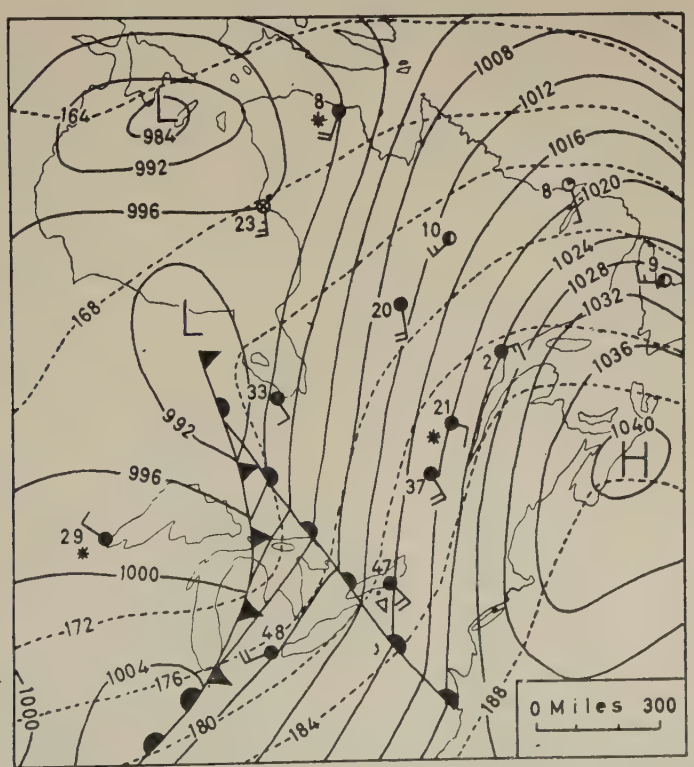

Figure 4. Westerly modified (Wm) and South-westerly (SW) types, 19 December 1957, m.s.l. and 500 mb 12 GMT.

Southerly (S) is associated with cyclones of the 'Atlantic polar frontal zone' (Hare 1950) which move northward from the east coast of the United States. Hare notes that maritime tropical air is not infrequently present aloft when these cyclones reach south-east Labrador. Thus, although the polar front may only appear over Newfoundland and the St. Lawrence on the m.s.l. map, precipitation falls in southern Labrador-Ungava from warm sector air aloft.

Easterly (E) represents in many cases a later stage of the S type. East coast depressions may become quasi-stationary over Newfoundland or move northwards to the Davis Strait. This results in E flow over at least the eastern part of the peninsula, such as is exemplified in Fig. 5.

Precipitation indices (including freezing precipitation and rain in winter II at Knob Lake and Seven Islands in particular) are high in the eastern part of the peninsula in both winters. In winter I, Goose Bay has a value of 0·22 in. and Harrington Harbour 0·29 in. In winter II indices of 0·26 in. at Knob Lake and 0·28 in. at Seven Islands reflect a slightly different pattern which results mainly from over-running at a quasi-stationary front over eastern Labrador-Ungava in early February 1958. Average maxima with E type in winter II are of the order of 32°F in the east and south-east, decreasing westwards.

North-easterly (NE) is essentially similar to the E type, but the pattern is characterized by high pressure over Greenland-Baffin Bay, strengthening the general E flow. The type is infrequent.

Northerly (N) occurs rather infrequently when a trough develops over the Labrador Sea–Davis Strait from a quasi-stationary cyclone near Newfoundland. N may represent the final stage of a sequence of S-E-N types. It tends to give modified maritime conditions – less precipitation and lower temperatures than E flow.

The weather conditions during anticyclonic cases are largely related to the origin of the air although precipitation amounts are generally low. The cases of the individual sub-types are on the whole too few to analyse. The recognition of the anticyclonic category is primarily useful in the consideration of the climatic characteristics of the other flow types under non-anticyclonic conditions.

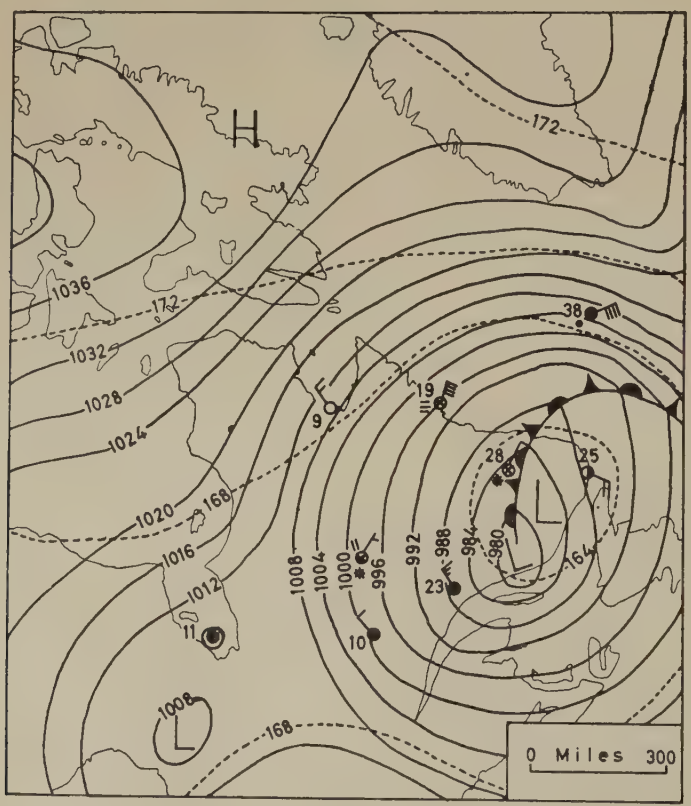

Figure 5. Easterly (E) type, 18 February 1957, m.s.l. 12 GMT; 500 mb 15 GMT.

5. Frequencies of the flow types

The total frequency of the types has been calculated from 1 November 1956 to 28 February 1958 (485 days) for the six regions, (Table 4). W type occurs on over 20 per cent of days in each region, with a maximum of 31 per cent in the south-west and the Lake Plateau. The north-west region is distinct from the others in having a 23 per cent frequency of NW flow, but the south-west region is the most ' continental ' with the virtual absence of S, E, NE and N types. The general anticyclonic category has a minimum frequency of 21 per cent in the north-east and a maximum of 28 per cent in the North Shore region.

TABLE 4. Airflow type frequencies

	Regions					
	North West	South West	North Shore	South East	North East	Lake Plateau
	Total frequency (1 November 1956 to 28 February 1958, 485 days) (per cent)					
A	22	26	28	23	21	22
NW	23	12	7	9	13	14
NWm	9	7	5	4	6	7
W	24	31	24	22	22	26
Wm	9	14	16	11	10	14
SW	1	6	8	7	3	4
S	–	–	2	5	1	1
E	5	1	7	14	13	7
NE	1	1	1	1	2	1
N	5	1	1	4	8	2
	Winter I (120 days) (per cent)					
A	22	29	37	27	25	27
NW	25	8	5	8	15	12
NWm	5	7	4	3	5	5
W	32	31	24	26	28	31
Wm	6	20	18	10	8	14
SW	–	2	6	5	2	3
S	–	–	3	6	1	1
E	3	1	1	10	5	3
NE	1	1	–	–	1	2
N	5	1	1	5	10	3
	Winter II (120 days) (per cent)					
A	21	25	23	26	23	22
NW	27	17	4	6	9	14
NWm	13	8	8	8	10	13
W	18	26	15	14	16	20
Wm	7	12	14	7	7	12
SW	2	4	8	4	2	3
S	–	–	2	5	2	1
E	5	2	18	21	18	8
NE	4	3	5	3	4	4
N	3	2	2	5	8	4

There are marked contrasts between the type frequencies for winters I and II. W flow is less frequent in all regions in winter II than in winter I and there is a corresponding increase of E and NE flow. The high frequency of E flow in winter II over eastern Labrador-Ungava accounts for a part of the temperature departures shown in Table 1. In the north-west, Lake Plateau and, particularly, the south-west region, the NW type is more frequent in winter II than winter I.

6. Significance tests

The validity of the airflow categories is examined by an analysis of the variance of precipitation values within and between selected flow types and by the application of χ-square tests to grouped temperature data. Daily maxima are employed for the latter since minimum temperatures are generally more subject to specifically local effects. The results of these tests, which are summarized in Table 5, indicate that the categories are on the whole reasonably discrete. Annual contrasts will arise from variations in dynamic influences, in particular the large-scale circulation patterns, and regional and local differences are to be expected in view of the effects of Hudson Bay and topography upon climate.

TABLE 5. Significance levels for tests of the airflow types

Airflow types	Station	Precipitation Analysis of variance (per cent)	Temperature χ-square (per cent)
WINTER I			
NW-W	Hopedale		4
	Knob Lake Nitchequon		0·5
	Port Harrison	1	Insignificant
	Fort Chimo	1	
NW-W-Wm	Knob Lake	0·1	
NW-W-N	Hopedale	2	
W-Wm	Seven Islands	1	
W-Wm-E	Goose Bay	0·1	
	Harrington Harbour	0·1	
Wm-SW	Harrington Harbour Seven Islands		2
E-N	Goose Bay Hopedale		Insignificant
WINTER II			
NW-NWm	Knob Lake Nitchequon		Insignificant
	Port Harrison		4
NW-NWm-W	Fort Chimo	1	
	Port Harrison	1	
NW-W	Fort Chimo		0·5
NWm-W	Knob Lake Nitchequon		1
NW-W-Wm	Fort Chimo	1	
	Knob Lake	Insignificant	
	Nitchequon	0·1	0·1
W-Wm	Fort Chimo Port Harrison		Insignificant
NWm-W-Wm-SW-E	Seven Islands	0·1	
Wm-SW	Harrington Harbour Seven Islands		Insignificant
E-N	Goose Bay Hopedale		0·5

The bracketed values in the χ-square test column indicate that temperature values for the two stations were considered together to provide adequate samples.

7. Developments of the study

More intensive consideration of the airflow types has included an additional classifying of the isobar curvature. However, the period of study is too short to provide sufficient cases for determination of the climatological parameters on this basis.

The strength of the geostrophic zonal flow between latitudes 45° and 65°N from 55-105°W and the meridional flow between the sectors 55-80°W and 80-105°W has also been investigated. Daily flow indices are calculated for m.s.l. and 500 mb from pressure or height values at points along the two latitude lines. Zonal flow is positive west to east; meridional flow is positive north to south. Examination of these indices and the airflow types over the Lake Plateau region shows that the most clear-cut relationships occur with NW and E types. With NW flow, zonal and meridional indices are almost entirely positive at m.s.l. and 500 mb. During E and NE flow, there is negative zonal and positive meridional flow at m.s.l. and mainly positive meridional flow at 500 mb. The flow indices display much greater variability with W, Wm and SW types.

The flow indices show an inconsistent relationship with the 700 mb zonal wind index between 35-55°N and 5°W-175°E of the U.S. Weather Bureau (Klein 1958).

The contrasting climatic conditions associated with individual airflow types during each winter season raises the possibility that the airflow categories are invalid. The statistical tests indicate that the classes are discrete and it is suggested that the inter-annual differences arise from the particular large-scale circulation patterns and the variable influence which Hudson Bay may have on air passing eastwards over it.

This study demonstrates the necessity for considering both large and small-scale circulations in synoptic climatology and indicates methods for inter-relating dynamic and synoptic climatology. The results of the study provide some guide for local station forecasting and have applications in palaeoclimatology. Labrador-Ungava was a major centre of ice-dispersal during the last glaciation and it is therefore a key area with regard to the climatological aspects of glaciation.

Acknowledgments

The author is indebted to the Director, Meteorological Branch, Department of Transport, Canada, for supplying temperature and precipitation data and to Professor F. K. Hare and Dr. S. Gregory for advice and criticism. The research was supported in part by the McGill Sub-Arctic Research Laboratory and in part by the Geophysics Research Directorate of the Air Force Cambridge Research Center, Air Research and Development Command, under Contract No. AF 19(604)-3865.

References

Anderson, R., Boville, B. W. and McClellan, D. E. 1955 *Quart. J. R. Met. Soc.*, **81**. p. 588.

Burbidge, F. E. 1951 *Ibid.*, **77**, p. 356.

Döll, L. 1937 *Aus dem Archiv. der Deutschen Seewarte*, **57**, p. 1.

Hare, F. K. 1950 Ph.D. Thesis, Montreal University, 2 vols., 440 pp.

Hare, F. K. and Montgomery, M. R. 1949 *Arctic*, **2**, p. 79 and 149.

Klein, W. H. 1958 *Weatherwise*, **11**, p. 7.

Sawyer, J. S. 1954 *Toronto Met. Conf. 1953, Proc. R. Met. Soc.*, p. 145.

Shaw, W. N. and Lempfert, R. G. K. 1906 'Life history of surface air currents,' *M.O. 174*, H.M.S.O., London.

Tanner, V. 1944 *Acta Geogr. Fennica.*, Helsinki, **8**, p. 288.

Thomas, M. K. and Titus, R. L. 1958 *Mon. Weath. Rev.*, U.S.W.B., **86**, p. 19.

Correspondence

551.578.46 : 311.214

Snowfall measurements in northern Canada

By Richmond W. Longley

Mr. C. I. Jackson's article (*Quart. J. R. Met. Soc.*, **86**, p. 273, 1960) emphasizes once again the problem of precipitation measurements in the Arctic. I wonder whether the source of error he discusses is not minor compared with other sources of error.

The frequency of falling snow crystals in the polar regions is amazing to anyone who goes there, no matter how much he has studied the recorded weather reports. The total deposit from these cannot be negligible. Moisture also comes from direct sublimation on the snow. There seems no method by which one can measure these accumulations.

But moisture from such sources is not the only precipitation that cannot be measured. Even when a ' measurable ' amount falls, it is seldom a ruler is used to determine that amount. There are two reasons. Daily totals of recorded measured snow are 0·2 in. or less on over 50 per cent of the occasions in the far north. The frequency of six-hourly totals of these small amounts must be much greater. Even when such small amounts lie uniformly over the surface, the value is usually estimated. Large amounts are usually accompanied by winds of 15 mi hr^{-1} or more. These will carry the falling snow into drifts, to make it necessary that the observer use his judgment in recording the total snowfall. When the wind reaches 20-25 mi hr^{-1}, snow from the ground is carried aloft. Under these circumstances there is no method by which an observer can state with confidence the amount that fell from the clouds.

Another error in the determination of the water content is in estimating the density of the fresh snow. The snow particles at Resolute, N.W.T., and probably at many other Arctic stations, were almost never the star-like aggregations of ice crystals familiar to residents of temperate latitudes. On most occasions they were snow pellets of 0·2 to 0·5 mm diameter. I have suspected that many of these were formed in the turbulent eddies above areas of open water from which some of the moisture came. With the light snow deposits that occur in the far north, it is impossible to obtain a sample of this snow in order to determine the density.

There would appear to be another method of determining the moisture from the snow. In these areas there is no melting during the winter, and very little evaporation. The snow cover of 30 April then equals the total winter precipitation to date. The water content should be determined using the mean snow depth on the ground and the mean density. Using the total accumulated snow fall, one might then determine a ' mean density of fresh snow.' Moisture from sublimation and traces would be included when this value was used with the recorded snowfall.

The difficulty with such a method concerns itself with measuring the snow on the ground. A study I made at Resolute during the winter of 1957-1958 (to be reported in the *Journal of Glaciology*) showed that the snow depth was a function of topography and the direction of the wind during the last major storm. Except in ravines and other protected places, it did not continue to accumulate as the winter progressed. A representative ' depth of snow on the ground ' over these barren lands then becomes impossible.

As a result of my two years at Resolute, and my consideration of this problem, I have concluded that we cannot know the moisture that comes to these north lands. The present method gives an underestimate, I am sure. At least the data from year to year are comparable.

Department of Mathematics,
University of Alberta,
Edmonton, Alberta, Canada.
20 June 1960.

Reply

By C. I. Jackson

I am grateful to Mr. Longley for his remarks on the problem of snow measurement and look forward to the appearance of his own paper on the subject.

In my paper I did not intend to minimize the importance of the errors discussed by Messrs. Bruce and Potter (1957) and by Mr. Longley. The purpose was rather to draw attention to the additional problem of traces which, so far as I am aware, has been discussed only by Neuberger (1944). The unusual conditions at Lake Hazen, so far as wind-derived errors are concerned, meant that the omission of trace records appeared to be the only factor which could satisfactorily explain the difference between the water equivalent of snow sections near to the station and the measured precipitation (this is discussed in more detail in Jackson, 1959, p. 88). The importance of this factor at Lake Hazen raised the question whether it might not be of significance elsewhere and the records of 200-300 traces in a single winter at Alert and Eureka suggest that the error is not a minor one.

On the question of direct sublimation, I agree that it is likely to be of significance, particularly at stations which frequently record temperatures between about 0°F and freezing point. At temperatures much below these values, however, my own experience is that it is much less important.

With most of Mr. Longley's other points I am in complete agreement, particularly the impossibility of obtaining a representative ' depth of snow on the ground.' The human errors alone which are involved in this method make me feel that the introduction of a gauge is necessary, despite the problem of eddying which it entails.

References

Bruce, J. P. and Potter, J. G. 1957 *Canad. Branch R. Met. Soc. Pap.*, **8**, 1.

Jackson, C. I. 1959 *The meteorology of Lake Hazen, N.W.T.*, **1**, Canada, Defence Research Board, Ottawa.

Neuberger, H. 1944 *Bull. Amer. Met. Soc.*, **25**, p. 183.

Physical-statistical rules as bases for forecasts of weather and weather-character

(Reviewed October 1959)

By F. Baur

The review of my book in the *Quarterly Journal* selects Rule 66 as an example. This appears regrettable inasmuch as various other rules find a much better physical interpretation in the book than this particular rule, for which at present no other explanation can be given than the tendency for persistence and the transfer of temperature from an adjacent area in the course of the general atmospheric circulation. Presumably, however, this particular rule was mentioned in the review because it applies to part of the United States and, therefore, was printed in both German and English, whereas most of the other rules in the book concern Central Europe and are printed in the German language only.

In mentioning Rule 66, however, the reviewer became the victim of an error. This needs to be pointed out, because from this error he arrives at a false conclusion. The reviewer writes :

> " In the example quoted, why is the New England winter temperature related to that at Winnipeg in October rather than September or November ? Presumably because the author either knew, from other work on the same data, or found through his own work, that the other months would give worse results."

Actually the October temperature of Winnipeg is not used; Rule 66 in fact reads as follows :

> " If *November* in Winnipeg is more than 3·5°F too cold and in Boston the first half of of December is too cold or not more than 0·2°F too warm it will be highly probable that in southern New England winter as a whole, on temporal and spatial average, will be colder than normal or in the extreme 0·9°F warmer than normal."

Table 18 of the aforementioned book shows that both the pre-conditions of Rule 66 were fulfilled 13 times in the period from 1873 to 1950. In all these cases the temperature of the following winter in ½ (Boston + New Haven) was below the normal value or only a few decimal points, at most 0·8°F, above the normal value.

It is thoroughly reasonable to take the average temperature of November instead of October or December for the deduction of the rule, since the rule is found in the section of the book entitled " Statistically significant rules, mainly based on tendency for persistence and repetition of circulation patterns " and moreover in the chapter of this section which deals with the atmospheric circulation over the North Atlantic in *November* in relation to the temperature of the subsequent winter in New England. Rules 65, 66 and 67 are, in a manner of speaking, merely the introduction to Rules 68 and 69, which have as their most important pre-condition the circulation over the North Atlantic. If October had been chosen for the Rule 66 it would not have been possible to speak of a tendency for persistence and of the influence of temperature anomalies in adjacent areas. Taking December would have meant, on the other hand, that one-third of the winter had been already included in the pre-conditions, so that the rule would have lost practical value. This objection may partly be raised against the second pre-condition of the rule, which involves the departure of temperature at Boston in the first half of December. This, however, means only one sixth of the winter. The contents of Rule 65 suggested the addition of this second pre-condition.

Forschungsstelle für Grosswetterkunde,
Bad Homburg,
Germany.
26 May 1960.

551.583

Synoptic and dynamic aspects of climatic change

By E. B. KRAUS

(Read 16 March 1960. Presented by Dr. E. T. Eady. See *Q.J.*, **86**, p. 1)

Mr. R. G. VERYARD : This is a very interesting paper and it certainly brings together a lot of useful information about climatic change, but, as in many papers on the subject, there are a number of assertions based on insufficient evidence and, as Dr. Kraus himself admits, there are several assumptions, some of which are very dubious.

In regard to the idea that climatic fluctuations may be related to an increased infra-red cooling rate in the upper air, particularly over the tropics, perhaps I might draw attention to a recent paper by Stranz (1959) who finds quite a high correlation between variations in solar activity and variations in the height of the tropical tropopause. This may lend some support to Kraus's suggestion.

Regarding the summary of climatic fluctuations during the last 100 years, from my own reading of the many papers on the subject, I find it very difficult to co-ordinate the results. Different workers have used different lengths of record and different reference periods. (Perhaps I should mention that this is a matter which I hope to get tidied up at the next meeting of the Climatological Commission of World Meteorological Organization). I would like to point out that such changes as have taken place are not all of the same sign. For example, Rubinshtein (1956) found reversed phases of temperature variation in Moscow and Barnaul in Siberia, and for the monsoon area, Pramanik and Jagannathan (1954) found an *increase* of rainfall in some areas and a *decrease* in others but with a tendency for deficient rainfall to be more frequent in the semi-arid zones. This latter result supports the findings of Kraus.

In regard to changes during the last glacial period with its interglacial interruptions, and the effort by Kraus to identify these changes with the changes in the last 100 years, I think it is important to get a time-scale clearly in our minds. If we equate the age of the oldest rocks – about 1,500 million years – to one year, then we would get the Quaternary period from about 1800 hr to midnight on 31 December with the last ice-free period a few minutes before midnight, and the period of instrumental meteorological observations and synoptic charts a few seconds before midnight. I cannot help feeling that it requires a lot of imagination to match climatic changes in the last 100 years or so with those in the last 10,000 or 20,000 years, especially when the dating of past climatic events may be in error by several hundreds of years. There may well be long-period fluctuations which we cannot yet identify – as Kraus himself admits when he discusses the effect of CO_2.

Regarding the contention of Kraus that a slight decrease in summer temperature might allow for the development of snowfields, this certainly appears to be true for Scotland where a change of only a few degrees is required for there to be permanent snow-beds or not. What is not clear and has yet to be determined is the dynamic effect of a large area of snow-cover on the motion of the atmosphere.

I would like to emphasize that a *mean* atmospheric circulation can be very misleading. In fact, there appear to be a whole spectrum of circulation patterns which vary in their incidence from day to day, season to season and year to year. Kraus considers that glacial periods were characterized by an intensified Hadley-type circulation in the tropics. But in a paper on related fluctuations of Trade Winds and northern climates, Bjerknes (1958) contends that the warming of the Arctic in the 1920's and 1930's can be understood only if there were an intensification of meridional eddy flux of heat in middle latitudes concurrently with an intensification of the Hadley circulation. Prof. Bjerknes produces Trade-Wind statistics to support his contention. He found a strengthening both of the north and south components.

Regarding the suggestion by Kraus that climatic fluctuations may be related to variations in the ultra-violet and to the ozone and CO_2 content, his special reference to circulation changes in the stratosphere and troposphere is of particular interest. In the Climatological Research Division of the Meteorological Office we have recently been looking at upper-air data for the tropics and have been very impressed by the changes, *especially at high levels*, not only from day to day, and from month to month, but from year to year. At the 50 mb level, i.e., in the lower stratosphere, the year-to-year variations of the monthly mean wind are quite remarkable. In one year there

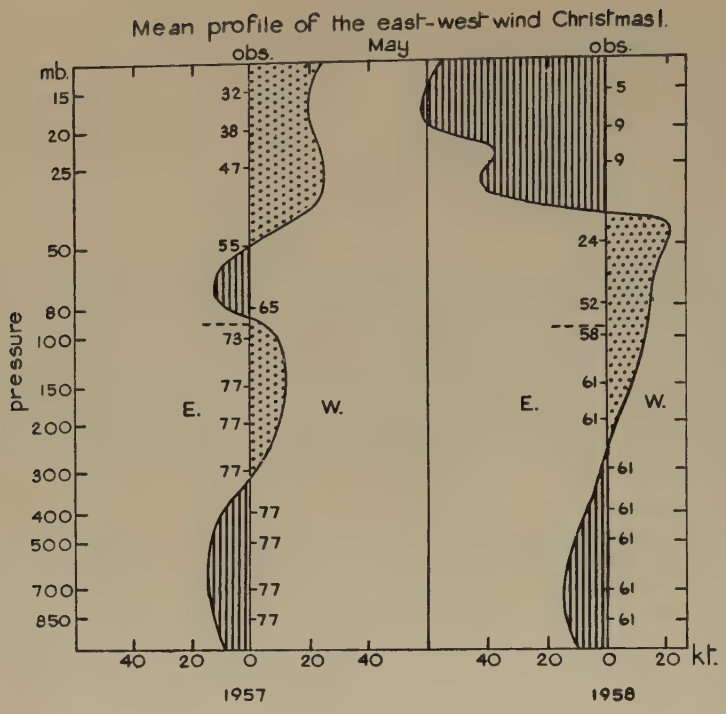

Figure 1

are westerlies, the next easterlies, and the following year westerlies – with the westerlies or easterlies showing up not only in the monthly mean but throughout the whole month. This is well illustrated by Fig. 1 for Christmas Island, 2°N, 20°W, May 1957/8. It will be seen that the text-book picture of the Berson westerlies at 50 mb with the Krakatoa easterlies reaching a maximum speed at 10 mb certainly does not hold good for every year. What we would like to know, of course, is to what extent there is a coupling between stratospheric and tropospheric circulations. Perhaps the I.G.Y. and I.G.C. data will facilitate this.

References

Stranz, D.	1959	'Solar activity and the altitude of the tropopause near the Equator,' *J. Atmos. Terr. Phys.*, **16**, Nos. 1-2.
Rubinshtein, E. S.	1956	Budyko, M. I., A. I. Voeikov, i Sovremennye Probl. Klim., Hydromet Publishing House, Leningrad, pp. 123-174.
Pramanik, S. K. and Jagannathan, P.	1954	'Climatic changes in India,' *Proc. I.A.M.*, Rome.
Bjerknes, J.	1958	'Related fluctuations of Trade Winds and northern climates,' *Geophysica*, **6**, No. 3-4.

Mr. H. H. Lamb : Dr. Kraus will certainly stimulate everybody's thinking on the subject of climatic change with this paper, as with his earlier ones on secular changes of rainfall. The real patterns of climatic change are, however, a good deal more complicated than the simple, grand design which he depicts in the paper presented today.

I suspect Kraus does less than justice to Simpson's theory, since it does in fact appear that (a) the last Interglacial was warmer than the present (cf. p. 2 of Kraus's paper) and (b) precipitation was heavy in the earlier stages of the last Ice Age. It seems quite possible that at the onset of glacial conditions world temperature was still rather higher than now, as required by Simpson, and only gradually sank, finally falling well below present levels, as the oceans became colder. However, Kraus is obviously right in emphasizing the *stronger* circulation of the glacial epochs, especially in summer : Simpson's Ice-Age summer-pressure distribution plainly needs correcting in this sense, as we see from consideration of the Southern Hemisphere today.

There seem to be three main points where Kraus's presentation may be misleading :

1. It is surely a mistake in principle to assume that all climatic changes must be attributable to the variations of any one factor. We all know that there are many things, varying all the time, which must cause climatic variations. Kraus himself is not consistently as rigid as this and I would accept that he has produced a good picture of how variations of O_3 and CO_2 (amongst other things) could operate to cause climatic changes; I support the notion that changing height of the tropopause is likely and must be important.

2. The argument which Kraus adduces to discount the influence of volcanic dust (p. 13 of his paper) is contrary to the facts. The general circulation, as demonstrated by many authors, did not decrease in vigour about the end of the last century; on the contrary its vigour increased and reached its maximum in about those years – especially in the 1920's and 1930's and some later years – when volcanic dust is reasonably supposed to have been at a minimum. The increase of circulation intensity can be seen in curves of pressure gradients in the northern and southern westerlies and in the Trades as well as in some measures of the strength of mean meridional currents, the peak intensity generally lying between 1910 and 1940. I would therefore enter a reservation in favour of volcanic dust as possibly an important agent in recent climatic fluctuations.

3. Kraus, in general, overstates the case for contemporaneity of climatic changes in many parts of the world. I think this means that he consistently underestimates the importance of terrestrial causes and terrestrial distribution patterns.

A few examples will show the need for qualification in this regard :

(a) The relatively wet period with high lake levels in south-eastern Australia beginning about 3,500 years ago is about a thousand years before the main increases of rainfall in the ' sub-Atlantic ' period given by Brooks for various parts of the Northern Hemisphere, though there do seem to have been brief foretastes of the sub-Atlantic climatic type in Europe around 2,000 and 1,300 B.C.

(b) As regards variations within the last 100 years, our empirical investigations at Harrow show there is no rule about poleward or equatorward movement of the subtropical highs (or the belt of westerlies) with increasing vigour of the circulation.

(c) These highs were at their most intense in both hemispheres during much of the first half of the present century. This did correspond to strong, well-developed westerlies and Trade Winds but coincided more or less with the time when (as Kraus has shown elsewhere) the equatorial rain belt was narrowest and the rains least.

I believe there are certain broad and simple facts to be discovered about the atmospheric circulation as a whole – for instance, the general increase of vigour since 1800-1850 – and Kraus's work is invaluable in encouraging the search for them. But great care is needed not to distort the facts by over-swift generalizations, particularly where these are suggested by some theoretical concept about the importance of any one variable.

Mr. L. C. W. Bonacina : I agree with Mr. Lamb that too much emphasis is often laid on single causes. In regard to the present paper I have always thought that Dr. C. E. P. Brooks's geographical theory and Sir George Simpson's solar radiation theory of Ice Ages are not mutually exclusive, there being room for both.

Simpson's theory is both elegant and logical; but surely he would be well advised to let the edge of the North Polar ice-cap now in latitude 75 deg. remain there in the middle of the next cold dry inter-glacial, due some 200,000 years hence, since the temperature will be the same as or slightly lower than, it is today. (See *Q.J.*, **85**, p. 334).

Brooks's theory deserves more reference than it has received in Dr. Kraus's paper. I do not think it is sufficiently realized that ice and snow possess, to an almost uncanny degree, the capacity to grow by their own cold. One sees this everywhere, both on the large and small scale.

On the large scale Antarctica and Greenland are veritable fortresses of cold capable of holding out against any amelioration of climate for a long time.

On the small scale, look at the Scottish snow-beds referred to by Mr. Veryard. My own studies of snowfall in the British Isles year by year have convinced me that ten successive summers with a sub-normal temperature of about 2 degrees F would go a long way towards restoring glaciers to our mountains. Thus the winter of 1950-51 was one of phenomenal snowfall at high-land levels and there is evidence that some of the immense drifts spilled over, so to speak, into the next autumn. Hence, under permanently colder conditions, such summer-surviving snow-belts would grow at an astonishingly rapid and accelerating rate.

Professor G. Manley : First let me congratulate Dr. Eady on his presentation of this comprehensive paper. He has indeed batted with success on what to him must be a strange wicket. I think Dr. Kraus is to be congratulated on his effort to provide us with a fresh synthesis of the results of a vast amount of recent work on a world-wide scale. Such an assemblage cannot but be both stimulating and provocative in our present state of knowledge. Mr. Veryard and Mr. Lamb have already asked several of the questions that occurred to me, so I shall merely ask whether we ought necessarily to assume that changes in the breadth of the equatorial rain belt would take place in the same sense all round the earth. After all, the fundamental feature of the Pleistocene glaciations was its asymmetrical development in the Northern Hemisphere. Would this not be likely to give rise to an equatorial rain belt of varying width ? According to the evidence of glaciation temperature fell by about 6°C in Kenya and Ecuador; but did it necessarily fall by the same amount in the Cameroons ? Unfortunately we have no mountains to tell us, and we have still a great deal of ocean to learn about from future core samples. In other words we still want more field evidence. To my mind it is not only the number, but also the wide variations in length of the several cold phases that presents a problem, coupled with their varying intensity in different parts of the world.

Dr. D. J. Schove : I am interested in the synoptic and dynamic aspects of climatic change from several viewpoints.

With regard to the recent climatic fluctuation, I have been collecting information on the differences between means for the periods 1851 to 1900 and 1901 to 1950 for each of the twelve months. The information received as a result of an appeal in the *W.M.O. Bulletin*, Geneva, Jan. 1959, p. 40, is in many cases consistent with the findings noted by Kraus in his previous papers and summarized by him on p. 2 of his paper. Thus east coast and tropical regions are often drier in the period 1901 to 1950. The pressure situation in Europe, however, shows an increased surface south-westerlies in most months but intensified monsoonal activity (with more north winds) in the summer months.

As far as the trends in general circulation are concerned, charts of pressure and wind in N.W. Europe since 1796 show, for the year as a whole, an increase in circulation similar to that found by Mr. Lamb for the month of January.

Glacials and pluvials are now regarded, on archaeological grounds, as largely synchronous in many parts of Africa. There are, nevertheless, some exceptions to this general rule, and a study of current rainfall trends would be interesting in this connection.

If we can assume that tropical rainfall regimes are always more intense and wider during periods of glaciation, it would help to resolve the chronology of the Permo-Carboniferous period. This was discussed in a recent paper on ' The climatic geography of the Permian,' (Schove, Nairn and Opdyke, *Geografiska Annaler*, Stockholm, 1958, p. 216 and correction sheet). It is tempting (although geologically unproved) to regard the wet phases of the coal measures of ' equatorial ' Europe as contemporary with glaciations of regions such as Australia, Africa and India (which then lay near the South Pole).

It would be interesting to see the conclusions of Kraus expressed in world maps, as current research will soon enable detailed comparisons to be made between the recent climatic fluctuations and the changes of the geological past.

Dr. D. M. Houghton : Dr. Kraus appears to have dismissed as unimportant in his considerations of climatic change any variations in the character of the earth's surface except those involving snow and ice. Some time ago (Houghton 1958) I showed that other and equally common changes in the condition of the earth's surface can materially alter the distribution of heat sources and sinks. For instance in low latitudes the change in albedo when green vegetation is parched, and this can occur over a very wide area, results in a loss of heat to the atmosphere comparable to the loss in high latitudes when earth becomes covered with snow. Does Dr. Kraus consider that such changes have no long-term influence on the earth's climate ?

Reference

Houghton, D. M. 1958 ' Heat sources and sinks at the earth's surface,' *Met. Mag.*, London, **87**, p. 132.

Mr. G. S. Callendar (*communicated*) : I was very interested to see that Kraus emphasized the importance of radiation heat losses from the atmosphere, because this aspect has been much neglected in the past, although it may well hold the key to the glacial periods.

There are, however, one or two points I should like to raise. For example, I think it possible that the tendency to revert to former rainfall regimes during the last decade or so, could be due to a re-establishment of equilibrium, rather than to any recession of the temperature climate. Several facts of observation support this conclusion, as follows :

(1) In the last 3 years, 1957-59 warm summers in Europe have caused increasing recession of the Alpine and Scandinavian glaciers, which, for a few years previously, had shown a tendency to slow down.

(2) In New Zealand, the very warm summers of 1954-57 and '59 have caused severe recession of the glaciers there.

(3) In Japan, the 10 years 1948-57 have been warmer than any decade since before 1880. (Even when allowance is made for ' urban increase ' at several stations).

(4) On the Canadian prairies, and adjacent plains of U.S.A. which Kraus mentions were down in 1945-51, mean temperatures for 1952-58 have been more than 1° above the 1901-30 average, and in eastern Canada to north-eastern U.S.A., as much as 2°F above.

These and other instances suggest that temperatures are still increasing in many regions. There has been, however, a tendency since 1948 for those in the sub-Arctic zone to fall to a level such that the temperature gradient between about 50 and 70°N Lat. approaches the average before the 1930's. But in the sub-Arctic zone advection rules the temperature fluctuations even more than elsewhere.

Referring to glacial recession, I cannot agree with Kraus's remark that ' this retreat was most noticeable at the beginning of the century.' It is true there was considerable retreat in North Atlantic regions around 1900, but it is since about 1930 that this has been most rapid, particularly in Europe, Iceland, New Zealand, the tropical mountains of Africa, etc.

The attached graph shows the excellent agreement between the percentage of Alpine glaciers retreating and the summer temperature at the high Alpine observatories. Correlations between sunshine or snowfall are relatively small because these elements have fluctuated in an irregular way, every few years, in this region.

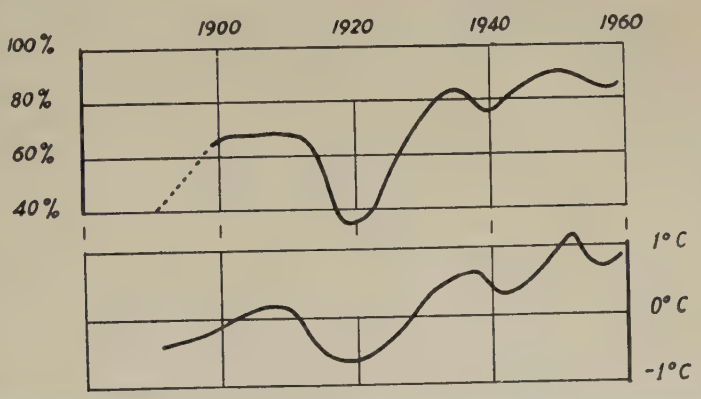

Figure 1. The lower curve gives 10 years' moving averages of deviation from the mean temperature (3·6°C) for June to August at Sonnblick (3 km), Säntis (2·5 km) and St Bernhard (2·5 km). The upper curve shows percentage of Swiss glaciers in retreat (5 years' moving averages, 60 to 80 glaciers, mean retreat 64 per cent).

Regarding the effect of CO_2, I think the chief influence of changes in its mixing ratio would be very much as Kraus suggests. That is in altering the rate of heat loss to space from the upper surface of clouds and from the warm dense layers of water vapour at low levels. The surface cooling in cold, or very dry regions would also be affected, but with surface temperatures above about 50°F there is usually enough water vapour near the ground to screen off most of the surface radiation in the wave lengths where CO_2 absorbs. Hence the most active influence of CO_2 absorption on the heat balance tends to progress to higher levels in the atmosphere as one goes from Pole to Equator.

I think Kraus's remarks about Simpson's solar theories of the glacial periods are justified. Simpson seems to have overlooked the fact that the extra latent heat, from the greatly increased precipitation his theory requires, would mean a warmer middle troposphere *in order that it could be radiated away to space sufficiently fast.* The resulting higher level for solid precipitation would make the formation of ice sheets on the northern continents even more impossible than under present conditions. I think present precipitation is perfectly adequate to form thousands of feet of ice in a few centuries provided summer melting is low enough. After all, the geologists give us thousands of years for the build up of the ice caps, so why worry about increased precipitation when a simple reduction of temperature will explain them. The great Antarctic ice cap probably has the lowest precipitation per square mile of anywhere of its size today. I fully agree with the conclusion that a moderate increase of world temperature should tend to augment the amount of ice on the Antarctic continent.

Dr. E. T. Eady (*in reply*) : I can only reply to the discussion from my own viewpoint, without committing Dr. Kraus to my views any more than I commit myself to every detail of his. Nevertheless it appears from the discussion that there are two basically different (though not incompatible) approaches to the problems of climatology. The first seeks to develop the logical consequences of certain plausible physical processes or mechanisms, as far as possible quantitatively, the aim being to discover which, if any, is compatible with ' observed ' (more usually inferred) behaviour. The second attempts to infer, as accurately and in as great detail as possible, what actually happened, the hope being that the interconnexions between phenomena will then become apparent. Though it is clear that *both* methods are essential and that no-one confines himself purely to one method, it is also clear that Kraus and I lean towards the first approach, and those Fellows who took part in the discussion lean towards the second. For this reason there was a certain amount of talk at cross purposes.

I do not deny (nor I think would Kraus) that there is insufficient evidence for some of his broad generalization nor that, as Mr. Veryard and Mr. Lamb pointed out, actual behaviour was vastly more complicated than Kraus's simple picture. Any attempt at devising a model of behaviour is bound, at the present time to be over-simplified. In fact it is precisely for this reason that models are necessary – to find out what features they do not explain so that they can be improved, the inter-relations between phenomena *not* being self-evident.

Brooks's theory of the growth of ice-sheets, referred to by Mr. Bonacina, seemed to be to me quite compatible with, or even implicit in, Kraus's model. The point would seem to be that Kraus was seeking an external *cause* which would set this process going. Simpson's theory on the other hand, was not implicit. Neither Kraus nor I regard this theory as flawless.

The point made by Dr. Houghton with regard to changes in the earth's albedo, though not implicit in the paper, is quite compatible with it, This but one aspect, like cloud amount, ocean temperatures, etc., which are important features of different climatic regions but which it is difficult to think of as *ultimate* causes. One aspect of the paper which may not be the least important is that it may help us to avoid chasing our own tails.

Dr. E. B. Kraus (*in reply, communicated*) : I shall only deal with the few points not answered completely by Dr. Eady's very clear summary of my views.

Mr. Veryard's contribution is interesting and constructive. The changes during the last 100 years are perhaps not quite as complex as he seems to suggest, considering the very similar pattern of change in regions as far apart as Eastern Australia, Eastern North America, East Africa (Nile), East Asia, and at the margin of the arid zone in India. As Veryard points out, this pattern of change is absent from the wetter parts of the monsoon areas (not only India, but also Indonesia, north-west Australia, and probably Mexico). My tentative explanation of this exception in earlier papers is not necessarily right, but the very fact of a systematic contrast between sub-tropical east-coast rainfall changes on the one hand, and the different pattern or absence of change in monsoonal or west-coast regions on the other hand, suggests an explanation in terms of the strength of the surface easterlies. The picture in high latitudes is admittedly much more confused.

I agree with Veryard's remarks about the time scale and the ' spectrum ' of atmospheric circulation patterns. We can only hope that the most frequent pattern in any period is also the one to have the greatest effect on soils, ice, vegetation and other items, on which we base our evidence. This assumption is admittedly very dubious, but prima facie, it is the most probable one to make. It is perhaps less the fact of change, than the relative stability of the climate over long periods which has to be explained.

Veryard's evidence of persistent high-level wind changes in the tropics is indeed very impressive and I am grateful that he brought this matter up.

Lamb's objection that the last interglacial was warmer than the present age is beside the point. Nobody denies this. We still live in an ice age and not in a true interglacial which appears to be characterized by an ice-free Arctic. Simpson's theory would be supported by evidence which could show that the Riss/Wurm Interglacial was considerably warmer than the Mindel/Riss Interglacial. This, I understand, is doubted by the majority of pleistocene geologists.

My view that the strengths of the sub-tropical maritime anticyclones decreased after the turn of the century, is based only on the observed decrease of east-coast rainfall from which a decrease of easterly wind velocities has been inferred. There may be other explanations though these would have to account for the observed phenomena.

Lamb states that it is surely a mistake to attribute all climatic changes to a single factor. The aim of my paper is stated explicitly in the Introduction – " I have tried to search for a physically plausible explanation, based on the minimum number of assumptions." This was qualified by my saying further that " a consistent explanation is not necessarily true." In fact, in the present case, it is more probably wrong than right, but it is surely reasonable to start with a simple model. We may learn something from proving that this model cannot account for all the observed changes – but a statement that the model must be wrong because it is too simple, is surely rather dogmatic. Of course, there are many other things that change as well, but this brings us back to the already discussed question of primary and modifying changes.

I accept Lamb's criticism on the non-coincidence of dates during the Hypsithermal.

Mr. Callendar's remarks about apparent changes during the last decade being possibly due to re-establishment of equilibrium, may well be correct. The period is much too short for any judgment about it to be on firm ground. His comments about alpine glacier retreat and similar temperatures are striking and the remarks about CO_2 and Simpson's theory are very interesting, but they do not seem to require any further comment. The same applies to Dr. Schove's statement.

Dr. Eady has already replied to queries raised by Mr. Bonacina and Dr. Houghton. His reply is also relevant to Professor Manley's remarks. I would only like to add that although vegetation changes in low latitude may well affect the radiation balance, they could only modify atmospheric conditions over the relatively small area of the margins of the continental arid zones. Three-quarters of the tropics are covered by water and the area susceptible to this type of change is only a very few per cent of the earth surface.

551.510.534

A synoptic study of day-to-day changes of ozone over the British Isles

By D. W. MARTIN and A. W. BREWER

(Read 16 March 1960. Presented by Dr. D. W. Martin. See *Q.J.*, **85**, p. 393)

Dr. R. S. Scorer : It is very dangerous to draw conclusions about the physical and dynamical processes by calculating correlation coefficients, when there are several simultaneous or special processes operating. To give an example of the kind of wrong conclusion that can be reached we might correlate the upward transfer of heat in the lower layers of the atmosphere with mean lapse rate for the day. Since the mean lapse rate is always stable it would be concluded that a stable lapse rate was required for the upward transport of heat, which is clearly untrue. In this example the error arises because the atmosphere is scarcely ever more than marginally unstable, and although such conditions exist generally for only a part of the day large amounts of heat are carried upwards. For the rest of the day the atmosphere is measurably stable and there is no transfer. The time mean of the stability is positive, and of the transfer is upwards. I am not suggesting that such an obvious error has been made in this paper, but there are processes which have been ignored or consciously omitted which may be highly correlated in a very unsymmetrical way with those which are considered, and if this were the case the correlation coefficients could be very misleading.

Dr. H. L. Penman : With the analysis complete, is the neglect of photochemical effects still considered to be a safe working assumption ?

Dr. J. M. Stagg (*President*) : Can Dr. Martin tell us what is the observational evidence for the first of the assumptions on which this work was based, namely that solar radiation makes no contribution to the day-to-day changes in total ozone ? There is considerable evidence that day-to-day variations do occur in the sun's output of short ultra-violet radiation in the region not far from the band which is responsible for the production of ozone. But perhaps these are due to different processes on the sun and do not necessarily vary together.

Mr. J. S. Sawyer : The causes of the relation between ozone changes, which are mainly above 100 mb, with the long-wave systems which are best developed around the tropopause level pose many unsolved problems for the dynamical meteorologist. Do the correlations between ozone amount and dynamical parameters show any seasonal variation ? A seasonal variation might be expected because the westerlies extend up into the ozone layers in winter but are replaced by easterlies above 100 mb in summer. A seasonal variation in the ozone relations might provide a useful clue to the dynamics.

Dr. C. D. Walshaw : I agree with Mr. Sawyer that it would be most interesting to examine the seasonal changes of the correlations, as we know from the work of Sir Charles Normand and Professor Dobson that the ozone amount and tropopause height, for example, are more closely associated in some seasons than in others.

I must confess that I am still rather uneasy about the possible influence of some types of observational error in calculations of this kind.

Mr. L. C. W. Bonacina : Are we to conclude from all that has been said that there is no definite relation of ozone production in the atmosphere to the solstices and equinoxes ? One might have thought at such high levels there would have been.

Dr. W. D. Martin (*in reply*) : This is the first study of its kind and Dr. Scorer's warning, that the techniques employed may suffer from serious inadequacies, is unexceptionable. However, as he says, it is not obvious that an analogue of his example operates in the transport of ozone.

The questions of Dr. Penman, Dr. Stagg and Mr. Bonacina concern the influence of solar ultraviolet radiation on total ozone amounts. The detailed calculations of Dütsch and Craig indicate clearly that it is extremely unlikely that photochemical action contributes to the ozone changes examined. In addition, observations on still days do not indicate a diurnal variation of total ozone, such as would be expected if solar radiation induced large ozone changes. The wavelengths which form ozone are absorbed at levels considerably above those where most of the ozone is thought to occur, so that while there are heights at which the ozone concentration is sensitive to changes of insolation, the proportion of the total ozone involved is negligible.

Insufficient data have been examined for Mr. Sawyer's question to be answered. Further studies would be valuable, and the present work suggests that the data are reliable enough to sustain them. Although the ozone data leave something to be desired, I shall be surprised if the errors to which Dr. Walshaw refers are so large as to lead to false conclusions about dynamical processes in the atmosphere.

Other discussion concerns the relative importance of meridional circulations and large-scale quasi-horizontal exchange processes in determining the annual and global distribution of ozone. In particular it is pointed out that the potential temperature of the ozone layer is higher in low latitudes (which are regarded as the source region for atmospheric ozone) than nearer the poles (which are regarded as ozone sinks). The implied radiational cooling with poleward transfer was considered to be evidence for a slow meridional circulation. Positive correlations of total ozone with northward velocity in the high stratosphere were considered merely to reflect the synoptic effects described in the paper.

551.510.53 : 551.513 : 551.557.2

The summer circulation of the arctic stratosphere below 30 km

By F. K. HARE

(Read 18 May 1960. See *Q.J.*, **86**, p. 127)

Mr. A. G. Matthewman : I am sorry Professor Hare has lost confidence in his Fig. 11. Cross-sections which I constructed through various fronts some years ago led me to the same kind of link-up between the tropopause and the boundaries of the frontal zone. Dr. Brewer's

objection that air flows across the ' tropopause-link ' shown above the warm airmass does not seem to me to vitiate the construction. Indeed Mr. Sawyer's findings on the location of frontal cloud relative to a frontal zone could be interpreted as due to a slow flux right through the frontal zone. A perfect frontal discontinuity of temperature would be impermeable but any actual frontal zone is only an idealized approximation, which should permit a slow flux of this kind.

Mr. J. MacDowall : I should like to ask if you have done any work on the difference between the antarctic and arctic atmospheres. Many of the features noted today bear a general resemblance to the behaviour of the antarctic atmosphere particularly in respect to the stratospheric circulations, but there are still some very great differences between the two Poles. In particular the spring rise in stratospheric temperatures and the total amount of atmospheric ozone over many years of arctic records has seldom or never been delayed as late as the corresponding seasonal increases in Antarctica in each of the past four years and the seasonal variation of total ozone in Antarctica differs from arctic variations at latitudes higher than 55°. It is apparent from arctic records that a significant breakdown in the winter type of cyclonic vortex in the stratosphere, with associated sudden dynamic warming effects, can occur suprisingly soon after the arctic midwinter ; this has not been observed in Antarctica where the breakdown appears to await the return of the sun. I should like to know whether your studies have revealed any factors which may lead to a better understanding of these differences.

Dr. J. M. Stagg (*President*) : Now that you have given convincing accounts of the circulation in the arctic stratosphere both in summer and winter, it would perhaps be useful to examine in some detail what happens in each of the two transitional periods separately. In addition to those sudden warmings in the lower stratosphere which you associate with temporary meridional flow during the change-over of circulation in the early spring months, is it also reasonable to infer that you would account for the spring maximum of ozone in high northern latitudes by the same kind of process ? Are there any corresponding events associated with the change back to the winter regime ?

Mr. J. S. Sawyer : In presenting your paper, Dr. Hare, you suggest that the structure which you had found in the summer stratosphere was inconsistent with theoretical calculations which indicate a continuous radiative loss of heat from the stratosphere. Can you explain a little more fully why this is so ?

Mr. L. C. W. Bonacina : Diagrams in the printed paper showing the seasonal course of temperature in the stratosphere and troposphere seem to suggest that these two parts of the continuous atmosphere are thermally independent of one another. Yet there may be a good deal of hidden connection, and I should like to ask Dr. Hare whether, for example, a proportion of long-wave radiation from the surface manages to escape absorption in the troposphere thereby raising the temperature of the stratosphere.

Dr. F. K. Hare (*in reply*) : I wish I could agree with Mr. Matthewman that the tropopause construction shown on my Fig. 11 is valid, but subsequent experience makes me pessimistic. I originally linked the tropical tropopause to the upper surface of the frontal zone because time and time again the observations suggested such a link. But of what can it consist ? The two surfaces are discontinuities of opposite sign in the thermal field; hence there must be a level near the jet-core where continuity pertains. Moreover, recent impressive results published by Danielson (1959) imply a very complex lamellar structure in the ' tropopause gap,' and in no case support the kind of link suggested by Mr. Matthewman : hence I am compelled to reject his defence of my own construction !

Mr. MacDowall raises a question of fundamental importance. In addition to the differences he mentions between the two hemispheres, there is the vital question as to whether baroclinic instability exists in the antarctic polar-night circulation. Undoubtedly it does exist in the Northern Hemisphere, and it can be argued (as I am about to do elsewhere in print) that the five-fold increase in kinetic energy displayed by the arctic winter vortex is due to typical baroclinic processes. Yet it has not been convincingly demonstrated that such processes are at work in the Antarctic, in which case the high intensity of the southern vortex is a dynamical puzzle. I am of the opinion (as yet with only flimsy support) that the premature sudden warmings of the northern vortex are due to a form of dynamical instability not yet defined by baroclinic theory, involving wholesale energy conversions from kinetic to potential form. It looks as if the southern vortex may ordinarily lack this form of instability, but I cannot yet suggest any good reason why.

Elsewhere my colleagues and I (1960a, 1960b) have suggested a link between the middle stratospheric circulation and total ozone content in a vertical column. These results, when published, will answer Dr. Stagg's question. In brief, we find that high ozone amounts occur when the middle stratosphere (i.e., 20 to 30 km) is dynamically warmed by subsidence. This happens

in the ridges of the winter baroclinic waves, and during the sudden warming episodes. We attribute both the sub-polar and the spring ozone maxima to the operation of these dynamical processes (which are complicated in more southerly latitudes by the well-known Normand effect due to the wave disturbances of the tropospheric westerlies). Very similar ideas have been elaborated by Godson (1960). In autumn, the polar stratospheric vortex is gradually re-established as an undisturbed barotropic system, in which ozone variation is very small.

In reply to Mr. Sawyer, I should like to disclaim any very profound significance to my remarks about the problem of radiative equilibrium. However, the situation does seem reasonably clear. The easterlies are almost devoid of disturbances, so that a lateral eddy transport of enthalpy cannot be invoked. Available computations of radiative flux divergence imply cooling rates of about 1°C day^{-1} in summer below 30 km. Yet temperatures remain steady for almost three months at about − 40°C. If we accept the estimate of a net radiative *cooling*, and discount eddy enthalpy transport, only a steady meridional circulation can account for the stability of temperature. It seems more likely, however, that radiative equilibrium exists, in which case the problem vanishes. It also seems very probable that the uniform cooling of about 0·3°C day^{-1} typical of September is a wholly radiative effect.

Mr. Bonacina's question is difficult to answer in specific terms. It is hard to believe, however, that infra-red from the surface exerts any very profound influence in the winter stratosphere : otherwise the warm stratosphere over the Gulf of Alaska ought to be matched by another warm ridge over the Norwegian Sea, where the winter stratosphere is very cold. In summer the thermal field is conspicuously free from longitudinal irregularities of the sort such an effect would require.

References

Allington, K., Boville, B. W. and Hare, F. K.	1960a	*Tellus*, **12**, 4.
Boville, B. W. and Hare, F. K.	1960b	Paper read before Canadian Branch, R. Met. Soc. (to be published).
Godson, W. L.	1960	*Quart. J. R. Met. Soc.*, **86**, p. 301.
Danielsen, R. F.	1959	*Arch. für Met., Geoph. und Bioklimat.*, Series A, **11**, 3, pp. 293.

551.551 : 551.501.45

An experimental system for directly recording statistics of the intensity of atmospheric turbulence

By J. I. P. JONES and F. PASQUILL

(Read 18 May 1960. Presented by Dr. F. Pasquill. See *Q.J.*, **85**, p. 225)

Professor P. A. Sheppard : The theory of diffusion which leads to the need for the technique described in this paper provides, I believe, a tremendous step forward in the problem of diffusion, the biggest step forward in more than a generation.

The problem of horizontal diffusion having reduced itself to a knowledge of the appropriately weighted variance of wind direction, we can now look on the latter as the entity to be described and Dr. Pasquill has shown us a technique for obtaining the description. We can also expect that the recently developed and developing description and theory of turbulence in terms of power spectra and stability parameters will provide a second entry to the new form in which the diffusion problem has been posed. Presumably a roughness parameter and a stability parameter should be sufficient to prescribe the required variance. What does Dr. Pasquill think about the corresponding problem in vertical diffusion in relation to the variance in inclination of the wind ?

Dr. F. Pasquill (*in reply*) : For many purposes I agree entirely with Professor Sheppard's suggestion that a roughness parameter and a stability parameter should be sufficient to prescribe the required wind variance. The technique described in our paper was indeed developed partly with the aim of acquiring, without prohibitive labour, the statistics which are necessary to establish

the relation between the wind variance and these parameters. As regards the corresponding problem in the vertical plane, the same treatment of diffusion is acceptable in so far as the diffusion is occurring in a region in which the systematic variation of turbulence with height may be neglected. This may be expected to be the case for at least some distance downwind of an elevated source, and certain unpublished data already suggest that a useful estimate of the distance at which the ground-level concentration is a maximum may even be made on this basis.

551.521.14

The reflection of short-wave radiation by vegetation

By. J. L. MONTEITH

(Read 18 May 1960. See *Q.J.*, **85**, p. 386)

Dr. F. K. HARE : In view of the dependence of reflectivity on the geometry of the vegetation, as seen in projection, to what extent does the height of observation above the vegetation surface affect measured values ?

Mr. J. S. SAWYER : I was interested in Dr. Monteith's results as giving an indication of the variations in the heat available to drive the general circulation of the atmosphere arising from changes in the albedo of the earth's surface. Am I right in deducing that variations of the heat input to the atmosphere of a few per cent between the same season in different years might arise from difference in the state of the vegetation over wide areas ?

Dr. J. L. MONTEITH (*in reply*) : For most of the measurements we were able to keep at least two plant heights above the ground where there was no change in reflection with increasing height. Rather to our surprise, we found that the reflection from grass growing to a height of 85 cm was virtually constant down to 60 cm above the ground. Apparently the top 26 cm, where there were few leaves, made no significant contribution to reflection.

On a climatological scale, differences in surface reflection will certainly alter the heat input to the atmosphere and I believe D. M. Houghton has studied the relative importance of such effects (*Air Ministry Met. Res. Cttee.*, M.R.P. No. 1005). The greatest difference is when dry soil is replaced by transpiring vegetation and vice versa. If the reflection coefficient for the soil exceeds that of the vegetation – a desert soil may have a reflectivity of 0·3 – reflected radiation and long-wave emission will increase or decrease together and there may be a large change both in net radiation and in total (sensible and latent) heat transfer from surface to atmosphere. But if the reflection coefficient of soil is less than for vegetation – and this will generally be true for agricultural soils – changes in reflection and in long-wave emission will have opposite sign and there may be little change in net radiation.

For a given surface, reflection coefficient may vary with season through its dependence on solar elevation, but for all the measurements reported here, elevation exceeded 40° and no attempt has been made to calculate how the mean daily reflection coefficient might change during the year.

L. F. RICHARDSON PRIZE

The Council of the Royal Meteorological Society has decided to institute a new award to be known as the L. F. Richardson Prize for the encouragement of research by young meteorologists. The prize will consist of £25 together with a book and will be awarded for meritorious papers contributed to the *Quarterly Journal* by Members who were under the age of 28 at the time the papers were submitted for publication. It is intended that the award shall be made annually, provided that a paper of sufficient merit has been received.

Proceedings at meetings of the Society

Special General Meeting, 15 June 1960

A Special General Meeting of Fellows was held to elect the Officers and Council for the year 1960-61.

Fellows had been circulated on 19 April with the list of nominations by Council for Officers and Council for the year 1960-61. No other nominations having since been received, the persons so nominated were declared to be elected unopposed in accordance with By-law 51.

The Officers and Council for 1960-61 were therefore elected as follows :

President

James Martin Stagg, C.B., O.B.E., M.A., D.Sc.

Vice-Presidents

Arthur George Forsdyke, A.R.C.S., Ph.D.
Richard Mead Goody, M.A., Ph.D.
George David Robinson, Ph.D., F.Inst.P.
Percival Albert Sheppard, Hon. A.R.C.S., B.Sc., F.Inst.P.

Vice-President for Canada

Warren Lehman Godson, Ph.D.

Vice-President for Scotland

Robert Cranna, M.A., B.Sc.

Treasurer

Brian Cecil Vernon Oddie, B.Sc.

Secretaries

George Arthur Bull, B.Sc., M.I. Inf.Sc. (Librarian)
Patrick John Meade, O.B.E., B.Sc., A.R.C.S.
John Stanley Sawyer, M.A. (Editor)
Richard Segar Scorer, M.A., Ph.D.

Councillors

John Alan Chalmers, M.A., Ph.D., F.Inst.P.
George Arthur Corby, B.Sc.
John Robert Dark Francis, B.Sc (Eng.), A.I.C.E.
Arthur Leonard Maidens, B.Sc.
John Lennox Monteith, Ph.D.
Paul Robert Owen, B.Sc., A.F.R.Ae.S.
Reginald Charles Rainey, Ph.D.
John Brodrick Rigg, M.A.
John Russell Thorp, O.B.E., M.A.
Gilbert Brian Tucker, Ph.D.
Charles Desmond Walshaw, M.A., Ph.D.
Henry Lionel Wright, M.A.

Ordinary Meeting, 15 June 1960

The following candidates were declared to have been elected that day by the Council :

Fellows

Adefemi, Samuel Ajai, A.M.I.Tech.G.B., Meteorological Services, Headquarters, Lagos, Nigeria, W. Africa.

Besley, Bryan Philip, 95 The Avenue, Sunbury-on-Thames, Middx. (*reinstatement*; resigned 1959).

Wood-Jones, Raymond Bernard, Ph.D., M.A., B.Arch., A.R.I.B.A., 15 Orrishmere Road, Cheadle, Cheshire.

Student Members

Rossington, Lionel George, 122 Ashurst Road, North Finchley, London, N.12.

Strang, David Don, 6 Will Street, Abbotsford, S.W.2, New Zealand.

Canadian Branch

Fellows

Gibson, Timothy Travers, B.Sc., M.A., c/o Department of Transport, Goose Bay, Labrador, Newfoundland.

Lawrynuik, Walter Donald, B.Sc., M.A., c/o Department of Transport, Goose Bay, Labrador, Newfoundland.

The following papers were read and discussed :

1. ' The fragmentation and electrification of freezing water drops ' by B. J. Mason and J. Maybank (*Q.J.*, **86**, p. 176).
2. ' Observations of precipitation elements in cumulus clouds ' by R. J. Murgatroyd and M. P. Garrod (*Q.J.*, **86**, p. 167).
3. ' Aircraft observations of rain and drizzle from layer clouds ' by F. Singleton (*Q.J.*, **86**, p. 195).

Summer Meeting, Dundee, 29 June-1 July 1960

The seventh two-day Summer Meeting of the Society was held at Queen's College, Dundee, University of St. Andrews, by kind permission of the Master, Professor A. M. Matheson, Q.C., M.A., LL.B., and the College Council.

The meeting was formally opened on the evening of 29 June at a reception at West Park Hall given by Professor Matheson and Mrs. Matheson accompanied by Miss Rhona Morrison, the Warden of the Hall. At the reception Professor Matheson made a short speech of welcome to the visiting Members of the Society to Dundee and Dr. J. M. Stagg, President of the Society, replied.

Dr. Stagg took the Chair at the first symposium on ' Convection.' Speakers included Dr. F. H. Ludlam on ' Convection in the atmosphere,' and Mr. C. Dixon on ' The initiation of convection in water.' After a discussion of these papers Mr. F. W. G. Warren read his paper on ' Gravity waves initiated by penetrative convection,' and Dr. R. P. Pearce presented his paper on ' Convection and frontogenesis,' and both papers were concluded with a discussion.

Mr. R. Cranna, Chairman of the Scottish Centre, took the Chair at the second day's symposium on ' Agricultural meteorology.' Papers were read by Dr. H. L. Penman on ' Weather in wheat ' and Dr. J. L. Monteith on ' The flux of CO_2 over a field of sugar beet.' After a discussion Mr. G. J. Day read a paper on ' Radiation climatology ' followed by Mr. R. W. Gloyne on ' Windbreaks – some physical effects.' The session concluded with a discussion of these papers.

Two enjoyable visits were made on Thursday afternoon, to the Freshwater Fisheries Laboratory of the Scottish Home Department and to the Central Control Hydro-electric Station of the North of Scotland Hydro-electric Board at Pitlochry.

On Friday afternoon a lunch was given in the City Chambers by the Lord Provost and the City Fathers, at which the Lord Provost made a speech welcoming the delegates of the Society to Dundee. Dr. Stagg replied expressing the thanks of the Society for the hospitality of the City. After lunch, visits were made to the Tidal Model of the Dundee Harbour Trust and to the Scottish Horticultural Research Institute, Mylnefield.

Council wishes to record its sincere thanks to Mr. G. A. Corby who acted as co-ordinator, and to Dr. R. P. Pearce and his colleagues on the local committee, whose efforts assured the success of the meeting.

An additional account of the meeting appeared in the October issue of *Weather*.

Summer Visit, 20 July 1960

The Summer Visit of the Society was held on 20 July 1960 at the Lasham Gliding Centre, near Alton, Hampshire, by kind invitation of the Lasham Gliding Society.

As a result of indifferent weather only about two dozen members attended. After Colonel H. V. S. Muller had given a few introductory remarks, the party was conducted round the hangars and workshops and introduced to the main types of sailplane.

Although the previously arranged demonstration of aerobatics was cancelled because of weather conditions, about a dozen members of the party were able to go for short flights round the airfield whilst others visited the launching site where the proceedings were explained by Colonel Muller and Dr. James.

A very pleasant informal tea was provided for the party in the Gliding Society's premises.

At the conclusion of the visit Inst. Cdr. J. R. Thorp expressed appreciation to Colonel Muller for a most enjoyable afternoon.

A full account of the visit will appear in the November issue of *Weather*.

Reviews

Dynamics of climate. Ed. by R. L. Pfeffer. London (Pergamon Press). 1960. Pp. xv, 137; Figs.; Tables. 35s.

This unusual volume is, in spite of its title, about the general circulation. It comprises an edited account of the proceedings at a conference on the application of numerical techniques to the general circulation problem. The conference, held in October 1955, was sponsored jointly by the Institute for Advanced Study, Princeton, and the Geophysics Research Directorate, Air Force Cambridge Research Center. The participants included well-known authorities in this field, from a dozen or more U.S. research establishments.

The formal contributions are presented in three sections. The first covers the numerical integration of models devised specifically for general circulation studies and includes stimulating contributions from Von Neumann, Charney, Smagorinsky and others, and also an account of Phillip's experiment. Another section deals with other studies, e.g., of energy considerations and the effects of heating and rotation. A third section reports some radiation work by Kaplan and King from which it is clear that the inclusion of radiative transfer processes in numerical models is likely to be an extremely difficult task. Finally the discussion is admirably summarised in an edited account, reconstructed from notes and tape recordings.

Publications recording verbatim the proceedings of major conferences and symposia, although of some value to a few specialists, have become something of an embarrassment in the literature, their object being largely defeated by the often considerable length, and the difficulty the non-specialised reader has in gaining a useful impression of the significance of the conference as a whole. The present volume is a very welcome change and succeeds because a great deal of effort has been applied to the editing of the proceedings in order to achieve a coherent account. It is unfortunate that in the achievement of this polished account there should have been a delay in its publication of over four years. However, progress in the field of numerical prediction and the general circulation is not so rapid that the book is badly dated and workers in this field will find much to interest and stimulate them.

G.A.C.

Sonnenstrahlung und Lufttrübung. By L. Foitzik and H. Hinzpeter. Leipzig (Akademische Verlag, Geest and Portig), 1958. Pp. ix. 309; 117 Figures; 66 Tables; 8 Folding charts. 43 D.M.

Here we have a sizeable book reviewing the transmission of solar radiation through the earth's atmosphere. The term ' Lufttrübung ' in the title corresponds to the similarly somewhat vague term ' turbidity ' in English meteorological literature, and solar radiation here is considered from both the point of view of its importance energetically and as a ' probe ' in the analysis of the composition of the atmosphere. The discussion of solar radiation has, however, been limited to a consideration of the direct, i.e., unscattered, solar radiation.

Theory, instrumental methods, and observational results are all presented, together with numerous references to work not discussed in detail. The size and limited scope of the book allow much more detailed discussions than have been possible with most reviews dealing with solar radiation in general, but the treatment still lacks the thoroughness and critical approach needed to single the book out as the standard text or reference work. Considerable pruning, however, could have been carried out in a number of the sections without any significant loss for the majority of readers and the space could have been used to provide a more balanced and valuable review. There is a need, for example, for a fuller treatment of the basic physics of the absorption mechanisms, and the theory given of molecular scattering certainly needs amplifying at least, and a different approach, emphasizing the physics of the problem, would be desirable for the newcomer to the subject. Further to these somewhat disappointing features the general plan of the work has scattered material best considered together. This, however, was probably unavoidable owing to the joint-authorship of the work.

Despite these criticisms the book would be quite useful to the newcomer to the field in supplementing the briefer general reviews and providing a valuable source of references to the original papers. In particular, the authoritative sections on standard pyrheliometric techniques and observations would be especially valuable to those commencing such techniques or attempting to make use of the available data.

D.B.L.

Weathercraft. By L. P. Smith. London (Blandford Press), 1960. Pp. 87; 63 Figures; 13 Photographs; Tables. 9s. 6d.

A first reaction to this carefully designed book is surprise that there have been so few, if any, similar attempts before; for, as presented by Mr. Smith, the subject seems admirably suited to introduce to the secondary-modern pupil some ideas of how to investigate.

The core of the book contains 28 experiments (some are graphical exercises or record analyses rather than experiments proper), in which emphasis is placed upon the variation in time and space of the familiar elements of climate (atmospheric humidity a notable absentee), and including a consideration of water movement in the soil – certainly a novel feature in a book at this level. The final section ' Weather in harness ' deals with the glasshouse and irrigation.

Throughout there is implicit insistence upon the need for statistical ' control,' and the resourceful teacher might well develop useful ideas on experimental layout and sampling methods from the experiments on soil and ground temperature variations.

The inherent difficulties of the subject do break out, and in particular I have doubts as to whether the concept of radiative exchange will mean much to the pupil without extensive preparation by the teacher via the more familiar ideas of (perhaps) radio : one example would be the difficulty of reconciling the insistence on screening thermometers (in chapter 1) and the extensive use of exposed spirit instruments (in chapter 10).

A detailed argument on matters of terminology and modes of expression is out of place but two misprints have been noted (viz., p. 10 for ' glass ' read ' grass '; p. 72, Fig. 63. The caption should surely read ' . . . . occasions on or *before* a given date,' not ' . . . . *after* . . . . ').

I doubt if some of the results will be as unambiguous as suggested – but this is not necessarily a disadvantage when introducing pupils to the realities of scientific investigation – and emphasizes that the book seems first and foremost a teacher's handbook rather than a more or less unaided class-text : certainly no one charged with the task of introducing natural science to the non-academic pupil can afford not to examine this book.

R.W.G.

Alfred Wegener. By Else Wegener. Wiesbaden (Brockhaus), 1960. Pp. 262 : 4 Sketch maps, 28 Pictures. 16.50 DM.

This is a charming and intimate biography, by his widow, of a very human man, a meteorologist and earth scientist of broad vision, whose consuming energy was directed by intense, boyish enthusiasms. An early love was for balloon flights, which Wegener began under Professor Berson at Lindenberg in the early years of the century and which ultimately involved his fiancée – the accounts of these exploits make good reading. But Wegener's greatest enthusiasm was for polar exploration, and this he first achieved by volunteering in 1906 at the age of 26 to join a Danish expedition to Greenland as meteorologist with the particular aim of obtaining upper-air observations by kite and balloon.

Much of the book is devoted to the logs of Wegener's Greenland journeys, including the last one on which he lost his life in 1930, to the correspondence which preceded them and the endless struggle to get the results written up and published.

It was in seeking support and equipment for the 1906 expedition that Wegener first met Köppen, who was then in charge of the upper-air station at Hamburg (where Wegener much later succeeded him) and whose daughter he married after some years of hoping and striving to secure a post which would bring in a steady income. It was not until 1924 that security was achieved in the long-desired form, that of a university professorship – actually at Graz in Austria. Long before this stage in his career Wegener was so heavily engaged in writing and lecturing commitments that polar expeditions came to be a necessary escape for nervous recuperation. He was, however, capable of refusing a chance to partake in an early airship expedition across the Pole because it would contribute much less to scientific knowledge than another expedition on the ground such as he proceeded to promote and organize.

All this is typical of the man and his devotion to the pursuit of knowledge. The descendant of a family of Lutheran pastors in Brandenburg and Silesia, Wegener was no nationalist. His friends were those of like mind anywhere in the world. It is interesting to trace the reactions of such a man to the facts and fictions of war and military training.

His continental-drift theory, which made him famous, was first conceived in 1911 when idly examining the pages of a new world-atlas. It was followed up over the years with his usual combination of scientific insight and restless persuasive zeal, through a long series of papers, lectures and journeys. The theory never won universal support, but is today perhaps more widely accepted than ever before on account of the new evidence of palaeomagnetism.

This book is of less interest for its scientific content than it will be to those who are similarly dominated by some single-minded purpose in scientific research and who encounter the same struggle for opportunities. Here is detailed experience of the necessary parts played by individual initiative, by personal support and criticism, by universities and state institutions and by funds such as those of the national academies of science. Also included are the place of the cigar, the Institute teas, the mountain holiday and the helping wife.

How much does science owe to the irrational intuitions and personal enthusiasms of its leading men ? The President of the Royal Society said in the recent Tercentenary Address : ' the full fruition of scientific work depends on three things : the desire to know, the initiative to find out and the awareness to apply.' Alfred Wegener possessed all three abundantly.

H.H.L.

Turbulent flows and heat transfer. Ed. by C. C. Lin, Oxford (University Press), 1960 (and Princeton University Press, 1959), pp. 549.

This is Vol. 5 of a series of twelve volumes on *High-speed aerodynamics and jet propulsion* which are being prepared under the guidance of a board whose chairman is T. von Kármán, who also provided the original initiative which got the series under way. Such a big undertaking has only been possible through

the generous support of the U.S. Defence Services. It involves about a hundred authors altogether, work by twelve of whom appears in this volume. The well-known *Modern developments in fluid mechanics* has obviously been taken as the model, and a generally high standard has been attained.

Meteorologists, however, are only indirectly concerned with most of the subject matter, because it is mainly of engineering interest, and the title of the series as well as of this volume must be continually borne in mind. There is nothing about hot plumes and buoyant convection because gravitational effects are not considered. The Richardson number does not appear anywhere in the whole book. Many of the difficulties connected with turbulence as found in the atmosphere, such as the problem of defining mean values, are not mentioned, which means that the sections dealing with the more fundamental aspects of fluid flow are unsatisfactory, philosophically at least, because the authors seem curiously blind to many interesting questions. The section dealing with jets is excellent and stimulating in many respects but ignores not only buoyancy but also the phenomenon of recirculation and other effects of rigid boundaries. This would not matter if there were no pretence to be comprehensive; but the references are so copious that these things deserve mention by comparison with much that is discussed.

The first section which is on ' Transition from laminar to turbulent flow,' makes reference to numerous papers (about two per page), mostly reporting experimental work on the Reynolds numbers at which various transitions are said to occur, but leaves one in a most uncertain state at the end about the mechanism. Evidently the author has not felt that in the present state (or ' status ' as this book is pleased to call it) of the subject, a more fundamental treatment is warranted, and one may therefore ask whether less space – it occupies 72 pages – should have been given to it.

The second section, entitled ' Turbulent flow,' occupies 120 pages containing much valuable material, but again betrays the engineer's unphilosophical instincts. For example, the transports along jets and wakes due to correlations between fluctuating quantities (even of the velocity fluctuation with itself !) are ignored. But this does not affect the answers obtained because the integrals from which the terms are omitted are only subjected to dimensional analysis, which fact, however, is obscured by the unnecessary assumption that a power law is obeyed. The reader is not made aware when one must assume similarity or when it must necessarily exist, and it seems that the author is content with any correct argument so long as it gives a correct answer. But if we are to understand the subject properly we need a more thorough discussion of assumptions, their sufficiency, their reasonableness, and their necessity, than we find here.

The third section, ' Statistical theories of turbulence ' is a good 58 pages. Again it leans very heavily, as it must, on its 100 references, but is much more theoretical and complete in itself and therefore of more value to meteorologists and others outside the special field of the series. The other sections, namely, ' Conduction of heat,' ' Convective heat transfer and friction in flow of liquids,' ' Convective heat transfer in gases,' ' Cooling by protective fluid films,' and ' Physical basis of thermal radiation,' have a mainly rocket-engineering interest. It is a pity that parts of this series which are the more fundamental, such as the first three sections of this book, cannot be available in slimmer, cheaper volumes to non-engineers, and perhaps the more technologically based sections would equally be welcomed separately by others.

Having a series of this kind has obviously got the subject surveyed pretty well, and efficient editing has avoided overlapping and produced interleaving which is very good in these days of so many books. But one does miss the excitement evident in an original and spontaneous work ; the authors are too uncommitted, drudging a little, escaping issues by making references. It would be interesting to see if the standard of authorship, which must certainly be acknowledged as high, could be raised by forbidding references in the text and providing instead a selected bibliography, with brief notes.

R.S.S.

Index

See following supplementary index for newly-elected Members

(Titles of books reviewed or otherwise noticed are printed in italics)

Accuracy of determination of the vertical distribution of atmospheric ozone from emission spectrophotometry in the 1043 cm^{-1} band at high resolution, The, 519

Adamson (J.), The compensation of the effects of potential gradient variations in the measurement of the atmospheric air-earth current, 252

Adkins (C. J.), Fragmentation and electrification of very small droplets, 186

Aircraft observations of rain and drizzle from layer clouds, 195

Alberta, Patterns of hailstorms in, 281

Andrews (J. B.) and B. J. Mason, Drop-size distributions from various types of rain, 346

Antarctic atmosphere, Seasonal and other temperature changes in the, 283

Arctic and sub-arctic areas in winter and spring, Total ozone and the middle stratosphere over, 301

Arctic stratosphere below 30 km, The summer circulation of the, 127, 576

Atlas (D.), W. G. Harper, F. H. Ludlam and W. C. Macklin, Radar scatter by large hail, 468

Atmospheric air-earth current, The compensation of the effects of potential gradient variations in the measurement of the, 252

Atmospheric electricity and their cause, Some recent changes in, 399

Atmospheric extinction of infra-red radiation, 371

Atmospheric inhomogeneities, Radar echoes from, 116

Ball (F. K.), A theory of fronts in relation to surface stress, 51

————, Control of inversion height by surface heating, 483

Barclay (F. R.), M. J. W. Elliot, P. Goldsmith and J. V. Jelley, A direct measurement of the humidity in the stratosphere using a cooled-vapour trap, 259

Baroclinic stability, A problem in, 237

Barry (R. G.), A note on the synoptic climatology of Laborador-Ungava, 557

Baur (F.), *Dir sommerniederschlage Mitteleuropas in den letzen 1½ Jahrhunderten and ihre Beziehungen zum Sonnenfleckenzyklus*, 432, 567

————, Physical-statistical rules as bases for forecasts of weather and weather-character, 567

Bearing and incidence of rainfall, A method of obtaining average, 408

Beechey (J. C.), Obituary, 293

Berg (H.), *Solar-Terrestrische Beziehungen in Meteorologie und Biologie*, 123.

Blackadar (A. K.), G. E. McVehil and H. A. Panofsky, The diabatic wind profile, 390

Brewer (A. W.) and D. W. Martin, A synoptic study of day-to-day changes of ozone over the British Isles, 575

Bryant (G. W.) and B. J. Mason, Photolytic de-activation of silver iodide as an ice-forming nucleus, 354 (Pl. III)

Byers (H. R.), *General meteorology*, 123

Campbell-Stokes sunshine recorder as an integrating actinometer, The use of the, 270

Canadian stations from *umkehr* observations, The vertical distribution of atmospheric ozone over, 512

Carbon-dioxide flux over a field of sugar beet, The, 205

Chalmers (J. A.) and M. W. Ramsay, Measurements on the electricity of precipitation, 530

Chalmers (J. A.) and J. E. Maund, Point-discharge currents from natural and artificial points, 85

Chalmers (J. A.) and M. Smiddy, Measurements of space charge in the lower atmosphere using double field mills, 79

Circulation of the arctic stratosphere below 30 km, The summer, 127

Circulation of the atmosphere, Interhemispherical features of the general, 156

Circulations in the atmosphere, Mean meridional, 277

Clay minerals and stony meteorities, Ice-nucleating properties of, 552

Climatic change, Synoptic and dynamic aspects of, 1, 569

Compensation of the effects of potential gradient variations in the measurement of the atmospheric air-earth current, The, 252

Computations of the variation of vertical velocity with pressure on a synoptic scale, Some, 318

Control of inversion height by surface heating, 483

Control of kinetic energy of the atmosphere by external heat sources and surface friction, On the, 437

Cumulonimbus clouds, Size-distribution of ice crystals in, 187

Cumulus clouds, Observations of precipitation elements in, 167

Deirmendjian (D.), Atmospheric extinction of infra-red radiation, 371

Determinant hypothesis for the superadiabatic wind and temperature, A, 232

Diabatic wind profile, The, 390

Direct measurement of the humidity in the stratosphere using a cooled-vapour trap, A, 259

Diurnal temperature variation during the polar night, The, 104

Douglas (R. H.) and W. Hitschfeld, Patterns of hailstorms in Alberta, 281

Drizzle from layer clouds, Aircraft observations of rain and, 195

Drop-size distributions from various types of rain, 346

Drop-size distributions in low layer clouds, Some observations of, 454

Duration of sunshine in Trinidad, West Indies, Solar radiation and the, 415

Durst (C. S.), The statistical variation of wind with distance, 543

Dynamic aspects of climatic change, Synoptic and, 1, 569
Ebdon (R. A.), Notes on the wind flow at 50 mb in tropical and sub-tropical regions in January 1957 and January 1958, 540
Eckel (O.), F. Sauberer and F. Steinhauser, *Klima und Bioklima von Wien*, Teil III, 123
Edwards (Pamela), Differing water budgets in two adjacent reservoirs, 412
Electrification of freezing water drops, The fragmentation and, (Pl. I), 176
Fragmentation and electrification of very small droplets, 186
Electricity of precipitation, Measurements of the, 530
Elliot (M. J. W.), P. Goldsmith, J. V. Jelley and F. R. Barclay, A direct measurement of the humidity in the stratosphere using a cooled-vapour trap, 259
Elliott (S. S.), Obituary, 294
Emission spectrophotometry in the 1043 cm^{-1} band at high resolution, The accuracy of determination of the vertical distribution of atmospheric ozone from, 519
Exchange of heat, moisture and momentum between *Hurricane Ella* (1958) and its environments 276
Experiments in numerical prediction using a stream function, A report on some, 504
Farbrother (H. G.) and C. W. Rose, A method of obtaining average bearing and incidence of rainfall, 408
Field mills, Measurements of space charge in the lower atmosphere using double, 79
Fjørtoft (R.), On the control of kinetic energy of the atmosphere by external heat sources and surface friction, 437
Fluxes and gradients in the lower atmosphere, Similarity theory in the relation between, 67
Foitzik (L.) and H. Hinzpeter, *Sonnenstrahlung und Lufttrübung*, 583
Forecasts of weather and weather-character, Physical-statistical rules as bases for, 567
Fournier D'Albe (E. M.) and I. G. Galindo Estrada, The use of the Campbell-Stokes sunshine recorder as an integrating actinometer, 270
Fragmentation and electrification of freezing water drops (Pl. I), 176
Fronts in relation to surface stress, A theory of, 51
Funk (J. P.), Measured radiative flux divergence near the ground at night, (Pl. IV), 382
Galindo Estrada (I. G.) and E. M. Fournier D'Albe, The use of the Campbell-Stokes sunshine recorder as an integrating actinometer, 270
Gangopadhyaya (M.) and H. Riehl, Exchange of heat, moisture and momentum between *Hurricane Ella* (1958) and its environment, 276
Garrod (M. P.) and R. J. Murgatroyd, Observations of precipitation elements in cumulus clouds, 167
Godson (W. L.), Total ozone and the middle stratosphere over arctic and sub-arctic areas in winter and spring, 301
Godson (W. L.) and C. L. Mateer, The vertical distribution of atmospheric ozone over Canadian stations from *umkehr* observations, 512
Goldsmith (P.), J. V. Jelley, F. R. Barclay and M. J. W. Elliot, A direct measurement of the humidity in the stratosphere using a cooled-vapour trap, 259
Gradients in the lower atmosphere, Similarity theory in the relation between fluxes and, 67
Green (J. S. A.), A problem in baroclinic stability, 237
Grid length to be adopted in numerical weather prediction, On the, 265
Gunn-Bellani radiation integrator, The performance of a, 91
Hailstorms in Alberta, Patterns of, 281
Hail, Radar scatter by large, 468
Hare (F. K.), The summer circulation of the arctic stratosphere below 30 km, 127, 576
Harper (W. G.), F. H. Ludlam, W. C. Macklin and D. Atlas, Radar scatter by large hail, 468
Heat, moisture and momentum between Hurricane Ella (1958) and its environment, Exchange of, 276
Heat sources and surface friction, On the control of kinetic energy of the atmosphere by external, 437
Heninger (S. K. Jr.), *Handbook of Renaissance Meteorology*, 433
Hinds (M. K.) and E. Knighting, A report on some experiments in numerical prediction using a stream function, 504
Hinzpeter (H.) and L. Foitzik, *Sonnenstrahlung und Lufttrübung*, 583
Hisdal (V.), The diurnal temperature variation during the polar night, 104
Hitschfeld (W.) and R. H. Douglas, Patterns of hailstorms in Alberta, 281
H.M.S.O., *Annual Report on the Meteorological Office for the year ending 31 March 1959*, (M.O. 659), 431
Houghton (J. T.) and J. S. Seeley, Spectroscopic observations of the water-vapour content of the stratosphere, 358
House (G. J.), N. E. Rider and C. P. Tugwell, A surface energy-balance computer (Pl. II), 215
Humidities near stratocumulus clouds. Observations from aircraft of temperatures and, 114
Humidity in the stratosphere using a cooled-vapour trap, A direct measurement of the, 259
Hurricane Ella (1958) and its environment, Exchange of heat, moisture and momentum between, 276
Huschke (R. E.) (Ed.), *Glossary of meteorology*, 431
Hutchinson (W. C. A.), Ice-crystal contact electrification, 406
Ice-crystal contact electrification, 406
Ice crystals in cumulonimbus clouds, Size-distribution of, 187
Ice-forming nucleus, Photolytic de-activation of silver iodide as an, (Pl. III), 354
Ice-nucleating properties of clay minerals and stony meteorites, 552
Incidence of rainfall, A method of obtaining average bearing and, 408
Infra-red radiation, Atmospheric extinction of, 371
Integrating actinometer, The use of the Campbell-Stokes sunshine recorder as an, 270
Interhemispherical features of the general circulation of the atmosphere, 156

Inversion height by surface heating, Control of, 483
Israel (H.), *Luftelektrizität und Radioaktivität*, 435
Jackson (C. I.), Snowfall measurements in northern Canada, 273
Jackson (C. I.), R. W. Longley, Snowfall measurements in northern Canada, 566
James (D. G.), Observations from aircraft of temperatures and humidities near stratocumulus clouds, 114
Jeffree (E. P.), Some long-term means from *The Phenological Reports* (1891-1948), 95
Jeffreys (Sir Harold), *The Earth : its origin, history and physical constitution*, 434
Jelley (J. V.), F. R. Barclay, M. J. W. Elliot and P. Goldsmith, A direct measurement of the humidity in the stratosphere using a cooled-vapour trap, 259
Jones (J. I. P.) and F. Pasquill, An experimental system for directly recording statistics of the intensity of atmospheric turbulence, 578
Jones (R. F.), Radar echoes from atmospheric inhomogeneities, 116
Jones (R. F.), Size-distribution of ice crystals in cumulonimbus clouds, 187
Kilinski (E. von), *Lehrbuch der Luftelektrizität*, 435
Kinetic energy of the atmosphere by external heat sources and surface friction, On the control of, 437
Knighting (E.), On the grid length to be adopted in numerical weather prediction, 265
———, Some computations of the variation of vertical velocity with pressure on a synoptic scale, 318
Knighting (E.) and M. K. Hinds, A report on some experiments in numerical prediction using a stream function, 504
Kraus (E. B.), Synoptic and dynamic aspects of climatic change, 1, 569
Kulkarni (R. N.) and K. R. Ramanathan, Mean meridional distributions of ozone in different seasons calculated from *umkehr* observations and probable vertical transport mechanisms, 144
Labrador-Ungava, A note on the synoptic climatology of, 557
Landsberg (H. E.) and J. Van Miegham (Eds.), *Advances in geophysics*, Vol. 6, 434
Lehnert (B.) (Ed.), *Electromagnetic phenomena in cosmical physics*, 123
Lin (C. C.), (Ed.), *Turbulent flows and heat transfer*, 584
Lodge (J. P.) (Ed.), *The atmospheric chemistry of chlorine and sulphur compounds*, Geophysical Monograph, 123
Long (I. F.) and H. L. Penman, Weather in wheat : an essay in micro-meteorology, 16.
Longley (R. W.), C. I. Jackson, Snowfall measurements in northern Canada, 566
Ludlam (F. H.), W. C. Macklin, D. Atlas and W. G. Harper, Radar scatter by large hail, 468
Macklin (W. C.), D. Atlas, W. G. Harper and F. H. Ludlam, Radar scatter by large hail, 468
Martin (D. W.) and A. W. Brewer, A synoptic study of day-to-day changes of ozone over the British Isles, 575
Mason (B. J.), Ice-nucleating properties of clay minerals and stony meteorites, 552
Mason (B. J.) and J. B. Andrews, Drop-size distributions from various types of rain, 346
Mason (B. J.) and G. W. Bryant, Photolytic deactivation of silver iodide as an ice-forming nucleus, (Pl. III) 354
Mason (B. J.) and J. Maybank, The fragmentation and electrification of freezing water drops (Pl. I), 176
Mateer (C. L.) and W. L. Godson, The vertical distribution of atmospheric ozone over Canadian stations from *umkehr* observations, 512
Maund (J. E.) and J. A. Chalmers, Point-discharge currents from natural and artificial points, 85
Maybank (J.) and B. J. Mason, The fragmentation and electrification of freezing water drops, (Pl. I), 176
McCormick (R. A.) and H. A. Panofsky, The spectrum of vertical velocity near the surface, 495
McVehil (G. E.), H. A. Panofsky and A. K. Blackadar, The diabatic wind profile, 390
Mean meridional circulations in the atmosphere, 277
Mean meridional distributions of ozone in different seasons calculated from *umkehr* observations and probable vertical transport mechanisms, 144
Measured radiative flux divergence near the ground at night, (Pl. IV), 382
Measurements of space charge in the lower atmosphere using double field mills, 79
Measurements on the electricity of precipitation, 530
Meridional circulations in the atmosphere, Mean, 277
Meridional distributions of ozone in different seasons calculated from *umkehr* observations and probable vertical transport mechanisms, Mean, 144
Method of obtaining average bearing and incidence of rainfall, A, 408
Meteorology become too professionalized ? Has, 295
Micro-meteorology, Weather in wheat : an essay in, 16
Moisture and momentum between *Hurricane Ella* (1958) and its environment, Exchange of heat, 276
Monteith (J. L.), The reflection of short-wave radiation by vegetation, 579
Monteith (J. L.) and G. Szeicz, The carbon-dioxide flux over a field of sugar beet, 205
———, The performance of a Gunn-Bellani radiation integrator, 91
Morgan (W. A.), Determination of the straight line of best fit to observational data of two related variates when both sets of values are subject to error, 107
Murgatroyd (R. J.) and M. P. Garrod, Observations of precipitation elements in cumulus clouds, 167
Notes on the wind flow at 50 mb in tropical and sub-tropical regions in January 1957 and January 1958, 540

Numerical calculation of the displacements of a stratified airstream crossing a ridge of small height, 326
Numerical prediction using a stream function, A report on some experiments in, 504
Numerical weather prediction, On the grid length to be adopted in, 265
Observations from aircraft of temperatures and humidities near stratocumulus clouds, 114
Observations of drop-size distributions in low layer clouds, Some, 454
Observations of precipitation elements in cumulus clouds, 167
Oddie (B. C. V.), The variation in composition of sea-salt nuclei with mode of formation, 549
Ozone and the middle stratosphere over arctic and sub-arctic areas in winter and spring, Total, 301
Ozone in different seasons calculated from *umkehr* observations and probable vertical transport mechanisms, Mean meridional distributions of, 144
Ozone over the British Isles, A synoptic study of day-to-day changes of, 575
Panofsky (H. A.), A. K. Blackadar and G. E. McVehil, The diabatic wind profile, 390
Panofsky (H. A.) and R. A. McCormick, The spectrum of vertical velocity near the surface. 495
Pasquill (F.) and J. I. P. Jones, An experimental system for directly recording statistics of the intensity of atmospheric turbulence, 578
Patterns of hailstorms in Alberta, 281
Penman (H. L.) and I. F. Long, Weather in wheat : an essay in micro-meteorology, 16
Performance of a Gunn-Bellani radiation integrator, The, 91
Pfeffer (R. L.), *Dynamics of climate*, 583
Phenological Reports (1891-1948), Some long-term means from, 95
Physical-statistical rules as bases for forecasts of weather and weather-character, 567
Photolytic de-activation of silver iodide as an ice-forming nucleus, (Pl. III), 354
Point-discharge currents from natural and artificial points, 85
Polar night, The diurnal temperature variation during the, 104
Potential gradient variations in the measurement of the atmospheric air-earth current, The compensation of the effects of, 252
Precipitation elements in cumulus clouds, Observations of, 167
Precipitation, Measurements on the electricity, of 530
Presidential Address by J. M. Stagg, Has meteorology become too professionalized ? 295
Priestley (C. H. B.), A determinant hypothesis for the superadiabatic wind and temperature profiles, 232
Problem in baroclinic stability, A, 237
Proceedings at meetings of the Society, 119, 288, 428, 580
Radar echoes from atmospheric inhomogeneities, 116
Radar scatter by large hail, 468
Radiation and the duration of sunshine in Trinidad, West Indies, Solar, 415
Radiation integrator, The performance of a Gunn-Bellani, 91
Radiative flux divergence near the ground at night, Measured, 382 (Pl. IV)
Rain and drizzle from layer clouds, Aircraft observations of, 195
Rain, Drop-size distributions from various types of, 346
Ramanathan (K. R.) and R. N. Kulkarni, Mean meridional distributions of ozone in different seasons calculated from *umkehr* observations and probable vertical transport mechanisms, 144
Ramsay (M. W.) and J. A. Chalmers, Measurements on the electricity of precipitation, 530
Rao (Y. P.), Interhemispherical features of the general circulation of the atmosphere, 156
Recent changes in atmospheric electricity and their cause, Some, 399
Reflection of short-wave radiation by vegetation, The, 579
Report of the Council for 1959, 416
Reviews :
Advances in geophysics, Vol. 6, (Eds.) H. E. Landsberg and J. Van Miegham, 434
Alfred Wegener, E. Wegener, 584
Annual Report on the Meteorological Office for the year ending 31 March 1959 (M.O. 659), H.M.S.O., 431
Arid-Zone hydrology, H. Schoeller, 291
Climatic Atlas of the Czechoslovak Republic, Hydro-met. Inst., 432
Cockle Park Farm, H. Cecil Pawson, 292
Contemporary physics, Vol. 1, No. 1, 1959, 123
Die Sommerniederschlage Mitteleuropas in den letzen 1½ Jahrhunderten und ihre Beziehungen zum Sonnenfleckenzyklus, F. Baur, 432, 567
Dynamics of climate, R. L. Pfeffer, 583
Electromagnetic phenomena in cosmical physics, (Ed.) B. Lehnert, 123
General meteorology, H. R. Byers, 123
Glossary of meteorology, (Ed.) R. E. Huschke, 431
Handbook of Renaissance meteorology, S. K. Heninger, Jr., 433
Introduction to theoretical meteorology, Seymour L. Hess, 290
Klima und Bioklima von Wien, Teil III, F. Steinhauser, O. Eckel and F. Sauberer, 123
Lehrbuch der Luftelektrizität, E. von Kilinski, 435
Luftelektrizität und Radioaktivität, H. Israel, 435
Radar meteorology, L. J. Batten, 292
Snow hydrology, United States Department of Commerce, 291
Solar-Terrestrische Beziehungen in Meteorologie und Biologie, H. Berg, 123
Sonnenstrahlung und Lufttrübung, L. Foitzik and H. Hinzpeter, 583
The atmospheric chemistry of chlorine and sulphur compounds, Geophysical Monograph (Ed.) J. P. Lodge, 123
The Earth : its origin, history and physical constitution, Sir Harold Jeffreys, 434
The theory of homogeneous turbulence, G. K. Batchelor, 291

The world around us, (Ed.) Sir Graham Sutton, 433
Theoretical hydrodynamics, L. M. Milne-Thomson, 433
Turbulent flows and heat transfer, C. C. Lin, (Ed.), 584
Turbulent transfer in the lower atmosphere, C. H. B. Priestley, 290
Weather, R. S. Scorer, 123
Weathercraft, L. P. Smith, 583
Richardson (L. F.) Prize, Announcement of, 579
Rider (N. E.), C. P. Tugwell and G. J. House, A surface energy-balance computer (Pl. II), 215
Riehl (H.) and M. Gangopadhyaya, Exchange of heat, moisture and momentum between *Hurricane Ella* (1958) and its enviroment, 276
Rose (C. W.) and H. G. Farbrother, A method of obtaining average bearing and incidence of rainfall, 408
Sauberer (F.), F. Steninhauser and O. Eckel, *Klima und Bioklima von Wien*, Teil III, 123
Sawyer (J. S.), Numerical calculation of the displacements of a stratified airstream crossing a ridge of small height, 326
Scorer (R. S.), *Weather*, 123
Sea-salt nuclei with mode of formation, The variation in composition of, 549
Seasonal and other temperature changes in the antarctic atmosphere, 283
Seeley (J. S.) and J. T. Houghton, Spectroscopic observations of the water-vapour content of the stratosphere, 358
Short-wave radiation by vegetation, The reflection of, 579
Silver iodide as an ice-forming nucleus, Photolytic de-activation of (Pl. III), 354
Similarity theory in the relation between fluxes and gradients in the lower atmosphere, 67
Singleton (F.), Aircraft observations of rain and drizzle from layer clouds, 195
Singleton (F.) and D. J. Smith, Some observations of drop-size distributions in low layer clouds, 454
Size-distributions of ice crystals in cumulonimbus clouds, 187
Smiddy (M.) and J. A. Chalmers, Measurement of space charge in the lower atmosphere using double field mills, 79
Smith (G. W.), Solar radiation and the duration of sunshine in Trinidad, West Indies, 415
Smith (D. J.) and F. Singleton, Some observations of drop-size distributions in low layer clouds, 454
Smith (L. P.), *Weathercraft*, 583
Snowfall measurements in northern Canada, 273, 566
Solar radiation and the duration of sunshine in Trinidad, West Indies, 415
Space charge in the lower atmosphere using double field mills, Measurements of, 79
Spectroscopic observations of the water-vapour content of the stratosphere, 358
Spectrum of vertical velocity near the surface, 495
Stagg (J. M.), Presidential Address – Has meteorology become too professionalized ? 295
Statistical variation of wind with distance, The, 543
Statistics of the intensity of atmospheric turbulence, An experimental system for directly recording, 578
Steinhauser (F.), O. Eckel and F. Sauberer, *Klima und Bioklima von Wein*, Teil III, 123
Stewart (K. H.), Some recent changes in atmospheric electricity and their cause, 399
Stratified airstream crossing a ridge of small height, Numerical calculation of the displacements of a, 326
Stratocumulus clouds, Observations from aircraft of temperatures and humidities near, 114
Stratosphere below 30 km, The summer circulation of the arctic, 127, 576
Stratosphere over arctic and sub-arctic areas in winter and spring, Total ozone and the middle, 301
Stratosphere using a cooled vapour trap, A direct measurement of the humidity in the, 259
Stream function, A report on some experiments in numerical prediction using a, 504
Sub-tropical regions in January 1957 and January 1958, Notes on the wind flow at 50 mb in tropical and, 540
Summer circulation of the arctic stratosphere below 30 km, The, 127, 576
Superadiabatic wind and temperature, A determinant hypothesis for the, 232
Surface energy-balance computer, (Pl. II), 215
Surface heating, Control of inversion height by, 483
Surface stress, A theory of fronts in relation to, 51
Sutton (Sir Graham) (Ed.), *The world around us*, 433
Symons Memorial Lecture for 1960 – On the control of kinetic energy of the atmosphere by external heat sources and surface friction, 437
Synoptic and dynamic aspects of climatic change, 1, 569
Synoptic climatology of Labrador-Ungava, A note on the, 557
Synoptic study of day-to-day changes of ozone over the British Isles, A, 575
Szeicz (G.) and J. L. Monteith, The carbon-dioxide flux over a field of sugar beet, 205
————, The performance of a Gunn-Bellani radiation integrator, 91
Taylor (R. J.), Similarity theory in the relation between fluxes and gradients in the lower atmosphere, 67
Temperature profiles, A determinant hypothesis for the superadiabatic wind and, 232
Temperature changes in the antarctic atmosphere, Seasonal and other, 283
Temperatures and humidities near stratocumulus clouds, Observations from aircraft of, 114
Theory of fronts in relation to surface stress, A, 51
Total ozone and the middle stratosphere over arctic and sub-arctic areas in winter and spring, 301
Trinidad, West Indies, Solar radiation and the duration of sunshine in, 415

Tropical and sub-tropical regions in January 1957 and January 1958, Notes on the wind flow at 50 mb in, 540
Tucker (G. B.), Mean meridional circulations in the atmosphere, 277
Tugwell (C. P.), G. J. House and N. E. Rider, A surface energy-balance computer (Pl. II), 215
Turbulence, An experimental system for directly recording statistics of the intensity of atmospheric, 578
Umkehr observations and probable vertical transport mechanisms, Mean meridional distributions of ozone in different seasons calculated from, 144
Van Miegham (J.) and H. E. Landsberg (Eds.), *Advances in geophysics*, Vol. 6, 434
Vegetation, The reflection of short-wave radiation by, 579
Vertical distribution of atmospheric ozone from emission spectrophotometry in the 1043 cm^{-1} band at high resolution, The accuracy of determination of the, 519
Vertical distribution of atmospheric ozone over Canadian stations from *umkehr* observations, 512
Vertical velocity near the surface, The spectrum of, 495
Vertical velocity with pressure on a synoptic scale, Some computations of the variation of, 318
Walshaw (C. D.), The accuracy of determination of the vertical distribution of atmospheric ozone from emission spectrophotometry in the 1043 cm^{-1} band at high resolution, 512
Water budgets in two adjacent reservoirs, Differing, 412
Water-vapour content of the stratosphere, Spectroscopic observations of the, 358
Weather in wheat : an essay in micro-meteorology, 16
Wegener (E.), *Alfred Wegener*, 584
Westaway (R. F.), Obituary, 294
Wexler (H.), Seasonal and other temperature changes in the antarctic atmosphere, 283
Wheat : an essay in micro-meteorology, Weather in, 16
Wilson (C. T. R.), Obituary, 293
Wind flow at 50 mb in tropical and sub-tropical regions in January 1957 and January 1958, Notes on the, 540
Wind with distance, The statistical variation of, 543
Witchell (W. M.), Obituary, 436

Supplementary Index

(*Newly-elected Members*)

Adefemi (S. A.), Fellow, 581
Bailey (T. W.), Fellow, 430
Baker (D. G.), Foreign Member, 428
Baker (Helen M.), Fellow, 120
Balchin (P. M.), Student, 289
Bardon (P. J.), Fellow, 288
Bennion (B.), Fellow, 430
Berry (K.), Fellow, 120
Besley (B. P.), Fellow (*Reinstatement*), 581
Bethell (J. P.), Fellow, 121
Bignell (K. J.), Student, 289
Blackall (R. M.), Fellow (*from Student*), 119
Burton (J. M. C.), Fellow, 430
Chalmers (W.), Fellow, 121
Cook (J. K.), Fellow, 428
Cox (A. E.), Fellow, 120
Cox (D. L.), Student, 122
Crosdale (A. L.), Fellow, 288
Cross (D. A. E.), Fellow, 120
Dalton (A. B.), Fellow (*from Student*), 121
Davies (D. L.), Fellow, 120
Dearing (E.), Fellow (*Reinstatement*), 428
Dessens (H. J. J.), Foreign Member, 428
De Silva (M. B. G.), Fellow, 121
Diver (A. A.), Fellow, 288
Dixon (C.), Fellow, 120
Edwards (M. G.), Student, 120
Elliott (J. A.), Fellow, 120
Epstein (E. S.), Foreign Member, 428
Fenn (M. G.), Fellow, 120
Fernandes (K. J.), Fellow, 121
Ford (M. W.), Fellow, 121
Gadd (N.), Student, 289
Gilead (M.), Foreign Member, 430
Gill (J. S.), Fellow, 430
Glennon (G. J.), Fellow, 121
Goldsmith (P.), Fellow, 121
Good (B. T. C.), Fellow, 288
Griggs (M.), Student 428
Gunton (H. E.) Fellow, 120
Haggett (R. C. F.), Fellow, 288
Hanson (W.), Student, 428
Harvey (J. G.), Fellow, 121
Heathcote (J.), Fellow, 121
Hirst (T. L.), Student, 120
Hofmeyr (W. L.), Fellow, 428
Horne (E.), Fellow, 119
Howell (Jacqueline A.), Student, 122
Hrynkiewiczmoczulski (M. B.), Fellow, 121
Hull (O. M.), Fellow, 119
Hutchins (I. A.), Fellow, 120
Hutchings (J. W.), Fellow, 288
Jackson (C. I.), Fellow (*from Student*), 122
Jeffries (B. L. A.), Fellow, 119
Karunatilleke (D. P. W.), Fellow, 122
Kington (J. A.), Fellow, 120
Kruger (E. G.), Foreign Member, 288
Laker (D. D.), Fellow, 430
Lamond (M. H.), Fellow, 119
Laverack (Barbara M.), Student, 289
Lealan (A. D.), Student, 289
Levett (R. E. K.), Fellow, 122
Lewis (J. B.), Student, 120
Limbrick (G.), Fellow, 120

Loewe (F.), Fellow (*from Foreign Member*), 430
Macarthur (G. G. S.), Student, 289
Madden (F. A. P.), Fellow, 120
Mané (U.), Foreign Member, 122
Manning (J. H. A.), Fellow, 288
Magor (Joyce I.), Fellow, 288
Martin (J. H. A.), Fellow (*Reinstatement*), 288
Miura (A.), Foreign Member, 288
Morrissey (E. G.), Student, 122
Muffatti (A. H. J.), Fellow, 122
Ohtake (T.), Foreign Member, 122
Paley (J.), Fellow, 122
Patrick (G. O.), Fellow, 122
Pennant (A. D. H.), Fellow, 119
Pereira (H. C.), Fellow, 288
Piéjus (P. C.), Fellow (*Reinstatement*), 428
Powell (J. M.), Fellow, 288
Prabhakar (D. R. L.), Fellow, 119
Price (T.), Fellow (*Reinstatement*), 120
Quereshi (M. Y.), Fellow (*from Student*), 119
Radcliffe (C. J.), Student, 289
Richards (J. M.), Fellow, 122
Rickers (D.), Fellow, 122
Rogers (P.), Fellow, 288
Ross (S. M.), Fellow, 288
Rossington (L. G.), Student, 581
Rushforth (Beryl), Student, 289
Rushforth (J. M.), Fellow, 120
Sen-Gupta (B. K.), Fellow, 430
Shepstone (B. J.), Fellow, 428
Shore (W. R.), Fellow, 122
Singleton (F.), Fellow (*from Student*), 430
Smith (C. E. A.), Fellow, 119
Smith (E. J.), Fellow, 288
Smith (S. D.), Fellow, 122
Sparrow (B. A.), Fellow, 288
Spence (Jean M.), Student, 120
Stafford (Margaret M.), Fellow, 428
Starling (E. A.), Fellow, 288
Strachan (D. G.), Fellow, 288
Strang (D. D.), Student, 581
Subrahmanyam (V. P.), 122
Symonds (K. A.), Fellow, 430
Taylor (B. H. T.), Fellow (*Reinstatement*), 119
Torrance (J. D.), Fellow, 288
Turner (A. M. R.), Student, 430
Turton (Margaret A.), Student, 289
Tyldesley (J. B.), Fellow, 122
Vanderelst (N. P.), Foreign Member, 288
Voisk (Sylvia V.), Student, 289
Wheeler (D.), Student, 289
Wilson (D. J.), Student, 120
Wood-Jones (R. B.), Fellow, 581
Woodacre (T. S.), Fellow, 120
Worsnop (A. R. S.), Fellow (*Reinstatement*), 119

Canadian Branch

(*Newly-elected Members*)

Barklie (R. H. D.), Fellow, 119
Catling (R. G.), Fellow, 122
Gates (A. D.), Fellow, 122
Gibson (T. T.), Fellow, 581
Lawrynuik (W. D.), Fellow, 581
McBride (J. H.), Fellow, 122
Schwarz (U.), Foreign Member, 430
Thacker (J. J.), Fellow, 430
Verge (R. W.), Fellow, 430

a new DECCA windfinding radar type WF2

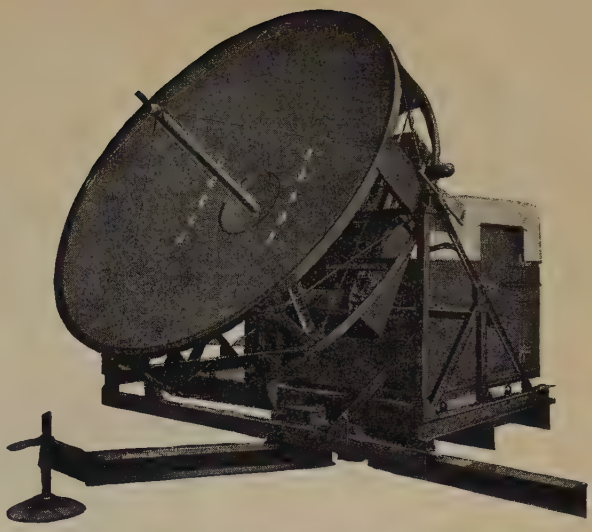

★ **High Performance**—A new high power transmitter increases maximum slant range to well beyond 150,000 metres. A smaller target can be used for normal ranges thus keeping operating costs to a minimum.

★ **Improved instrumentation** making the equipment suitable for one man operation and still further improving the day to day economy of the primary radar windfinding system.

★ **Variable beamwidth aerial** producing a broad beam for picking up the reflector target at the start of an ascent at night in bad weather.

★ **Re-designed operators cabin** with built-in air conditioning and all-round accessibility to electronic units.

Developed from Type WF1 which is in service with some 20 meteorological authorities, the new Decca Windfinding Radar is easy to operate and maintain, and is capable of providing regular, accurate upper wind data at low operating cost.

lower daily operating costs

reflector ranges in excess of 150 km

one man operation

a simple efficient proven system

DECCA RADAR

DECCA RADAR LIMITED · LONDON · ENGLAND

DR 109b

PYRHELIOMETER

For the Measurement of SOLAR RADIATION

Eppley Pyrheliometers are used for solar radiation measurements at ninety-eight weather stations in the continental United States, Canada, Alaska, Greenland, Iceland, Caribbean Sea, and the Pacific Ocean. Sixty-two of these stations are under the direction of the United States Weather Bureau.

The Eppley Pyrheliometer was adopted as standard equipment by the Weather Bureau after considerable experimentation. It was found to be the best instrument so far tested by the Bureau.

Used in conjunction with a suitable recorder, the Eppley Pyrheliometer will provide an accurate and reliable record of total solar and sky radiation on a horizontal surface.

Bulletin No. 2 on Request

THE EPPLEY LABORATORY INC.

Scientific Instruments

20 Sheffield Avenue Newport, Rhode Island, U.S.A.

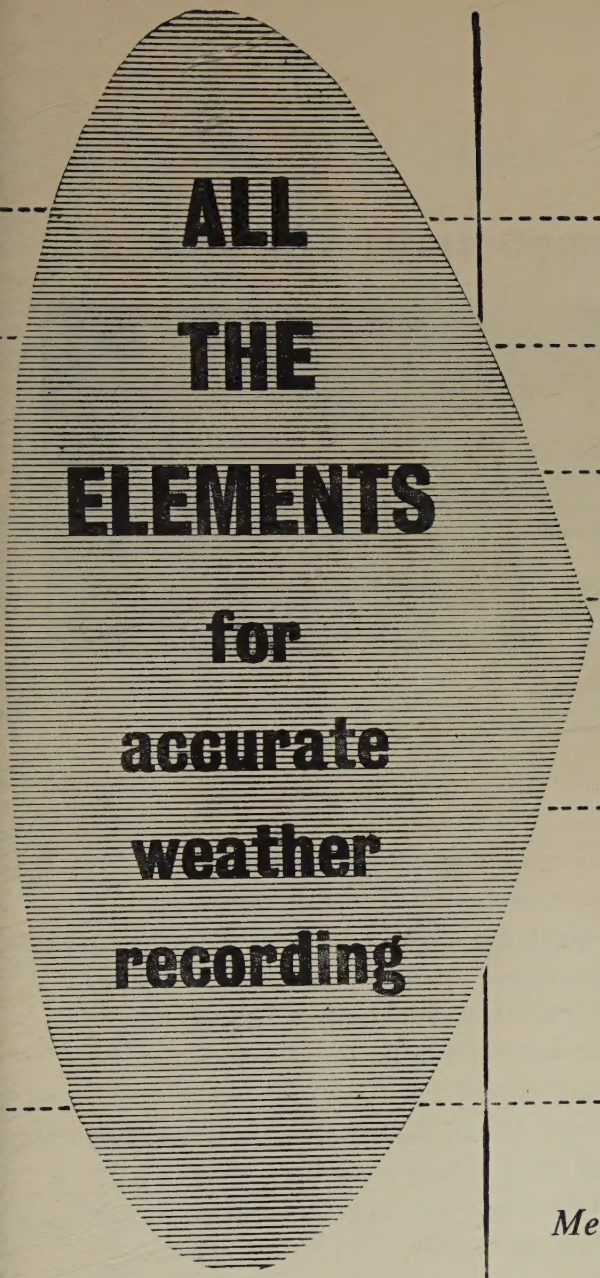

Thermometers

Hygrometers

Barometers

Rain Gauges

Sunshine Recorders

Wind Direction and Velocity Indicators, etc.

Meteorological Instruments by

NEGRETTI & ZAMBRA LTD

Manufacturers of instruments for the indication, recording, controlling of :— Temperature, pressure, liquid level, volume, specific gravity, humidity, etc.

122, REGENT STREET, LONDON, W.1
'Phone: REGent 3406. 'Grams: Negretti, Piccy, London
Branches : Birmingham, Cardiff, Glasgow, Leeds, Manchester, Nottingham.
Agents or Subsidiaries in most countries.

Mufax

THROUGHOUT THE WORLD

9

IN THE AIR

TRANSATLANTIC FLIGHT

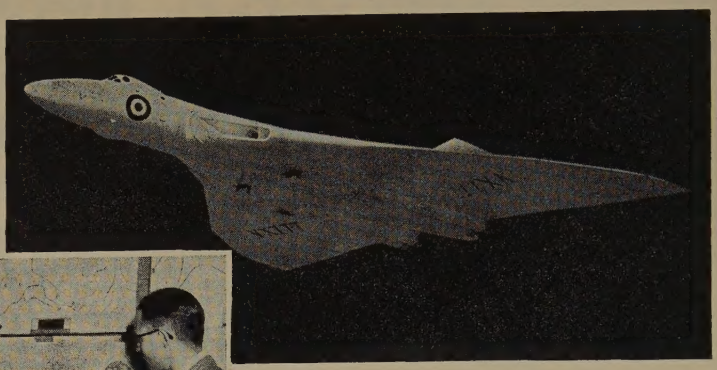

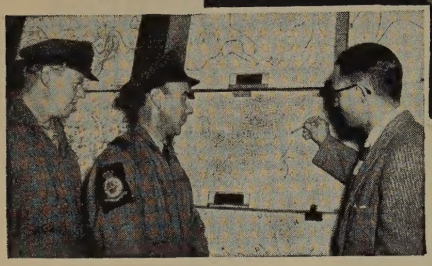

Early one Sunday morning a Royal Air Force Vulcan jet bomber swept off a Canadian runway on the first non-stop transatlantic jet flight out of Station Trenton. Before take-off, the crew was briefed on weather conditions expected throughout the trip. This was the first briefing ever provided by the forecast officer for a non-stop transatlantic flight. The lower photograph shows Mr. D. H. Parkinson, the senior station meteorological officer, discussing the latest Mufax weather chart recordings with Wing Commander A. C. L. Mackie, the Captain, and F/L J. R. Ward, the navigator.

MUIRHEAD

MUIRHEAD & CO. LIMITED, Beckenham, Kent, England.
Tel : Beckenham 4888.

MUIRHEAD INSTRUMENTS LIMITED, Stratford, Ontario, Canada.
Tel : 271–3880

MUIRHEAD INSTRUMENTS INC., 441 Lexington Avenue, New York 17, N.Y., U.S.A.
Tel : Murray Hill 2–8131.

431

Marconi 3cm Storm Warning Radar

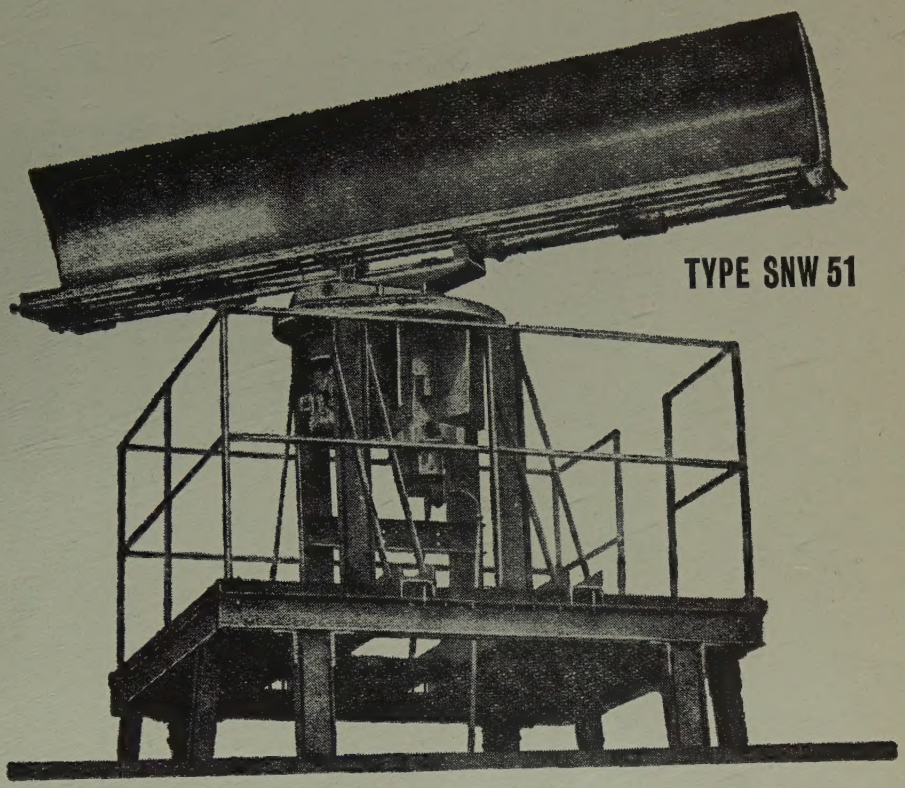

TYPE SNW 51

Marconi's Storm Detection Radar, Type SNW 51 is specially designed to present an accurate picture of storms and rain-producing clouds over ranges up to 200 n.m. It can therefore meet the needs of Meteorological Departments and Airport Authorities, particularly where it is required to derive information from inaccessible areas. Features include:— High Power Working, High-gain Tiltable Aerial (remote-controlled from display unit). Full Off-Centring Facility (enabling any sector to be expanded to cover the whole area of the tube). Remote Displays, Static or Mobile Versions available.

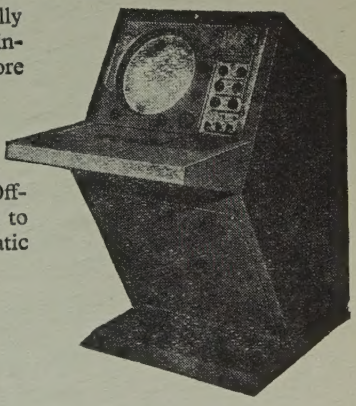

MARCONI

COMPLETE CIVIL AND MILITARY RADAR INSTALLATIONS

MARCONI'S WIRELESS TELEGRAPH COMPANY LIMITED, CHELMSFORD, ESSEX, ENGLAND

M6A

F. DARTON & CO. LTD.

Makers of :

THERMOGRAPHS
BAROGRAPHS
HYGROGRAPHS
PRECISION HAIR HYGROMETERS
ALTIMETER CALIBRATORS
KEW PATTERN BAROMETERS
FORTIN'S PRINCIPLE BAROMETERS
GRASS & SOLAR THERMOMETERS
RAIN GAUGES, etc.

All enquiries to : Established 1834

WATFORD FIELDS, WATFORD, HERTS

Tel. : WATFORD 26019 & 26010

Prepared under the auspices of the Royal Meteorological Society

CLOUD STUDY

A PICTORIAL GUIDE

By F. H. Ludlam and R. S. Scorer
D.I.C., F.R.Met.S. M.A., Ph.D., F.R.Met.S.

Published by John Murray

Foreword by R. C. SUTCLIFFE, O.B.E., Ph.D., F.R.S.
(President of the Royal Meteorological Society 1955-57)

This is a new and authoritative guide, suitable for the novice yet indispensable also to the more expert reader. It is the work of two authors who have taken a leading part in the post-war research which has so greatly improved our understanding of clouds. It is illustrated by 73 photographs (six in full colour), each accompanied by a full descriptive caption.

Size $9\frac{1}{4} \times 6\frac{1}{8}$ *ins.* 80 *pages* 12*s.* 6*d. net*

Orders (with remittance) to Assistant Secretary, 49 Cromwell Road, London, S.W.7

Price to Members of the Royal Meteorological Society : **12s.** *post free*
Non-Members : **13s. 6d.** *post free*

Printed in Great Britain in Horley Series by The Salisbury Press Ltd., Publicity House, Wilton Road, Salisbury, Wilts. (23908)